STRONTIUM RELEASING COMPOSITE RESINS CEMENTS

by

Kathleen MacDonald

Submitted in partial fulfillment of the requirements

for the degree of Doctor of Philosophy

at

Dalhousie University

Halifax, Nova Scotia

February 2018

This thesis is dedicated to my loving husband Neil. This work was fuelled by your support, motivation, and mid afternoon coffee deliveries. It could not have been done without you.

Table of Contents

List of Tables . . . . . **viii**

List of Figures . . . . . **xiii**

Abstract . . . . . **xiv**

List of Abbreviations and Symbols Used . . . . . **xv**

Acknowledgements . . . . . **xx**

Chapter 1 Introduction **1**

Chapter 2 Literature review **7**

2.1 Osteoporosis and osteopenia 7

2.1.1 Epidemiology 7

2.1.2 Pathophysiology of osteoporosis 9

2.2 Percutaneous spinal augmentation 28

2.2.1 Pain relief efficacy of vertebral augmentation 29

2.2.2 Subsequent vertebral fracture following percutaneous vertebral augmentation 37

2.2.3 Prophylactic percutaneous vertebroplasty 38

2.2.4 Vertebroplasty materials 41

2.3 Bioactive glass 59

2.3.1 Bioactive glass degradation reaction 60

2.3.2 Bioactive glass as therapeutic ion release systems 64

Chapter 3 Rationale **69**

Chapter 4 Experimental work **77**

4.1 Modulation of strontium release from a tertiary borate glass through substitution of alkali for alkali earth oxide 77

4.1.1 Author contribution statement 77

4.1.2 Abstract 77

4.1.3 Introduction 78

4.1.4 Methods 80

4.1.5 Results 84

4.1.6 Discussion 87

4.1.7 Limitations 95

4.1.8 Conclusion 95

4.2 The feasibility and functional performance of ternary borate-filled hydrophilic bone cements: targeting therapeutic release thresholds for strontium 96

4.2.1 Author contribution statement 96

4.2.2 Abstract 96

4.2.3 Introduction 97

4.2.4 Results 100

4.2.5 Discussion 109

4.2.6 Materials and methods 117

4.2.7 Conclusions 121

4.3 Mechanical loading, an important factor in the evaluation of ion release from bone augmentation materials 123

4.3.1 Note on composition selection 123

4.3.2 Author contribution statement 125

4.3.3 Abstract 125

4.3.4 Introduction 126

4.3.5 Results 129

4.3.6 Discussion 131
4.3.7 Conclusion 137
4.3.8 Methods 137

4.4 A pilot implantation study of borate glass filled hydrophilic bone cements 140
4.4.1 Author contribution statement 140
4.4.2 Abstract 140
4.4.3 Introduction 140
4.4.4 Materials and methods 141
4.4.5 Results 143
4.4.6 Discussion 147

Chapter 5 Conclusion 149

Bibliography 163

Appendix A Peak Exothermic Setting Temperatures 194

Appendix B Cytotoxicity testing of cement extracts 196

Appendix C Additional animal study data 198

List of Tables

Table 2.1 Clinical trials investigating the efficacy of strontium ranelate for the treatment of osteoporosis in post-menopausal women. . . . 22

Table 2.2 Clinical trials evaluating the efficacy of PVP and BKP for the treatment of painful VCFs (part 1 of 3) 32

Table 2.3 Clinical trials evaluating the efficacy of PVP and BKP for the treatment of painful VCFs (part 2 of 3) 33

Table 2.4 Clinical trials evaluating the efficacy of PVP and BKP for the treatment of painful VCFs (part 3 of 3) 34

Table 2.5 Ideal properties for PVP materials as reported by Lewis[1] . . . 42

Table 2.6 Two-paste composition of ceramic reinforced Bis-GMA based cement[2]. 51

Table 2.7 Mechanical Properties of Commercially Available Injectable Bone Cements[2]. 52

Table 4.1 Glass compositions by molar fraction of pre-fired material, and actual compositions revealed in compositional analysis (molar percentage and standard deviation). 81

Table 4.2 Corrected Akaike informative criteria table comparing linear and quadratic fits to boron ion release. 94

Table 4.3 Compositions of resin phase, and glass loading of the cement compositions, in weight percentage. 100

Table 4.4 ATR-FTIR peak locations with corresponding cement component, and functional group. 102

Table 4.5 Multiple t test statistics results comparing Sr release levels between the 3 loading conditions investigated 130

Table 4.6 Comparison of model fits between linear release model (surface controlled release), and power series release (with allowance for burst effect). 132

Table 4.7 Two paste chemically cured resin system (wt%). 138

Table 4.8 Histological and histomorphometry results for sham, glass filled, and unfilled defect sites, 8 weeks post implantation. 145

Table B.1 Criteria for the evaluation of cytotoxicity. Materials with cytopathology scores below 2 considered non cytotoxic. Positive cytotoxic response considered mild for scores of 3, and severe for scores of 4. 197

Table B.2 Cytotoxicity scoring results 197

Table C.1 Histologic evaluation scoring rubric used for the evaluation of implant response, adapted from ISO 10993 199

Table C.2 Detailed histomorphometry findings of implant response to glass filled (strontium releasing) implant sites, evaluated 8 weeks post implantation. 200

Table C.3 Detailed histomorphometry findings of implant response to unfilled resin (non strontium releasing) implant sites, evaluated 8 weeks post implantation. 201

Table C.4 Detailed histomorphometry findings of sham defect sites, evaluated 24 days post operation due to early sacrifice related to decreased appetite. 202

Table C.5 Detailed histological findings of glass filled (strontium releasing) implant sites 8 weeks post implantation. 203

Table C.6 Detailed histological findings of unfilled resin (non strontium releasing) implant sites 8 weeks post implantation 204

Table C.7 Detailed histological findings of sham defect sites, evaluated 24 days post operation due to early sacrifice related to decreased appetite. 205

List of Figures

Figure 2.1 Prevalence of osteoporosis in industrialised countries by sex, and age[3]. 8

Figure 2.2 Cortical and Trabecular bone structure[4]. 10

Figure 2.3 Steps of bone remodelling process, (left to right): quiescence, resorption, reversal, formation, mineralization, and return to quiesence[4]. 12

Figure 2.4 CaSR pathways initiated by strontium ion binding in OBL and OCLs. 19

Figure 2.5 Prevalence of fracture locations in the thoracic and lumbar spine demonstrating increased succeptability to fracture in the thoracolumbar junction. 26

Figure 2.6 Illustration demonstrating the augmentation of a VCF though the use of PVP, indicating the insertion of a large bore needle into the fractured vertebral body under fluoroscopic guidance, and full fill of vertebral body providing internal cast[5]. 29

Figure 2.7 Illustration of the steps of PVP on 1) a fractured vertebrae, including 2) the insertion of a large bore needle into the fractured vertebral body under fluoroscopic guidance, and insertion of collapsed bone tamp into the vertebral body 3) the inflation of the bone tamp generating a void for cement fill while pushing endplates apart restoring vertebral body height,4) injection of bone cement into the bone void providing an internal cast[5]. . 30

Figure 3.1 Hydroxyethyl methylacrylate monomer structure, showing highly polar hydroxyethyl side chain 74

Figure 4.1 XRD analysis of all nine glass compositions showing two amorphous peaks, at 2θ values of approximately 25 and 45, corresponding to 3 and 4 coordinated boron centers in the glass. . . 85

Figure 4.2 Fraction of four coordinated boron content by post-fired strontium content. 85

Figure 4.3 Variation in glass transition temperature with post-fired strontium content. 86

Figure 4.4 Variation in glass density with post-fired strontium content. . 86

Figure 4.5 Ion release profiles for boron and strontium release of all nine glasses studied. Strontium release profiles show a linear release with respect to the root of time, characteristic of diffusion-controlled release. Boron release profiles vary among glass compositions, with low sodium glasses displaying diffusion-controlled release, while high sodium glasses demonstrate a decrease in boron release over time, indicating a precipitation reaction. . . 88

Figure 4.6 Ion release efficiency for strontium and boron release (expressed as a percentage of initial element loading released) showing a transition from preferential boron release to preferential strontium release with time. 89

Figure 4.7 Linear increase in rate constant of strontium ion release from glass series with increasing strontium content ($R^2 = 0.95$). . . 90

Figure 4.8 Cement (a) working times, and (b) setting times, significant differences are marked with "$*$"($p<0.05$) or "$**$"($p<0.01$). . . 101

Figure 4.9 Representative ATR-FTIR spectra collected on unset cement pastes (red and pink traces for paste one and two respectively), and set cement samples (blue trace) of cement composition A1 (15 % HEMA, 55 % glass). 101

Figure 4.10 DC measured through ATRFTIR analysis with standard deviation, showing increased DC as the HEMA content increased, ($p < 0.01$, unless otherwise noted. 103

Figure 4.11 Cement biaxial flexural strength (MPa) at 1, 7, 30 and 60 d incubation, with standard deviations. 104

Figure 4.12 Cement weight gains over 60 d of incubation in PBS (with standard deviations), and weight loss from max (calculated as difference between maximum weight gain, and final weight gain at 60 d) as a measure of glass filler loss. 105

Figure 4.13 Sr release from cements into PBS in mg/l, relative to (A) *in vitro* OBL activation threshold [6]; (B) serum Sr concentration reported in the Treatment of Peripheral Osteoporosis (TROPOS) study (10.8 mg/l) [7] and (C) *in vitro* OCL inhibition threshold [8] 107

Figure 4.14 Ion release efficiency as % of initial elemental loading for B and Sr demonstrating preferential release of B from the cements. . 108

Figure 4.15 Representative SEM images of resin surfaces for (a) control unreacted surface of group E, 60 % glass cement (b) Group E 60 % glass cement, 1 d of incubation in PBS; (c) group E 60 % glass, 60 d of incubation in PBS; (d) group A 60 % glass, 1 d of incubation in PBS; and (e) group A, 60 % glass 60 d of incubation in PBS, demonstrating the development of a Sr rich surface precipitate 110

Figure 4.16 Schematic of two paste resin fabrication, all compositions represented in weight percentage. 118

Figure 4.17 Biaxial flexural strength of 45 % HEMA composites, fabricated without TEG DMA inclusion. Samples prepared as per section 4.3.8, and assessed for biaxial flexural strength as per section 4.2.6. 124

Figure 4.18 Working time of 45 % HEMA composites, fabricated without TEG DMA inclusion. Pastes prepared as per section 4.3.8, and assessed for working time as per 4.2.6. 124

Figure 4.19 Setting time of 45 % HEMA composites, fabricated without TEG DMA inclusion. Pastes prepared as per 4.3.8, and assessed for setting time as per 4.2.6. 125

Figure 4.20 Mass gain (measured as difference between dry and wet weight) during cement incubation under various loading conditions, denoting statistically significant difference between unloaded and cyclic compression conditions. 130

Figure 4.21 Cumulative release of (a) boron, and (b) Sr ions under various loading conditions, demonstrating Fickian diffusion under cyclic loading, and less Fickian diffusion in unloaded and static compression loaded incubation. 131

Figure 4.22 Sr release from cements into SBF in mg/l, relative to (A) *in vitro* OBL activation threshold[9] (B) serum Sr concentration reported in the Treatment of Peripheral Osteoporosis (TROPOS) study[10], and (C) *in vitro* OCL inhibition threshold [8]. 133

Figure 4.23 Rate of Sr release as equivalent days (7,200 cycles of compression) relative to (A) *in vitro* OBL activation threshold[9] (B) serum Sr concentration reported in the Treatment of Peripheral Osteoporosis (TROPOS) study[10]. 136

Figure 4.24 Histologic response, 8 w post implantation, Goldners Trichrome stain low magnification (10 x, subfigures a, b,c) and high magnification (subfigures d, e, f). Sham defects (a, d) showing fibrous infiltrate, unfilled resins (b, e) showing mineralized bone formation at implant surface (stained green) and glass filled resins (c, f) evidence of unmineralised osteoid formation (stained red/orange) and implant surface irregularity. 144

Figure 4.25 Mirco CT of implants sites, 8 weeks post implantation, (a) glass filled resin cylinder showing high contrast between glass filled material and surrounding bone tissue, along with the protrusion of the cement cylinder out of the defect site and (b)unfilled showing the formation of mineralized bone covering the defect opening 146

Figure A.1 Peak exothermic temperatures of cement curing. 195

Abstract

While vertebroplasty has proven effective in relieving pain and stabilizing fractures in osteoporotic patients, it currently fails to address the underlying pathology. Strontium releasing composite resin cements, based on borate glass reinforced hydrophilic resin, may present a method of incorporating anti-osteoporotic therapy into a vertebroplasty material, however a thorough understanding of the release of strontium is needed in order to tailor ion release to achieve and maintain therapeutic thresholds. To achieve this goal, strontium-sodium-borate glasses were investigated to assess the effects of composition on glass properties and ion release. While strontium release was found to be diffusion controlled, high sodium glasses resulted in borate precipitation, possibly presenting a mechanism of mitigating cytotoxicity without limiting strontium release. When incorporated into a Bis-GMA, TEG-DMA , HEMA resin, this material was found to maintain sufficient handling properties for this intended use. Lower HEMA content cements decreased in strength from 44 to 28 MPa over 60 days, strength was maintained for high HEMA contents (16 MPa), an unusual finding for composite resins. Increased HEMA resulted in increases in borate release efficiency (up to 15%) as expected; strontium release was limited (<1.8%) by the formation of strontium phosphate precipitates on the resin surface, demonstrating strong mineralization potential. Strontium release greatly increases in calcium rich SBF, demonstrating the importance of the ionic environment. Ion release under mechanical loading (an implantation variable frequently overlooked in the evaluation of ion release from orthopedic materials) was investigated to assess the effect of compression on release kinetics. While both cyclic and static compression resulted in decreased water sorption, the release of both strontium and boron was increased. This significant increase in ion release demonstrated an important limitation to the unloaded ion release experiments commonly performed. In a pilot implantation model, strontium-releasing cement demonstrated significant implant swelling, and direct tissue integration. New bone formation however was greater surrounding a non strontium releasing control resin, demonstrating that the beneficial effects were likely imparted by the highly hydrophilic resin, and not strontium release. While materials demonstrated significant release of strontium ions under in vitro testing conditions, no in vivo therapeutic effect was observed.

List of Abbreviations and Symbols Used

μm	Micro meter
°C	Degrees Celsius
%	Percent
™	Trademark
AIDS	Acquired immune deficiency syndrome
Al	Aluminium
ALP	Alkaline phosphatase
ANOVA	Analysis of Variance
ASTM	American society for testing and materials
ATR-FTIR	Attenuated total reflectance Fourier transforms infrared
B	Boron
Bis EMA	bisphenol A ethoxylate dimethacrylate
Bis-GMA	Bisphenol A glycidyl methacrylate
BMD	Bone mineral density
bn	Billion
BPO	Benzoyl peroxide
C	Carbon
C.	Approximately
Ca	Calcium
CAD	Canadian dollar

CAMOS	Canadian multicenter osteoporosis study
CaSR	Calcium sensing receptor
cm	Centimetre
DC	Degree of conversion
DHPT	Dimethyl-p-toludine
DNA	Deoxyribonucleic acid
DSC	Differential Scanning Calorimetry
e.g.	For example
EDS	Energy-dispersive X-ray spectroscopy
ERK	Extracellular signal-regulated kinase
FRAX	Fracture risk assessment tool
g	grams
GPa	GigaPascal
h	Hour
HA	Hydroxyl apatite
HDPP	High density polyporpylene
HEMA	Hydroxyl ethyl methacrylate
Hz	Hertz
i.e.	That is

ICP-AES	Inductively coupled plasma atomic emission spectroscopy
ISO	International Organization for Standardization
ITAM	Immunoreceptor tyrosine based activation motif
kN	kiloNewton
Li	Lithium
MAS NMR	Magic angle spinning nuclear magnetic resonance
Mg	Magnesium
mg	Mili gram
micro CT	Computed Tomography
min.	Minute
mL	Mililiter
mM	Mili molar
mm	Milimeter
mol	Molar
MPa	Mega Pascals
Na	Sodium
O	Oxygen
OBL	Osteoblasts
OCL	Osteoclasts
OPG	Osteoprotegrin

P	Phosphorous
Pas	Pascale seconds
PBS	Phosphate Buffered Saline
PMMA	Poly methyl methacrylate
ppb	Parts per billion
ppm	Parts per million
PTFE	Poly tetra fluoroethylene
PVP	Percutaneous vertebroplasty
RANKL	Receptor activator of nuclear factor k ligand
RR	Risk ratio
s	Second
SBF	Simulated Body Fluid
SEM	Scanning Electron Microscope
SF 36 PCS	Short form 36 physical component summary
Si	Silicon
Sr	Strontium
TEG DMA	Triethylene glycol dimetracrylate
TII	Therapeutic inorganic ion
US	United States of America
VAS	Visual analogue scale

VCF	Vertebral compression fracture
Wnt	Wingless related protein
wt%	Weight percent
XRD	X-ray diffraction

Acknowledgements

First and foremost, my thanks go to Dr. Daniel Boyd for his support, guidance, and motivation through this project. Thank you for you putting your faith in me, and dedicating your time and energy to help guide me through. Thank you for always making your students a priority, and fostering a sense of teamwork and community. Your work ethic and integrity make you an incredible mentor.

To my committee members Dr. Mark Filiaggi, Dr. Paul Gratzer and Dr, Clem Higginbotham, thank you for your time, insight, encouragement and guidance. Meetings with you have always been productive and encouraging reflections on my growth as a student.

To Dr Hanson and Dr Price, thank you for your sharing technical expertise and insights.

Thanks my fellow Boyd lab group researchers Sharon, Xiao, Sammi, Katie, Brett, Nancy, Victoria, Lauren, Jensen, Amanda, Camryn. Not only have you guys provided invaluable tips and assistance in the lab, but were a genuine pleasure of a team to work with. Thank you for being both colleagues and friends through this journey. A special thanks to Nancy, Lauren and Katie, there were weeks when our coffee dates were all that preserved my sanity.

To Gordie and Alicia, thank you for sharing your invaluable laboratory expertise. You assistance in setting up experiments, finding lab equipment and just generally making a lab run smoothly definitely helped speed my research along.

My genuine thanks to Susan, for going above and beyond in keeping our lab running. Thank you for spending countless hours trouble shooting equipment with me, and managing to keep me laughing the whole time. Thanks for always being in your office for another report of broken equipment, or just for a chat about your

childrens' latest antics.

Finally thanks to all my friends and family who patiently accepted my absenteeism while supporting my pursuit of this degree. You all provided much needed support and outlets to stress.

Chapter 1

Introduction

Osteoporosis is a degenerative disease characterized by a decrease in bone mineral density (BMD), and changes to bone architecture, culminating in significant reductions in bone strength. It is a prevalent disease that, globally, affects over 70 % of women over 65 years old, and is associated with increased fracture risk and compromised fracture healing capacity[11]. While traditional osteoporosis therapies such as bisphosphonates have been used to slow the progression of bone loss, the coupled nature of bone remodelling may result in adverse effects when used over extended periods[12]. More recently, strontium (Sr) ranelate therapy has been found to be effective in reversing the loss of BMD, by decoupling bone remodelling[13]. The pharmaceutically active component of strontium ranelate is the strontium ion, which serves to increase osteoblast (OBL) activity, promoting bone deposition, while simultaneously decreasing osteoclast (OCL) activity, and bone resorption[6].

Despite the efficacy of anti-osteoporotic agents in reducing fracture risk, high profile media reports detailing rare side effects, as well as the lack of readily recognisable symptoms, have lead to low levels of patient compliance and persistence[14, 15, 16]. As such preventative therapies are underutilized, and the prevalence of osteoporotic fracture remains high. It is estimated that 1 in 3 women, and 1 in 5 men will experience an osteoporotic fracture during their lifetime![17]. In the Canadian context, osteoporosis results in a 2.3 billion Canadian dollars (CAD) burden (per annum) on the health care system. These direct, and indirect costs are associated with ca. 138,600 fragility fractures, >25 % of which are vertebral compression fractures (VCFs)[17].

Percutaneous vertebroplasty (PVP) has emerged as a minimally invasive method

to rapidly stabilize VCFs. This procedure involves the injection of bone cement into the fractured vertebrae, serving to minimize fracture movement, and reinforce weakened bone[18]. While PVP has shown considerable pain relief for patients, it (as well as the cements currently used) has been criticised due to the high rate of subsequent VCFs[19]. These subsequent fractures have been reported to occur in ca. 33 % of patients within three years of PVP[20]. This high rate of VCF was initially proposed to be a consequence of the mechanical mismatch between the bone and the injected cement[21]. However, cements with enhanced mechanical properties meant to better match bone have failed to reduce the incidence of fractures when compared to traditional poly methyl methacrylate (PMMA) cements in both (i) *ex vivo* mechanical testing, and (ii) clinical trials[22, 23]. More recently, studies into the rate of vertebral body fracture, subsequent to PVP, have found links to kyphotic angle and bone compactness at the level of fracture (both measures of bone quality and osteoporotic progression)[24, 25].

As osteoporosis is a progressive disease, it has been hypothesised that the high rate of subsequent fracture is due to the high risk of fracture seen with the patient population. It is not a true complication of PVP, and can not be addressed through alterations to cement mechanical properties. Accordingly, treatment of the underlying pathology, beyond fracture fixation, is recommended to reduce the rate of subsequent VCFs[26]. One approach which may provide a mechanism to both mechanically reinforce a vertebrae and prevent subsequent fracture is the use of PVP cement capable of releasing anti-osteoporotic therapy. Due to the strontium ion's ability to act at a local level on both OCLs and OBLs, strontium would be an ideal therapeutic for release from such a material. Success in this approach however, would be dictated by the cements' ability to release strontium ions at necessary therapeutic levels, while maintaining the key characteristics necessary for use in PVP, notably injectability, radioopacity, mechanical strength and biocompatability.

A similar therapeutic inorganic ion (TII) release approach has been successfully

utilized in the dental field to reduce the occurrence of caries through the release of fluoride ions from bioactive glass reinforced composites[27]. As (non fluoride releasing) composite resin materials have also been developed for use in orthopaedic applications, such a material may offer potential for TII release in PVP. For example, Stryker's Cortoss®, an approved PVP material, has been demonstrated to release both calcium and phosphate ions from the degradation of its filler phase to allow for direct bone integration[28]. While investigation into the use of strontium containing bioactive glasses in resin composites for PVP has shown promise, it is surprising that limited studies exist which comprehensively investigate the underlying mechanism(s) of strontium ion release for such materials. Understanding of the mechanism of release in a therapeutic biomaterial is essential to ensuring that therapeutic thresholds are reached and maintained over time. With respect to strontium, the minimum release levels required for the uncoupling effect has been reported to be 88 mg/l, while an exposure duration of 15 to 22 d is required to achieve full response[6, 29, 30].

While bioactive glasses have been demonstrated to release component ions in aqueous solution, the majority of these compositions have been based off silicate glass networks[31]. Due to the high silica content, their reaction mechanisms result in the condensation of a silicate gel layer following ion leaching, resulting in decreased mass transport, and a decay in ion release over time[32, 33]. Borate based glasses, in contrast, undergo bulk dissolution in aqueous environments providing both sustained, and highly tailorable ion release kinetics[34, 35]. However, while favourable for long term ion release applications, borate glass networks are less well understood than their silicate counterparts. Due to the ability of glass modifiers to generate non bridging oxygens, or increased boron coordination, the relationship between glass compositions, the resulting glass network, and glass dissolution kinetics is not readily apparent[36].

Previous studies aiming to alter ion release from dental cements have demonstrated that hydrophylicity modifications are effective in increasing hydration based

filler degradation, however such changes negatively impact cement strength[37]. Similar deleterious effects on cement strength have been reported with uncoupled resin filler interfaces[38]. While borate networks offer potential advantages in their enhanced degradation reactions, the lack of silica content prevents the use of silane coupling commonly used to improve mechanical strength. As such, this work aims to investigate the use of such an uncoupled borate glass reinforced hydrophilic resin composite to better understand the compositions property relationship of such a material, leading to better understanding of their potential, and limitations for use as ion releasing biomaterials. To provide a focus on the mechanisms of ion release a three step experimental approach was used to investigate the ion release under physiologically relevant conditions. The first investigation looked into the glass structure and degradation kinetics (in isolation) to provide a strong understanding of the role of glass degradation in the release of ion from the composite resin's filler phase. The second experiment focused on the effects of both glass loading and resin hydrophilicity on both ion release, (as well as the cement setting reaction), and mechanical strength. The third experiment investigated the effects of mechanical loading on the ion release kinetics to provide insight into the accuracy of unloaded ion release experiments as currently reported in the literature. In addition to these three experimental works investigating ion release, a pilot animal study was conducted. This implantation study compared a hydrophilic resin phase in isolation to an ion releasing composite to gain information on local tissue response, and provide guidance for the design of further animal studies.

To provide context to the research conducted, this document will consist of four sections: a literature review, a experimental rationale, an experiment section which outlines the work completed, and finally a conclusion section with unifies the findings of the experimental work and looks towards future work. In the literature review an overview of bone physiology, osteoporosis, VCF management, and bioactive glass dissolution is covered. These topics are presented to provide context to the project

goals. An overview of bone physiology and osteoporosis are presented to provide an understanding of the unique treatment goals for osteoporotic patients suffering VCFs. An overview of VCF management techniques provide a background on the requirements for PVP materials, and previous work done in the field, as well as the challenges faced by both the technique and the materials currently in use. An overview of previous approaches utilised to incorporate drug release into PVP materials is also presented. This information provides context to the challenge associated with various techniques used to deliver strontium from injectable bone cements. Finally an overview of bioactive glass dissolution is presented to highlight the challenges faced in understanding ion release from borate glasses. In the second section of this thesis, the rationale of the study design is presented. The third section consists of the manuscripts which comprise the scholarly contributions of the work. The first, "Modulation of strontium release from a tertiary borate glass through substitution of alkali for alkali earth oxide", was published in the Journal of Non Crystalline Solids, and studies the degradation properties of a series of borate based bioactive glasses. This work was completed both to expand our knowledge of borate glasses, but also to fully characterise the release characteristics of the glass filler particles in isolation. The second paper, "The feasibility and functional performance of ternary borate-filled hydrophilic bone cements: realizing therapeutic release thresholds for strontium", published in the Journal of Functional Biomaterials, studies the effects of both resin and borate glass filler on cement properties, as well as the release kinetics of strontium in a non mechanically loaded environment. The third publication, "The effects of mechanical loading on the dissolution of inorganic fillers in composite resin cements" has been submitted for publication in Scientific Reports, and demonstrates the importance of mechanical loading when determining the release kinetics from composite resin cements. Finally the fourth publication, "Pilot implantation study of a borate glass filled hydrophilic bone cement" has been submitted for publication in

Materials Letters, and explores the use of a New Zealand White rabbit model to elucidate implantation effects from the studied material. Collectively these publications help to develop a deeper understanding of the role of glass structure, resin composition, and implantation environment on the ion release behaviour of borate glass reinforced bone cements. As the final component of this thesis, a conclusion section is presented, which unites the findings from the four experimental publications, and discusses potential directions for future work in this field.

Chapter 2

Literature review

2.1 Osteoporosis and osteopenia

The term osteoporosis refers to abnormally porous bones, which are weak and prone to fracture. Osteoporosis is defined as a BMD (of the total hip) of 2.5 standard deviations below the healthy population mean ($t < -2.5$). Osteopenia, a milder form of the disease, is often a precursor to osteoporosis, and is defined as a BMD which is 1.0 to 2.5 standard deviations below the healthy population mean ($-1.0 > t > -2.5$)[4, 39]. Irrespective of pathology, decreases in BMD are associated with changes in trabecular architecture, resulting in (i) a lower number of trabeculae of greater width, and (ii) a decrease in transverse connections between them[40]. This reduced density, and opened lattice network, results in great decreases in the load bearing capacity of bones, resulting in a high risk of fracture[4, 11, 40]. While BMD measurements are considered the defining factor of osteoporosis, the diagnostic tool of choice in Canada is the Fracture Risk Assessment tool (FRAX), which quantifies patients risk factors for osteoporotic fracture[39].

2.1.1 Epidemiology

The prevalence of osteoporosis is greater in women than men, increases with age, and varies greatly between regions and races (Figure 2.1). Osteoporosis is estimated to effect one in three Canadian women, and one in five Canada men during old age[41, 11]. This age-related form of osteoporosis is referred to as primary osteoporosis, the most prevalent form of the disease[41]. In women, this is also referred to as post-menopausal

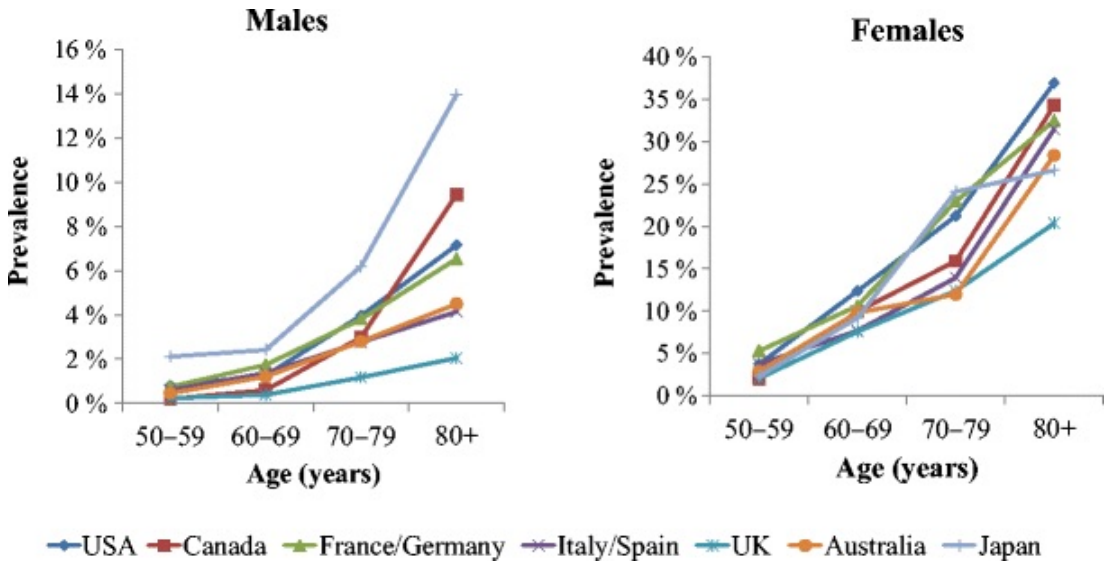

Figure 2.1: Prevalence of osteoporosis in industrialised countries by sex, and age[3].

osteoporosis, due to the temporal link with post-menopausal decreases in oestrogen levels[4]. Primary osteoporosis can also occur in men but shows a later onset, usually following a drop in testosterone, and typically presents in octogenarians[11, 3]. Secondary osteoporosis, on the other hand, is not associated with age related changes, but is a side effect of medication (most commonly glucocorticoids) or other disease states (diabetes, AIDS, hypertension , etc.)[4].

The large regional and racial variations in the prevalence of osteoporosis are associated with strong genetic links to peak BMD. An epidemiological study of the relative risk of osteoporosis between racial groups in the United States (a racially diverse population base) found a risk ratio of (i) 0.55 for women of African descent, (ii) 0.95 for women of Native American descent, (iii) 1.05 for women of Asian descent, and (iv) 1.2 for women of Hispanic descent relative to the Caucasian population[42]. Given its high prevalence, osteoporosis places a large burden on health care systems, primarily due to the increased incidence of fracture. For example, in Canada 138,600 osteoporotic fractures were reported in 2010. These fractures most commonly occurred in the vertebrae (27 %), distal ulna (22 %) and proximal femur (15 %)[4]. The direct costs associated with the treatment of these fractures was estimated to

be 2.3bn CAD. When long term treatment (i.e. indirect costs) is included, the costs on the Canadian health care system rise to 3.9bn CAD[17]. While the condition is preventable, few early symptoms are recognized due to the pathophysiology of the disease, leading the condition to be both underdiagnosed, and undertreated[16].

2.1.2 Pathophysiology of osteoporosis

Osteoporosis presents with varying pathophysiology, arising from the cumulative effects of the patients' age, genetics and other environmental factors. To better understand these changes, healthy bone development and remodelling must first be understood.

Physiology of healthy bone

Bone tissues are made up of a combination of spongy trabecular bone which is surrounded by a shell of compact cortical bone. The combination of mineral and organic fibrous matrix found in bone gives it both mechanical strength as well as resistance to cyclic loading. To maintain fatigue resistance bone tissues undergo a cycle of constant remodelling, the combined effect of three cell lines: OCLs, OBLs and osteocytes. This remodelling cycle is both continuous, and guided by mechanosensory feedback, allowing for bones to adapt to local loading levels[43, 44, 45]. Along with mechanical loading a number of hormonal signals serve to regulate bone remodelling and strength throughout our lifetime.

Rigidity and compressive strength are imparted by the mineral matrix, which is composed of tightly packed crystalline HA, that imparts roughly 66 % of the bones dry weight[46]. The fibrous collagen matrix in turn imparts toughness, supporting tensile loads, and provides nucleation sites for the crystallization of the mineral matrix[46]. The mechanical endurance of bone is greatly increased through its dynamic metabolism, which allows for the resorption of damaged tissue and deposition of new bone mass[45].

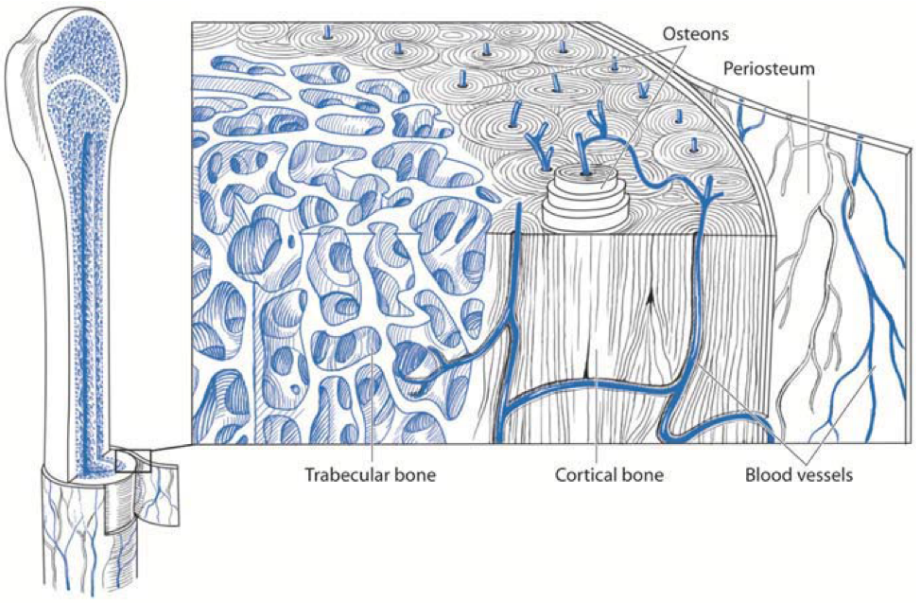

Figure 2.2: Cortical and Trabecular bone structure[4].

Histology of bone

While cortical bone is a compact network of Haversian systems (also referred to as osteons), trabecular bone is formed by an open network of trabeculae (Figure 2.2)[46, 44]. Haversian systems are ordered structures, which radiate from central Haversian canals. These canals are hollow passages, which allow for blood and lymph vessels to pass through cortical bone. The matrix of the osteon is deposited around the canals, in concentric lamella radiating outward, and is maintained by the osteocytes. In contrast trabeculae are thin struts, primarily aligned in the direction of the principle stresses in bone, and do not have a highly ordered concentric structures, or designated blood flow[43]. The blood flow needed to support metabolism in trabecular bone is instead supplied from the rich vascular network of the bone marrow which fills the voids between trabeculae[46, 44]. During youth, this bone marrow is hematopoietic, gradually transitioning to fatty marrow with age as the demand for new blood cells decreases[46].

Bone remodelling

As mentioned, bone metabolism in both healthy and pathological states consists of the combined action of three cell types: OCLs, OBLs, and osteocytes. These three cell types act in coordinated, membrane separated areas, referred to as bone remodelling compartments[47]. These compartments provide an isolated environment facilitating intracellular signalling and feedback (Figure 2.3). OCLs are multinuclear hematopoietically derived cells which are formed by the fusion of multiple macrophage like cells[43, 48]. The differentiation of OCLs is mediated by signalling from colony stimulating factor and the binding of the receptor activator of nuclear factor k ligand (RANKL), and immunoreceptor tyrosine based activation motif (ITAM) [49]. OCLs primarily serve to resorb both the mineral and protein matrix of bone. Although resorption occurs at low levels throughout the bone, micro-damage to the tissue activates signalling pathways which recruit OCLs to the site of damage through the activation of inflammatory pathways responsible for the production of RANKL[50]. Fully differentiated OCLs produce osteoprotegrin (OPG) a decoy RANKL receptor which serves to provide negative feedback to further resorption[48]. Bone mineral resorption results in the release of calcium into the bone remodelling unit space which serves as further negative feedback to both the differentiation and survival of OCLs.

This increase in extracellular calcium concentration also serves to recruit OBLs to the area of resorption. OBLs are secretory cells which act to replace lost fibrous and mineral matrix from resorption sites[46, 43]. OBLs are differentiated from mesenchymal cell lines through the signalling of the calcium sensing receptor (CaSR), wingless related protein (Wnt) and Notch pathways[51]. Fully differentiated OBLs secrete RANKL, and as such, serve to increase the differentiation and activity of OCLs[49, 52]. Along with increased calcium concentrations, areas of high mechanical loading also serve to recruit OBLs to increase the local strength of bone though osteocyte mediated pathways[50]. OBLs deposit the new bone matrix, both organic

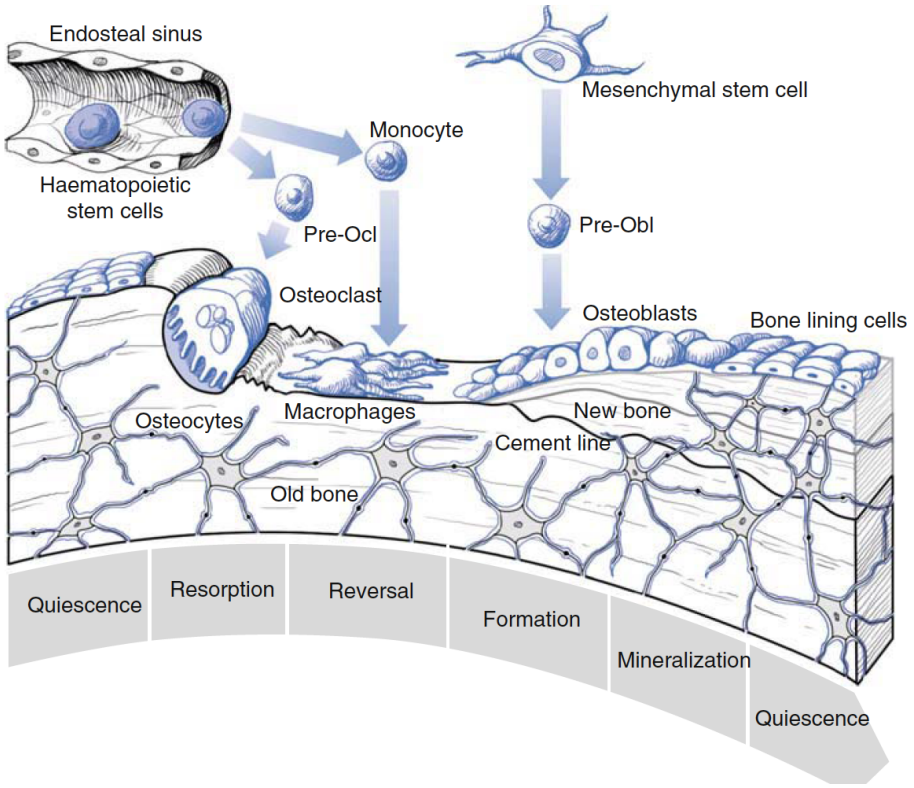

Figure 2.3: Steps of bone remodelling process, (left to right): quiescence, resorption, reversal, formation, mineralization, and return to quiesence[4].

and mineral components, around themselves which gradually eliminates their blood supply. As the blood supply drops, 80 % of the OBLs undergo apoptosis, while the remaining cells differentiate into osteocytes[46].

When the activity of OBLs and OCLs is balanced, no net change in BMD or mass occurs, and gradual bone turnover allows for high endurance in cyclic loading[46, 45]. Osteocytes are important regulators of bone metabolism, acting not only as mechano-transducers to adapt bone to mechanical loading, but also serving to recruit remodelling units to areas of micro damage[46]. Osteocytes alter bone metabolism through the production of a number of growth factors including fibroblast growth factor (FGF) and bone morphogenic protein (BMP)(essential in OBL differentiation), sclerostin (provides negative feedback to OBLs), as well as RANKL (essential in OCL differentiation)[50]. Along with direct OBL-OCL feedback provided by the RANKL pathway, local calcium cycling caused by formation and dissolution of mineral matrix serves to balance the effect of OBLs and OCLs[53].

While a number of cell level signalling pathways serve to regulate local bone turnover, a number of systemic and environmental factors have been recognised to alter bone metabolism on a skeletal level. In healthy individuals, BMD increases through youth and peaks in the early thirties, followed by a gradual decrease through middle age[46]. Increased height, weight or level of activity all serve to increase bone deposition through osteocyte mediated pathways[46]. In addition, increased dietary calcium and vitamin D (including exposure to sunlight) serves to increase bone deposition through the alteration of systemic calcium levels. On the other hand, PTH increases resorption of bone by increasing OCL activity, to raise circulating calcium[11, 4, 54]. Increases in bone resorption are also favoured by: ageing, decreasing androgen levels (especially following menopause), glucocorticoid use, immune compromisation, diabetes and cardiovascular diseases[4, 54, 11]. Although decreases in BMD are considered a natural part of ageing, severe decreases in BMD can result in osteopenia, or osteoporosis, and a high risk of fracture[4, 11].

Pathophysiology of osteoporosis

Early theories speculated that the loss of oestrogen induced OBL bone deposition was a direct causative factor for primary osteoporosis[55]. More recently however, it has been recognized as the cumulative effect of multiple genetic and environmental factors. As proposed by Raisz, in a review of the pathophysiology of osteoporosis, the reduced BMD which characterizes the disease may be caused by one, or more, of three causative pathways: (i) a low peak bone mass during youth, (ii) an excessive rate of bone resorption, or (iii) insufficient new bone deposition to match a healthy resorption rate[56]. With respect to the first pathway, large scale genetic surveys have demonstrated strong variability in peak BMD, with a heritability factor of 0.46 to 0.84[57]. These findings have been supported by the discovery of single nucleotide polymorphisms for both the CaSR as well as the Wnt pathway. These genetic variations play an important role in the low peak BMD in Asian and Hispanic populations respectively, leaving them at high risk of both primary and secondary osteoporosis[58, 59]. Considering the second pathway, post-menopausal osteoporosis has been linked with an increase in RANKL signalling, which induces pathologically increased OCL activity and bone resorption [49, 60]. Secondary to this OCL activation, increased OBL activity is also induced by changes in oxidative state, but not to an extent capable of matching the resorption rate. The resulting imbalance is especially deleterious to trabecular bone, where unchecked resorption pits perforate trabecular struts, altering load distributions and preventing their replacement[56]. Finally, the third pathway is associated with rare genetic disorders, and low levels of calcium and vitamin D[59, 61].

While all three pathways contribute to low BMD, the progressive loss of bone mass with advanced age is strongly associated with excessive OCL activation (i.e. the second pathway). Animal models have demonstrated that while post-menopausal oestrogen deficiency is associated with increased bone resorption, it is not due to its

role as a sex hormone. Rather, the loss of oestrogen following menopause results in increased oxidative stress, activating inflammatory pathways, thereby increasing Tissue Necrosis Factor A (TNF-a)production, and ultimately leading to the up regulation of RANKL and OCL differentiation[62]. Age related oxidative stress can thus explain the decrease in BMD in both male and female populations, with increased impact on post-menopausal women due to the high reliance on oestrogen as an antioxidant[63]. A number of diseases linked to secondary osteoporosis similarly result in increased bone resorption due to increased oxidative stress and inflammation, including arthritis, diabetes, cardiovascular disease, obesity and autoimmune disorders[64, 65, 66].

While some causes of secondary osteoporosis can be linked to inflammation or oxidative stress, its pathophysiology varies greatly with comorbidities and medications. For example, renal disease and hyperthyroidism have deleterious effects on bone strength, due to their effect on circulating PTH and calcium levels[67]. These effects are mediated through the CaSR on both OBLs, to decrease new bone formation, and OCLs to induce increased bone resorption[68]. On the other hand, glucocorticoids which are used to reduce inflammation (and would thus be expected to increase BMD), have been demonstrated to decrease Wnt signalling and reduce circulating OPG. The net result of glucocorticoids on bone remodelling is a combination of both strong anti-anabolic and catabolic effects[69, 70]. The dual negative effects on BMD from glucocorticoid use is an important example of the overlap between multiple regulating pathways which underlay the pathogenesis of osteoporosis, making it a challenging condition to target and treat effectively[56].

Preventative osteoporotic interventions

The first line of treatment for osteoporosis is dietary supplementation with calcium and vitamin D, which both act to support and maintain BMD [4, 39]. Along with these supplements, various pharmaceutical therapies are available to slow the loss of bone mass[71]. These therapies are traditionally classified as either antiresorptive,

or anabolic therapies depending on their mechanism of action[4]. Due to the highly coupled nature of OBL and OCL cells however, these therapies serve to effect both cell lines through coupled increases, or decreases in their metabolic activity[4, 54]. While various therapeutic options are available, the low rate of treatment, as well as low compliance with pharmaceutical therapies, has resulted in a crisis of care in osteoporosis[16]. Multiple compounding factors contribute to these low levels of effective treatment, including; (i) a lack of recognition of the disease[72], (ii) a failure to see the condition as a true pathology and not a sign of advancing age[73], and (iii) mistrust of pharmaceutical options due to a number of high profile adverse reactions in the media[74].

Antiresoprtive therapies

Antiresorptive (or anti catabolic) therapies target OCLs, and decrease the rate of bone resorption. However, these therapies also generate a coupled decrease in OBL activity and new bone formation[4, 71]. Although these therapies are effective in generating a net decrease in bone resorption, they also decrease mirco-damage repair, and thus allow for the accumulation of damage to the tissue[48]. For example, bisphosphonates are the most commonly used form of antiresorptive therapy for the treatment of osteoporosis in post-menopausal women[39]. Bisphosphonates are synthetic analogues to pyrophosphate, allowing the drug to be incorporated into the mineral matrix of bone. The drug is subsequently released during resorption, and is taken up by OCLs causing an alteration in adenosine triphosphate (ATP) synthesis and decreases in cellular activity[75]. Alternative formulations induce cytoskeletal changes that prevent attachment to bone and result in apoptosis[76]. Long term studies into the efficacy of various bisphosphonate formulations demonstrate significant reductions in VCF risks (up to a RR=0.41 for Risondronate) after 5 years of use[12]. However, extended periods of bisphosphonate use ($\geq$ 6 years) have been linked to decreased fracture reduction efficacy and increased risk of osteonecrosis[12].

In respect of the latter, this is primarily seen in bones which receive low mechanical loads, such as the jaw[48]. Osteonecrosis is often linked to a failure to undergo normal tissue remodelling following trauma (often minor dental surgery) due to the potent inhibition of bone metabolism. As such bisphosphonates have also been linked with increased time to union following fractures[77]. For these reasons, while bisphosphonate treatment remains the first line pharmaceutical intervention for osteoporosis in Canada, they are not recommended for long term continuous use[39].

In addition to bisphosphonates, anti RANKL antibodies have emerged as an antiresorptive therapy for the treatment of osteoporosis[78]. These agents act to prevent RANKL mediated differentiation of OCLs. Denosumab^{TM}, an anti RANKL antibody, has demonstrated equivalence, and in some cases superiority, when compared to bisphosphonates for the maintenance of BMD in post-menopausal osteoporotic women[79]. In addition, this therapy has demonstrated efficacy in reducing VCF rate by up to 68 %. However, long term data relating to safety and efficacy is not yet available and there are concerns that (i) long term effects may be similar to bisphosphonates, and (ii) there may be the potential for unwanted immunological response rendering the treatment ineffective over time[80].

Anabolic therapies

In contrast to antiresorptive therapies, anabolic therapies target OBLs to increase new bone deposition. Although they serve to increase BMD, they are unable to slow bone resorption and result in an altered trabecular architecture[4]. The most promising anabolic osteoporosis therapy is recombinant PTH, which has demonstrated up to a 9 % increase in BMD following one year of administration[81]. The increased rate of OCL activity, which is caused by these therapies, can result in a decrease in the overall number of trabecular struts, and the formation of large plate like trabeculae which are prone to buckling failure. These architectural changes result in bone strengths that are disproportionately low relative to the measured BMD [40].

While effective, recombinant PTH therapy is associated with high costs, and a low half life, requiring daily subcutaneous injections[15]. These features exacerbate issues of patient non-compliance frequently seen in the treatment of osteoporosis[4].

Strontium ion therapy

Where conventional osteoporosis treatments have traditionally shown coupled increases or decreases in bone metabolism, strontium based therapies have emerged as uncoupling agents with the advantages of both (antiresorptive and anabolic) systems [4, 54]. Strontium ions, administered orally as strontium ranelate (2000 mg/d) have been shown to be effective in both increasing OBL activity while simultaneously decreasing OCL activity[10]. Phase II clinical trials focusing on post-menopausal women have shown a net increase (2.97 %) in BMD, while maintaining healthy trabecular architecture[82]. Increases in BMD, after stable strontium ion exposure, have been recognised since the 1910s but were initially attributed to the larger atomic mass of strontium being substituted into the bone matrix in place of calcium[83, 84]. It has more recently been recognised that strontium is bioactive beyond its ability to incorporate into the mineral matrix of bone, having marked effects on OBLs, OCLs, and endocrine glands which serve to regulate BMD [29, 13, 82, 85, 86].

Mechanism of action of strontium ion therapies

The response of bone tissue to strontium ions has been shown to comprise both a rapid and a slow response, indicating the involvement of multiple signalling pathways [85, 86]. The first receptor shown to be targeted by strontium ions was the CaSR (Figure 2.4), and further investigations have revealed that the FGF receptor is also a target for the drug[54, 87]. Strontium ions, as divalent cations, are capable of activating the CaSR as type 2 agonists, in effect increasing the sensitivity of the receptor to calcium ions in the environment[87, 9]. This action can be seen in the parathyroid

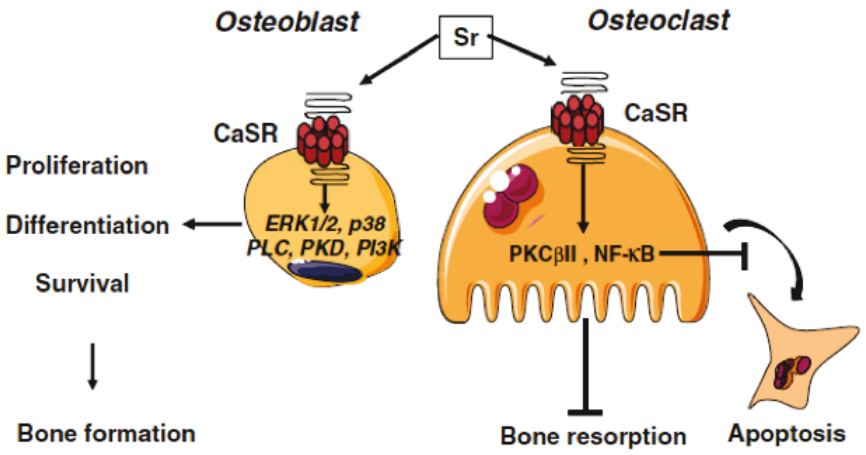

Figure 2.4: CaSR pathways initiated by strontium ion binding in OBL and OCLs.

tissue as well as directly in OBLs and OCLs imparting both local and systemic effects upon strontium exposure[87]. The CaSR is essential in the remodelling theory of bone (OCL resorption of the mineral matrix serves to liberate calcium into the local environment, increasing OBL recruitment, while providing negative feedback on OCLs activity), and as such its activation is the key to strontiums ability to decouple bone turn over[85]. On a systemic level, CaSR activation in the parathyroid results in a decrease in PTH production, resulting in increased renal excretion of calcium, and up regulation of OBL activity to decrease plasma calcium levels[85]. Local effects of strontium ions on OBLs and OCLs are mediated through multiple G coupled protein related signalling pathways including: (i) extracellular signal-regulated kinase 2 (ERK1/2),(ii) Wnt pathways, (iii) protein kinase C II and (iv) the nuclear factor k B/RANKL pathways[88]. These pathways culminate in the up regulation of the production of collagen and alkaline phosphatase (ALP) in OBLs[9]. Conversely, in OCLs, the ultimate effect of strontium signalling through the CaSR is an alteration of actin dependent attachment to the extracellular matrix. This results in a reduction of the efficacy of resorption enzymes and an increased rate of apoptosis[30].

Therapeutic threshold of strontium ions

Strontium has been shown to be effective in altering OBL and OCL activity, and its effective dose is known to be dependant on calcium concentrations *in vitro*[9]. Reginster et al. reported the ED_{50} for OBLs *in vitro* to be (i) 5.4 mM when administered alone, or (ii) 0.4 mM when co-administered with 2.0 mM calcium[82]. This dependence on calcium concentration is due to the action of strontium as a type 2 agonist,[87, 9]. Other *in vitro* trials have found increased OBL activity to occur at concentrations as low as 0.1 mM, indicating that low doses may be sufficient to mediate beneficial effects[6]. The apoptotic OCL CaSR response however, shows a much greater threshold, with and LD_{50} of 20-30 mM *in vitro*[30, 85]. Conversely, OCL differentiation is inhibited at levels as low as 1.0 mM in macrophage differentiation cultures[6]. This OCL inhibition concentration serves as the threshold to the uncoupling effect of strontium, with doses between 0.1 and 1 mM acting only as anabolic agents through local pathways[85, 88]. While little evidence of (stable) strontium related toxicity in healthy humans has been reported, strontium contamination of haemodialysis fluids (>100 mg/l) has been linked to serum strontium concentrations of 235 mg/l resulting in osteomalacia[89]. These findings indicate that control of the therapeutic dose of strontium exposure is essential in the utilization of strontium as an anti-osteoporotic agent.

Clinical efficacy of strontium ion therapy

In vitro data on strontium ion therapy has translated well with respect to clinical efficacy. Strontium ranelate, sold under the trade name Protelos (Servier Laboratories), is amongst the most studied strontium carrier salts for oral dosing[90]. While early studies demonstrated effective increases in BMD, the radiographic measurement methods traditionally used, could not distinguish between calcium and strontium inclusion in the bone matrix, and as such overestimated clinical efficacy. Subsequent

trials combined both radiographic BMD analysis with biopsy ashing, to develop correction curves capable of providing more accurate measurements, without the need for continuous bone biopsies. Summary data pertaining to clinical trials of strontium ranelate efficacy are presented in (Table 2.1). Reginster et al. conducted a clinical trial in which strontium ranelate was orally administered at doses of 0, 125, 500 and 1000 mg/d along with calcium supplementation (500 mg/d) to post-menopausal women over 24 months[82]. Patients receiving the highest dosage exhibited a net increase in BMD of 5.53 % (once corrected for strontium content using a correction factor of 10 % BMD / mol% Sr), while control groups exhibited decreases in BMD of up to 0.98 %. Subsequent research by Reginster et al. found a 44 % decrease in VCF risk for patients who received strontium ranelate at 2000 mg/d[10].

With specific respect to spinal osteoporosis, the Spinal Osteoporosis Therapeutic Intervention (SOTI) trial, conducted by Roux et al. found that strontium ranelate resulted in preferential improvements in the bone quality of vertebral bodies for post-menopausal women[91]. This study further reported a 15.8 % increase in (corrected) BMD in the lumbar vertebrae compared to a 7.1 % increase in femoral neck density, indicating its highly effective nature in targeting osteoporosis in the spinal column. This increase in vertebral BMD resulted in a 49 % decrease in the risk of new VCFs. As strontium ions are known to have localized effects on cell metabolism, with preferential benefit to vertebral BMD, these finding suggest that strontium ion delivery into a vertebral body could serve as a mechanism to directly improve local bone quality.

Clinical burden of osteoporotic fracture

Traumatic skeletal fractures occur at loading levels not typically seen in every day activities and are frequently the result of a major fall, sporting injury or motor vehicle accident[94]. Conversely, fragility fractures occur at every day loading conditions and are due to a weakened bone state, most commonly caused by osteoporosis[75]. As osteoporosis or osteopenia affects over 70 % of women in old age, there are over 9

Table 2.1: Clinical trials investigating the efficacy of strontium ranelate for the treatment of osteoporosis in post-menopausal women.

Trial	**Trial Info**	**Dosing**	**Findings**	**Ref**
Early Dosing Ranging Study	Placebo Controlled Multi Center Double Blind Dose Ranging Early Postmenopausal 2 year	0.125, 500, 1g/d	BMD increase Lumbar spine: 1.41 % at 1g/d Total hip: 3.2 % at 1g/d	[82]
TROPOS (Treatment of peripheral osteoporosis study)	Placebo Controlled Multi Center Double Blind Post-menopausal 3 years	2g/d	49 % reduction in VCF BMD increase: Lumbar spine: 14.4 % Femoral neck: 8.3 %	[7, 92]
STRATOS (Sr ranelate for treatment of osteoporosis)	Placebo Controlled Multi Center, Double Blind Dose Ranging Post-menopausal 2 year	0.5, 1.0, 2 g/d	BMD increase Lumbar spine: 1.4 % at 0.5 g/d 3.0 % at 2g/d	[93]
SOTI (Spinal Osteoporosis Therapeutic Intervention)	Placebo Controlled Multi Center Double Blind Early Post-menopausal 4 year	2g/d	35 % reduction in VCF risk BMD increase: Lumbar Spine: 15.8 % Femoral Neck: 7.1 % increase	[91]

million osteoporotic fractures reported globally every year[11]. The disease increases the risk of fracture at all skeletal sites, and has a disproportionate effect on the rate of fracture of the spine, distal radius, hip and humerus, which are referred to as major osteoporotic fractures[95]. The prevalence and rate of major osteoporotic fractures follows that of osteoporosis. As such, major osteoporotic fractures represent 75 % of clinical fractures experienced by women aged 75-85[95]. These fracture sites are put at a disproportionate risk from osteoporotic bone loss due to their high fraction of trabecular bone, which is more severely affected by osteoporosis due to alterations in trabecular architecture[40]. Beyond the initial pain and treatment costs, osteoporotic fractures have significant deleterious effects on quality of life and mortality. The Canadian Multicenter Osteoporosis Study(CAMOS) found the relative risk ratio for death to be 4.19 for participants that experienced a hip fracture during the study. Similarly, patients that experienced VCFs during the study had relative risks of death of up to 2.53 when compared to patients without fractures[96].

Although decreases in BMD are a defining feature of osteoporosis, the disease is often unrecognised, or untreated until the occurrence of an osteoporotic fracture[16]. It has been estimated that only 30 % of osteoporotic patients are correctly diagnosed, and less than 15 % of those patients will receive preventative therapies[4]. Because of the difficulties in identifying osteoporosis the WHO has suggested that screening resources for otherwise healthy women be targeted towards patients who have suffered a fragility fracture[4, 40]. While the utilization of FRAX and other non diagnostic risk assessment tools is improving the ability to identify and treat women at risk, poor patient compliance remains a challenge. In respect of the latter, a study of patient behaviour following diagnosis reported that only 55 % of women continued to regularly take anti osteoporotic therapy past one year, and only 40 % of patients achieved compliance rates necessary to achieve a clinical reduction in fracture risk after three years[14]. This overall challenge of low diagnosis, treatment, and compliance rate is referred to as a “crisis of care”, leaving patients at high risk of osteoporotic

fracture[16]. This challenge is further complicated in the prevention of VCF, where an initial fracture is associated with a sharp increase in fracture risk, due to alterations in mechanical loading of the spine[11, 40].

Vertebral compression fractures

The high incidence of osteoporotic VCFs is caused by a combination of disproportionate bone loss in the spine, as well as deteriorating biomechanics associated with ageing[24, 25]. The CAMOS study , estimates that 1 in 4 Canadians over the age of 50 show vertebral deformities related to VCFs[97]. VCFs result in decreased vertebral height, thoracic volume (and thus functional lung capacity), balance and mobility as well as increased kyphosis and pain at the level of fracture[98]. Altered biomechanics result in a significant increase in fracture risk after an initial VCF, both in the vertebral column as well as at all other skeletal sites (e.g. hip fractures). Less than 50 % of patients who suffer an osteoporotic VCF have received preventative therapies; usually due to a lack of early diagnosis, as well as a lack of patient compliance[16]. While nearly half of all osteoporotic VCFs are asymptomatic, being discovered during unrelated medical examinations, symptomatic fractures cause pain, loss of function and decreased quality of life requiring immediate treatment[99].

Aetiology of vertebral compression fractures

Vertebral compression fractures most commonly occur in the lower thoracic or upper lumbar levels due to the changes in loading mechanics in the transition from lordotic to kyphotic curvature; leaving the vertebral bone more susceptible to changes in load distribution (Figure 2.5)[94]. These fractures most commonly occur in an anterior wedge shape, as the neural arch provides increased support to the posterior section of the vertebral body, and postural stresses such as lifting and carrying frequently shift the centre of mass forward[100]. While decreased BMD plays an important role in the aetiology of VCFs, a number of additional factors contribute to

their high rate of incidence in ageing populations. Age related changes to the load distribution through the intervertebral disks, spinal instability due to decreased activation of postural muscles, and increased spinal kyphosis resulting from postural changes all contribute to the complex aetiology of VCFs[98, 100]. As such osteoporosis screening alone to assess fracture risk is poorly effective in reducing the rate of VCFs. This is demonstrated by the need to screen 1300 patients over 5 years to effectively prevent one VCF[101]. Effective prevention and treatment should serve to address all factors which contribute to VCFs in order to best serve patient needs.

With respect to age related degeneration of intervertebral disks, it has been established that there is a progressive decreases in the hydrostatic pressure of the nucleus pulposus, resulting in non-uniform stress distribution to the vertebral endplate. In particular, a ring of high stress is generated along the edges of an effected vertebral body causing endplate deflection, and ultimately altering the load distribution to the underlying trabecular network[98]. Injury to the superior intervertebral disk is reported to be present in 39 % of fractured vertebral bodies, demonstrating a correlation between intervertebral disk degeneration and VCFs[102]. While no definitive mechanism has been established to identify the initial incident which causes degeneration, damage to vertebral endplates and intervertebral disks provides positive feedback accelerating the deterioration of hard and soft tissues[103]. As such, the risk of a VCF is not based solely on bone strength, and may be prevented though both osteoporotic treatment and biomechanical interventions which improve load distribution in the spine.

An initial VCF also increases the risk of a subsequent fracture 4-7 fold over the general population[11, 100]. This is referred to as the vertebral fracture cascade, and has many contributing factors. The anteriorly wedged shape commonly seen in VCFs leads to an increased kyphotic angle, which increases the lever arm of the upper body weight acting on the surrounding vertebrae, thereby greatly increasing effective loading[100]. Furthermore, local inflammation and pain lead to decreased

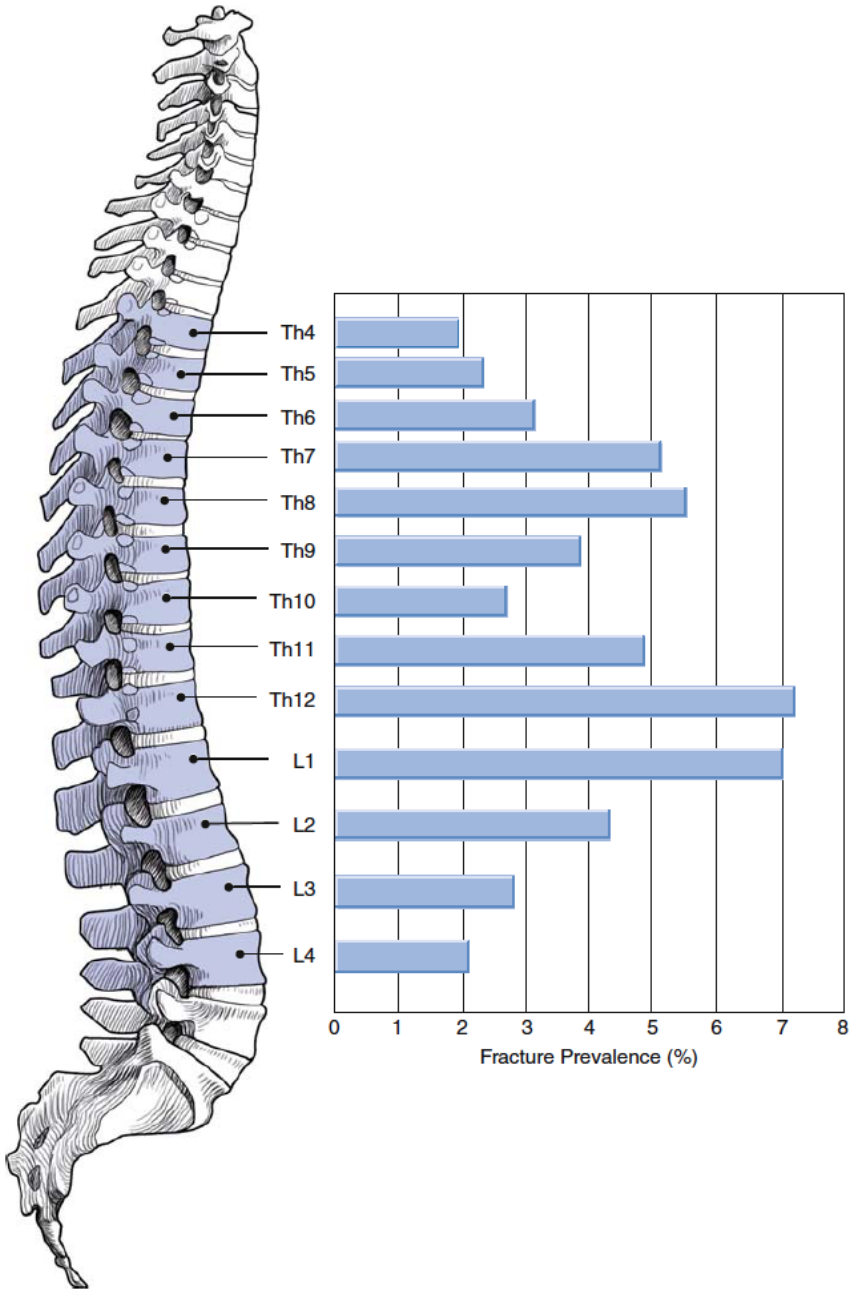

Figure 2.5: Prevalence of fracture locations in the thoracic and lumbar spine demonstrating increased succeptability to fracture in the thoracolumbar junction.

muscle tone and increased trunk sway, further destabilizing the load distribution in the spine and increasing fall risk[104]. As such, early intervention to decrease pain and return mobility and quality of life play an important role in reducing the vertebral fracture cascade. In the case of osteoporotic VCFs the underlying bone deterioration, which lead to the first VCF, is also a contributing factor to the increased incidence of subsequent fracture[40, 100].

Vertebral fracture management

Vertebral compression fracture management presently focuses on pain management and may include: analgesic therapy, bed rest, bracing, rehabilitative exercises or surgical intervention[104, 105, 18]. Bed rest, bracing and rehabilitative therapy all focus on reducing fracture motion, promoting proper alignment of the spine and preventing trunk sway to promote proper fracture healing and decrease discomfort[105]. There is great variation in the clinical guidelines for optimal VCF management, due, in part, to a lack of clinical evidence to support various conservative management techniques[106]. For example, bed rest remains a recommendation of both the American Academy of Orthopedic Surgeons, and the National Institute for Health [107]. On the other hand, there exists evidence of increased bone resorption due to inactivity, as well as an increased risk of deep vein thrombosis, and it is therefore discouraged the American Association of Family Physicians[106, 99]. A study comparing the efficacy of the use of analgesics, bed rest, back bracing, and walking aids for the management of VCFs was demonstrated to achieve an average reduction in visual analogue scale (VAS) pain score from 7.2 to 2.2 over three months, with a further decline in pain to 1.4, after one year. While a significant pain reduction was achieved and maintained for the majority of study participants, one in three patients failed to achieve a reduction in pain with conservative treatment and required further intervention[99]. For these patients, percutaneous vertebral augmentation in the form of PVP and balloon kyphoplasty (BKP) offer options to rapidly restore vertebral strength and relieve

pain[18]. While clinical guidelines vary greatly on recommendations for the treatment of VCFs, recommendations for the prevention of new fractures are consistent and encourage the use of anti-osteoporotic therapy as the most effective method of reducing new fracture occurrence, a goal not met by current vertebral body augmentation techniques or materials[26].

2.2 Percutaneous spinal augmentation

Percutaneous vertebroplasty (Figure 2.6) is a minimally invasive procedure that allows for the injection of bone cement into a vertebral body under fluoroscopic guidance. This procedure was first performed in 1984 to treat a painful spinal hemangioma, and has since been used for the fixation of VCFs[108]. Rapid pain relief was noted in its first application, a finding which has been substantiated by subsequent clinical trials which compare the procedure to traditional fracture management techniques[20, 109]. While PVP was first performed in France, the first procedures to take place in the United States were performed in 1993. Due to its early success, the technique rapidly gained popularity, and by 2010 over 300,000 procedures had been performed [110]. This procedure reduces both hospital stay times and infection risk versus invasive fracture fixation techniques, while also reducing the need for anaesthesia, as it may be performed under conscious sedation[18, 108]. Cement injections are performed through large bore needles (11- 15 gauge) which are inserted into the vertebral body through the pedicle[82]. Injected cement volumes typically range from 2.5 to 4.5 ml, with the cement being allowed to cure while the patient remains prone on the procedure table.[18, 111].

Balloon kyphoplasty (Figure 2.7) is a similar percutaneous vertebral augmentation technique which allows for the partial correction of kyphotic deformity. This procedure includes the transpedicular insertion of a high pressure inflatable bone tamp

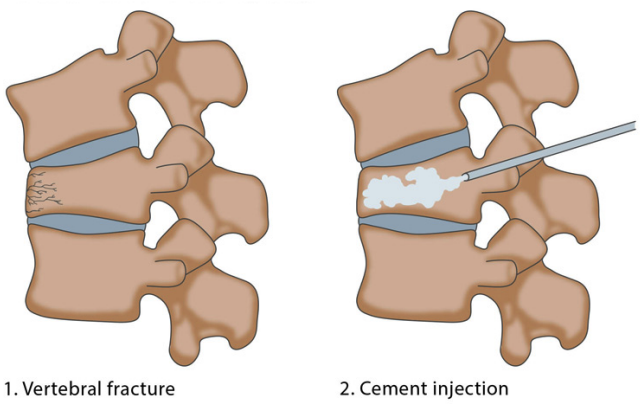

Figure 2.6: Illustration demonstrating the augmentation of a VCF though the use of PVP, indicating the insertion of a large bore needle into the fractured vertebral body under fluoroscopic guidance, and full fill of vertebral body providing internal cast[5].

into the fractured vertebral body. Once in place, the bone tamp is inflated, compacting surrounding trabecular bone and partially restoring vertebral body height[112]. The resultant bone void is then filed with a more viscous injectable bone cement, stabilizing the vertebrae in this expanded position. BKP allows for both fracture stabilization, and decreased kyphosis, however, it requires additional procedure time (approximately 1.5 h), the use of general anaesthesia, and an added equipment cost of 3,578 CAD per patient (above the 187 CAD equipment cost of PVP)[113].

2.2.1 Pain relief efficacy of vertebral augmentation

A number of clinical trials have investigated the efficacy of PVP and BKP, most commonly assessing pain relief, as well as the rate of subsequent fracture. These clinical data are summarised in Table 2.2 to 2.4. When compared to conservative treatment techniques, vertebral augmentation was reported to provide significant improvement in patient pain relief in initial open label trials[114, 115]. In one of the largest studies of its kind, the Vertos II trial compared PVP to conservative fracture management. It was reported that PVP resulted in a reduction in VAS pain scores of

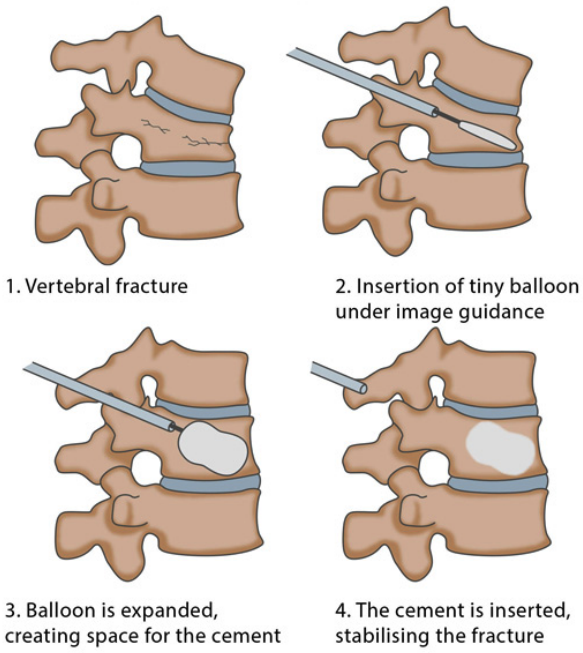

Figure 2.7: Illustration of the steps of PVP on 1) a fractured vertebrae, including 2) the insertion of a large bore needle into the fractured vertebral body under fluoroscopic guidance, and insertion of collapsed bone tamp into the vertebral body 3) the inflation of the bone tamp generating a void for cement fill while pushing endplates apart restoring vertebral body height,4) injection of bone cement into the bone void providing an internal cast[5].

5.2 and 5.7 points after 1 and 12 months respectively while, conservative treatments reduced VAS scores by 2.7 and 3.7 points at equivalent follow up[114]. In a similar open prospective trial, in which fracture age of up to 12 months was included (in contrast with the VERTOS 6 week cut off), a 42 % reduction in pain was seen with the PVP group compared to a 25 % reduction in pain for the control group after 2 months. No significant differences were observed vis-à-vis long term benefits past 12 months[115]. With respect to quality of life (as assessed by the Qualeffo questionnaire), immediate improvement was reported for the PVP cohort, while conservative treatment demonstrated improvements only after six months. Similar results were found in a trial including patients with an average of 3 pre-existing VCFs, where improved pain relief compared to conservative treatment was reported, but only for time points of up to 6 months[116]. While open label trials have consistently demonstrated increased efficacy compared to conservative treatment, placebo controlled trials have shown greater variation in outcomes, leading to significant criticism of the technique.

In double blinded studies, control groups were subjected to a sham procedure meant to mimic PVP[122, 123, 124]. These control patients were sedated, placed prone on the procedure table, injected with a local anaesthetic at the level of fracture, soft tissue incisions were made, surface pressure was applied to the spine, as well as tapping noises and the mixing of bone cement. These actions were all intended to mimic the experience of PVP for the patient. In these trials, most notably those by Kallames et al. (INVEST), and Buchbinder et al., no significant differences were reported in pain relief over an extended time period, and as such a decrease in the popularity of PVP occurred[117, 119]. These trials however have subsequently been critiqued due to weak inclusion criteria, allowing for the inclusion of patients not generally thought to be suited for PVP[122]. The inclusion criteria did not discriminate based on fracture age, which is recognised as an important indicator of success. In particular fractures under four months old are considered ideal candidates for PVP, while patients with chronic fractures report low success rates for pain

Table 2.2: Clinical trials evaluating the efficacy of PVP and BKP for the treatment of painful VCFs (part 1 of 3)

Trial	Trial Type	Inclusion Criteria	Cohorts	Primary Outcomes	New Fracture Rate
VERTOSS II[114]	Open Label Multicenter	>50 y/o Fracture <6w VAS>5	PVP + Vit D Bisphos. Cal.	Vas Decrease 5.2 pts. at 2 mo 5.7 pts. at 12 mo	16.4 % (15/91)
			Conservative Vit D Bisphos Cal	VAS Decrease 2.7 pts. at 2 mo 3.7 pts. at 12 mo	24.7 %(21/84)
			Findings	Sig.	Non Sig.
Effect of VP on Pain relief, QoL, and incidence of new VCF...[115]	Prospective Controlled Single Center	Fracture <12 mo VAS >4 MRI edema	PVP	Qualeffo Improv. Sig all time pts. VAS Decrease 3.0 at 2 mo	26.5 % (17/64)
			Conservative (analgesics, calcitonin)	Qualeffo Improv. Sig at t >6 mo VAS Decrease 1.6 at 2 mo	13.1 % (8/61)
			Findings	Sig. at t<6, & t<2	Sig.
Randomized Control Trial of PVP vs Opt. Med Man for the Relief of Pain and Disability in Acute Osteoporotic VCFs[116]	Single Blind Randomized Control Trial Single Center	Fracture >1 w, <12 mo MRI edema	PVP	VAS Decrease 5.1 at 1 mo 6.2 at 12 mo 6.6 at 36 mo	2.5 % (1/40)
			Conservative (analgesics, Vit D, Bisphos, Ca, Calcitonin)	Vas Decrease 0.8 at 1 mo 3.1 at 12 mo 3.5 at 36 mo	14.2 %(6/42)
			Findings	Sig for t<12 m	Sig.

Table 2.3: Clinical trials evaluating the efficacy of PVP and BKP for the treatment of painful VCFs (part 2 of 3)

Trial	Trial Type	Inclusion Criteria	Cohorts	Primary Outcomes	New Fracture Rate
INVEST[117]	Randomized, Multicenter Double Blind, Placebo Controlled	>50 y/o Fracture <12 m VAS >3	PVP	VAS Decrease 3.01 at 1 mo 3.44 at 12 mo RDQ decrease 6.46 at 1 mo 6.37 at 12 mo	Not Reported
			Sham (subcut lidocaine, periosteal bupivacaine, skin incision, pressure/tapping, cement mixing)	VAS Decrease 2.56 at 1 mo 2.54 at 12 mo RDQ Decrease 4.52 at 1 mo 5.62 at 12 mo	
			Findings	Non Sig.	
VAPOUR Trial[118]	Randomized, Multicenter, Double Blind, Placebo Controlled	Fracture <6w NRS>7	PVP	NRS below 4 44 % of patients at 2w 69 % at 6 mo	7.3 % (3/41)
			Sham(Subcutaneous lidocaine, skin incision, needle placement, tapping/pressure)	NRS below 4 21 % of patients at 2w 47 % at 6 mo	6.9 % (2/43)
			Findings	Sig at t = 2w	Non Sig.

Table 2.4: Clinical trials evaluating the efficacy of PVP and BKP for the treatment of painful VCFs (part 3 of 3)

Trial	Trial Type	Inclusion Criteria	Cohorts	Primary Outcomes	New Fracture Rate
Randomized Trial of PVP for painful osteoporotic VCF [119]	Randomized, Multicenter, Double Blind, Placebo Controlled	Fracture <12 mo MRI edema	PVP	VAS Decrease 1.5 at 1w 2.4 at 6 mo	7.8 % (3.38)
			Sham (skin incision, lg. gauge needle placement, tapping, mixing of cement)	VAS Decrease 2.1 at 1w 1.9 at 6 mo	10 % (4/40)
			Findings	Non Sig	Non Sig
FREE Trial[120]	Randomized, Multi Center	>21 y/o Fracture <3 mo MRI edema VAS>4	BKP	SF 36 PCS	33 %(38/115)
			Conservative (analgesics, bed rest, bracing, rehab., walking aids, osteoporosis treatment)	BKP>PVP, 5.2 pts at 1 mo BKP>VPV 1.5 pts at 12 mo	25 %(24/95)
			Findings	Sig.	Non Sig
A Randomized Trial Comparing BKP to PVP for VCFs due to Osteoporosis [121]	Randomized, Unblinded 24 mo	Fracture <6 m MIR edema	PVP	VAS decrease 4.6 pts at 3 mo 4.3 pts at 12 mo 4.0 pts at 24 mo	27.4 % (40/146) at 3 mo 43.5 % (57/131) at 12 mo 57.7 % (64/111) at 24 mo
			Balloon KP	VAS decrease 4.5 pts at 3 mo 4.5 pts at 12 mo 4.0 pts at 24 mo	23.3 %(35/150) at 3 mo 35.7 % (50/140) at 12 mo 49.1 % (54/110) at 24 mo
			Findings	Non Sig	Non Sig

relief[125]. Furthermore, the investigational PVP safety and efficacy (INVEST) trial, widened inclusion criteria due to low enrolment numbers to include patients with a VAS pain score as low as 3[117]. While both study and control groups experienced an *ca.* 30 % decrease in VAS pain scores, no significant difference was found between the groups, due to a combination of the large variability in VAS pain score ranking, and the inclusion of patients suffering only mild pain. A further critique of these two trials was their inability to distinguish between the cause of pain in the patient as either mechanical pain from the fracture (which would respond to PVP), or soft tissue pain due to height loss (which would only respond to height restoration of the vertebrae)[124]. It has also been noted that the volume of cement injected in these studies was significantly lower than recommended levels for stabilization (2.8 ml vs 4.0 ml), potentially resulting in insufficient mechanical reinforcement[124]. The sham procedure selection was challenged in study conducted by Wilson et al. which compared the efficacy of (a) local bupivulcan injection at the level of fracture to (b) the results from the INVEST trial, finding no significant difference in patient outcomes[126]. This study demonstrated that the injection of local aesthetic, used in the sham procedures, served to break the pain cycle, and was effective in providing long term pain relief for patients. As such, the "sham procedure" typically used in blinded PVP trials does not serve as an appropriate control for the evaluation of pain relief, resulting in the underestimation of efficacy.

To address the shortcoming of early blinded clinical trials, investigations with more restrictive inclusion criteria are currently under way, and show positive outcomes for pain relief following PVP[114]. Early results have emerged from the "Vertebroplasty for acute painful osteoporotic fractures" (VAPOUR) trial, which investigated the efficacy of PVP with stringent procedural, and inclusion requirements[118]. The procedural restrictions required cement filling from end plate to end plate, pedicle to pedicle and posterior cortex to anterior third to ensure stability. Furthermore, patient selection was restricted to those with an initial VAS score greater than 7, and a

fracture age of under 6 weeks. Early six month follow up data has reported significant improvements in VAS pain ratings at all time points investigated (3 d to 6 months) when compared to a placebo control. Furthermore, the best pain relief outcomes were reported in patients with fracture age under 3 weeks at the time of intervention[118]. In this study 41 % of the subjects who underwent PVP had a reduction in numeric rates pain scale from 7 or greater (sever pain) to 4 or below (minor pain) following treatment, indicating a clinically relevant reduction in pain. While effective in providing rapid pain relief, PVP is incapable of addressing the postural changes associated with VCFs, and as such BKP has emerged as an alternative technique to build upon this success.

Clinical trials comparing BKP with conservative treatment (Table 2.2) have reported similar results to those investigating PVP. The Fracture reduction evaluation trial followed 300 patients who received either BKP or conservative treatment of acute fractures (ongoing oedema confirmed by MRI). This study demonstrated significant improvement in pain as assessed through the "short form 36 physical component summary" (SF 36 PCS). These improvements over conservative care however were not maintained, decreasing from a 5.2 point benefit to a 1.5 point benefit between 1 and 12 months[120]. Limited clinical trial data is available directly comparing the efficacy of PVP to BKP. One non blinded multicenter trial was conducted comparing the procedures, finding no significant differences in patient outcomes (SF 36 PCS, Oswestry Disability index, VAS pain) between procedures[121]. It is of note however, that the trial was terminated early due to low enrolment, reaching only one third of the intended patient cohort. While limited direct comparisons are available, pain relief results have been similar between the two procedures in prospective studies[110]. Furthermore, a meta analysis of 29 clinical trials comparing the pain relief outcomes of PVP and BKP has concluded that no difference in pain controls is achieved at early, or extended time points (up to 12 months)[112]. While clinically effective in pain relief, legitimate criticism to both vertebral augmentation techniques has emerged,

due their inability to slow the progression of the vertebral fracture cascade.

2.2.2 Subsequent vertebral fracture following percutaneous vertebral augmentation

The second most frequently reported complication following vertebral augmentation is the incidence of adjacent VCFs (with the first being cement leakage outside of the vertebral body)[18, 108]. Subsequent VCF rates of 33.5 % in the three years following PVP have been reported[20]. BKP also results in a high rate of subsequent fracture, with two year subsequent fracture rates of approximately 47 %[127]. Initial reports believed that this rate of subsequent fracture was due to the high stiffness of the injected cement increasing mechanical forces on adjacent vertebrae[23]. Clinical data however, has not consistently demonstrated a significant increase in subsequent fracture rate when compared to conservative management, challenging this theory[114, 115, 116, 118, 119, 120, 121]. Many studies have been conducted in an attempt to better understand this phenomenon and an alternative hypothesis has been proposed[20, 25, 24, 128]. Specifically, that it is the underlying bone pathology, most commonly osteoporosis, which results in the high rate of subsequent fractures[129]. Furthermore, it is of note, that the conservative management techniques used to treat the control patients in two of the open label clinical trials included the use of anti osteoporotic agents, known to reduce VCF risk[119, 115]. No anti-osteoporosis treatment was provided for patients receiving PVP, therefore direct comparison between fracture rates would be an inappropriate evaluation of procedural risk.

In support of this hypothesis, Muijs et al. and Tseng et al. have both reported similar rates of adjacent and non adjacent fractures subsequent to PVP[24, 130]. Tseng et al. however highlighted a temporal difference in the time to fracture; adjacent fractures occurred on average 71.9 d following augmentation, while non adjacent fractures occurred 286 d after augmentation. Alterations in local load distributions due to kyphotic angle were proposed as the causative mechanism in this study[24].

Wang et al., in a mechanical study simulating vertebral loading following PVP found kyphotic angle to be the best predictor of adjacent fracture[25]. While temporal differences, as marked by Tseng et al., have yet to be fully explained, many theories contributing to this phenomenon have been proposed including: difficulty in identifying the time of fracture onset, greater losses in BMD being reported in patients who elect to undergo PVP, and higher levels of activity following PVP[25, 24]. While kyphotic angle has been linked to subsequent VCFs, meta analysis studies comparing BKP to PVP have failed to demonstrate a reduction in fracture rate between techniques[121].

Although commonly referred to as a complication of PVP, subsequent VCF is part of the natural progression of osteoporosis, and is due to the steady decline in BMD [25]. While PVP serves to reinforce and stabilize the fractured vertebrae it does not address the underlying osteoporotic changes to the bone, allowing for further decline in BMD due to the progressive nature of the disease. In order to decrease the rate of subsequent fracture in osteoporotic patients, treatment must serve both the mechanical and therapeutic needs of the patients[26].

2.2.3 Prophylactic percutaneous vertebroplasty

While PVP is typically performed following a fracture, there has been recent investigations into its use as a prophylactic measure to prevent vertebral collapse in osteoporotic patients[131, 132, 133, 134, 128]. In such an application PVP presents a method of reinforcing a weakened vertebrae which may be at risk of fracture. Most commonly this approach is taken at levels adjacent to fractured vertebrae, in a combined therapeutic and preventative procedure which attempts to decrease the high rate of adjacent level fracture seen following PVP[133]. While the procedure has been suggested to help prevent adjacent VCFs, the technique has been criticized for unnecessary patient risk associated with multi level augmentations[135, 136].

Multiple *ex vivo* cadaveric biomechanical models have investigated the effect of

prophylactic PVP on the load distribution, and failure load of vertebral bodies adjacent to therapeutically augmented sections, with conflicting results. Oakland et al. found: (i) decreases in vertebral body stiffness following prophylactic PVP, (ii) increasing loss of vertebral height with increasing cement stiffness, and (iii) no increase in failure strength following augmentation[128]. Investigations into the effect of loading angle, in turn, have concluded that while no increase in vertebral failure load following prophylactic augmentation is seen during on axis loading (simulating healthy biomechanics), a significant increase in the off axis fracture load (simulating altered mechanics due to kyphotic deformity) is observed[137]. This suggests that prophylactic PVP is successful due to its ability to increase the resistance to off-axis loading as would be expected to occur at a level adjacent to a wedged VCF. Such a finding is significant, as PVP has only mild height restorative capabilities.

An investigation into the effect of cement distribution within the anterior third of the vertebral body has highlighted significant correlation with the rate of adjacent VCFs. In the cases of greatest fill, where cement extends past the vertebral endplate (leakage into the intervertebral disk space) the rate of subsequent fracture was reported to be 44 % over a 2 years. If cement fill extends to, but does not pass the endplate, the rate of adjacent fracture decreases to 29 %. Finally, in cases where the cement did not extend past the trabecular space, adjacent fracture was reduced to 7 %[138]. From these findings, it was suggested that adjacent level fracture may be preventable through the use of prophylactic adjacent level augmentation in cases where cement leakage into the intervertebral space is noted intraoperatively. Such findings are further backed by the lack of efficacy of prophylactic PVP at preventing adjacent vertebral body fracture following hight restoring BKP, where off axis loading would not be expected to occur[139].

Studies into the clinical efficacy of prophylactic PVP have demonstrated a reduction in new fracture rate from 16.8 to 4.5 % at 3 months, and 22.4 to 9.7 % at 12 months[134]. A greater effect was seen in a study by Yen et al. (follow-up was of up

to 4 years) with only 3 % of patients who underwent prophylactic PVP experiencing an adjacent level fracture, while 39 % of patients who received only therapeutic PVP experienced new adjacent level fractures[132]. The rate of success of adjacent level prophylactic vertebral augmentation was found to be greatest when multi level segments were augmented in both the cranial and caudial directions resulting in a fracture risk reduction odds ratio of 2.61 compared to therapeutic PVP alone[133]. As PVP has a lower hospital cost than height restoring BKP, with similar patient outcomes[112], the combination of therapeutic and preventative vertebroplasty may offer a cost effective method of addressing the biomechanical changes which result in subsequent adjacent vertebral body fractures offering an optimized long term outcome.

While effective in reducing adjacent fracture, prophylactic PVP has also been critiqued due to increased patient risk, potentially deleterious alterations to bone remodelling, and speculation that fracture risk will not be improved, simply shifted to the next vertebral level causing an ongoing problem. While multi-level augmentation procedures of fractured vertebrae are known to be high risk due to the increased risk of cement embolism[136], leakage risks are significantly lower in cases of multilevel prophylactic augmentation. When assessed through intraoperative fluoroscopic imaging, leakage rate in non fractured vertebrae are reported to be 1.4 %, compared to 26 % in fractured vertebrae[133]. Concerns of long term stress shielding have similarly been disproven, with in silico computational modelling studies reporting that, contrary to previous fears of stress shielding and bone resorption, increased bone volume is seen over time when cement boundary does not extend to the end plates[131]. The third criticism, that prophylactic augmentation may spare a one vertebral body at the expense of another has no basis in clinical evidence. Similar rates of non adjacent subsequent VCFs following prophylactic and therapeutic PVP have been reported, indicating no increased risk between interventions[132]. As such, computational modelling, and clinical outcomes suggest the preventative vertebroplasty may

have beneficial effects on local bone health, preventing fracture and allowing for adaptive remodelling. While initial studies are promising, in silico modelling is limited by our knowledge of the response of tissue at the bone cement interface, and may be negatively impacted by fibrous encapsulation, or thermal damage. Improvements to the bone cement interface, as well as the combination of therapeutic bone cements with this procedure may provide even greater benefit allowing for treatment of the underlying disease state, while providing support to off axis loading to ameliorate the rate of subsequent VCFs.

2.2.4 Vertebroplasty materials

Ideal vertebral augmentation materials

During a comprehensive review of the literature on injectable bone cements used for PVP, Lewis compiled a list of ideal cement properties (Table 2.5)[1]. While this list of cement characteristics outlines key design criteria for PVP materials, many of the criteria lack quantitative goals (such as "easy injectability" and "mechanical properties similar to bone"). This lack of specificity stems from both a large variation in physician preference of handling properties (measures of the ease of use and timeframe for injectability) as well as natural variations in the mechanical properties of the implantation environment. While largely used as a guide for the development of PVP materials, this review did not include the requirement to address underlying bone pathologies, which is an essential component of VCF management[26, 39]. Nonetheless, this review provides basic guidelines for critical features required by a PVP material, which can aid in the development of next generation therapeutic bone cements.

To allow for safe and predictable injection into the fractured vertebral body, the cement is required to be radiopaque, have an appropriate 'paste like' viscosity, and

Table 2.5: Ideal properties for PVP materials as reported by Lewis[1]

Desired Cement Characteristic	**Rationale**
(≥2 mm Aluminium)	Allow for fluroscopic imaging
Constant Viscosity	Ease of injection, reduced leakage
Working Time of 6-10 min	Provide sufficient time for injection
Setting time of 15 min	Allow rapid patient mobilization
Mechanical properties similar to bone	Provide support and prevent stress shielding
Low curing temperature (<50°C peak or <45°C sustained)	Prevent thermal damage to local tissue
Macroporosity (>100 μm)	Allow for tissue ingrowth
Microposority (<10 μm)	Allow for blood and lymph circulation
Osteoconductive/Osteoinductive	Promote new bone growth and integration
Bioactive	Promote integration with surrounding tissue

provide setting and working times sufficient for the procedure to be performed (Table 2.5). High radiopacity, equivalent to at least 2 mm of Al is required for easy fluoroscopic imaging of the cement, ensuring proper fill, and the early detection of leakage during injection. This level of radiopacity can be achieved through the use of inherently radiopaque materials such as bioactive glasses, or through the addition of heavy metal salts to non radiopaque bone cement formulations. With respect to the latter, the addition of radiopacifying salts can lead to a reduction in mechanical performance, with potentially cytotoxic leaching of both the radiopacifying agent and unreacted monomer from the implanted cement. The latter, being associated with decreases in the extent of polymerization[140]. Collectively this can compromise safety, efficacy and performance of the cement and the procedure. These effects were highlighted in an animal study comparing the response to PMMA cements loaded with either 10 or 30 wt% $BaS0_4$, finding that increased radiopacifier content lead to fragmentation of the cement along implant boundaries, and increased inflammatory

response after 90 d of implantation[141].

Along with high radiopacity to allow for visualization, appropriate viscosity must be neither too low, allowing for extravasation, or too high, requiring excessive injection pressures. Viscosity requirements for PVP are subjective and vary with clinician preference. Boger et al. attempted to quantify these values and found that the ideal viscosity, based on radiologist preference, ranged from 23 to 30 Pas during PVP procedures[142]. Ideally cement viscosity would remain constant over the injection period, allowing for constant injection pressures to be used, this is difficult to achieve however due to the continual progress of the curing reaction of conventional materials, which is either a free radical polymerization in acrylic cements, or a precipitation reaction in calcium phosphate cements (CPC).

The final property required for injectability is an appropriate working and setting time to allow sufficient time for the procedure to be performed. Working and setting time are also determined by physician preference, with an ideal working time of 6-10 min commonly cited in the literature[1]. This working time allows for the augmentation of multiple vertebrae at a time if necessary. Materials with extended working times have also been developed with working times of up to 20 min, this allow for greater time for trocar placement which may be needed in multi-level, or bipedicular augmentations[143]. Furthermore longer working times may be required if a single fluoroscopy field is available, as procedure time would be increased due to the need to frequently reposition in the filed of view. Setting times of 15 to 20 min are considered ideal, allowing for patient transfer to be performed sooner, and reducing time in the interventional radiology suite.

While PVP cements must provide appropriate injectability, the mechanical properties of the set cement must also be considered, with an ideal cement for PVP matching those of the surrounding vertebral bone. This requirement however is open to a wide range of interpretations due to the variations between healthy and osteoporotic bone, as well as trabecular or cortical bone. Mechanical testing of trabecular

bone shows mean ultimate compressive strengths of 9 MPa, with a range as wide as 1 to 30 in patients with a BMD in the healthy range[144, 145]. Elastic modulus for healthy vertebral trabecular bone has been reported to have a mean value of 513 MPa, however this can be reduced by up to 12 % in patients with osteoporosis[146, 145]. While trabecular bone provides up to 90 % of the loading support of the vertebrae, the cortical shell provides a much greater stiffness with an elastic modulus of over 12,000 MPa, and a compressive strength of 167 to 215 MPa[147]. An ideal bone cement should have a high mechanical strength while maintaining a stiffness that approaches that of the surrounding bone to minimize shielding. While there is little census on an exact value, low stiffness and a compressive strength of over 30 MPa are frequently used a guideline for PVP materials[1].

Finally the cements impact on local tissue response must also be considered. Along with injectability, and appropriate mechanical strength, the cement should ideally provide low curing temperature, porosity, osteoconductivity and "bioactivity". The first of these requirements as listed by Lewis, low curing temperature is required to minimize the risk of thermal necrosis to the surrounding tissue, a risk associated with the heat generated during free radical polymerization. Osteonecrosis is recognised to occur at temperature of 50°C or greater which are maintained for one minute (min), while temperatures of 45°C or greater which are maintained for 30 min may cause sensory nerve damage[148]. Porosity is desired on both the micro and macro scale, to allow for fluid circulation, and bone ingrowth respectively. Micro pores on the scale of <10 μm allow for the circulation of blood and interstitial fluids into the cement, providing nutrients for tissue ingrowth. Macro pores of >100 μm in diameter allow for the ingrowth of bone into the material, ensuring a strong mechanical interlock occurs[149]. While a porous cement structure is desirable, the voids created by air entrapment during acrylic cement mixing significantly decrease fatigue performance, presenting a trade-off between porosity and strength[150]. A similar trade off between

porosity and cement strength is seen in CPCs[151]. Biocompatability, including osteoconduction, and osteoinduction are also desired in a bone cement. Osteoconduction as defined by Lewis is the promotion of growth of existing bone. Such a property is beneficial as it provides interdigitation and mechanical interlock with bone. Osteoinductive cements in turn encourage the development of new bone growth, which may allow for the development of bone at areas inside of the cement bolus[149]. New bone growth is especially advantageous in cements which exhibit shrinking upon curing, allowing for and voids created to be filled with new tissues. Such properties are essential to develop a tightly linked pseudo composite from the interlock of bone and cement, capable of increasing the stiffness of the augmented vertebrae[152].

While a number of commercially available injectable bone cements have been successfully used in PVP, none satisfy all the characteristics of an ideal PVP material. Three main varieties of commercially available injectable bone cements have been used in PVP; PMMA, calcium phosphate or composite resin cements, each system with their respective strengths and drawbacks.

Poly methyl methacylate cements

The most commonly used cement formulation for PVP is PMMA, these cements are derived from those used for arthroplasty fixation[153]. Injectable PMMA cements are composed of a powder of polymeric beads, which is mixed with a liquid monomer component (metheylmethacrylate). To allow for free radical polymerization benzoyl peroxide (BPO) is added to the polymeric powder components, while dimethyl-p-toluidine (DHPT) is added to the liquid monomer components[154]. Although each component is stable on its own, once mixed this initiator system serves to generate free radicals, leading to the polymerization of the liquid methacrylate monomer, causing progressive curing. The addition of the polymer powder to the cement serves to increase viscosity, decrease setting time, decrease exothermic heat of reaction, and

divert crack propagation in the set product[153]. Along with the polymer and initiation systems radiopacifying salts are added to allow for visualization of the cement under fluroscopy[154].

Although PMMA products have remained popular, there are a number of drawbacks recognised in the literature for their use in vertebral augmentation[153, 154, 155, 156]. PMMA cement is not capable of bonding with bone, and vertebral fixation is achieved solely though mechanical interlock. The bone cement interface is further compromised due to polymerization shrinkage, which not only generates strain on the surrounding trabecular, but also results in the formation of microvoids at the cement surface[152]. Due to the lack of bonding, crack propagation has been reported at the bone cement interface, resulting in movement of the cement bolus relative to the surrounding bone[23]. This movement has been linked to the formation of a free moving fibrous capsule around the cement, compromising the mechanical integrity of the vertebrae[157]. The response of local tissues may be further impacted by the high setting temperatures (41-95°C), which exceed the temperature threshold of thermal damage[148, 158]. Furthermore, incomplete curing has been shown to result in the leaching of unreacted monomers from the cement, resulting in toxicity. Monomer leaching is confounded by the need for the addition of radiopacifiers at high rates, which decrease the extent of polymerization[153, 156]. PMMA based cements have also been criticized for their stiffness (1.2 to 1.4 GPa[159]) which is greater than that of trabecular bone (344 MPa[147]). To address shortcomings associated with PMMA cements, calcium phosphate and composite resin cements have been developed as alternatives, providing less exothermic setting reactions, reduced rates of fibrous encapsulation, allowing for direct bone integration, and varying extents of resorbability.

Calcium phosphate cements

Calcium phosphate bone cements were first developed in the 1980s as bone void fillers, and have been proposed as a more bioactive alternative to PMMA based bone

cements[160]. These cements are composed of a soluble calcium phosphate powder and an aqueous liquid phase. Upon mixing, the initial calcium phosphate powder phase dissolves, resulting in super saturation of the solution, and finally solidification through the precipitation of interlocking crystals. The final calcium phosphate phase is typically a hydroxyl apatite (HA) phase, however some cement formulations first harden into a metastable brushite phase which is then converted into HA *in vivo*[161]. This setting reaction generates little exothermic heat[161]. Furthermore, due to the interlocking crystal structure these materials are inherently micro porous allowing for fluid transport through the material. While the high calcium content imparts radiopacity, the similarity to bone mineral matrix results in low contrast with tissues, requiring further opacifiers to be added[162]. These materials have been successfully used as an alternative to bone grafts where they have demonstrated a decreased risk of loss of fracture reduction by up to 68 % in metaphyseal fractures in various appendicular bones[163]. Many challenges exist however to translating this success into PVP materials due to poor mechanical properties and poor injectability.

Some CPCs have been demonstrated to be resorbable following implantation, this effect is thought to be due to their similarity to natural bone HA matrix[164]. As their degradation releases calcium into the local environment they have the potential to induce increased bone deposition through calcium mediated OBLs recruitment[46]. The mechanical properties of these cements however are much lower than those of PMMA cements with compressive strengths frequently below 20 MPa, and the materials are prone to brittle fracture, especially under torsion or shearing forces[165, 166]. Furthermore the degradation of the cement leads to further loss of strength with time, leading many to conclude the materials are inappropriate for use in osteoporosis where bone remodelling is compromised and long term mechanical support would be needed from the PVP material[167, 168]. Along with difficulties in achieving sufficient mechanical strength, CPCs are prone to filter pressing, resulting in phase separation during injection. This phenomena results in the formation of a non-homogeneous

material, with high variability in porosity, strength and setting time due to decreases in powder to liquid ratio during injection[169].

Poor cement injectability, assessed as the fraction of cement which can be extruded from a syringe fitted with a large bore needle without phase separation and loss of cohesiveity is also a challenge for the use of CPCs in PVP[169]. To overcome this challenge, as well as to improve mechanical strength, various organic additives have been incorporated, acting to increase liquid phase viscosity and therefore improve cohesion and reduce porosity (a major predictor of cement strength). The addition of collagen fibres for example has been shown to increase the compressive strength of an α-tricalcium phosphate cement formulation from 15 to 32 MPa, while increasing injectability from 15 to over 50 %[170]. This modification however results in an increase in material cytotoxicity, a decrease in cellular proliferation on the cement surface, and a decrease in ALP activity, potentially negating their proposed advantages over PMMA. Hydroset^{TM}, a commercially available injectable CPC incorporates polyvinyl pyrrolidone into its liquid phase to increase cohesivity and has similarly demonstrated improved injectability. However, compressive strength remains low (<25 MPa after 24 hs of incubation in distilled water) and rapidly decreases with time (<15 MPa after 7 d)[165].

While cement degradation is considered by some to be a beneficial quality, allowing for the ingrowth of new bone to eventually replace the cement, this resorption reaction has been demonstrated to be highly variable. In a study of the use of an injectable CPC, Calcibon^{TM}, for the augmentation of traumatic vertebral body fractures it was noted that resorption varied from 0.3 to 35.3 % after 12 months[168]. This finding led study authors to conclude that the use of such a material for vertebral augmentation outside of healthy patients experiencing traumatic fracture (ie osteoporosis patient or patients with osteolytic legions) would be inappropriate due to the unpredictable deterioration in mechanical strength associated with resorption. These conclusions highlight the need for bone cements which are capable of both providing

mechanical strength, but also improving local bone quality to reduce the risk of future fracture. Cement degradation studies for Hydroset^{TM}, similarly demonstrates a large variation in degradation with a loss of 8.1 ± 4.9 % of implanted material present after 6 months[171]. Furthermore, it was noted that material degradation was limited to the cement surface with no bone ingrowth, and only surface remodelling occurring. Animal studies investigating the effect of calcium phosphate phase on the rate of reaction have demonstrated that resorption is dependent not only on material properties, but may also the site of implantation[172]. Such effects are hypothesized to result from interactions with blood flow and the setting cement, resulting in cement "wash out". This "wash out"phenomena has been reported to occur due to low cement cohesivity, where the weak interactions between the powder particles allow for the penetration of fluids into the cement. This results in the dilution the liquid phase, delaying the saturation effects necessary for crystal formation, and ultimately generating large fluid filled pores and a granular, non-uniform material. Reinforcement with degradable fibre such as poly-lactic-co-glycolic acid has been used as a method to both increase mechanical strength and provide macroporosity in an attempt to improve bone ingrowth[171, 173]. Such a technique has been demonstrated to increase overall cement degradation (up to 66 % resorption after twelve weeks of implantation) and allow some bone ingrowth (approximately 7 % of initial cement volume at twelve weeks), however the mismatch between degradation and ingrowth lead to the loss of implant integrity.

While injectability and cohesivity are often considered a challenge for the use of injectable CPCs, the lack of free flowing cohesivity also results in a decreased rate of cement extrusion, offering a potential advantage. This was quantitatively assessed in an animal study comparing the extrusion of a high viscosity PMMA cement to that of a (carboxyl methyl cellulose) fiber reinforce CPC. In this study, leaks extending more than half a millimetre beyond the defect boundary were decreased from 6 % of the injected cement volume for PMMA to a negligible value with the CPC

(∼0 %)[173]. The risks associated with poorly cohesive materials however extend beyond effects on cement strength, with reports of laryngeospasm and tachycardia in otherwise healthy patients being potentially linked to bolus calcium release during cement implantation[174]. Foreign body response, and macrophage activation has been linked to the granular nature of poorly cohesive CPCs, lasting up to four weeks, and is greater in brushite cements than HA cements[175, 172]. Such an effect may be of increased concern in patients with primary osteoporosis, where bone resorption and OCL activation are linked to increased inflammatory pathway activation of macrophage cell lines[176]. As such, CPCs may not only fail to provide the long term mechanical strength necessary for vertebral body augmentation, but may also further exacerbate the unbalanced resorption experienced in these patients. While CPCs have improved on some of the drawbacks of PMMA cements, improving bone integration, preventing thermal damage, prolonging working time, they fail to meet other key requirement. Accordingly, composite cements have thus been developed that utilise an inorganic filler phase to reinforce a resin matrix. These cements have been developed to combine the advantages in injectability and mechanical strength seen in acrylic cements with the decreased fibrous encapsulation, increased bone bonding and ion release seen in CPCs.

Reinforced resin composites

A ceramic reinforced bisphenol A glycidyl methacrylate (Bis-GMA) composite bone cement (Table 2.6), has been developed as an alternative to PMMA or calcium phosphate based bone cements, and is currently marketed as Cortoss®. The filler phase of this composite is composed of a combination of silica, silane treated bioactive combite, and silane coupled barium boro-alumino silicate. This combination offers mechanical reinforcement, radiopacity, and the ability to directly couple with bone tissue due to calcium and phosphate release[28]. Cortoss® is formulated as a two paste liquid system, which is dispensed through a proprietary injecting device, preventing the mixing

Table 2.6: Two-paste composition of ceramic reinforced Bis-GMA based cement[2].

Paste A	**Paste B**
Bis-GMA	Bis-GMA
TEG DMA	
Silane Treated Bioactive Combite	Teg DMA
Silica	Silane Treated Barium Boro-Aluminosilicate
BPO	Silica
	DHEPT

of the initiator system and polymerization until the time of injection, and is marketed as a "snap set" cement due to the lower setting time allowed by this system[177]. This design, in theory, allows for constant, predictable injection viscosity and reduces the required working time. The mechanical properties (Table 2.7) have been proposed to be more closely matched to cortical bone than those of PMMA, decreasing stress shielding [2]. While such a cement sets in a similar free radical polymerization reaction to PMMA, the incorporation of large molecular weight monomers, as well as inorganic fillers, results in a significantly lower peak exothermic temperature and shrinkage[159].

Animal trials comparing the local bone response following the implantation of either Cortoss® or PMMA in a rabbit femoral defect model demonstrated a significant increase in new bone formation with the use of Cortoss®[28]. Similarly, Cortoss® was shown to decrease fibrous encapsulation, allowing for direct bone bonding. This material is also of interest for the augmentation of stripped out orthopaedic screws, as it has demonstrated a significant increase (over 4.5 times greater) in rod pull out force when compared to PMMA at time points between 6 and 72 weeks[28]. Both direct bone deposition, and increased pull out force, are attributed to the inclusion of bioactive ceramic filler.

Open prospective trials comparing the efficacy of Cortoss® to traditional PMMA cements in PVP have shown significant decreases in VAS pain scores and Oswestry

Table 2.7: Mechanical Properties of Commercially Available Injectable Bone Cements[2].

Property	**Units**	**Cortical Bone**	**Composite Resin**	**PMMA**	**PMMA**	**CaP**
Static Compressive Strength	MPa	167-215	200	80	111	24 [a]
Tensile Strength	MPa	70-140	62	31	37	3-10 [b]
Modulus	GPa	14.7-19.7	8.2	3.5	3.7	0.24 [a]
Tensile Modulus	GPa	10.9-14.8	10.5	3.4	3.0	NA
Compressive Creep Strain	50 MPa 24h	NA	<1%	20%	NA	NA
Compressive Endurance	50 MPa	NA	$>10^7$	$\sim 10^5$	NA	NA

[a] [165]
[b] [178]

disability indexes, at both three and 12 months[23]. It was initially hoped that a two paste system would result in lower rates of cement leakage by allowing for more consistent viscosity during the injection period, and increased radiopacity improving cement visualization[28]. However, clinical results demonstrated that rates of leakage were comparable to those with PMMA (63.8 % for both materials) albeit the average volume of leakage was significantly lower with the composite resin than PMMA (0.14 ml and 0.20 ml respectively)[23]. This may improve patient safety as lower volumes of cement leakage have been linked to lower risk of complications[179].

Although improvements in histological response, cement leakage volumes, and handling properties have been achieved through the use of a composite resin, the risk of subsequent fracture remains high[23]. Clinical data comparing the effectiveness of Cortoss® to PMMA found that no significant decrease in subsequent fracture rate was found between material (27.8 % vs 31.9 % for PMMA)[180]. These findings are consistent with subsequent biomechanical studies which have demonstrated that cement stiffness is not a major predictor of subsequent fracture rates. Rather,

research investigating the link between cement stiffness and the rate of subsequent fracture conducted by Wang et al. found that the compactness ratio was a better predictor of subsequent fracture than the mechanical properties of the cement[25]. As such, purely mechanical improvements to PVP materials will not prevent VCFs from occurring. Current treatment guidelines for VCF patients at high risk to re-fracture is to address both fracture stabilization, as well as providing treatment for the underlying disease state to slow the progression of bone loss[26]. While PMMA and composite resin cements offer an advantage over CPCs through the maintenance of consistent mechanical strength during implantation, all three materials fail to provide improvements to local bone quality. In order to address this concern, a number of approaches have been used to develop therapeutic bone cements, capable of providing local drug release in an aim to improve tissue response.

Therapeutic bone cements materials

While therapeutic bone cements in the context of this work refers primarily to cements capable of providing anti-osteoporotic effect, a variety of other therapeutic goals for drug delivery have been investigated, providing insight into the design of such materials. The first pharmaceutical compounds to be delivered from bone cements were antibacterial agents, used to minimize the risk of biomaterial based infection in cemented arthroplasties. These materials have significantly decreased the risk of deep tissue infection (RR 0.41), decreased revision rates, and decreased cost of treatment[181, 182]. Due to this success, materials of a similar concept have been developed aiming to treat other underlying pathologies which complicate bone cement implantation; including (i) the use of antimetastatic drugs to treat osteolytic metastasis[183], (ii) the inclusion of anti inflammatory drugs to reduce post surgical inflammation[184], (iii) the inclusion of growth factors to promote bone formation (most notably BMP)[185] and (iv) the inclusion of anti-osteoporotic drugs to increase

local BMD and strength[186, 187]. The essential challenge in the design of these materials is loading the therapeutic agents in a manner that allows for their predictable release, in an active format, within the therapeutic range[188]. Such materials must be designed to meet minimal thresholds required for efficacy, without inducing undesired cytotoxic responses (apart from metastatic drugs where controlled cytotoxicity is a desirable endpoint). Along with the design criteria required for efficient drug delivery, therapeutic bone cements must also maintain the general requirements for a bone cement, including handling properties, strength, setting reaction and long term stability.

Antibiotic loaded PMMA cements were first generated through the "off label" inclusion of antibiotic powder into commercially available cements, and ready made cements are now available and widely used for this purpose[189]. In cemented arthroplasties, they have succeeded in reducing the infection rate by 50 % in both primary, and revision procedures[190]. Much like the inclusion of radiopacifiers, the inclusion of antibiotics may decrease the degree of polymerization and reduce the strength and stiffness of the cement, however the loss in mechanical strength is not thought to be clinically relevant as PMMA cements generally exceed the mechanical strength requirements for both vertebroplasty and arthroplasty applications[189]. As acrylic cements experience very little water infiltration, drug release is surface mediated, and rapidly decays over time[191, 192, 189]. In a study of the effect of fatigue loading on antibiotic release it was found that full tension compression reversal loading generates an increase in the release of antibiotics into solution[191, 192]. Microcrack propagation at the surface of the cement, increasing the surface area available for drug release was though to be the mechanism through which release was altered. While such a mechanism is sufficient for the prevention of surgical infection, where long term release is unnecessary, PMMA cements offer a poor base for long term dosing due to these limitations.

Anti-osteoporotic cements

Due to the high prevalence of osteoporotic VCFs a number of approaches have been taken to design bone cements capable of increasing BMD and treating the underlying osteoporosis. Anti-osteoporotic drugs which have been incorporated into experimental bone cements include oestrogen, bisphosphonates and strontium ions[183, 193, 194, 164]. Unlike in antibiotic loaded cements, long term drug release is desired in these materials due to the chronic nature of the disease. The inclusion of the bisphosphonate zoledronic acid into a PMMA cement exhibited surface mediated burst release, similar to the release kinetics seen in antibiotic loaded cements, with a release plateau reached after 4 d (incubation in distilled water)[183]. This large burst release resulted in 10 to 50 % cytotoxicity, which while proposed as beneficial for the treatment of osteolytic metastases, would greatly decrease the bone remodelling potential in osteoporosis patients.

Strontium has also been incorporated into PMMA cements for proposed anti-osteoporotic effects in the form of strontium substituted HA, modified with linoic acid to increase water sorption to prolong release. While this technique did allow for a more hydrophilic cement with prolonged release, strontium release *in vitro* did not exceed 2μM, and was not significantly different from non-strontium loaded controls at early time points (<7 d)[194]. While such a cement is being investigated for clinical use in PVP, it is unlikely to offer true anti-osteoporotic effects due to the low release levels, which are well below therapeutic doses for the ion. Improved bone integration compared to PMMA as reported in animal studies is likely to occur due to improved water contact angle and calcium phosphate release in a manner similar to Costoss^{TM}. Similarly improved localised responses may have been provided through the addition of strontium in place of $BaSO_4$ to impart radiopacity. While these changes are beneficial, no long term improvement to bone quality can be expected to occur due to strontium release. To overcome the difficulties associated with

burst release from PMMA acrylic cements, calcium phosphate based cements have been the preferred base for such materials providing extended release through bulk degradation[195, 187]. Additional advantages are provided by the non exothermic setting reaction, which mitigate concerns of thermal degradation of the loaded drug.

Bisphosphonate loaded CPCs have demonstrated decreased burst release, and increased long term release compared to bisphosphonate loaded PMMA cements. While this approach allows for the inclusion of Alendronate or Pamidronate into CPCs without cytotoxic effect on MG63 cells *in vitro*, it also results in significant losses in mechanical strength due to decreased crystal propagation (from 22±2 to 13±2 and 13±1 MPa for the inclusion of alendronate and pamidronate at 1.0 mM concentration respectively)[164]. Such cements have demonstrated *in vivo* efficacy, as demonstrated in a osteoporotic sheep model where an increase in bone volume (from 40 % in controls to 80 % for bisphosphonate loaded cement), with improved bone quality (as assessed through trabecular pattern, an indicator of the interconnectedness of the trabecular lattice) being observed[167]. This material however was deemed only suitable for prophylactic use by study authors due to brittleness. Furthermore, bisphosphonate may result in delayed fracture healing rates as they inhibit the OCL activity required to resorb damaged bone matrix prior to regeneration, making a bisphosphonate releasing cement a poor candidate for fracture fixation[77].

The incorporation of 0.5 % oestradiol into a CPC resulted in release profiles which were mediated by the serum calcium concentration *in vivo*[193]. While such a model is potentially beneficial for calcium deficient osteoporotic patients, the first line treatment of osteoporosis is calcium supplementation which would result in decreased release efficiency[39]. Furthermore, while osteoporosis has been linked to oestrogen deficiency following menopause, it is not a lack of oestrogen effect which causes the pathology, rather inflammation resulting from the loss of the antioxidant action of oestrogen, causing the activation of oxidative stress pathways[62, 196]. As such, the inclusion of oestrogen in CPCs which have been linked to local inflammatory reactions

would likely negate the efficacy of such a therapeutic[175, 172].

The incorporation of strontium into CPCs has been the most popular design approach for the formulation of an injectable bone cement with anti osteoporosis potential[197]. Two major challenge exists with this approach however. Firstly, as CPCs solidify through the entanglement of long needle like HA crystals, strontium loading is limited to <10 % of the calcium content of the cement, the point at which major disruption to the HA lattice occurs preventing elongation[198]. Similarly, as strontium phosphates are more soluble than calcium phosphates at physiological pH, strontium loaded CPCs experience accelerated degradation kinetics, rapidly losing their initial mechanical strength[198]. The incorporation of strontium in the liquid phase of a CPC was demonstrated by Tadier to provide sustained strontium release, over the three weeks investigated, up to 200 mg/l. This sustained release however was caused by crystal degradation leading to increased cement porosity (up to 68 % after release testing), resulting in crack propagation through the cement[195]. Similarly strontium carbonate substitution into a β tri CPC was successful in generating a predictable zero order release profile, with up to 60 mg/l release[199]. These materials however did not generate any improved cell proliferation, had very short setting times (between 1.25 and 2.5 min) and compressive strengths below 7 MPa, making them unsuitable candidates for PVP.

Panzavolta similarly combined strontium chloride addition in the liquid phase with the addition of gelatin in an attempt to address both anti-osteoporotic drug release and improve mechanical properties of a CaP cement. While these modifications provided nearly two fold increases in ALP activity (a measure of OBL activity), and increased cell proliferation, they also resulted in setting times of over 50 min, rendering them impractical for use in PVP[200]. The effect of such strontium additions on the mechanical properties of the cements varies between studies, with reports of both increased or decreased compressive strength, likely dependent on the strontium loading used; with lower strontium loadings (under 5 %) resulting in increased strength,

and losses of strength seen thereafter[201, 202]. While CPCs have demonstrated increased, and sustained strontium ion release, difficulties with their translation into functional PVP materials capable of meeting the requirement of proper handling properties and mechanical strength remain.

Alternative approaches to the development of strontium releasing cements have utilised the inclusion of a strontium eluting inorganic phase in either a composite cement, or an ionomeric cement. A Hong Kong based research group has developed a strontium HA containing bone cement, which is currently undergoing clinical trials. This material is a resin reinforced composite cement, based off a Bis-GMA, TED-GMA, PEG-MA blend[203, 200]. The material showed a 60 % increase in OBL proliferation over a traditional HA material *in vitro*, and increased bone deposition over PMMA cements *in vivo*. The mechanical strength however has been found to be lower than current PVP materials (compressive strength of 40.9 MPa, bending strength of 31.3 MPa, bending modulus of 1.4 GPa), yet likely to be sufficient for the application[203]. Little information however is provided as to the release of strontium from this material leaving it unclear if the beneficial effect is gained due to strontium incorporation, or is similar to the improved integration and response seen with other composite resin cements. To further build upon the improved biocompatability of composite resins, the use of reinforcing phases capable of providing long term, high level strontium release at therapeutically relevant levels could offer a mechanism of providing anti-osteoporotic efficacy and improved local bone quality. Other approaches have focused on the use of strontium eluting bioactive glasses, primarily in ionomeric cements[159, 204, 205, 206]. These materials all showed increased OBL proliferation in *in vitro* studies. A strontium containing ionomeric cement developed by Johal et al. also show increased rates of bone repair in Wistar rat models. However the glass ionomeric cement contained aluminum, a material currently contraindicated for use in bone cements[204]. Although research into the development of aluminum free ionomeric cement is underway, many suffer from low mechanical strength or

handling characteristics, and none of these cements have reached the clinical trial phase[159, 205, 206]. While these bioactive glass based systems show promise, they provide limited long term release potential due to the rapid decay in ion release kinetics commonly reported with silicate based glasses[33]. The use of alternative glass formulation tailored to provide extended release could thus be beneficial, offering potential for the use of borate based bioactive glasses which demonstrate more uniform degradation kinetics.

2.3 Bioactive glass

The term bioactive glass was first used in the 1960s to describe phospho-silicate glasses capable of directly bonding to hard tissues following implantation[207]. Since its initial use, the definition of bioactive glass has expanded to recognize a much boarder range of both compositions and applications. In the broadest sense the term bioactive glass now refers to any glass capable of generating a desired host response, which may include direct tissue integration, controlled degradation/resorption, or bioinnert glasses which remain unchanged following implantation[208, 31, 209, 27]. The original Bioglass^{TM} series was developed to overcome issues with fibrous encapsulation in hard tissue engineering, and allows for direct bone integration through the development of a bone like HA layer on the surface of the glass[207]. These materials were later shown to also be capable of bonding to non calcified tissues, again through the formation of an HA like surface layer, expanding their area of application[210]. The direct tissue integration demonstrated by many bioactive glasses is due to the complex surface reaction that takes place upon immersion in an aqueous environment, resulting in the release of glass components into solution, and the formation of an altered surface layer[211, 212, 213, 214]. While newer generations of bioactive glasses do not exclusively demonstrate bone bonding behaviour, the degradation of bioactive glasses in aqueous implantation environments remains as the primary material characteristic

manipulated to control biological response. Thus, the understanding of glass corrosion mechanisms has been at the centre of bioactive glass development.

2.3.1 Bioactive glass degradation reaction

The first studies into the reaction of bioactive glasses within the implantation environment were conducted on a series of glasses composed of silica, phosphorous, calcium and sodium oxides by Hench and Clark in 1978[33]. This study proposed a five step surface reaction governed the formation of HA at the surface of the glass following exposure to water as follows: (i) proton exchange and rapid release of alkali ion glass modifier components into solution, resulting in an increase in pH, (ii) silica network hydrolysis, (iii) supersaturation of the solution with silica resulting in the precipitation of a silica gel layer, (iv) saturation of local solution with phosphate and calcium, causing precipitation on the silica gel surface, and (v) the rearrangement of the surface precipitate layers to form a crystalline HA. Clear evidence of reaction steps one and two exist from the alkali silicate glass literature[33, 215]. These two reactions are consistent with traditional alkali silicate glass corrosion studies in which glass modifier are released, and a modifier depleted surface layer forms upon exposure to water. The decrease in ion release kinetics and silica release observed in the Bioglass^{TM}series was hypothesized to be due to the increasing thickness of this altered layer formed resulting in decreased water infiltration and reaction.

While solution pH has been proposed to govern these reactions, with the increase in local pH being responsible for the switch from ion exchange to network hydrolysis, these reactions have since been demonstrated to occur simultaneously[216]. Furthermore, the saturation based formation of the silica gel layer and the calcium phosphate layer has also been shown to occur simultaneously with steps 1 and 2, challenging the stepwise mechanism initially proposed[217, 218]. Such a simultaneous reaction counters the passivating layer theory in which the reaction is slowed due to the formation of the silica gel layer, as there is evidence that the silica gel layer forms *beneath* the

calcium phosphate rich layer. Furthermore, such a diffusion controlled model would be predicted to result in diffusion gradients in the altered layer, a characteristic that is not present in many reacted bioactive glass surfaces, rather banding patters are occasionally seen with depth profiles displaying alternating layers of high and low modifier content[214, 212]. Despite these substantial flaws, the Hench model of glass dissolution has remained largely accepted model by the bioactive glass community.

Alternative glass dissolution models

It was initially believed that only a narrow range of glass compositions could present bioactivity (in terms of HA formation and bone bonding), requiring high phosphate and modifier contents to provide the ion release and solution saturation required. Subsequent studies however, have demonstrated that HA formation can occur in glasses with a much broader compositional range, leading to the expansion of glasses considered bioactive with silica, phosphate, alumina, boron and germanium networks all being investigated[32, 27, 209]. Furthermore, interest in the possible network intermediates or modifiers has greatly expanded leading to more diverse glass structures. Due to this new broader range of bioactive glasses, alternative dissolution reactions have been suggested[219]. In a model proposed by Hill in 1996 the surface reaction is proposed to occur in a sequence similar to that suggested by Hench and Clark but without the release of silica into solution and subsequent precipitation. Rather this model proposes the untangling of a linear silica polymer network following the removal of glass modifiers and subsequent relaxation to form a gel. This model better predicts the release of silica, as there is no peak and decrease as would be predicted by Henchs model[218]. It also offers some predictive ability as the network connectivity (the average number of bridging oxygen species per network former) can be used to predict how easily such a network will untangle and reform, with the best bioactivity results around a network connectivity of 2. While this model expands on the four-component model presented by Hench allowing for composition based

predictions on glass reactivity, (most notably explaining the role of aluminum addition), its predictive abilities fail with glasses which comprise a large fraction of (or are entirely formed from) boron oxide. While such a model would suggest that boron addition increases network connectivity, and thus decreases the reactivity of the glass, an opposing trend is observed, with borate glasses demonstrating more rapid rates of reaction[220, 221, 222, 223, 34, 224]. Furthermore, banded reaction surfaces again remain unexplained by this model. In this linear polymer model of glass degradation saturation effects remains an important factor in the formation of the altered surface layer, however both calcium and phosphate free glasses have been shown to generate such a surface layer. These findings suggest that the reaction may be surface mediated and not controlled by saturation effects as initially proposed[225, 226].

Nuclear glass dissolution models

While most bioactive glass literature remains focused on the Hench dissolution model, glass research from the field of nuclear waste containment glass has focused on interfacial reactions models. These models suggest the simultaneous dissolution and reprecipitation of a thin surface layer at the boundary of hydration of the glass[227, 228, 229, 230]. Nuclear waste containment glasses are highly resilient glasses designed to contain spent nuclear fuel as glass components. As such they are more varied in composition, and their degradation reaction has been studied over longer time frames, in more extreme conditions, offering valuable kinetic insight into the corrosion mechanism of multicomponent oxide glasses.

A number of important findings have emerged from this field which directly counters the accepted glass dissolution models from the biomaterials community. Alteration layers have been demonstrated to spontaneously form a striated lamellar structure with areas of low and high modifier content, suggesting diffusion gradients do not govern their formation[228, 231]. Isotope doped ageing environments have

disproven that silica is precipitated from solution (with the exception non physiologically relevant extreme pH conditions), rather the gel layer formed is residual modifier depleted glass network, which was never released into solution (similar to Hills linear polymer network theory)[230, 232, 233]. Finally, recent advances in analytical techniques have allowed for high resolution compositional analysis which has revealed atomically sharp transitions between the pristine core glass and the modifier depleted altered surface layer[227, 228, 234]. These sharp transitions offer further evidence that the surface layer is not resulting in a diffusion limiting passivating layer as previously proposed.

These findings suggest that a simultaneous interfacial dissolution and reprecipitation reaction govern the reaction of oxide glasses in aqueous solution. Such an interfacial dissolution and reprecipitation reaction has been suggested to govern the weathering of naturally occurring minerals as far back as the 1950's, however experimental techniques were incapable of identifying such a mechanism until 2007[234]. This model suggests that the glass networks dissolves at the hydration boundary, simultaneously reforming into a more stable alteration layer, where low solubility glass components are retained while highly soluble components are released into solution[227, 229]. Atomically thin layers of altered glass form as the hydration front advances, with each layer representing a unique time point in the reaction[233]. This is the basis of the formation of striated layers as the respective saturation points for various glass components is reached, resulting in their precipitation into the alteration layer, and thus depleting the solution, allow for further removal in subsequent layers. The overall rate of reaction is governed by both the solubility of the glass components as well as the molar volume of the altered layer relative to the initial glass volume[231]. If the alteration product is more dense than the original glass, the altered layer formed would have an insufficient volume to cover the surface, resulting in the formation of micro channels. The porosity formed would provide rapid water

transport to the surface of the unreacted glass, sustaining modifier release. Alternatively, if alteration products formed are of a lower density, the layers can fully cover the glass surface, and water must diffuse through the bulk of the material, slowing the progression of the hydration front [235].

While such an interfacial dissolution and reprecipitation glass degradation model is not fully formed, it does offer a kinetic basis allowing for the comparison of relative dissolution rates based on the solubility of glass components, and the diffusivity of the alteration products formed. While it has not gained popularity in the bioactive glass community, it offers a great advantage as it allows for the consideration of a much broader range of glass components. furthermore, such models can provide an explanation for the role of the local implantation environment through the effects of solution fluid flow in the surrounding area. The reaction of borate glasses for example, which can be explained by neither Hench's or Hills models of bioactive glass degradation, could be understood through the lens of interfacial dissolution and reprecipitation. Such a model would suggest that boron, due to it's high solubility would result in the loss of a large fraction of the glass to solution, and as such the resulting alteration layer would fail to cover the glass surface. As such extensive water infiltration would be possible, prolonging the release of glass modifiers, as has been demonstrated in experimental work.

2.3.2 Bioactive glass as therapeutic ion release systems

Therapeutic inorganic ions have been demonstrated to alter cellular metabolism as enzyme cofactors, or by acting as direct molecular signals[27, 236]. As such they can be used to treat a variety of pathologies in a similar manner to typical organic drug molecules. The most widely recognized TII is lithium which has been used as a mood stabilizing drug due to its ability to disrupt glycogen synthase kinase-3β (GSK-3β) signalling[237]. Similarly, strontium ions have been demonstrated to lower calcium signalling thresholds, uncoupling OCL and OBL activity in bone remodelling

resulting in increased bone deposition and reduced bone resorption[88, 29, 13].

Therapeutic inorganic ions offer a variety of advantages over traditional organic drug molecules for localized delivery, as they are thermally stable allowing for easy processing, their molar weights are much lower than that of most traditional drug molecules, requiring low levels of therapeutic loading, and ions are less prone to enzymatic deactivation once release into solution. Furthermore, in the case of bioactive glasses, TIIs can be directly incorporated into the glass network without additional drug loading steps. These advantages have generated research interest for the development of therapeutic bioactive glasses aiming not to integrate with surrounding tissue, but to alter local metabolism through the release of TIIs as degradation products. Such glasses have been used in a variety of applications to allow for antibiotic, angiogenic, antimetastatic, and osteoinductive properties[27, 236]. Due in part to the wide use of bioactive glasses in hard tissue engineering, a number of TIIs aiming to improve bone regeneration have been investigated including zinc, magnesium, cobalt, copper, boron and strontium[27]. A crucial step in the development of a TII releasing glass, is the ability to identify the required concentrations of the ions to elicit biological response, and prevent toxic effect, as well as the biological fate of the ion once released *in vivo*[238]. In this regard, the use of strontium ions has a great advantage through the depth of knowledge gained on the effect of strontium on bone in the development of strontium ranelate. Like their bone bonding predecessors, the success of ion releasing bioactive glasses relies on a thorough understanding of the interaction of the glass network and the aqueous environment into which they will be implanted, as this reaction governs the rate of ion release and thus local dosing.

For such systems aiming to treat chronic conditions such as osteoporosis, ensuring prolonged and effective release kinetics is essential. While silicate glass systems have remained the most commonly studied form of bioactive glasses, the decay in ion release kinetics is not ideal in such application as cation release decay can occur as early as a few hours after implantation[31]. Bioglass45S5 (46.1 SiO_2, 2.6 P_2O_5, 26.9

CaO, 24.4 Na_2O; in mol%), the first bioactive glass composition studied, for example shows a plateau of ion release between 4 and 12 hs of incubation at physiological pH[239, 240]. While the substitution of SrO for calcium oxide in such a glass system was shown to extend the time until release plateau, it remained in the order of hours[241]. Such a rapid decay in release kinetics has been proposed to result from the formation of a passivating layer on the glass surface, often the calcium phosphate layer required for osteointegration[33]. Nuclear glass dissolution models predict that such a layer is the result of the low solubility silica relative to the glass modifiers included, resulting in the generation of a silica rich passivating layer which limits diffusion, and potentially results in the precipitation of secondary phases on the glass surface[229]. While such characteristics are desirable for a bone bonding application they serve to limit their functionality as ion releasing materials. Early investigation into the incorporation of borates into bioactive glasses suggested that boron resulted in less reactive glasses with either delayed bone bonding, or lack of bone bonding seen following implantation[212, 213]. These findings were challenged in ion release studies which demonstrate increased rates of release despite the lack of calcium phosphate layer formation[223]. Due to the high solubility of borate (>40g/l at 37°C) relative to silica (<0.2 g/l at 37°C) borate glasses allow for a greater extent of glass degradation before secondary phases such as HA precipitates occur, preventing the rapid plateau seen in silicate glasses[242, 190]. As such borate based bioactive glasses, which show both greater overall degradation, as well as sustained degradation reactions, would provide an advantage over silicate glasses for the release of TIIs.

Boron based bioactive glasses

Boron oxide has long been recognized to readily form an oxide glass from melt quench techniques, allowing for lower melting temperatures, and melt viscosities than silicate glasses[243]. As such, the inclusion of boron oxide into glass melts can improve ease of manufacturing and, reduce temperatures (and therefore energy consumption)

required for melting. While early implantation studies of bioactive borate glasses were thought to fail due to lack of surface reaction[31, 244, 220, 222]. For example, the switch from a silicate to borate based glass network lead to a tripling of the time to HA formation in a study of the surface reaction of glass fibres in SBF[222]. While this would suggest that borate glasses offer a slower reaction, greater concentrations of both calcium and phosphorous were seen in solution. The basis of this finding is the highly soluble nature of boric acid (>40g/l at 37°C) allowing for sustained release without the formation of precipitates[242]. Due to the limited formation of surface precipitates borate based glasses allow for sustained water infiltration, prolonging the dissolution reaction relative to silicate glasses.

While borate glasses have been demonstrated to show extensive glass network degradation (tailorable between 2 to 25 % weight loss over 7 d)[35], the exact mechanism is still debated. Studies of a B, Ca, Mg, Na, K glass system concluded that borate glasses release glass modifiers in stoichiometric proportion to the (alkali and alkali earth) modifiers contained, contrary to the ion exchange reaction seen in silicate glasses[34, 224]. The inclusion of phosphates and borates in the initial incubation media was been shown to increase the rate of ion release, a finding which contradicts previous saturation based glass dissolution models[34]. Studies of B, Sr, Ti and B, Sr, Ti, Na glasses in turn have suggested that while alkali oxide modifier release is proportional to time, the release of boron and strontium were non linear[35]. While Ti addition resulted in decreased in BO_4 coordination in both sodium containing and sodium free glasses in this study, it resulted in increased Sr and B release only for sodium free glasses, with no significant effect seen in sodium containing glasses. This again counters the linear polymer theory of glass degradation suggesting that network connectivity does not predict glass reactivity in borate networks. The investigation of a B, Sr, Na, La system in turn demonstrated that the addition of lanthanum was capable of generating linear ion release kinetics, demonstrating the importance of ionic complexes in the degradation process of purely borate glasses[245]. As glass

modifiers in borate glasses are often less soluble than boric oxide, modifier addition may serve to decrease overall glass degradation rates.

Furthermore, very little glass research focused on borate based glasses (less than 2 % of glass science articles published in 2013 focused on borate based systems), leaving the effects of modifier addition on glass structure (which can alter the molar volume of the glass, and has marked effects on glass degradation) poorly understood[246]. Despite our lack of understanding of the degradation reaction of borate bioactive glasses they have been used successfully in wound healing applications. For example, the use of copper doped borate bioactive glass has been demonstrated reduce healing time and improve angiogenesis in full thickness dermal defect animal models[247].

Despite these promising applications, the field of borate based bioactive glasses is limited by our depth of understanding of the composition-structure-property relationships of these materials. In a recent review of borate glasses for scientific and industrial applications, two challenges faced by the field were noted, which are of particular interest to their use as degradable biomaterials[248]. The first challenge is that much of our understanding of borate network structure is based on dated publications, limited by the analytical techniques of the time, and could be improved if fundamental studies were repeated with modern analytical techniques. The second is that the vast majority of these early publications focused on the inclusion of silicates, alumina or lead to increase glass durability, leaving little information on how highly degradable borates behave in isolation. In order to best utilize borate glasses for the release of TIIs, better understanding of how modifier inclusions alter the glass network,and thus degradation behaviour, is needed. As such, the first step in working towards a material capable to delivering long term strontium ion release for an anti-osteoporotic application is to develop a better understanding of borate glass networks and how they can be manipulated through compositional changed to modulate ion release.

Chapter 3

Rationale

According to the 2010 clinical practice guidelines for the diagnosis and management of osteoporosis, the focus of osteoporosis treatment should be on prophylactic measures to reduce the risk of fracture[39]. As such ideal fracture interventions would address the osteoporotic progression in order to reduce the risk of subsequent fracture and not just mechanically stabilize the bone. While a variety of systemic osteoporosis therapies are available and highly effective in the prevention of osteoporotic fracture when properly administered, they suffer from low patient compliance[16]. A study into the effect of low compliance on the efficacy of bisphosphonate therapies in American women (covered under private drug insurance) estimated that as few as 48 % of patients maintained compliance level required to experience any clinical benefit following 3 years of treatment[14]. Such low levels of compliance and continuance is referred to as a crisis of care for the condition, with new fracture rates failing to drop despite the availability of new and effective treatment to treat the disease.

To address the treatment of painful VCFs resulting from osteoporosis, PVP has offered a safe and effective method of reducing patient pain and improving quality of life[115]. While this method is effective in alleviating osteoporotic fracture related pain, it has been linked to high rates of subsequent fracture (as high as 33.4 % over three years follow up). This high rate of fracture is linked to off axis loading of adjacent vertebral bodies, and the underlying osteoporotic bone loss which caused the original fracture[20]. BKP may have improved upon this technique though the use of a height restoring bone tamp, reducing kyphotic deformity, however study results are not conclusive with reports of both decreased and increased subsequent fracture

rates[112, 249] . This method while offering improvement in height restoration over traditional PVP has a much greater procedure cost both due to increased staffing demands (due to the requirement of general anaesthesia, as well as increased duration) as well as increased equipment cost of 3,578 CAD per patient[113].

Prophylactic augmentation of non fractured, adjacent vertebral bodies at risk of collapse has emerged as a low cost alternative to BKP, increasing resistance to off axis mechanical loading, preventing further height loss, and reducing the rate of adjacent vertebral body fracture[139, 134, 128]. There are however uncertainties as to the effect of prophylactic PVP on the local bone quality. In silico modelling has suggested that high stiffness cement does not result in stress shielding of trabecular bone as initially proposed, rather it may increase loading, promoting remodelling while providing improved mechanical support[131]. The translation of such findings to implantation environments is questioned however due to concerns of local biocompatability with PMMA based cements which show evidence of fibrous encapsulation and suboptimal incorporation with tissue[28]. For optimal long term efficacy in reducing fracture risk, materials used in prophylactic PVP should provide long term mechanical stability (which can not be maintained by current calcium phosphate materials) as well as direct bone integration providing improved load distribution and remodelling.

The integration of anti osteoporosis therapy in the form of strontium ions into a composite resin cement could provide a mechanism of improving integration over PMMA based cements, while providing the long term mechanical stability required. Such a material could be used both for fracture fixation, and prophylactic augmentation to prevent fracture in high risk individuals. A bone cement capable of releasing anti osteoporosis agents could serve to further increase the efficacy of prophylactic PVP in osteoporotic patients, improving the local remodelling process surrounding the cement. While various attempts have been made to include anti osteoporotic agents into bone cements, these materials have either failed to address temporal release requirements, or to achieve therapeutically effective dosing, or failed to meet

the mechanical and handling requirements for a PVP cement.

This work will aim to investigate the feasibility of a borate glass reinforced composite resin cement, and to understand the effect of material composition on its dissolution characteristics. Composite resins have been selected due to previous reports of improved bone integration as well as their ability to release TII from the inorganic filler phase. Borate glass fillers will be investigated due to their sustained degradation kinetics as a possible method to improve the duration of TII release. Due to the limited knowledge of the effects of borate glass compositional changes, initial investigation into the effect of glass modifiers on glass structure will be used to tailor ion release. Modifications to both glass and resin components will be used to modulate the ion release profile with a goal of reaching therapeutic thresholds, reported to be between 8 and 88 mg/l[8, 6]. Ion release kinetics, mechanical properties and localised response in a small animal implantation model will be assessed in aim of generating long term therapeutic potential in a PVP material.

TIIs have successfully been used in biomaterials as therapeutic agents[236]. TIIs provide advantages through reduced chemical or thermal inactivation in the delivery device[250]. Previous work has targeted the release of ions as antibacterial, angiogenic, and neurogenic agents[236]. The majority of the research investigating TII delivery however has focused on bone regeneration and integration. Previous materials have released Ca, Mg, P, Zn, Sr, all with therapeutic aims. Strontium ions are known to be effective in increasing bone turnover and new bone deposition, with low levels of toxicity, and are thus a promising TII for release from biomaterials[251]. Furthermore, as a mono atomic ion, strontium is not subject to metabolic degradation or inactivation, nor is it preferentially excreted in patients with normal calcium balance[10]. For these reasons strontium is an attractive therapeutic agent for incorporation in a bone augmentation material.

Although some previous methods have shown promise in the therapeutic release of strontium a mechanistic understanding of ion release and its role in modulating cell

response is limited in the literature. Furthermore, many of the strontium releasing materials previously studied sacrificed material handling or strength to incorporate strontium; resulting in suboptimal materials for use in PVP. Modulation of strontium release is essential to ensure adequate release levels are reached and sustained. Previous research demonstrated different therapeutic thresholds for OBLs and OCLs to be between ∼8 and ∼88 mg/l respectively. While the majority of work focuses solely on OBL response, which demonstrates a significantly lower threshold[30, 9, 82, 8]. Specifically strontium mediated changes in proliferation and differentiation requires 15 or 22 d for OBLs and OCLs respectively[6]. While these mechanisms have been recognised by the cell biology community, little research has investigated methods of modulating release form therapeutic biomaterials beyond increased loading. In order for a strontium releasing bioactive cement to be effective as an anti-osteoporotic agent is must be capable of releasing strontium at a therapeutically effective level and maintain release for a therapeutic duration.

This combination of tailorability, and degradability in bioactive borate glasses makes them an ideal vehicle for ion release. Metal oxides in borate glasses, unlike in silicate glasses, can play multiple roles, acting as both network stabilizers or modifiers due to borons unique ability to exist in both three fold and four fold coordination[252, 253, 36]. The behaviour of a metal oxide in borate glass is determined by the concentration in which they are added, with a sharp change in behaviour seen in the proximity of 16-20 mol% concentration for alkali metals, and 30 mol% for alkali earth metals when used in a binary glass network, a phenomena commonly referred to as the borate anomaly[253, 254, 36]. As such the correlation between the degree of glass network disruption and metal oxide content cannot be calculated imperially[243]. A tertiary borate glass consisting of boron, strontium and sodium oxides was selected for investigation in this work aiming to better understand the effects of alkali oxide for alkali earth oxide substitution. This series of glass compositions maintains a boron content in the anomalous range (70 mol%)

substitution Na_2O (0 to 16 mol%) for SrO (30 to 14 mol%). While SrO was chosen a TII, Na_2O has been selected due to it's low cytotoxicity, being a common component of bioactive glass compositions. The substitution of these two oxides should give information on the importance of divalent cation network cross linking on the degradation behaviour of borate bioactive glasses. Along with the characterization of glass degradation (though the analysis of ion release), glass properties (density, glass transition) and glass structure (through NMR), glasses were analysed for compositional changes during firing (which have been previously been hypothesised to alter borate bioglass degradation[219]).This work should allow not only for the design of a glass with long term strontium release potential but also improve our fundamental knowledge of borate glasses.

Previous work has shown that the modulation of cement hydrophilicity can also be used to control the amount of water sorption into cement, and as such the elution of cement components. As borate glass networks are known to degrade due to hydration based reactions, control of cement hydrophilicity should allow for control of the glass degradation kinetics, and as such the release of TIIs from the glass. In a polymer based cement this can be done through the incorporation of hydroxyethyl methacrylate (HEMA, Figure 3.1), a highly hydrophilic monomer that has been shown to increase water uptake into copolymers[37]. While the incorporation of 10 % HEMA into a dental composite was shown to have not appreciable effect on ion release, the incorporation of up to 30 % by weight has been shown to double ion release[255]. Such gains in hydrophilicity and ion release are countered by losses in mechanical strength however, which have been reported to be as great at 40 % when a 50 % HEMA blend was used[37]. A design space between 15 and 45 % has thus been selected to investigate the trade off between ion release and cement mechanical properties. Along with ion release and mechanical properties, characterization of the cement setting and handling properties were used to assess if such a material could be of potential use in PVP.

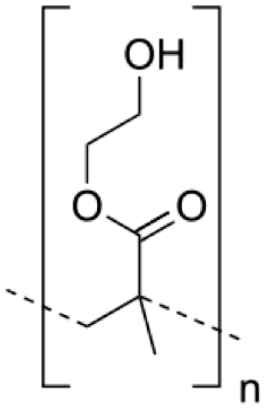

Figure 3.1: Hydroxyethyl methylacrylate monomer structure, showing highly polar hydroxyethyl side chain

Modulations in polymer hydrophilicity have previously been used in drug delivery materials to alter release kinetics. Hydrophilic polymers serve to draw water into the system, which allow for drug release, but also cause swelling in the polymer network. In highly compliant hydrogel systems mechanical loading has been used to counter this swelling behaviour leading to load responsive materials. Cyclic loading in particular has been demonstrated to cause significant increases in the release of reversibly bound hydrophilic drugs due to the alteration in the dissolved drug content within material voids during loading[256]. While PVP materials are much stiffer materials than their drug releasing hydrogel counterparts, they are also subjected to high mechanical loading. While unloaded, static, *in vitro* release assessment has remained the standard method of evaluating the release from therapeutic bone cements, the implantation environment would subject the material to high levels of cyclic compressive loading. While a number of factors have been investigated to better extrapolate *in vitro* release levels to *in vivo* behaviour in ion releasing materials, including alterations to the ionic composition of the solution, and flow through modelling, the effect of mechanical loading remain largely unexplored. To gain a better understanding of the effects of the mechanical environment and how this may alter ion release behaviour the final experimental component aims to subject the materials to physiologically relevant

mechanical loading elution environment. This experiment will assess if alteration in mechanical loading alter water sorption or ion release kinetics to determine if mechanical loading has an effect on ion release, and how this information could be use to better design elution testing protocols for such materials.

Finally, while composite resins have demonstrated significant improvements in local tissue response over PMMA based materials, the alterations suggested in this work would present significant deviations from previous formulations. High concentrations of HEMA may be beneficial in promoting water infiltration, however, the lower molecular weight and single methacrylate functionality of this monomer leave it more prone to leaching, imparting potential toxicity[257]. Similarly, the high rate of borate glass degradation relative to traditional fillers poses potential for burst release. For such a material to be successful in providing long term ion release to the surrounding bone, direct bone contact would be necessary, and as such, any fibrous encapsulation presents a barrier to ion transport and therapeutic potential. Due to the potential for local irritation imparted by leaching of both glass and polymer components in this novel cement formulation, a pilot implantation study is justified to assure that proper tissue integration is possible. To satisfy this goal, a New Zealand White rabbit femoral defect study presents an established load bearing orthopaedic implant model which could provide insight into the local tissue response. To assess if any deleterious effects are imparted by either the resin or glass phase, a comparison of precast cylinders of both a borate glass loaded composite resin, and an unfilled highly hydrophilic resin will be made. Along with initial implantation response, such a study could provide guidance for the design of future animal studies aiming to assess the therapeutic potential of a strontium releasing hydrophilic composite resin cement.

As a collection these four experiments will serve not only to investigate the feasibility of achieving therapeutically relevant release levels from a strontium releasing borate glass reinforced composite resin cement, but also serve to better understand the underling mechanisms which govern ion release and cement behaviours. This

increased knowledge could be used to further the study and design of ion releasing biomaterials by identifying key factors which control ion release, and the effect of the mechanical loading on ion release.

Chapter 4

Experimental work

4.1 Modulation of strontium release from a tertiary borate glass through substitution of alkali for alkali earth oxide

K. MacDonald[1], M.A. Hanson[2], D. Boyd[1,3]

[1]School of Biomedical Engineering, 5981 University Avenue, Dentistry Building, Dalhousie University, PO BOX 15000, Halifax, NS, Canada, B3H 4R2

[2]Department of Chemistry and Institute for Research in Materials, 6274 Coburg Road, Dalhousie University, PO BOX 15000, Halifax, NS, Canada, B3H 4R2

[3]Department of Applied Oral Sciences, 5981 University Avenue, Dentistry Building, Dalhousie University, PO BOX 15000, Halifax, NS, Canada, B3H 4R2

4.1.1 Author contribution statement

K.M. and D.B. conceived and designed the experiments, and revised the manuscript; K.M. performed the experiments, analysed the data, and wrote the paper. M.A.H. collected MAS-NMR data and provided MAS-NMR expertise

4.1.2 Abstract

The effect of the substitution of Na_2O for SrO in a series of nine borate glasses was studied to understand the effect of alkali for alkali earth oxide substitution in the boron transition range. Glasses were analysed for post-firing composition, density, glass transition, ^{11}B MAS-NMR and ion release in a simulated physiological condition (immersion in PBS at 37°C over time points of 1, 7, 30 and 60 d). Post-compositional

analysis revealed decreases in boron and sodium content during glass firing, and allowed for improvements in composition property relationships. Increased substitution of sodium resulted in decreases in glass density, glass transition, and non-bridging oxygen fraction in the glass. Strontium ion release kinetics were governed by Fickian diffusion and were not altered by the substitution of sodium for strontium in the glass. Boron ion release varied from pure Fickian diffusion controlled to a parabolic release demonstrating precipitation with high sodium contents.

4.1.3 Introduction

Bioactive glasses have been used in a variety of biomedical applications due to their ability to: (a) integrate with surrounding tissue, (b) fill defect or voids, (c) guide tissue regeneration (d) release TIIs [208]. These materials have been particularly successful in the field of hard tissue engineering where they have been shown to support the remineralization of dentin as well as the regeneration of bone tissue [31]. This remineralizing effect is believed to be due in part to high local mineral content resulting from network dissolution, as well as the ability of certain TIIs to alter local cellular behaviour[208, 31, 258, 259]. TIIs from bioactive glass dissolution products have also been shown to be beneficial in soft tissue applications, such as the release of copper ions, resulting in altered growth factor expression and improved angiogenesis[260, 261].

Strontium is a TII of particular interest in the field of bone regeneration. Strontium ions having been shown to effect bone cell metabolism of both OBLs and OCLs to elicit an increase in bone mineralization[29, 6]. This therapeutic effect on bone metabolism has been shown to occur at both the systemic level (altering hormonal pathways which control bone metabolism) and at a local level through direct cell stimulation [29, 6, 88]. Due to its ability to alter bone metabolism in the local environment strontium has potential application for local release from biomaterials [27]. Furthermore it has been shown to alter cell metabolism at low doses (8.8 mg/l), with

a large therapeutic window increasing its ease of utilization[29].

While glass dissolution byproducts may be beneficial for tissue regrowth, rapid dissolution and burst release from bioactive glasses can have a toxic effect or compromise mechanical stability at the implant site[208]. For example Fu et al. found that borate ions released for bioactive glasses resulted in both decreased proliferation and osteogenic potential (assessed by ALP assay) of murine MLO-A5 cells *in vitro*[262]. Reports of losses in compressive strength (associated with glass degradation) following incubation in simulated body fluid (SBF) can vary from 40 to 80 % depending on the composition of the glass[221]. Further to loses of mechanical strength, borosilicate glass designed for rapid dissolution and conversion into HA can decrease DNA synthesis up to 78 % in *in vitro* conditions, while a slow conversion analogue glass showed no inhibition[263]. A balance of network stability to reduce toxicity and degradation to allow tissue integration is often sought through modification of the glass network, this however requires an understanding of composition structure relationships.

Recent research into borate based bioactive glasses has shown highly tailorable degradation rates. For example in the borate glass series investigated by Hasan et al. the total mass loss varied from 2 to 22 % over 21 d through variation of glass composition[35]. A similar mass loss range of 3-20 % was reported in a single week in the work of Abdelghany et al.[264]. However, for borate based glass systems our understanding of the underlying composition-structure-property relationships lags behind that of other glass systems, partially due to the low fraction of glass science studies which focus borate glasses (2 % of USA publications while 20 % focused on silicate glasses between 2007 and 2013)[246]. For binary borate glasses composition-structure relationships have been well studied through the use of NMR, Raman and infrared spectroscopy for alkali or alkali earth containing glasses[253, 244, 252, 265, 254, 266]. These studies have focused primarily on the generation of four fold coordinated boron or non-bridging oxygens through the addition of modifying oxides and their effect on

the glasses density, thermal, and optical properties[253, 265, 266, 254]. These structural studies have explained the basis of the borate anomaly with a change in borate coordination occurring at higher modifier contents, and non-bridging oxygen formation at lower modifier contents. This change in structural role of glass modifiers results in a non-linear, parabolic, relationship between modifier content and glass properties such as density and glass transition[265]. Furthermore mixed alkali effects have been investigated in tertiary borate glasses and have been shown to have a dramatic effect on the transition region changes the region of inflection for glass properties[267]. The effect of mixtures of alkali and alkali earth metals however has not been as well studied for its effect on glass degradation kinetics.

Bioactive borate glasses remain of interest despite these difficulties due to their high variability in dissolution rates making them highly tailorable, providing potential for use in the delivery of TIIs. This study aims to investigate the TII release potential of a tertiary borate glass through the substitution of sodium (an alkali oxide) for strontium (an alkali earth oxide) and study the effect of this substitution on glass structure, and stability. This was undertaken through fabrication of a series of tertiary glasses in which Na_2O (0-16 mol% fraction) was substituted in for SrO (30-14 mol% fraction) while maintaining boron oxide concentration constant (70 mol% fraction). This glass was investigated to elucidate structure, stability, density, and glass transition. Post-synthesis composition analysis was performed to allow for more accurate composition structure and composition property relationships to be investigated.

4.1.4 Methods

Glass synthesis

Nine glasses were synthesized through rapid quenching of oxide melts according to the compositions listed in Table 4.1. Materials were weighed out and transferred

Table 4.1: Glass compositions by molar fraction of pre-fired material, and actual compositions revealed in compositional analysis (molar percentage and standard deviation).

Glass	Theoretical compositions (mol%)			Final Compositions (mol%)		
	B_2O_3	SrO	Na_2O	B_2O_3	SrO	Na_2O
BSr_{30}	70	30	0	67.5(0.7)	32.5(0.7)	
BSr_{28}	70	28	2	68.4(0.5)	31.4(0.5)	0.2 (0.01)
BSr_{26}	70	26	4	68.9(0.8)	27.6(0.9)	3.5 (0.1)
BSr_{24}	70	24	6	67.8(0.6)	25.4(0.5)	6.8 (0.1)
BSr_{22}	70	22	8	68.5(0.7)	23.8(1.0)	7.7 (0.3)
BSr_{20}	70	20	10	69.2(0.2)	21.1(0.1)	9.7 (0.1)
BSr_{18}	70	18	12	69.7(0.8)	18.0(0.1)	12.3 (0.03)
BSr_{16}	70	16	14	66.0(0.5)	17.3(0.8)	16.7 (0.4)
BSr_{14}	70	14	16	67.4(0.1)	15.5(0.9)	17.1 (0.2)

into jars, mixed in a dry blender for 1 h, then packed into Pt/Rb crucibles. Packed crucibles were placed in a Carbolite high temperature furnace at room temperature, then the temperature was raised by 50 °C/min to 500 °C, held for 1 h to calcinate and ramped by 50 °C/min to 1100 °C. The final melting temperature was held for 1 h before quenching between stainless steel plates. The resulting glass was ground using a planetary ball mill (Pulverisette 7) and sieved to retriever sub 45 μm powder (ASTM standard sieves, Cole Parmer). Particle size distribution was verified through laser diffraction of a wet suspension using a Mastersizer 300 model laser diffraction particle size analyser using distilled water as the dispersant.

Post-synthesis composition verification

Glass digests were performed in triplicate on all 9 glass compositions using 50 mg of glass dissolved in 10 ml of ultra pure hydrochloric acid (37 % Ultra Trace, Sigma Analytical) in an HDPP digest vial. Each vial was capped, gently agitated, and heated to 35°C for 2 h to ensure full dissolution of the glass powder. Glass digests were then diluted in 2 % HCl for ICP analysis of B, Sr and Na content. Elemental analysis of glass digests and extracts was performed by inductively coupled plasma

optical emission spectroscopy (ICP OES) on a Perkin Elmer Optima 8000 using a 2 % HCl suspension media, nitrogen carrier gas and an argon flame. Calibration curves were produced using Perking Elmer pure ICP standards. All samples were measured in triplicate and recorded as the mean of 3 readings. Actual (post-firing) compositions were used for all composition structure and composition property analysis.

X ray diffraction analysis

XRD was performed on all glass samples to verify amorphicity using a Bruker AXS D8 diffractometer (Department of Physics, Dalhousie University, Canada). The system utilized Cu-K radiation, a Gbel mirror, a Vantec-2000 area detector, and a copper target. Samples were measured over a scattering angles range from $10° < 2\theta < 110°$ (step size: 0.033°), with a step time of 0.5 s.

Structural characterization

Network structure of the nine glass compositions was investigated using ^{11}B MAS NMR experiments. NMR measurements were acquired on a 16.4 T Bruker Avance NMR spectrometer (^{11}B Larmor frequency= 224.67 MHz) using a 2.5 mm HX probe head operating in single resonance mode. ^{11}B parameters were calibrated on solid $NaBH_4$, which was also used as an external chemical shift reference (42.1 mg/l relative to BF_3Et_2O). Two spinning speeds were acquired for each sample: 25 kHz (32 transients acquired per sample) and 10 kHz (4 transients acquired per sample). A 0.56 s pulsewave used for all experiments, corresponding to a pulse angle of roughly 15°. Spin lattice relaxation times were determined by saturation recovery and ranged from 6 to 7 s. Five times this value was used at the pulse delay. As the stator gives a considerable boron background, the spectrum of an empty rotor was also acquired under identical conditions at each spinning speed. This spectrum was phased and adjusted for intensity before being subtracted from the experimental spectra.

Glass density

Density measurements were performed using a gas pynctometer (Micromeritics AccuPyc II 1340) with a helium purge gas, and 1 cm^3 chamber insert, packed with approximately 0.75 g of glass powder. Three glass samples were analysed for each composition with measurements taken as the mean of 10 readings.

Thermal analysis

Glass transition temperatures were determined for each of the nine glasses through differential scanning calorimetry using a TA Instruments Q200 DSC (TA instruments, Grimsby, Canada) fitted with an S type thermocouple. 30 mg glass samples were heated in platinum pans at a heating rate of 10°C/min from 100 to 800°C. Glass transition temperatures were determined as the onset of inflection as determined using Q series software (TA Instruments, Grimsby, Canada).

Ion release evaluation in simulated physiological conditions

Glass extracts were prepared in triplicate using 0.1 g of glass powder placed in a 15 ml conical tube with 10 ml of phosphate buffered saline (PBS) solution. Tubes were capped and agitated to distribute glass particles, then incubated at 37°C for 1, 7, 30, 60 and 90 d. Following incubating samples supernatants were filtered through a 0.2 μm syringe tip filter, and diluted in 2 % hydrochloric acid for ICP analysis of Sr and B content (Na measurement omitted due to high background measurements in PBS). All ion release measurements were reported in mg/l for assessment of therapeutic potential.

Statistical analysis

All statistical analysis was performed using Prism 6 software (GraphPad Software Inc., La Jolla, USA). Significant differences between glass properties were determined using one-way ANOVA following linear regression of glass properties using least squares. Multilinear regression was performed using least squares analysis in R. Differences in ion release between time points and compositions were assessed using two way ANOVA analysis followed by Tukey's honest significance test, at significance levels of $p < 0.01$ and $p < 0.001$. Strontium and borate ion release profiles were fitted to linear, one phase and two phase exponential decay models, and fits were compared using a corrected Akaike's informative criteria to correct for variation in fit parameters between models[268].

4.1.5 Results

All glasses exhibited a decrease in boron content, of 0.3 to 4.0 %. Losses of sodium content were seen in glass compositions with theoretical sodium content of 10 % or lower, while those with 12 % sodium or greater showed increases in sodium content (Table 4.1). No significant differences in glass composition were found between any two adjacent glass pairings (i.e. initial strontium contents of 30 and 28, 28 and 26 etc). XRD analysis of all nine glasses showed no sharp peaks, indicating an amorphous glass structure free of identifiable crystalline species (Figure 4.1). The fraction of tetrahedral coordinated boron varied from 39.2 to 43.2 % in the glass series investigated (Figure 4.2). Linear regression to actual strontium content showed no significant effect on boron coordination ($p > 0.1$). However, multi-linear regression (generated through least squares regression in R), which accounted for boron content, showed both boron and strontium to have a significant effect on boron coordination in the glass ($p < 0.02$).

Glass transition temperatures varied from 520 to 641 °C with a linear increase

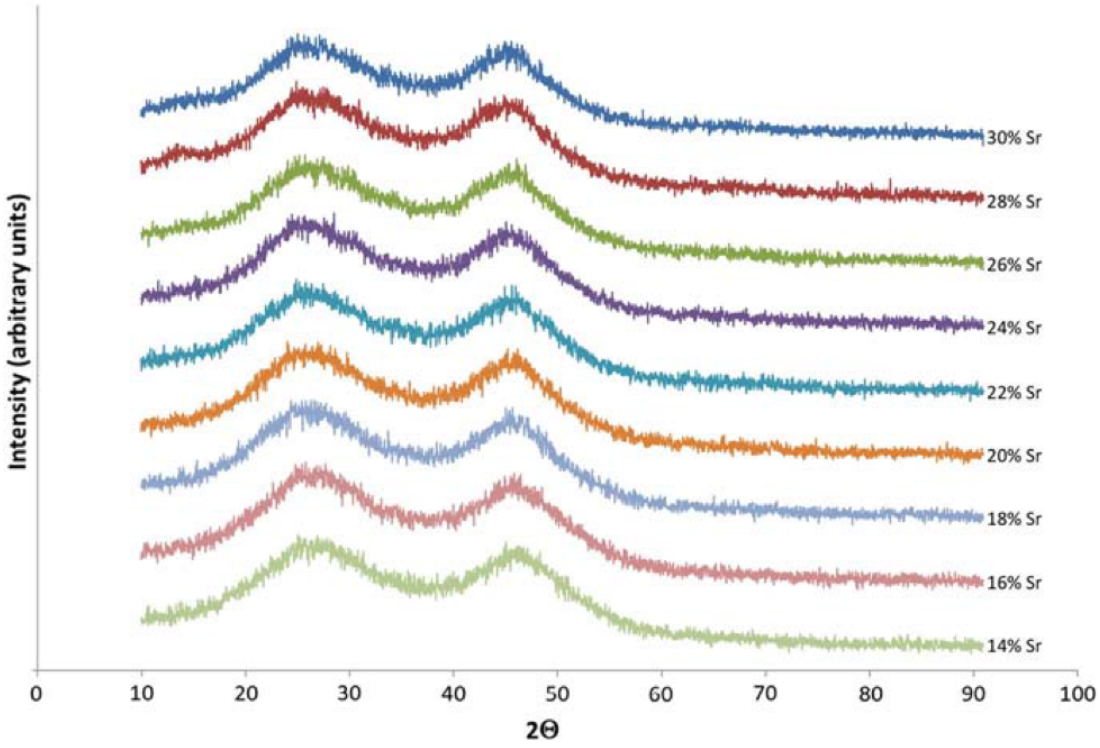

Figure 4.1: XRD analysis of all nine glass compositions showing two amorphous peaks, at 2θ values of approximately 25 and 45, corresponding to 3 and 4 coordinated boron centers in the glass.

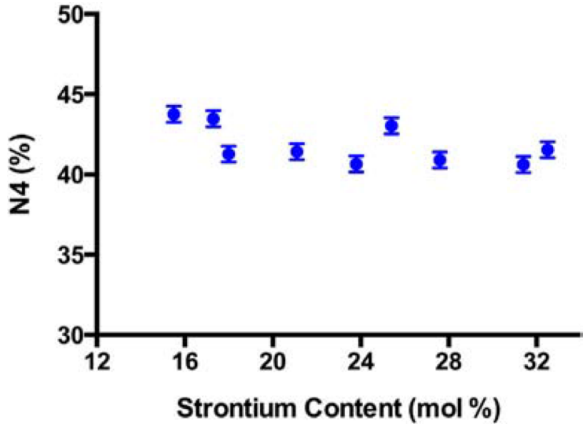

Figure 4.2: Fraction of four coordinated boron content by post-fired strontium content.

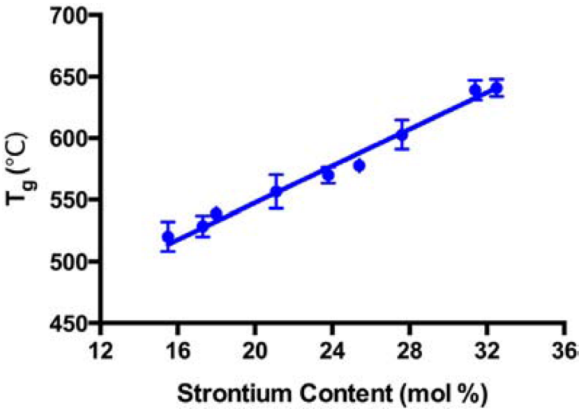

Figure 4.3: Variation in glass transition temperature with post-fired strontium content.

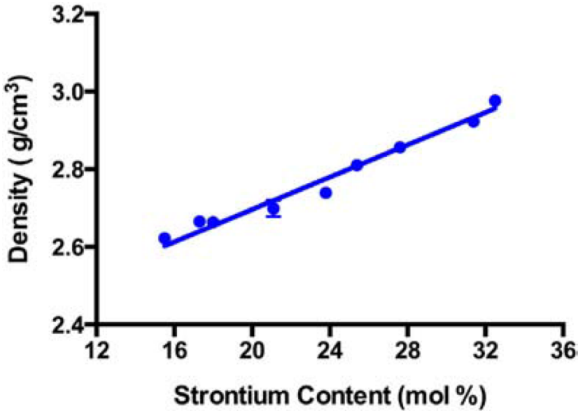

Figure 4.4: Variation in glass density with post-fired strontium content.

in glass transition temperature being seen with increased (actual) strontium content (R^2=0.98) (Figure 4.3). A similar correlation (R^2= 0.97) was seen between glass density and strontium content with values ranging from 2.62 to 2.98 g/cm^3 (Figure 4.4).

Strontium ion release increased with increased strontium content and time with the highest release of 1418 mg/l seen with the 30 % Sr glass at 60 d, and lowest release of 18 mg/l strontium at 1 d with 14 % Sr. Strontium release efficiency (% of initial strontium loading released from the glass) ranged from 1 to 7 % at one d with a maximum release efficiency of 20 to 41 % seen at 60 d (Figure 4.6). Release efficiency was greatest in the 30 % Sr glass, while the 18 % Strontium glass showed the lowest efficiency in strontium release. Strontium ion release increased linearly with the root

of time as seen in Figure 4.5 for all nine glasses analysed, suggesting that Fickian diffusion was the dominant mode of release. Linear regressions showed high goodness of fit with R^2 values ranging from 0.85 (30 % Sr) to 0.99 (18 % Sr). Rate constants for strontium release (slope of linear regression of release plotted against $t^{1/2}$) increased linearly with increasing strontium content, as seen in Figure 4.7 ($R^2 = 0.95$).

Boron release levels were greater than strontium release levels for all glasses and time points with the greatest boron release seen at 60 d with the 30 % Sr glass (1760 mg/l) and the lowest release of 420 mg/l seen with the 20 % Sr glass at one d. Boron release efficiency ranged from 6 to 7 % at one d, reaching a maximum of 16 to 24 % at 60 d (Figure 4.6). The fraction of boron released after one d of incubation exceeded the fraction of strontium released for all glass compositions, however, at later time points greater efficiency in strontium release was achieved by all glasses. Boron ion release kinetics altered between glass compositions with low strontium content glasses showing a decrease in cumulative release over time. A comparison of linear and quadratic fits of ion release was performed using a corrected Akaike informative criteria, with results presented in Table 4.2. High strontium glasses (30, 28, 26 % Sr) were linearly proportional to $t^{1/2}$ (as was seen with strontium release) while low strontium glasses (24, 22, 20, 18, 16, 14 % Sr) showed a parabolic release with respect to $t^{1/2}$ showing a decrease at the 60 d time points.

4.1.6 Discussion

All nine glass compositions were found to form a glass through plate quenching without evidence of crystallization or phase separation through XRD and thermal analysis. Post-fabrication compositional analysis (Table 4.1) revealed changes (B_4%) in glass composition, and lead to increased linearity for composition property relationships (specifically for density and glass transition).

The variation in tetrahedral boron content did not show a strong correlation to

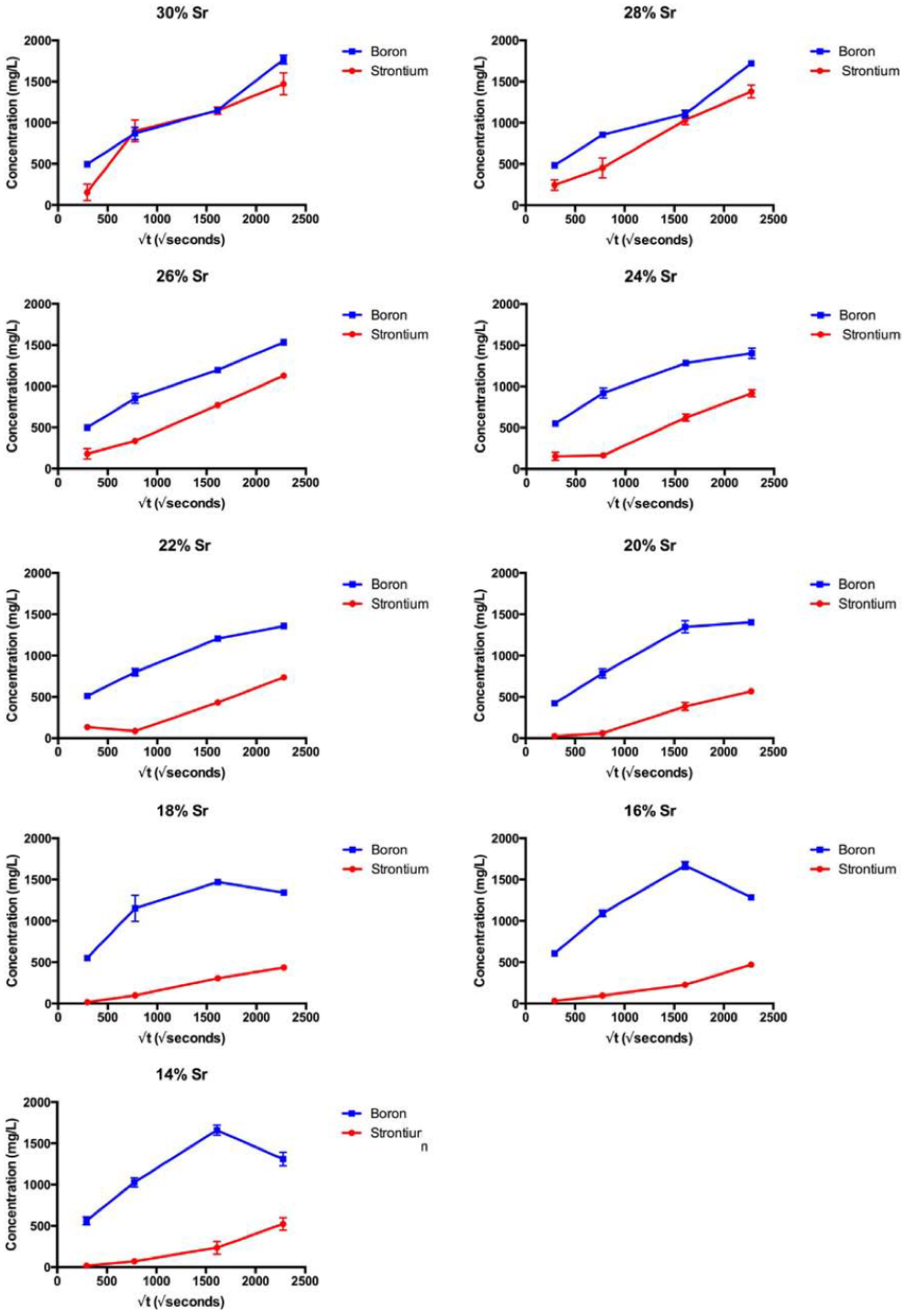

Figure 4.5: Ion release profiles for boron and strontium release of all nine glasses studied. Strontium release profiles show a linear release with respect to the root of time, characteristic of diffusion-controlled release. Boron release profiles vary among glass compositions, with low sodium glasses displaying diffusion-controlled release, while high sodium glasses demonstrate a decrease in boron release over time, indicating a precipitation reaction.

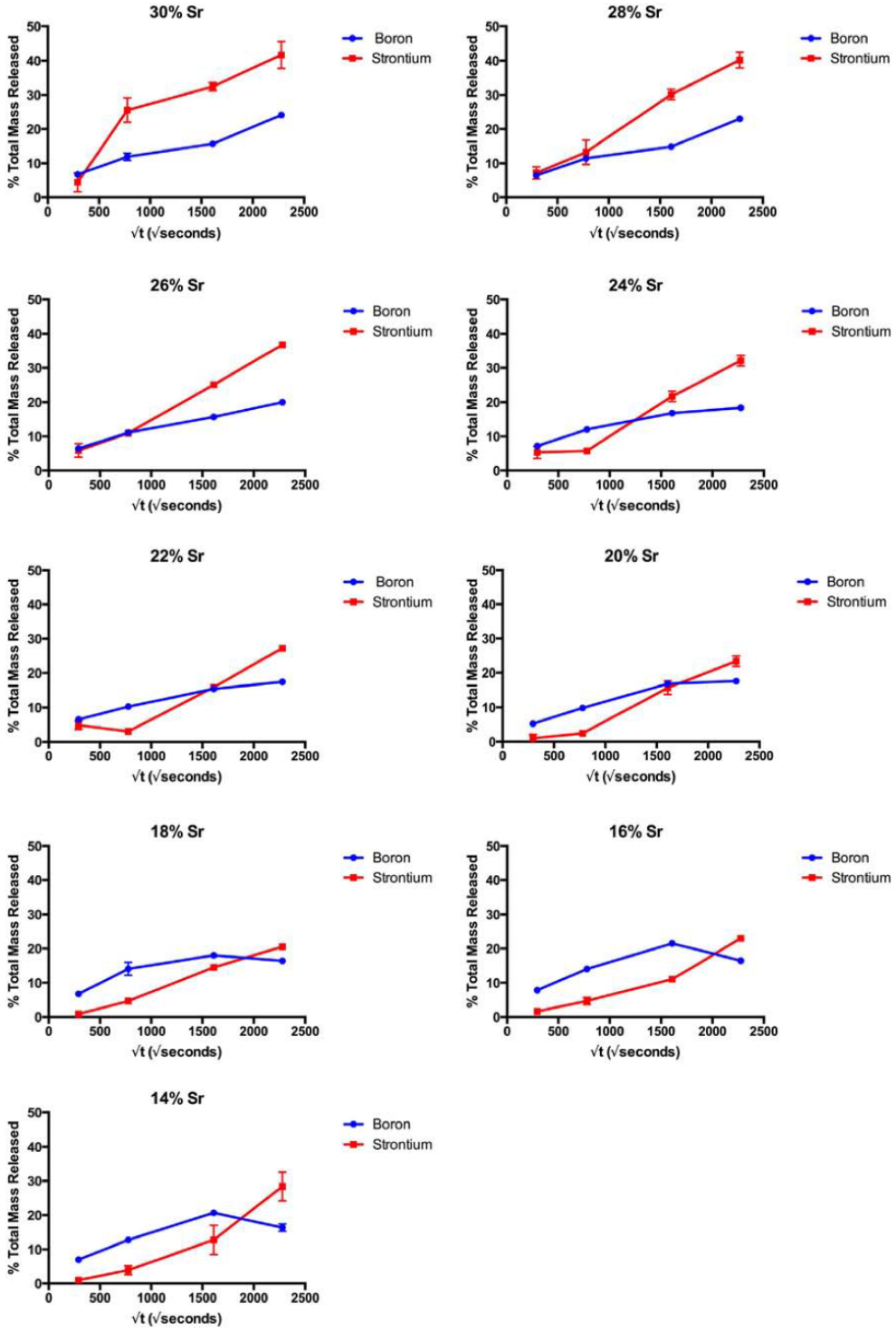

Figure 4.6: Ion release efficiency for strontium and boron release (expressed as a percentage of initial element loading released) showing a transition from preferential boron release to preferential strontium release with time.

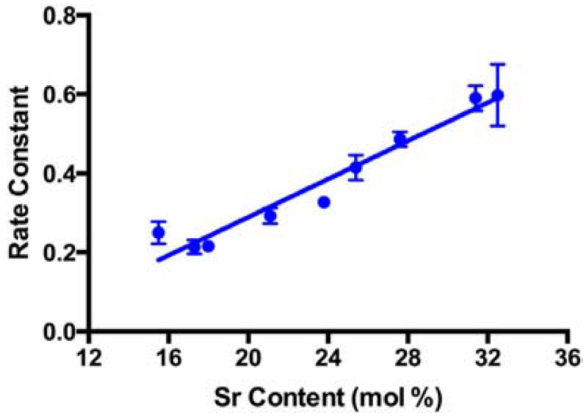

Figure 4.7: Linear increase in rate constant of strontium ion release from glass series with increasing strontium content ($R^2 = 0.95$).

theoretical glass compositions,when a single variable linear model was used for analysis (R^2 adjusted of 0.25). Post-fabrication compositional analysis of glass was essential in understanding the effect of strontium for sodium substitution in the glasses studied, as the variation in boron content loss during firing masked the effect of glass modifiers. This was demonstrated by the lack of fit for a linear strontium model, while strontium demonstrated a statistically significant effect ($p < 0.05$) when incorporated in a multi linear model, which accounts for boron losses, as seen in Table 4.1. This improvement in model fit remains statistically significant when corrected for the increased model complexity using a corrected Akaike informative criterion at a significance level of 0.05.

When the variation in boron content between glass compositions is accounted for it becomes clear that an increase in strontium content results in a decrease in the fraction of tetrahedral coordination (Table 4.1). This trend is in agreement with previous work done with alkali borates which showed that smaller monovalent ions favour the production of tetrahedral boron coordination's as their small size allows for closer bonding to the BO_4^- centre, while larger ions favour the generation of a nonbridging oxygen [254]. However, glass density follows a linear trend in relation to strontium content, most likely due to the increase in the molar weight of the

glass caused by the incorporation of high molar weight strontium. A similar trend was found in a series of Si, Ca, Na (70 % Si, 30-X% Ca, X% Na) glasses in which strontium was substituted for sodium resulting in a linear decrease in density and glass transition with increasing sodium addition [269]. Glass transition also increased linearly with strontium content despite evidence of decreased N_4, indicating a more open network. These results suggest that strontium ions may play a structural role in the glass serving to increase network rigidity, despite the increased content of non-bridging oxygen. Potentially attributable to the increased oxygen coordination surrounding modifier ions serving to stabilize the glass network [265, 254]. While the effect of substituting an alkali oxides into the glass shows similar changes in glass properties for both borate and silicate glass, the structural origin of this change differs. While sodium is commonly used to decrease glass density and increase glass reactivity through network disruption in silicate glasses, this mechanism is not seen in borate glasses. Instead an increase in boron coordination was seen which would suggest a less reactive glass despite the decreased density.

The linear release of strontium ions with respect to the root of time suggests that Fickian diffusion is the rate-determining step for strontium ion release. This is consistent with previous studies into the ion release mechanism from bioactive glasses in which the release of glass modifiers occurred through hydration and proton exchange, at a rate governed by the diffusion of water into the system[31, 223, 219]. Non-zero intercepts of the linear release profiles provide evidence of a burst release effect. This has also been noted in other bioactive glasses studied for ion release and is commonly attributed to fine surface powder generated during the dry grinding of glass. While this release mechanism is seen with bioactive silicate glasses over a short time frame, diffusive release remained constant over 60 d for the glasses studied. This sustained release could offer benefits over silicate bioactive glasses for extended TII delivery.

The linearity between strontium content in the glass and rate constant of release

provides further evidence of Fickian diffusion controlled release. This rate constant, a product of the initial concentration of the leachate and the diffusivity of the system, varied linearly with strontium content, indicating equal diffusivity in all glasses studied. This further supports evidence that the increased molar mass of strontium resulted in the increased glass density, as a change in network structure would result in an altered diffusivity of the glass. Similar parabolic kinetics were seen for boron release and mass loss in tertiary Na_2O, CaO, B_2O_3 glasses studied by George and Brow, which showed the formation of a Ca-phosphate surface layer acting as a diffusion barrier[34].

Further work by George and Brow investigated the dissolution of a Na, Ca, K, Mg, P containing borate glass, and found ion release ratios remained constant relative to boron release over 7 d of incubation, indicating uniform dissolution of the glass network[224]. Results in the current study in turn show a preferential release of strontium from the glass, increasing with time up to 60 d, indicating a non-uniform leaching of glass modifiers is occurring. Furthermore, while diffusion controlled release was seen for strontium, boron release displayed a reduction in cumulative ion release over time in low strontium glasses. At early time points, low strontium glasses lead to increased boron release, which would be consistent with the NMR results suggesting increased non-bridging oxygen, and therefore decreased hydrolysis needed to release boron from the network. The development of a parabolic release with respect to the root of time however is not consistent with a purely hydration controlled release and can be attributed to the presence of sluggish precipitation kinetics. Precipitation was not seen in either of the studies performed by George and Day, however the time frames investigated were notably shorter than the current study.

As seen in Table 4.2 the relative probability of a parabolic release profile greatly increases with sodium content, with low sodium glasses following purely diffusion controlled kinetics, and precipitation only seen in high sodium glasses. Such a polymerization of borate solutions has been previously shown to be stabilized by the

presence of alkali ions in solution as demonstrated by Brinker et al. who reported a linear increase polyborate polymerization with lithium oxide addition[270]. Furthermore extensive glass dissolution may result in the alkalization of the solution, greatly decreasing the solubility of polyborates in solution. While similar precipitations reactions are seen at the surface of silicate glasses resulting in a protective film, the precipitation seen in these glasses does not result in altered strontium release mechanisms over the time period studied. Through this mechanism it is possible that while sodium substitution in a borate glass does not decrease glass dissolution, it may serve to decrease boron release through the generation of a non-protective film. Such a non-protective film could be beneficial for the delivery of TIIs, allowing for selective ion release and preventing toxic boron accumulation.

Strontium ion release levels for all glasses far exceeded the threshold for CaSR activation in MG62 OBL like cells *in vitro* (0.47 μg/l) for all time points investigated. Similarly, the release range on 433 to 1471 mg/l after 60 d is well above the *in vitro* levels required to induce OCL apoptosis (8.8 mg/l Sr^{2+}). Strontium ranelate therapy at an oral dosage of 2 g/d has been reported to result in plasma strontium concentrations between 6 and 10.6 mg/l, and has demonstrated clinically significant increases in BMD and bone strength. This therapeutic threshold was exceeded by all compositions for all time points tested suggesting possible efficacy of these glass dissolution by products for the improvement of bone quality. A systemic toxicity threshold for strontium ions is not well established due to the high variability of absorption in oral dosing, and limited information on non-oral exposure routes[29, 271, 251]. *In vitro* assessment of strontium toxicity to periodontal ligament derived fibroblast through exposure to strontium ranelate in cell culture indicated an onset of toxicity at 5 % solution, the equivalent of 1706 mg/l Sr[271]. While the release levels seen in this study remain below the *in vitro* toxicity threshold for fibroblast indicated by the study by Er et al., such results are difficult to extrapolate to *in vivo* conditions and further testing would be justified

Table 4.2: Corrected Akaike informative criteria table comparing linear and quadratic fits to boron ion release.

	30 %Sr	28 % Sr	26 % Sr	24 % Sr	22 % Sr	20 % Sr	18 % Sr	16 % Sr	14 % Sr
Simpler model	Straight line	Straight line	Straight line	Straight line	Straight line	Straight line	Straight line	Straight line	Straight line
Probability it is correct	74.37 %	71.45 %	64.25 %	0.02 %	0.15 %	9.90 %	b0.01 %	b0.01 %	b0.01 %
Alternative model	Quadratic	Quadratic	Quadratic	Quadratic	Quadratic	Quadratic	Quadratic	Quadratic	Quadratic
Probability it is correct	25.63 %	28.55 %	35.75 %	99.98 %	99.85 %	90.10 %	N99.99 %	N99.99 %	N99.99 %
Ratio of probabilities	2.90	2.50	1.80	5184.20	651.59	9.10			
Preferred model	Straight line	Straight line	Straight line	Quadratic	Quadratic	Quadratic	Quadratic	Quadratic	Quadratic
Difference in AICc	2.130	1.835	1.172	17.11	12.96	4.417	21.14	28.53	18.71

4.1.7 Limitations

While this study aimed to quantify composition structure relationships in tertiary borate glasses, only the role of borate in the system was probed through the use of ^{11}B MAS-NMR. Divalent cations have been reported to act in varying roles in a borate glass, however their role could not be identified through Sr NMR due to the low natural abundance of ^{87}Sr, and relatively low strontium content of the glasses studied. As stated in the methods measurements of sodium loss from the glasses were omitted due to the high background of sodium in the buffered saline solutions. While glass dissolutions studies could have been performed in water to allow for sodium measurements, PBS was selected as a closer approximation to physiological conditions. Specifically, due to the role of proton exchange in bioactive glass degradation, a buffered solution was chosen to prevent large variations in pH which would alter the reaction environment from what would likely be seen in an implantation setting.

4.1.8 Conclusion

The substitution of sodium for strontium in a borate based bioactive glass resulted in a decrease in glass density and glass transition. Post compositional analysis was required to generate composition structure relationships, revealing that sodium favoured the generation of N_4 coordinated boron centres where as strontium favoured the generation of non-bridging oxygen. Increased sodium content resulted in parabolic ion release curves for boron release, indicating the presence of a non protective film during incubation in PBS. This resulted in decreased boron release while providing sustained, Fickian diffusion controlled strontium release over a 60 d time frame, exceeding therapeutic thresholds for both OBLs and OCLs.

4.2 The feasibility and functional performance of ternary borate-filled hydrophilic bone cements: targeting therapeutic release thresholds for strontium

K. MacDonald[1], R.B. Price[2,3], D. Boyd[1,3]

[1]School of Biomedical Engineering, Dalhousie University,

Halifax, NS B3H 1X7, Canada;

[2]Department of Dental Clinical Sciences, Dalhousie University,

Halifax, NS B3H 1X7, Canada;

[3]Department Applied Oral Sciences, Dalhousie University,

Halifax, NS B3H 1X7, Canada

4.2.1 Author contribution statement

K.M. and D.B. conceived and designed the experiments, and revised the manuscript; K.M. performed the experiments, analysed the data, and wrote the paper. R.B.P. contributed ATIR-FTIR expertise

4.2.2 Abstract

We examine the feasibility and functionality of hydrophilic modifications to a borate glass reinforced resin composite; with the objective of meeting and maintaining therapeutic thresholds for strontium release over time, as a potential method of incorporating anti-osteoporotic therapy into a PVP material. Fifteen composites were formulated with the hydrophilic agent hydroxyl ethyl methacrylate (HEMA, 15, 22.5, 30, 37.5 or 45 wt% of resin phase) and filled with a borate glass (55, 60 or 65 wt% of total cement) with known strontium release characteristics. Cements were examined with respect to degree of cure, water sorption, strontium release, and biaxial flexural strength over 60 d of incubation in PBS. While water sorption and glass degradation increased with increasing HEMA content, strontium release peaked with the 30

% HEMA compositions, scanning electron microscope (SEM) imaging confirmed the surface precipitation of a strontium phosphate compound. Biaxial flexural strengths ranged between 16 and 44 MPa, decreasing with increased HEMA content. Degree of cure increased with HEMA content (42 to 81 %), while no significant effect was seen on setting times (209 to 263 s). High HEMA content may provide a method of increasing monomer conversion without effect on setting reaction, providing sustained mechanical strength over 60 d.

4.2.3 Introduction

Strontium (Sr) has been demonstrated in various *in vivo* models to improve bone mass[272] and strength[273], leading to its subsequent use as a treatment for osteoporosis [29]. While oral Sr therapy (i.e., Servier Laboratories Sr ranelate), has demonstrated up at a 49 % reduction in VCF rate[7], early clinical trials predated a full understanding of the mechanism-of-action of Sr on bone[274]. Further research has since identified both localized and systemic effects associated with Sr[6, 54]. Beyond local efficacy, Sr also demonstrates accumulation in bone tissue, potentially providing sustained therapeutic effect following dosing[275, 83]. The discovery of its localized efficacy (and underlying mechanisms) has consequently lead to the investigation and development of therapeutic biomaterials for targeted local release of Sr ions[88, 276, 277].

From a design input standpoint, it is now recognized that the mechanism-of-action of Sr ions on bone metabolism relates to an uncoupling effect on OBL and OCL metabolism, which acts through the CaSR in both cell lines. Specifically, increases in proliferation and activity have been reported to occur at minimum Sr levels ranging from 8.7 mg/l[6] to 35 mg/l[82] while OCL inhibition occurs at higher Sr concentrations of 88 mg/l under *in vitro* conditions[6, 8]. Strontium also requires a sufficient duration of exposure, of over 20 d before the full benefit is achieved[6, 30]. While a minimum effective Sr dose is difficult to establish for localized release, it is agreed

that the effective dosage window is large due to its relatively low toxicity[278, 271]. Accordingly, localized release systems may target between 8.7 mg/l and 88 mg/l of Sr, the therapeutic threshold for OBLs and OCLs respectively.

The development of Sr-releasing injectable bone cements for the augmentation of osteoporotic VCFs, is an area of particular interest in the literature[200, 203, 201, 204, 202, 279, 194]. Despite predating much of the clinical evidence, and the detailed mechanistic understanding of Sr as an anti-osteoporotic agent, such materials have provided enhanced bone integration relative to controls[194, 195, 280]. Nonetheless, these studies lacked the guidance of accepted therapeutic threshold limits required for altered bone metabolism (including temporal dependencies), and, as such, the assessment of Sr release relative to these levels has not been widely studied. To develop an effective Sr releasing biomaterial capable of exerting an anti-osteoporotic effect, concept materials must be approached from a drug-device combination development standpoint. It must be engineered to provide both: (i) the necessary Sr release levels and (ii) maintain this therapeutic level over the duration required to achieve optimized therapeutic efficacy[6, 30].

A Sr releasing anti-osteoporotic cement must also maintain the characteristics necessary of a PVP material, including sufficient sustained mechanical strength, injectability, and biocompatibility[1]. Bis-GMA based composite resin cements (e.g., Cortoss®, Orthovita, Malvern, PA, USA) have demonstrated improved biocompatibility relative to conventional PMMA cements for vertebral body augmentation, while simultaneously proving a method of TII release from the inorganic filler phase[28]. As such Bis-GMA based composite resins present an ideal base for the development of a PVP material capable of releasing Sr at a therapeutic level. Previous studies aiming to release therapeutic agents from such dimethacrylate cements (both in dental and orthopaedic applications) have utilized hydrophilic monomer additions to increase water sorption, and therefore mediate subsequent ion (or drug) release in a controlled fashion[281, 282, 283]. For example the incorporation of HEMA into a Bis-GMA,

triethylene glycol dimethacrylate (TEG DMA) system has been shown to double the total ion release from composite dental cements[284].

While this approach has proven to be effective in increasing water sorption and release, the filler phase of composite cements is frequently based on phosphosilicate glasses, which show limited degradation kinetics (that decay rapidly over time)[208], and are thus unlikely to provide sufficient sustained release. While phosphosilicate bioactive glasses show a rapid decay in ion release, borate based glasses can be designed to release ions both through leaching as well as through the direct hydrolysis of the glass network, allowing for sustained ion release kinetics[224]. A previously investigated borate glass showed preferential, diffusion controlled release of Sr with 38 % percent of initial Sr content released over 60 d[285]. While they present many advantages for use in therapeutic ion delivery, fully borate based bioactive glasses cannot be silanized, potentially weakening the filler matrix interface[286]. This effect may be magnified by the effect of adding HEMA, which has previously been reported to decrease mechanical strength by as much as 40 %[37].

Arising from these questions, and limitations, this study has been designed to investigate the degradation kinetics of a series of borate-glass composite resin cements to assess the feasibility and functionality of such a system as a therapeutic Sr releasing biomaterial for use as a PVP material. To achieve this goal, a well-characterized borate glass with Fickian diffusion-controlled Sr release kinetics[285] has been selected for use as a reinforcing agent, in a Bis-GMA, TEG DMA, HEMA blend resin phase. This study is designed to assess the effect of both resin hydrophilicity as well as glass filler content (55-65 % of total cement weight) on cement handling characteristics, strength, water sorption, and Sr release over a 60 d time frame with a view to establishing Sr release levels capable of achieving the 88 mg/l required for uncoupling, for over 20 d to achieve maximum therapeutic efficacy.

Table 4.3: Compositions of resin phase, and glass loading of the cement compositions, in weight percentage.

Composite		**Group**				
		A	**B**	**C**	**D**	**E**
		1 2 3	4 5 6	7 8 9	10 11 12	13 14 15
Resin	Bis-GMA	41.474	37.725	33.975	30.225	26.475
Phase	TEG DMA	41.474	37.725	33.975	30.225	26.475
Part	**HEMA**	15	22.5	30	37.5	45
One	BPO	2	2	2	2	2
Resin	Bis-GMA	42	38.25	34.5	30.75	27
Phase	TEG DMA	42	38.25	35.5	30.75	27
Part	**HEMA**	15	22.5	30	37.5	45
Two	DHEPT	1	1	1	1	1
Glass		55 60 65	55 60 65	55 60 65	55 60 65	55 60 65

4.2.4 Results

Cement handling properties

The working times for the cements examined (Table 4.3) ranged from 150 to 255 s (Figure 4.8), cement setting time ranged from 209 to 263 s (Figure 4.8). While decreases in working time with increasing HEMA content were seen for some cement compositions (significant difference between composition A1 and B1, D1, E1; composition B1 and E1; composition C1 and E1; composition C2 and E2; composition E3 and A3, B3, C3), no overall trend was noted. No significant differences were seen between cement setting times.

ATR-FTIR Degree of conversion

Attenuated total reflectance Fourier transform infrared (ATR-FTIR) spectra showed characteristic peaks for resin, glass filler and initiation system as seen in Figure 4.9, with main peak assignments provided in Table 4.4.

Small variations were seen between the two unset resin pastes, with weak peaks at 1767 and 1790 cm^{-1} , indicating the presence of BPO initiator [289]. Spectra collected from both the (i) pastes and (ii) set cements included peaks at at 1717 cm^{-1},

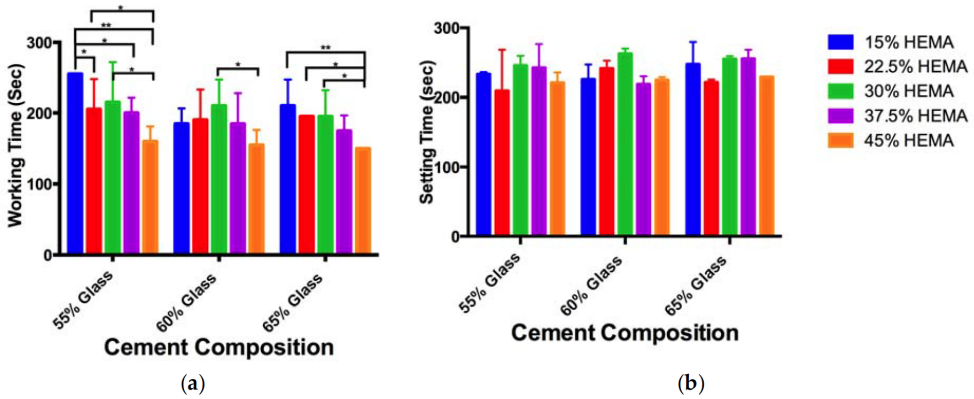

Figure 4.8: Cement (a) working times, and (b) setting times, significant differences are marked with "∗"($p<0.05$) or "∗∗"($p<0.01$).

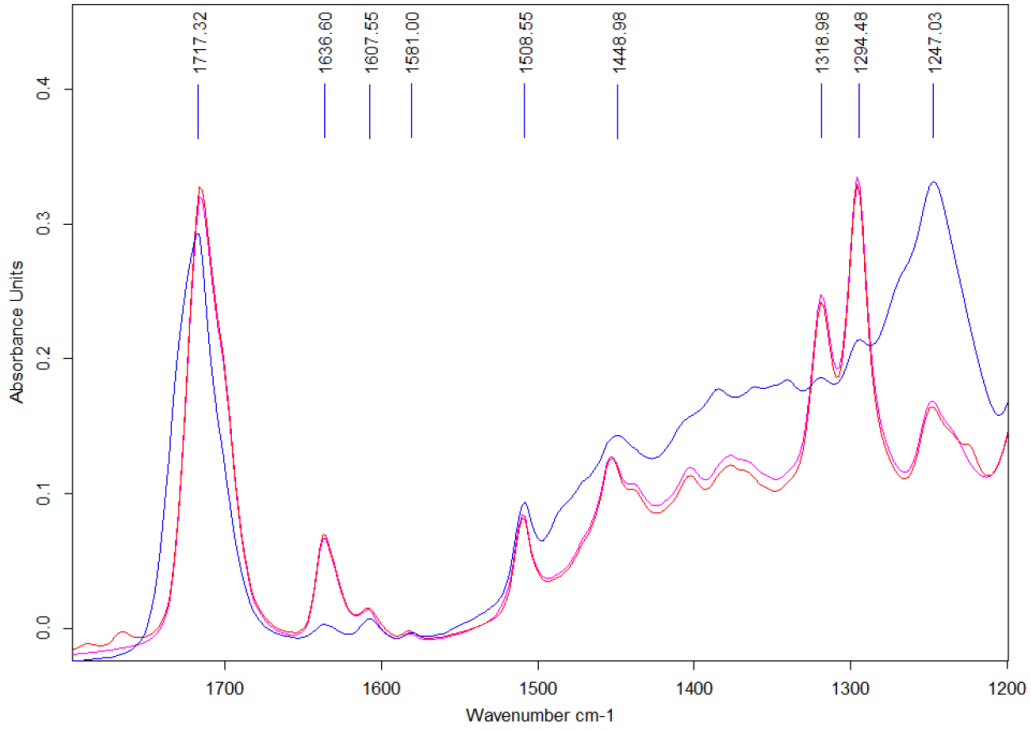

Figure 4.9: Representative ATR-FTIR spectra collected on unset cement pastes (red and pink traces for paste one and two respectively), and set cement samples (blue trace) of cement composition A1 (15 % HEMA, 55 % glass).

Table 4.4: ATR-FTIR peak locations with corresponding cement component, and functional group.

Band Region (cm^{-1})	**Cement Component**	**Functional Group**	**Reference**
1700-1720	Resin	C=O and C=O hydrogen bonding	[287]
1630-1640	Resin	C=C double bonds	[275]
1600-1610	Resin	Aromatic rings	[275]
1500-1520	Glass	Non bridging oxygen stretching	[288]
1280-1320 (2 peaks)	Glass	Boron-oxygen ring vibrations	[288]
1240	Glass	Ortho and pyro borate asymmetric bond stretching	[288]
1747&1790	Initiator	Benzoyl peroxide ring vibration	[289]

1637 cm^{-1}, and 1608 cm^{-1}, arising from the carbonyl, aliphatic and aromatic regions respectively. Peaks attributable to the borate glass filler are visible in the region of 1508 cm^{-1} (non bridging oxygen bond stretching), 1300 cm^{-1} (boron oxygen ring vibrations), and 1240 cm^{-1} (asymmetric bending of pyro and ortho borate groups) [288]. The degree of conversion (DC)for set cements (Figure 4.10) varied between 42 % (composition A1) and 81 % (composition E3). Significant increases in the DC were seen with increasing HEMA content for cements with equal glass content. Similarly, significant increases in the degree of conversion were seen between 55 % and 65 % glass loadings for equal HEMA contents, but not the 55 % and 60 %, or 60 % and 65 % pairing.

Biaxial flexural strength

Cement biaxial flexural strength granged from 16 MPa to 44 MPa after 24 h, and 16 to 28 MPa at the 60 d time point.

Increasing HEMA content resulted in significant decreases in cement strength at all time points investigated ($p < 0.01$). Increased glass loading resulted in significant decrease in cement strength at the 60 d time point only ($p < 0.01$). A significant

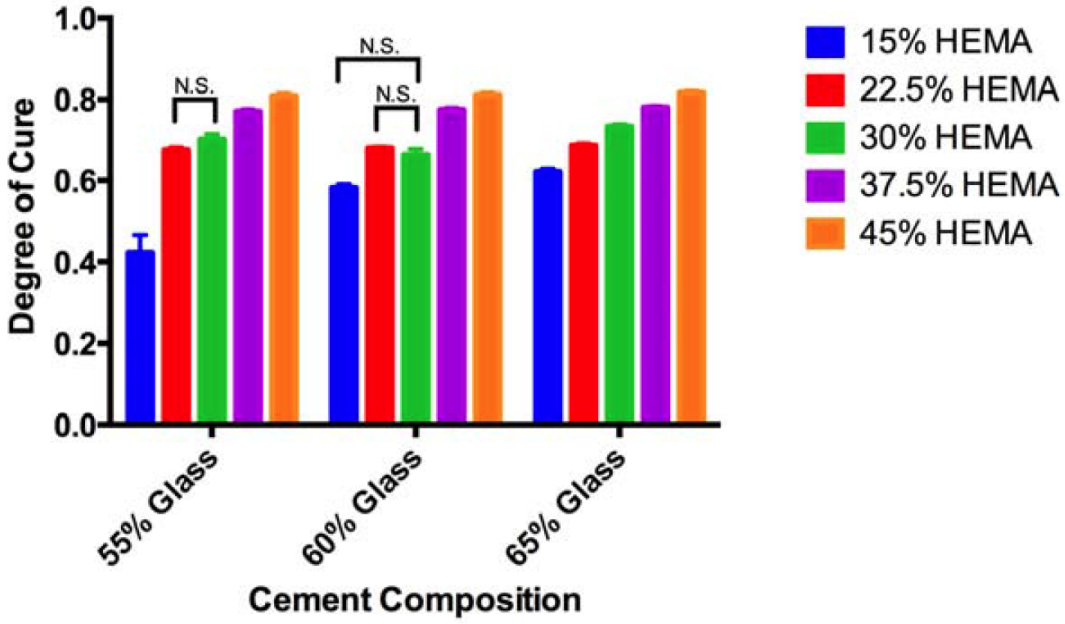

Figure 4.10: DC measured through ATRFTIR analysis with standard deviation, showing increased DC as the HEMA content increased, ($p < 0.01$, unless otherwise noted.

decrease in cement strength between the 1 and 60 d time points was seen for compositions of group A and B ($p < 0.01$), while cement compositions of group E increased in strength over 60 d ($p < 0.01$).

Cement water sorption and weight loss

After 24 h, increasing mass gain (1.3 to 5.8 %) of specimens was associated with both increased HEMA and glass content in the resin composites (Figure 4.12). Peak mass gain occurred after 14 d for cements of group C, D and E. Conversely cements of group A and B did not achieve peak mass gain until 30 d of incubation.

Maximum mass gains ranged from 11.3 % (A3, 30 d) to 16.4 % (C1, 14 d) of initial dry weight. Glass loading had no effect on the long-term mass gain for compositions of group A, B and C, while glass loading exerted a significant effect for group D and E compositions. HEMA content initially resulted in significant increases in mass gain

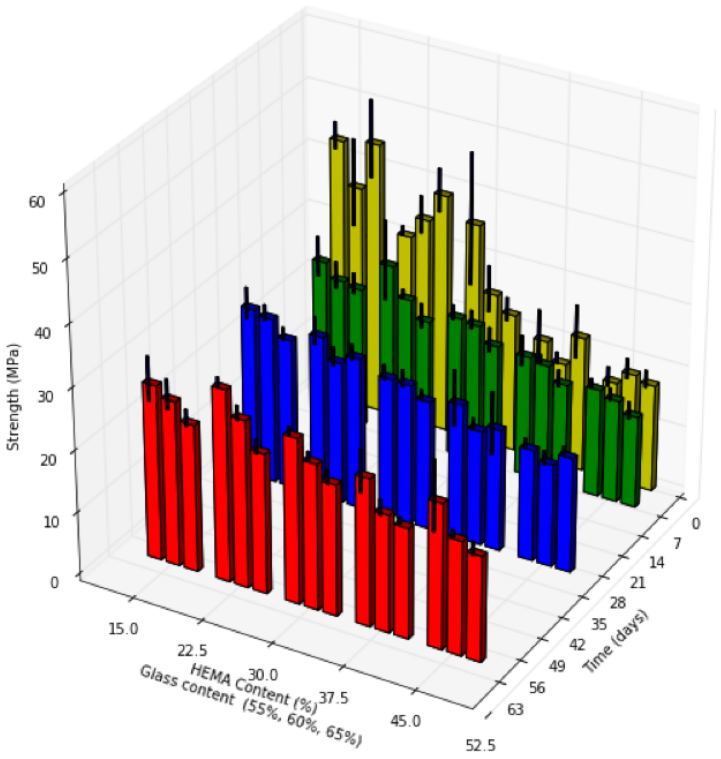

Figure 4.11: Cement biaxial flexural strength (MPa) at 1, 7, 30 and 60 d incubation, with standard deviations.

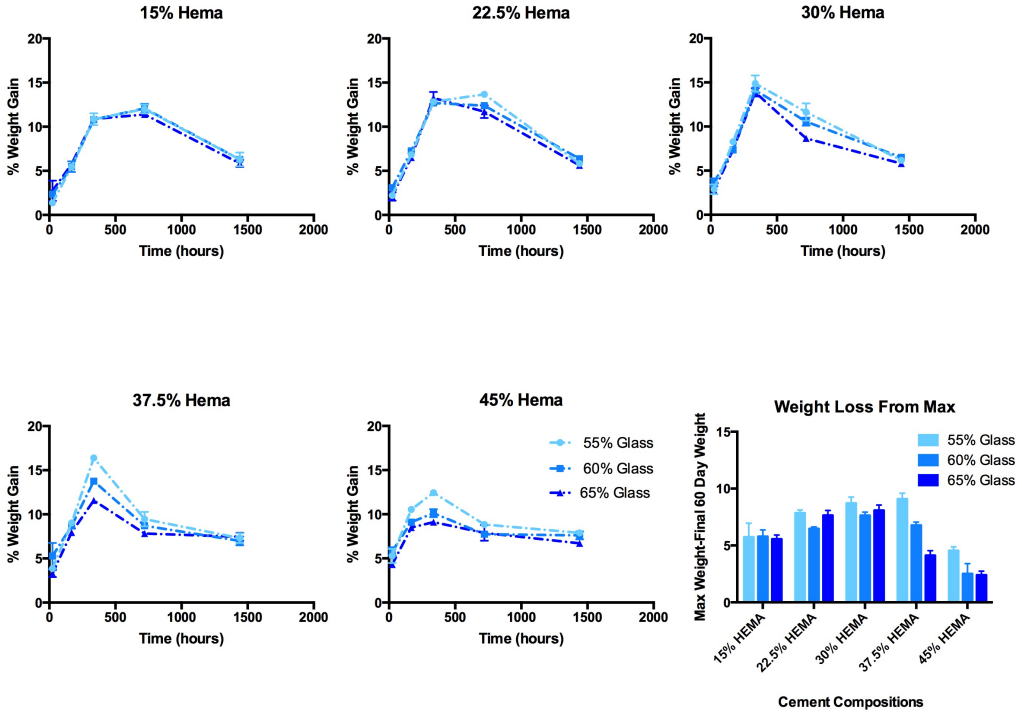

Figure 4.12: Cement weight gains over 60 d of incubation in PBS (with standard deviations), and weight loss from max (calculated as difference between maximum weight gain, and final weight gain at 60 d) as a measure of glass filler loss.

for all glass loadings; no significant effect was seen at extended time points. While sample mass decreased between 30 and 60 d, it is assumed that hydration increased, and decrease in mass is due to glass filler loss. As such, mass loss between the maximum weight achieved, and the final weight at 60 d was used as a proxy measure of glass degradation. Mass loss from peak weight gain was found to be the greatest in group C.

Ion release

Total Sr release from cements ranged from 9 to 32 mg/l following 60 d of incubation in PBS (Figure 4.13). These release levels corresponded to between 0.3 and 1.8 % of the Sr initially present in the samples (Figure 4.14). B release levels were much greater ranging from 67.7 to 183.6 mg/l, the equivalent of 4.6 to 12.9 % of the initial B content at the 60-d time point.

No significant differences in Sr release levels were seen between the compositions after 1, 7 and 14 d. Following 30 d of incubation cements of groups C, D and E released more Sr than group A and B samples ($p < 0.01$). After 60 d of incubation, samples from group C released significantly more Sr than all other HEMA loadings ($p < 0.01$). Release efficiency of Sr, measured as the % of initial Sr loading which was released into solution ranged from 0.3 to 1.3 % after 60 d, while release efficiency of B reached a maximum of 8 to 15 %. Previous investigation into the dissolution kinetics of the glass filler used showed preferential release of Sr from the glass network utilized in this study (i.e., the release efficiency of Sr was greater than the release efficiency of B) [285]; conversely, the cement extract data in this study showed greater release levels for B relative to the Sr release. As B release shows the degradation of the glass network, it is assumed that Sr is in fact released concurrently from the glass during degradation, but is not free in solution.

SEM analysis confirmed large regions of a Sr and phosphate containing precipitate at the surface of cement samples, showing evidence of crystallization at later time

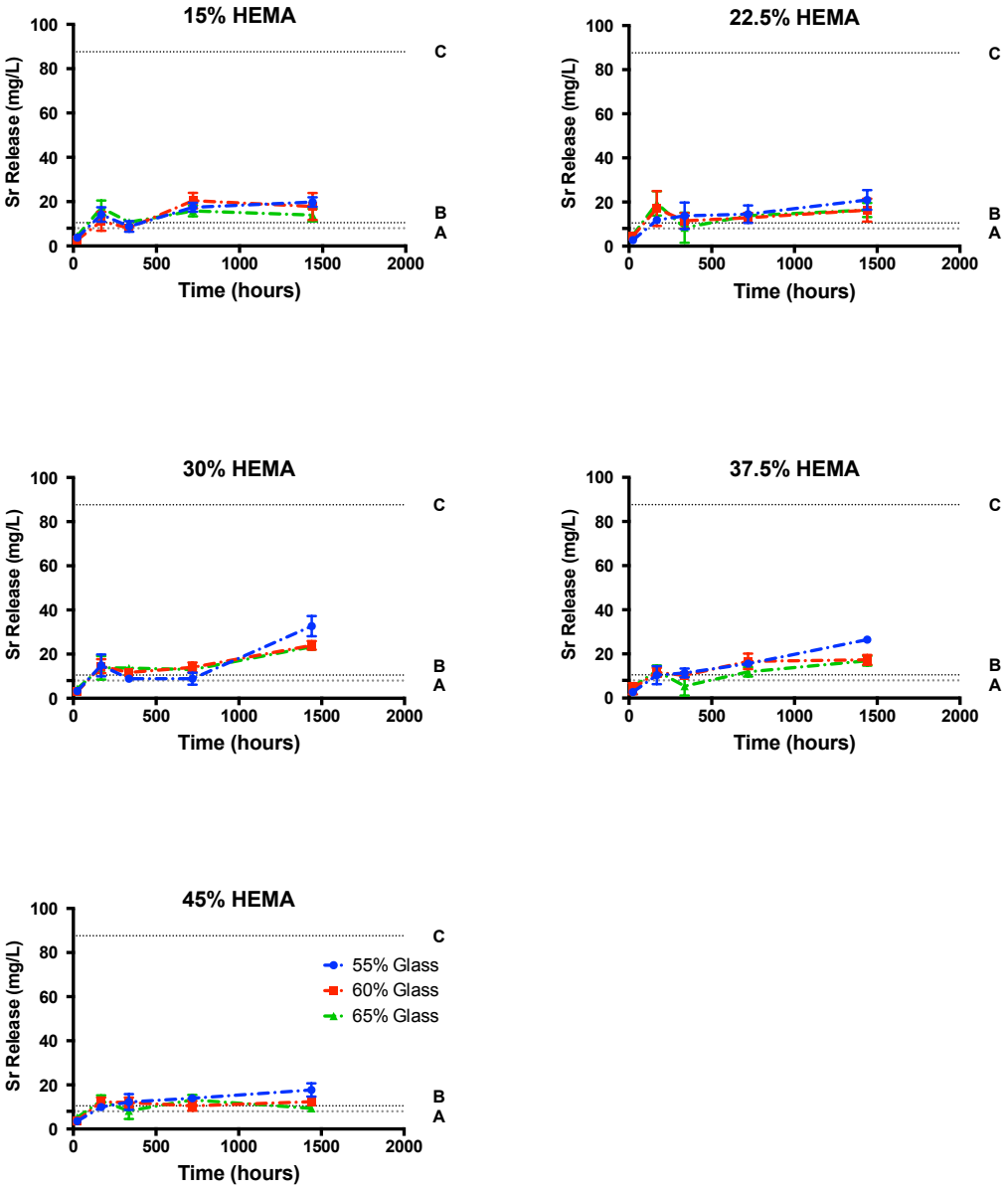

Figure 4.13: Sr release from cements into PBS in mg/l, relative to (A) *in vitro* OBL activation threshold [6]; (B) serum Sr concentration reported in the Treatment of Peripheral Osteoporosis (TROPOS) study (10.8 mg/l) [7] and (C) *in vitro* OCL inhibition threshold [8]

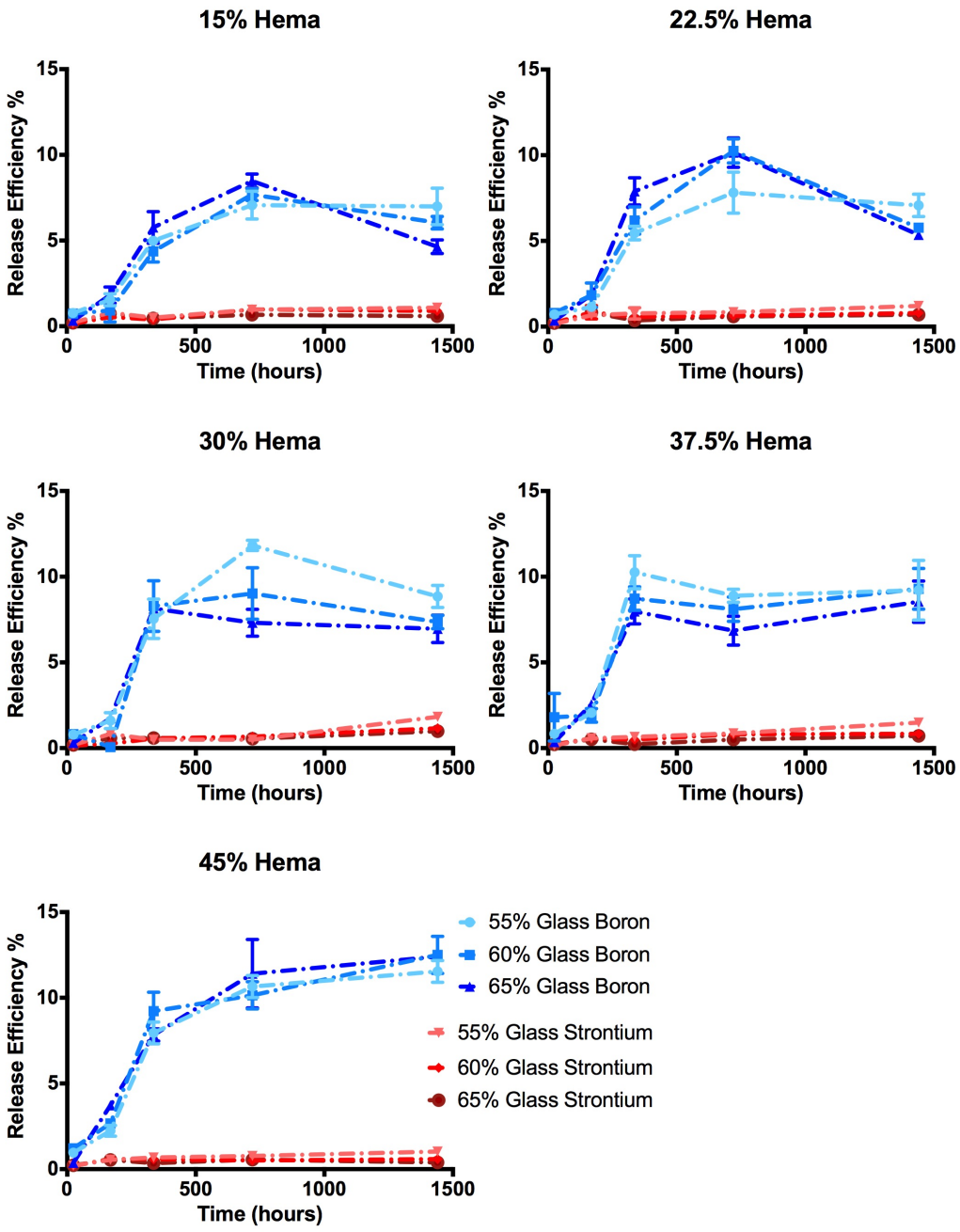

Figure 4.14: Ion release efficiency as % of initial elemental loading for B and Sr demonstrating preferential release of B from the cements.

points (Figure 4.15). After a single d of incubation, Sr phosphate precipitates were found on the surface of the glass filler for cements of group A, while group E cements displayed more dispersion of these deposits on the surface of both filler and resin phase. Energy-dispersive X-ray spectroscopy (EDS) analysis of the unreacted resin (Figure 4.15) revealed a surface Sr content of 4.63 % Sr by weight, while reacted surfaces had Sr contents of 18 to 33 % after one d of incubation, increasing to 20 to 45 % after 60 d. Sr enriched areas also showed between 6 and 10 wt% phosphate.

4.2.5 Discussion

The inclusion of HEMA, up to 45 % of the resin weight was achieved without significant reduction of the cement setting time. While some variations in cement working time were observed, this is likely due to the subjectivity of the measurement method, as previously reported[290]. The observed setting times were below the 20 min target frequently cited in the literature as a requirement for PVP materials[1]. Nonetheless, Cortoss, a two paste composite resin, is clinically utilized and has a reported setting time of 5-8 min for this indication[28]; as such the setting times reported for the experimental cements in this paper may not represent a clinical limitation. Specifically, if a similar "mix on demand"system were to be utilized for the experimental cements, it may eliminate the time for hand mixing, and simplify work flow in the clinic. Should extended handling characteristics be necessary it is known that prechilling the resins can extend the handling characteristics by up to 79 %[158, 291]; such an increase would leave the setting time of the cements investigated in this study within the range of those reported for Cortoss®.

Aside from the clinical determinants of setting, the DC is an important predictor of safety and performance; both in terms of mechanical strength, and biological performance. With respect to the latter it is known that unreacted monomers serve to plasticize the polymer matrix, reducing cement strength. This was demonstrated by Ferracane Berge and Condon who reported a 75 % increase in flexural strength

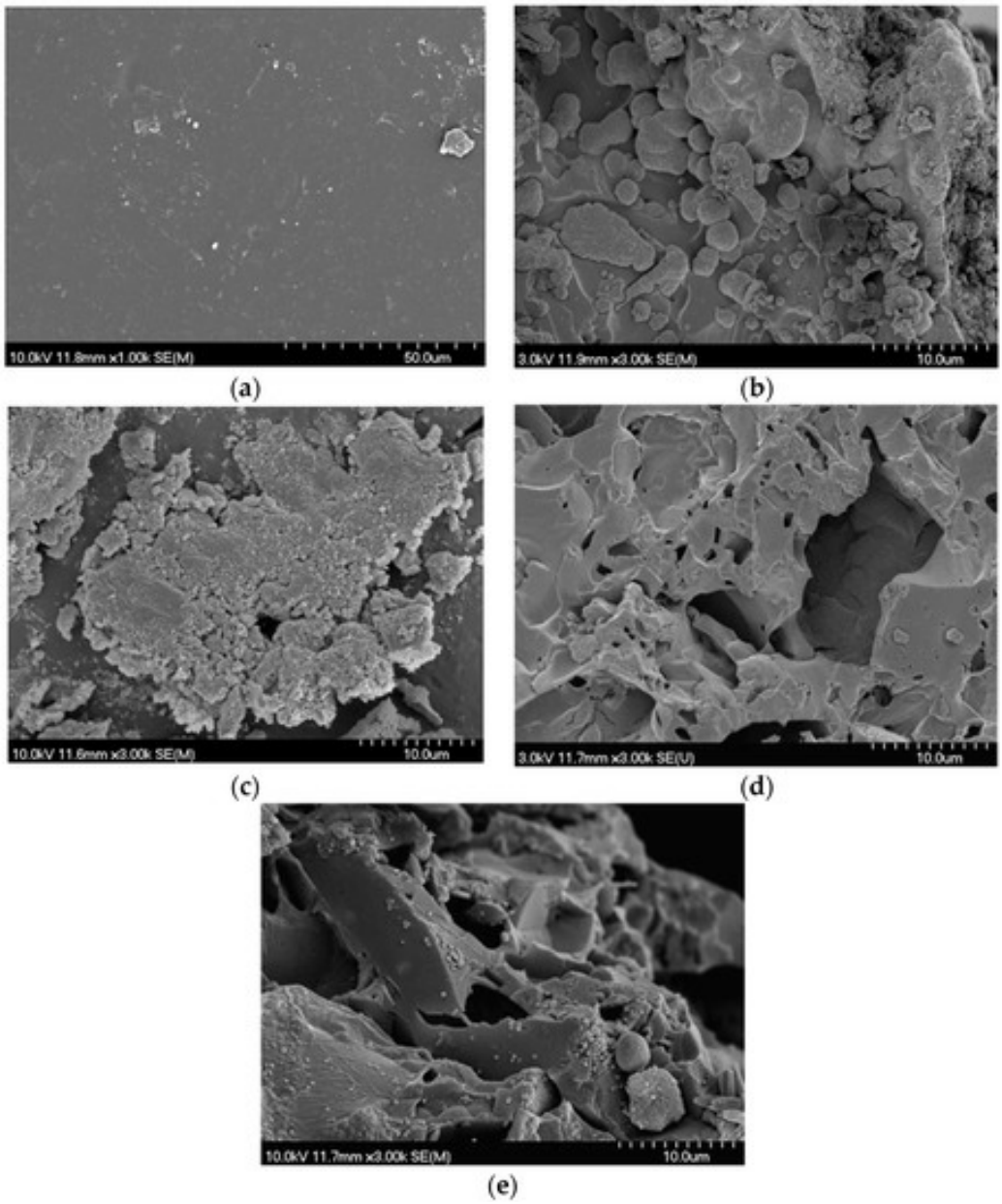

Figure 4.15: Representative SEM images of resin surfaces for (a) control unreacted surface of group E, 60 % glass cement (b) Group E 60 % glass cement, 1 d of incubation in PBS; (c) group E 60 % glass, 60 d of incubation in PBS; (d) group A 60 % glass, 1 d of incubation in PBS; and (e) group A, 60 % glass 60 d of incubation in PBS, demonstrating the development of a Sr rich surface precipitate

through improved DC[292]. The remaining unreacted monomer may be leached into the surrounding environment, increasing the probability of the occurrence of harm to local tissues[293]. The degrees of conversion previously reported for Cortoss®range from 76 to 86 % depending on storage conditions, similar to the results seen in this study, however for the latter (i.e., Cortoss®) measurements were performed using differential thermal analysis and not ATR-FTIR[158]. Measurements of DC may vary up to 10 % between methods, with varying reports of over or underestimation[287, 294]. DC measurements in this study were much greater than those reported for adhesive resins with similar co-monomer compositions (30-60 %), which showed a decreasing DC (as measured though ATR-FTIR) with increasing HEMA content, as opposed to the increase seen in this study[37]. A report of increased degree of polymerization with increased HEMA content, similar as to what was seen in this study however, was seen when comparing Bis-GMA HEMA blends to Bis-GMA, TEG DMA, HEMA blends in the study of amorphous calcium phosphate resin composites developed by Antonnuci, where conversion rates ranged from 79.3 to 89.9[287]. These conflicting reports have been attributed to either the lower reactivity of HEMA relative to Bis-GMA decreasing the DC[37], or alternatively, the low viscosity of HEMA imparting greater mobility allowing for greater cure[287]. While HEMA is less cytotoxic than both Bis-GMA and TEG DMA, its smaller molecular size, single methacrylate functional group and greater hydrophilicity result in higher rates of leaching, giving it a greater impact on resin cytotoxicity in dental materials[293]. The data reported in this paper indicate that increased HEMA content may be beneficial for these materials beyond increasing hydration of the matrix; specifically we observe a high level of cure for the cements examined in this work, which will reduce the concentration of unreacted monomers available for leaching, and as a consequence may improve the biological response.

From a mechanical performance standpoint, the biaxial flexural strengths of the compositions studied ranged from 44 down to 16 MPa (1 d), dropping to between 28

and 16 MPa (60 d). Biaxial Flexural strengths previously reported for commercially available PVP materials are significantly higher than the materials examined in this work. Previously reported biaxial flexural strengths for PMMA bone cements are 99 to 113 MPa after 1 and 30 d in SBF respectively, while strengths reported for Cortoss® range from 96 MPa to 59 MPa after 1 and 30 d respectively[159]. While Cortoss® s two paste system is packaged preloaded in a mixing/extruding device, the cements in this study were hand mixed to accommodate the small sample size and large number of compositions investigated. Such hand mixing has previously been linked to increased porosity and decreased mechanical strength due to the inclusion of air pockets during mixing when compared to mechanically mixed cements, this may partially explain the lowered flexural strength[149]. The lower biaxial flexural strengths seen in this study also likely results from the substitution of HEMA a small mono-functional methacrylate for the larger Bis-GMA dimethacrylate. While high Bis-GMA content provides increased mechanical strength, the inclusion of smaller co-monomers as diluents is necessary for workable orthopaedic or dental materials to reduce the viscosity of the resulting cement[295]. In this study, both TEG DMA, and HEMA served as diluents. Increased mechanical strength may be achieved for these cements through the elimination (or reduction) of TEG DMA content, allowing for increased Bis-GMA content, while maintain proper viscosity solely through HEMA addition. As high HEMA content cements demonstrated no loss of mechanical strength over time, with no appreciable effect cement setting time, and improved the DC, such a blend may provide improved long term strength and reduced cytotoxicity without compromising cement handling properties.

While no application specific standard exists for flexural strength of PVP materials, a 50 MPa minimum flexural strength is dictated by ISO 5833 for acrylic bone cements used in arthroplasty fixation. Much lower flexural strengths are required in non arthroplasty fixation cements, such as Hydroset, a CPC designed for void filling which has a biaxial flexure strength of 9 and 6 MPa at 1 and 30 d of incubation in a

SBF[165]. The decrease in cement strength seen with time with both Cortoss® and Hydroset was seen with the compositions of group A and B in this study, higher HEMA content cements however did not share this trend. The apparent ability of high HEMA content cements to maintain strength over time, despite the greater extent of glass filler degradation seen, may be explained by one of two factors: a more rapid loss of strength preventing the initial starting strength from being measured at the 24 h time point, or the formation of Sr phosphate precipitates within the resin as evidenced by SEM. While the current cement resin blend studied is unlikely to provide the water sorption required for extensive Sr deposits to form within the bulk of the material, the biaxial flexural test is sensitive to surface effects, and therefore may represent a surface strengthening effect form the mineral deposit seen[296].

Another interesting finding of this work were the changes in sample mass observed as a function of time. We propose that this observation encompasses three phenomena; (i) water sorption; (ii) glass dissolution (as shown through ion release); and (iii) the precipitation of Sr and phosphate mineral on the surface of the cements (as evidenced by SEM and EDS, Figure 4.15). The influence of these concurrent phenomena cannot be isolated based on the existing study design, and as such no mechanistic model for Sr ion release could be accurately fitted to our ion release data from the cements. The earlier onset of maximum weight gain in high HEMA content cement indicated a more rapid loss of glass filler, which was verified though the increased release of B into solution. Collares et al., studied a series of adhesive resin blends with similar HEMA content ranging from 15 to 50 % of resin blend (in a Bis-GMA, TEG DMA, Bis EMA blend), and reported water sorption of 74.7 to 174.1 $\mu g/cm^3$ following 7 d of incubation in distilled water. The 7-d weight gains observed in this study ranged from 95 to 187 mg/cm^3, orders of magnitude greater. Possible explanations for the large difference in mass gain could be both the macroporosity imparted by the incorporation of degradable glass filler, as well as the precipitates seen on the surface of the cements leading to overestimating of water content. It is also of note

that the DC seen in Collares study were much lower, and thus cured adhesive resins would contain a large fraction of unreacted HEMA, which is less hydrophilic than in its polymerized state, and may have lead to mass loss through leaching.

The effect of glass filler content on weight gain varied with HEMA concentration, high HEMA compositions showed decreasing weight gain with increasing glass content, while low HEMA compositions showed little to no effect of glass filler fraction. Similar results were seen in a study of amorphous calcium phosphate reinforced resins, where it was noted that the effect of glass filler on water sorption was dictated by the relative hydrophilicity of the two phases[287]. Similarly in this study, low HEMA content cements showed no change in water sorption with changing glass content, as hydrophilicity did not differ sufficiently between the two phases.

The relative release ratios of B and Sr seen in this study varied greatly from the release profiles reported for the glass (in isolation); the glass filler used is this study has previously been shown to exhibit preferential Sr release over 60 d (release efficiencies of 46 % and 19 % for Sr and B respectively)[285]. In this investigation, the release efficiency of B increased with increasing HEMA content (Figure 4.14), indicating that glass network hydrolysis did increase with HEMA content and water sorption, as expected. This trend however did not translate to increased Sr release into the solution. Previous investigation of the glass filler in isolation reported that (i) a single homogeneous glass phase was formed; and (ii) Sr release was governed by the diffusion of water into the glass network[287]. It can thus be assumed that as B release indicates the hydrolysis of the glass network, an equal or greater fraction of Sr must have been lost from the glass filler, despite not being measured in the solution. As B release reached between 8 % and 15 % of the initial B loading in the cements at the 60 d time point, it can be assumed that Sr release was equal to or greater than 8 to 15 %, ten times what was seen in the solution (0.3 to 1.3 % of initial Sr loading). As such, it may be reasonably concluded that at a minimum 8 to 15 % of the loaded Sr (equivalent to B release levels) was release from the glass filler greatly exceeded all

therapeutic thresholds, exceeding 100 mg/l after 14 d.

As B release measurements demonstrated extensive glass network dissolution, which conflicted with Sr release measurement through ICP-OES, SEM imaging was performed to ascertain the fate of the Sr released from the glass. SEM and EDS analysis of cement surfaces showed the development of large amounts of a Sr and phosphate-containing precipitate, which was not previously seen during the dissolution of the glass filler phase in isolation, in which Sr release concentration of up to 1127 mg/l were reported without deviation from Fickian diffusion kinetics[285]. This finding indicated that the discrepancy between release efficiency of Sr and B from the cements was the result of Sr being chelated in the form of a precipitate from solution following glass filler degradation. The formation of this precipitate would be favoured not only by the mass transport constraints enforced by the resin phase of the cement, but also the polarizable oxygen groups present in the resin phase due to the high HEMA contents. Previous studies into the calcification of copolymer blends in abiotic solutions have shown increases in the rate of calcification with increasing polar oxygen pendant groups, specifically increasing HEMA content[297]. In the current study, it is likely that the increase in resin polar oxygen severed to chelate Sr from solution, generating nucleation sites for phosphate in a similar manner, resulting in the formation of the precipitate in the resin phase. While increasing HEMA content effectively increased resin hydration and served to increase B release, the concurrent increased chelation of Sr reduced the efficacy of Sr release. Due to these conflicting mechanisms, maximum Sr release was achieved in the cements of group C.

The formation of the Sr phosphate precipitates may be further exasperated by the incubation conditions selected. As calcium phosphates have a lower degree of solubility than Sr phosphates, the chelation of Sr may be artificially enhanced due to the use of a calcium free incubation media. Furthermore, Sr phosphates have been demonstrated to undergo spontaneous ion exchange substitutions to form stable calcium phosphates in calcium rich environments. Through such a mechanism it is

possible that these precipitates may provide both enhanced cellular attachment, and prolonged Sr release through ion exchange. Testing of these materials under more dynamic conditions, in a calcium-rich environment, may provide information into the stability of this precipitate, and the potential of this layer to act (i) as a reservoir of Sr or as (ii) a site for cellular attachment.

Overall the Sr release from the materials developed and investigated in this study ranged between 9-32 mg/l after 60 d of incubation; falling within the range previously reported for increased OBL activity, but well below that of the OCL inhibition threshold *in vitro*. A study of Sr substituted dicalcium phosphate dihydrate cements at loading of up to 8 % of cement weight allowed for Sr release levels of 20 mg/l over 3 weeks, similar to levels seen in this work[195]. While the Sr-containing CPCs demonstrated improved cell proliferation and ALP expression over plastic tissue culture plates, they did not offer an advantage over purely calcium-based controls. Schumacher et al. reported maximum Sr release levels of 13 mg/l from Sr substituted CPCs, and was able to demonstrate a significant increase in OBL proliferation and differentiation in comparison to a calcium phosphate control at these release levels, with indirect cell culture methods[298]. These previous results may indicate that these release levels in this study are sufficient for *in vitro* efficacy, however the development of the precipitate masked our ability to determine total Sr release. Based on the present data, the Sr release levels observed are likely insufficient for an uncoupling effect *in vitro*.

The serum Sr levels required for the uncoupling effect are much lower than those required *in vitro* (10.5 mg/l) which may be a result of the systemic effect of Sr through the parathyroid gland, or the cell culture methods used. While OBL OCL communication is known to play an important role in the control of bone metabolism, *in vitro* efficacy levels have largely focused on monoculture conditions, leaving true localized *in vivo* requirements for uncoupling unclear. Serum Sr concentration required for uncoupling are achieved by many of the cements investigated (all but group E), and

as such may have some beneficial effect towards uncoupling of bone turn over. Furthermore, it is possible that the use of calcium-rich media may prevent Sr chelation, increasing Sr release up to tenfold, well above the 88 mg/l reported for the inhibition of OCL activity. Further investigation into the effect of incubation media on Sr release, and the *in vitro* efficacy through dual culture conditions could provide guidance for the further development of materials designed for the local release of Sr.

4.2.6 Materials and methods

Cement fabrication

Borate glass containing 70 % B_2O_3, 26 % SrO and 4 % Na_2O (mole fraction) was synthesized as per MacDonald et al., and sieved to retrieve <25 μm particles[285]. Particle size distribution was verified using a laser particle size analyser, in aqueous dispersant (Mastersizer 3000, Malvern, Malvern, Worcs, UK), and confirmed as d_{10} = 3.38 μm, d_{50} = 12.1 μm, d_{90} = 26.4 μm. A series of 15 twopaste resins (Figure 4.16, Table 4.3) were fabricated through varying mixtures of HEMA (Aldrich Chemistry, USA), TEGDMA (Aldrich Chemistry, St. Louis, MO, USA), and BisGMA (Aldrich Chemistry, USA). BPO (Sigma Aldrich,St. Louis, MO, USA) and DHEPT (Aldrich Chemistry, St. Louis, MO, USA) were added to paste one and two respectively, for each composition, to form a chemical initiation system[38]. Resin components were shielded from light to prevent photo initiation of BPO, and placed in a shaking incubator at (37°C, 2 Hz) overnight to reduce resin viscosity and allow for mixing. Resin mixtures were refrigerated until further use, and hand spatulated with the appropriate weight of glass to form both paste components as needed.

Cement handling characteristics

Cement working times were assessed in triplicate as described by Dickey et al.[299]]. Cement setting time was determined to be equal to the time to reach 50 % of the

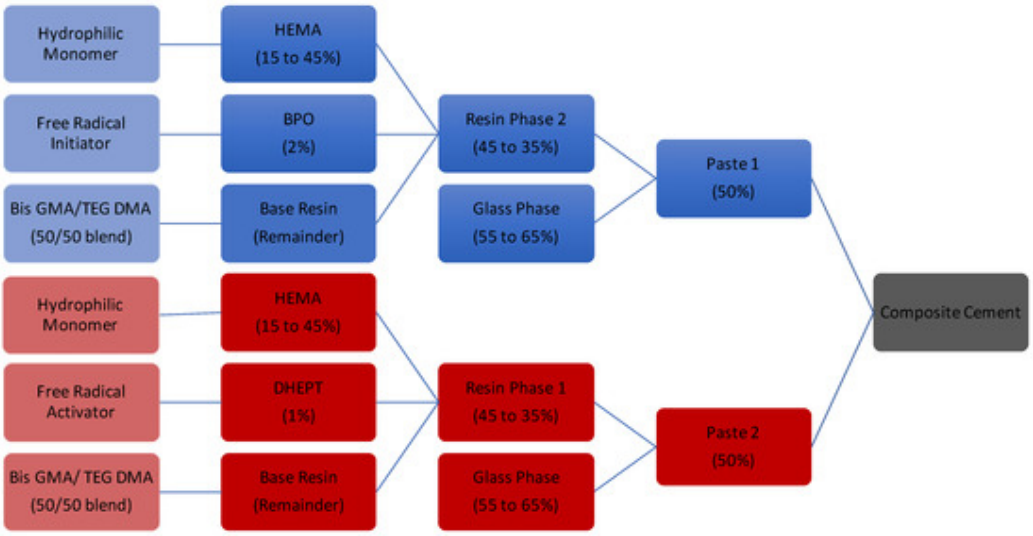

Figure 4.16: Schematic of two paste resin fabrication, all compositions represented in weight percentage.

exothermic peak following the mixing of the two pastes, as per established international protocols[300]. Dimensions of the curing mold used were reduced to 30 mm diameter and 15 mm height, to reduce the material needed for testing to 10 g/sample.

Degree of conversion

ATR-FTIR analysis was performed on both unset and set cements to assess the degree of conversion via observations of the relative decrease in the aliphatic carbon-carbon double bond (C=C) peak at a wave number of 1638 cm^{-1}. Set samples were generated through hand spatulation on a dental pad using equal amounts (1 g) of pastes one and two. Subsequently, cements were transferred into poly tetra fluoroethylene (PTFE) moulds (7 mm $\oslash$ 1 mm), sandwiched between acetate sheets, and clamped between steel plates to set a room temperature for 1 h[301]. The cement samples were then scrapped of excess material (i.e., flash), removed from moulds and stored for 24 h in a desiccator prior to analysis. Three discs were produced for each cement composition with two measurement locations used for each disc (n = 6). Unset cement spectra were collected through measurements of individual paste components (n = 3 per paste,

total n = 6 per cement composition). ATR-FTIR measurements were performed on a TENSOR 27 system (Bruker, Billerica, MA USA) using a diamond attenuated total reflectance (ATR) crystal (Golden Gate, Specac, Orpington, Kent, UK). Spectra were collected as the average of 6 scans, between 1200 cm^{-1} and 1800 cm^{-1} at a resolution of 4 cm^{-1}. To assess the stability of the individual pastes 500 spectral scans were gathered over 120 min. DC for all samples was calculated through the ratio of absorbance peaks centred at 1638 cm^{-1} and 1608 cm^{-1}, representative of the unreacted methacrylate functional groups and aromatic rings of the Bis-GMA respectively[302]. For each cement composition, the DC was calculated as the relative ratios of the methacrylate peak area before and after curing normalized to the aromatic peak area, using Equation 4.1;

$$DC = 1 - [(A_m/A_a)_{set}/(A_m/A_a)_{unset}] \tag{4.1}$$

Where Am is the area of the methacrylate peak (1638 cm^{-1}) and Aa is the area of the aromatic control peak (1608 cm^{-1})[302]

Biaxial flexural strength

Cement disks (15 mm ⊘ 1 mm) were fabricated in PTFE moulds, and allowed to cure for 1 h in ambient conditions[302]. Following removal from the moulds the cement disks were placed in PBS (35 ml/sample), and incubated in a shaking incubator at 37 °C, 2 Hz for 1, 7, 30 and 60 d (n=5 per condition). Following incubation each sample was patted dry, measured in duplicate for diameter (accuracy of 0.1 mm) and mounted in a ball on 3 ball biaxial flexural testing rig. Testing was undertaken using an Instron 3400 (MA, USA) system fitted with a 2 kN load cell at a strain rate of 1 mm/min. Sample thickness was measured in triplicate following sample rupture at the crack origin. Fracture loads were converted into biaxial flexure strengths using the methods described by Chung et al. using Equation 4.2 and Equation 4.3.

$$\sigma_{biaxial} = \frac{3P(1+\nu)}{4\pi t^2}\Big[1 + 2ln\frac{a}{r_o^*} + \frac{1-\upsilon}{1+\upsilon}\Big(\frac{2a^2 - r_o^{*2}}{2c^2}\Big)\Big] \tag{4.2}$$

$$r_o^* = \sqrt{(1.6r_o^2 + t^2)} - 0.675t \tag{4.3}$$

P is the load at failure, v is the Poissons ratio, (assumed to be 0.24), t is sample thickness, a is the radius of the support circle, c is the radius of the sample, and r_o is the radius of central loading ball[296].

Cement water sorption and weight loss

Cement samples were generated through hand spatulation on a dental pad using equal amounts (1.5 g) of pastes one and two. Subsequently, cements were transferred into stainless steel split ring cylindrical moulds (4 mm ⊘ 6 mm), sandwiched between acetate sheets, and clamped between steel plates to set a room temperature for 1 h[301]. The cement samples were then scrapped of excess material, removed from moulds, weighed for dry mass, placed in 10 ml (1 cm^2/10 ml) of PBS, capped, and stored in a shaking incubator (37°C, 2 Hz) for 1, 7, 14, 30, or 60 d respectively (n = 3/time point). Following incubation samples were removed using a disposable spatula, patted dry, and wet weights were recorded. Subsequently, the extract medium was capped and stored in a refrigerator until ion release analysis.

Ion release profiles

Extracts generated through the cement water sorption studies over 1, 7, 14, 30 and 60 d were decanted, and diluted in 2 % ultrapure hydrochloric acid (Fluka, Mexico City, Mexico) for ICP analysis of Sr and B content (Na measurement omitted due to high background measurements in PBS)[285]. ICP-OES analysis was performed using an Optima 8000 (Perkin Elmer, Waltham, MA, USA) with a 2 % hydrochloric acid suspension media, nitrogen carrier gas and an argon flame. Calibration curves were

produced using certified Perking Elmer Pure ICP standards (Perkin Elmer,Waltham, MA, USA). All samples were measured in triplicate and recorded as the mean of 3 readings. All ion release measurements were reported in mg/l for assessment of therapeutic potential, and normalized to initial sample content for assessment of degradation kinetics.

SEM analysis of weight loss samples

SEM images were collected for 15 % HEMA and 45 % HEMA samples following 1 and 60 d of incubation in PBS. Samples were sputter coated with a gold-palladium coating using a Lecia EM ACE200 (Wetzlar, Germany). BS-SEM images were collected using an Hitachi S4700 FED (Hitachi, Chula Vista, CA, USA) operating at 3 kV, 15 μA, under 30 time magnification, or 3 kV,16.5 μA, 250 times magnification.

Statistical analysis

Statistical analysis was performed using Prism 6 (GraphPad Inc., LaJolla, CA, USA) for the two-way ANOVA (assessing effect of HEMA and glass content) with a Tukey multiple comparison test, at a significance level of 0.05. Time effects were analyzed using a two way ANOVA, with repeated measures, with a Tukey multiple comparison test. Peak fitting of Fourier transform infrared (FTIR) data was performed using Python (Python Software Foundation,Wilmington, DE, USA).

4.2.7 Conclusions

Increasing the HEMA content of the cements led to an increase in mass gain and degree of cure without significantly effecting cement setting time. While filler network hydrolysis increased with increased water sorption (as evidenced through increased B release), the relative release ratio of Sr to B dropped with increasing HEMA content. It was confirmed that this observation was associated with precipitation of a Sr phosphate phase on the surface of the cements, suggesting an interaction between free Sr

and the resin phase under the experimental conditions utilized. The concentration of Sr required for *in vitro* OCL inhibition was not seen under the study conditions. However, the materials did release and maintain Sr at the levels required to increase OBL proliferation. Further investigation into the effect of incubation conditions on the rate of Sr release (namely the effect of calcium in the incubation media, and mechanical loading) may provide further insight into the mechanism of ion release from such materials, and allow for more accurate extrapolation into *in vivo* conditions.

4.3 Mechanical loading, an important factor in the evaluation of ion release from bone augmentation materials

4.3.1 Note on composition selection

While section 4.2 investigated a series of composite resins based on a Bis-GMA, TEG DMA, HEMA blend, in advancing to mechanically loaded release investigations a change was made to a Bis-GMA HEMA blend. As initial experiments revealed the greatest extent of overall glass degradation, with the unique finding of maintained strength over time for the 45 % HEMA blends, a 45 % HEMA loading was selected for further work. The high HEMA content alleviated the need for TEG DMA as a diluent. To counter the increased viscosity of the TEG DMA free resin, filler particle size was changed from 25 μm to 45μm. Biaxial flexural strength was evaluated for this new resin blend, filled with 55, 60 and 65 wt% glass after 24 h in PBS as per 4.2.6 and demonstrated significant increases in cement strength over the TEG DMA containing cements due to the increased Bis-GMA content (Figure 4.17). Similarly, both working and setting times were marginally extended (Figure 4.18, Figure 4.19), bringing the working time above the 150 s required for two paste systems. While the 55 % glass loading had the greatest biaxial flexural strength, the 60 % glass loading was ultimately chosen for further investigation due to its more paste like consistency. This material has a biaxial flexural strength of 30 $\pm$ 1.9 MPa, a working time of 155.0 $\pm$ 8.7 s, and a setting time of 209 $\pm$ 18 s .

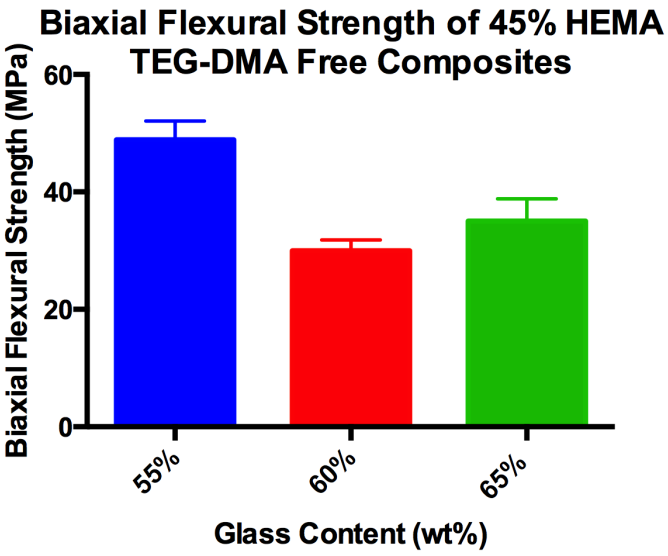

Figure 4.17: Biaxial flexural strength of 45 % HEMA composites, fabricated without TEG DMA inclusion. Samples prepared as per section 4.3.8, and assessed for biaxial flexural strength as per section 4.2.6.

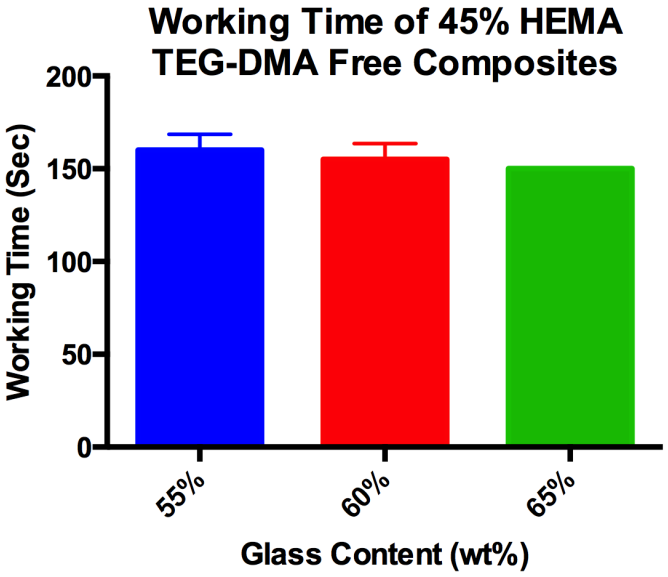

Figure 4.18: Working time of 45 % HEMA composites, fabricated without TEG DMA inclusion. Pastes prepared as per section 4.3.8, and assessed for working time as per 4.2.6.

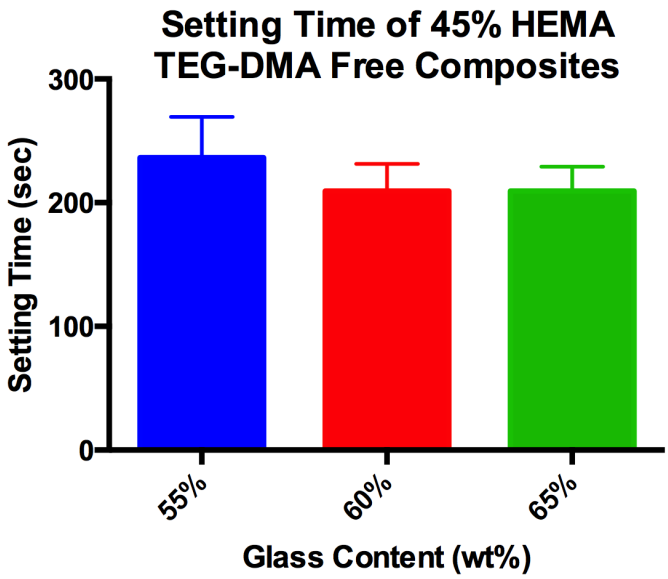

Figure 4.19: Setting time of 45 % HEMA composites, fabricated without TEG DMA inclusion. Pastes prepared as per 4.3.8, and assessed for setting time as per 4.2.6.

K. MacDonald[1], D. Boyd[1,2]

[1]School of Biomedical Engineering, Dalhousie University, Halifax, NS B3H 1X7, Canada;

[2]Department Applied Oral Sciences, Dalhousie University, Halifax, NS B3H 1X7, Canada

4.3.2 Author contribution statement

K.M. and D.B. conceived and designed the experiments, and revised the manuscript; K.M. performed the experiments, analysed the data, and wrote the paper.

4.3.3 Abstract

The controlled release of TIIs from biomaterials is an emerging area of international research. One of the foci for this research is the development of materials, which spatially and temporally modulate therapeutic release, via controlled degradation in the intended physiological environment. Crucially however, our understanding of the

release kinetics for such systems remains limited, particularly with respect to the influence of physiological loading. Consequently, this study was designed to investigate the effect of dynamic mechanical loading on a composite material intended to stabilize, reinforce and strengthen vertebral bodies. The composite material contains a borate glass engineered to release strontium as a TII at clinically relevant levels over extended time periods. It was observed that both cyclic (6 MPa 2 Hz) and static (4.3 MPa) compressive loading significantly increased the release of strontium ions. The observed alterations in ion release kinetics suggest that the mechanical loading of the implantation environment should be proactively considered when evaluating the ion release kinetics.

4.3.4 Introduction

Percutaneous vertebroplasty provides rapid fracture fixation for osteoporotic VCFs, resulting in rapid pain relief for 88 % of patients [109]. Despite the positive impact that PVP has on the quality of life for patients, subsequent fractures (in adjacent vertebrae), refractory to the original, are frequently associated with procedural outcomes. While the aetiology of adjacent fractures is complex, there is consensus in the literature that principal contributory factors, are compromised bone health (e.g. osteoporosis), and anatomical misalignment(s) caused by kyphotic deformity [25]. To address these factors, prophylactic augmentation of adjacent vertebrae has been proposed, and demonstrated, to increase fracture load [137]; thereby providing a means to mitigate subsequent fracture rates. Furthermore, as subsequent fractures have been linked to the progression of osteoporosis, the inclusion of therapeutically active agents, capable of slowing the progression of osteoporosis is considered to add further benefits for patients undergoing PVP whilst improving patient outcomes.

One approach to achieving a therapeutically active biomaterial for PVP has been

associated with the inclusion of strontium ions (Sr^{2+}), a therapeutically active inorganic ion, into PVP bone cements. Several clinical studies have confirmed the beneficial effects of pharmacologically active Sr^{2+} on bone quality [275, 83, 303, 304, 305]. The concomitant mechanism of action associated with Sr^{2+} is related to its ability to act as both (i) an antiresorptive and (ii) an anabolic agent on bone metabolism [6, 9, 30]. However, while Sr^{2+} has beneficial effects on bone quality, through direct action on OBLs and OCL cell lines[88], its release levels must be controlled to ensure temporal maintenance of Sr^{2+} levels within the therapeutic window. While a variety of approaches have been used to incorporate Sr into orthopaedic biomaterials[200, 298] little work exists with respect to investigating such devices as drug releasing systems (i.e. TII release systems); particularly with respect to investigating the release kinetics and temporal maintenance of therapeutic thresholds[306].

For composite resin cements, intended for both dental and orthopaedic applications, hydrophilic modifications have been used to alter ion release kinetics. Such modifications increase water sorption and therefore degradation of the inorganic filler phase; frequently a bioactive glass[255, 284]. As filler degradation, and ion release are dependent on the movement of water through the system, it is constrained by hydrostatic forces. Furthermore, the rate of glass dissolution has been shown to vary greatly depending on solution effects, slowing rapidly in constrained volumes when degradation products can accumulate at the glass-solution interface[307]. Due to the complexity of the implanted *in vivo* environment, and the ethical restrictions on the use of animal models, simplified *in vitro* elution models are frequently used to assess drug release. In particular, changes to the elution media (including ionic concentration and organic molecule interaction), along with flow through conditions have been explored to better understand those factors which govern *in vivo* release kinetics[308, 309] .

However, the effects of dynamic loading on TII release, has received little attention

by comparison. This gap in our knowledge is significant, especially given the emergence of research pertaining to metals in medicine, and in particular with respect to the temporal modulation of therapeutic metal ion release from biomaterials[236, 27]. In drug-releasing hydrogel materials, cyclic compressive loading has been demonstrated to significantly increase the rate release of reversibly bound drug particles[256]. This effect is attributed to variations in hydrostatic pressure, creating a periodic reversal of water flow in and out of the material. During unloaded phases, hydrophilic forces draw unsaturated fluid into the material generating swelling forces. In this unsaturated environment, water-soluble drugs are rapidly released into solution. Conversely, during the compressive loading phase compressive strain drives fluid from the material voids, into the bulk solution, which is replaced with unsaturated fluid in the next unloaded phase, continuing the cycle. While PVP materials are much less compliant than hydrogel materials, the addition of small hydrophilic mono-functional monomers, such as poly-HEMA to composite resins has been shown to not only alter water sorption behaviour but also to reduce the modulus of elasticity of composite resins by up to 40 %[310]. As such hydrophilic modifications of composite resin cements may result in loading dependent alterations of bioactive glass filler degradation kinetics. Accordingly, to design a Sr^{2+} releasing bone cement which can provide appropriate *in vivo* levels of ion release, the ion release kinetics under mechanically loaded conditions must also be fully considered.

This study aims to examine how dynamic loading of hydrophilic composite resins alters the movement of water into and out of the system, while also providing insights into the mechanisms of Sr^{2+} release from such materials. The methods and data generated in this paper may further help to evaluate and regulate the performance of ion releasing medical devices in the future. Accordingly, and to achieve the research objective, a highly degradable borate glass was selected as the reinforcing phase for a resin composite bone cement comprising conventional constituent polymers. The glass phase selected for this work has been previously studied, and is known to provide for

Fickian controlled diffusion of Sr^{2+} up to 60 d[285]. A highly hydrophilic Bis glycydil dimethacrylate (Bis-GMA), HEMA polymer blend was chosen as the resin phase of the composite; with the particular ratios of glass and HEMA content being based on previous investigations by MacDonald et al. to maximize ion release efficiency over 60 d[306]. Cement specimens produced in this study were exposed to three incubation conditions while immersed in SBF; (i) cyclic compressive loading, (ii) static loading, and (iii) an unloaded control condition. Ion release into solution was assessed using ICP-OES.

4.3.5 Results

Water sorption by cement samples was significantly decreased during cyclic loading ($p < 0.05$), with no decreases in water sorption being observed under static compression relative to unloaded samples (Figure 4.20). The highest ion release levels were seen under cyclic compression loading, with the cumulative release of Sr and B reaching 68 and 57 mg respectively at 48 h (Figure 4.21). Cumulative release under static compression reached maximums of 24 and 22 mg for Sr and B respectively, while unloaded conditions achieved a maximum of 21 and 17 mg respectively. A significant increase in Sr release was seen in both the static and cyclic compression loading conditions relative to the unloaded control samples (Table 4.5), with the cyclic loading showing the greatest effect on cumulative ion release levels.

Akaikes informative criterion comparison of surface controlled, and diffusion controlled release models, preferred the more complex power series diffusion controlled release for all data sets (Table 4.6). When fitted to a modified Korsemyers Peppas model (with allowance for burst release effect [311]) power coefficients were (i) 0.499, 0.1835 and 0.360 for the release of Sr and (ii) 0.510, 0.306, 0.440 for the release of B under cyclic compression, static compression, and unloaded conditions respectively. While the initial glass composition contained Sr:B at a mass ratio of 1.62, Sr:B release ratios ranged from 1.8 to 1.1 with no significant differences found between incubation

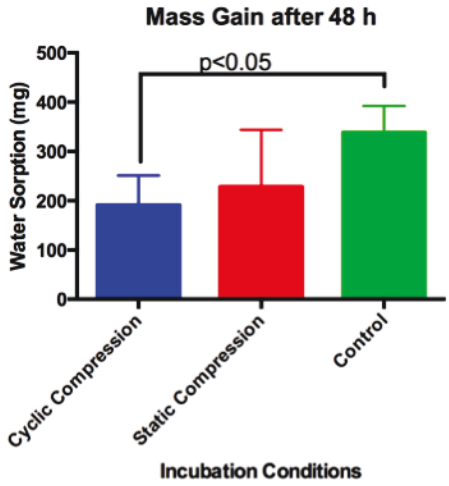

Figure 4.20: Mass gain (measured as difference between dry and wet weight) during cement incubation under various loading conditions, denoting statistically significant difference between unloaded and cyclic compression conditions.

Table 4.5: Multiple t test statistics results comparing Sr release levels between the 3 loading conditions investigated

Time (h)	Cyclic Compression Static Compression	Cyclic Compression Unloaded	Static Compression Unloaded
1	N.S.	<0.01	<0.05
2	<0.01	<0.01	<0.01
3	<0.01	<0.05	N.S.
4	<0.01	<0.01	<0.05
6	<0.01	<0.01	<0.01
8	<0.01	<0.01	<0.05
12	<0.01	<0.01	N.S.
24	<0.01	<0.01	<0.05
36	<0.01	<0.01	N.S.
48	<0.01	<0.01	N.S.

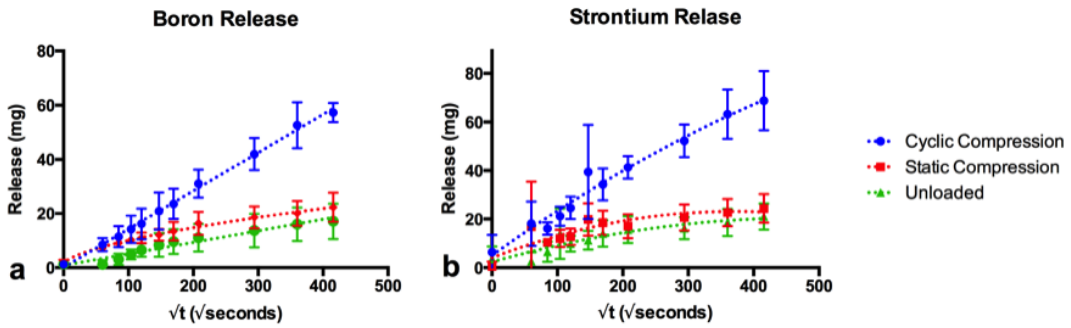

Figure 4.21: Cumulative release of (a) boron, and (b) Sr ions under various loading conditions, demonstrating Fickian diffusion under cyclic loading, and less Fickian diffusion in unloaded and static compression loaded incubation.

conditions. Significant decreases in the Sr:B release ratios were seen between time points of 1, 2 and 3 h, and the 36 and 48 h time point under the unloaded condition only.

4.3.6 Discussion

Sr release (24-48 mg/l after 48 h) was much higher than previous studies of a similar material in PBS. Elution studies of a 45 % HEMA, 26.5 % Bis-GMA, 26.5 % TEG DMA (added as a diluent to reduce viscosity) resin composite reported Sr release levels below 4 mg/l after 24 h, and below 20 mg/l after 60 d[306]. Release of B however was similar to previously reported values of 16 mg/l at 24 h in both unloaded and statically compressed samples. These results suggest that the ionic composition of the elution media is of greater consequence for sparingly soluble elements such as Sr. Cumulative Sr release remained above the *in vitro* efficacy levels for OBL proliferation, but below *in vitro* OCL inhibitory levels (Figure 4.22) [9, 10]. The serum Sr levels in the Treatment of Peripheral Osteoporosis Study (TROPOS), which reported a a significant reduction in fracture rate, were reached after 2 h under cyclic loading or 4 h under static compressive or unloaded conditions demonstrating that the potential for anti-osteoporotic effect is increased under mechanical loading. Much greater overall release, under the cyclic loading condition, suggests that the static

Table 4.6: Comparison of model fits between linear release model (surface controlled release), and power series release (with allowance for burst effect).

Comparison of Fits	**Cyclic Compression**	**Static Compression**	**Unloaded**
Simpler model	First order polynomial (straight line)	First order polynomial (straight line)	First order polynomial (straight line)
Probability it is correct	<0.01 %	<0.01 %	<0.01 %
Alternative model	Power series: Y=A*X^B + C	Power series: Y=A*X^B + C	Power series: Y=A*X^B + C
Probability it is correct	>99.99 %	>99.99 %	>99.99 %
Ratio of probabilities			
Preferred model	**Power series: Y=A*X^B + C**	**Power series: Y=A*X^B + C**	**Power series: Y=A*X^B + C**
Difference in AICc	46.64	29.51	18.78

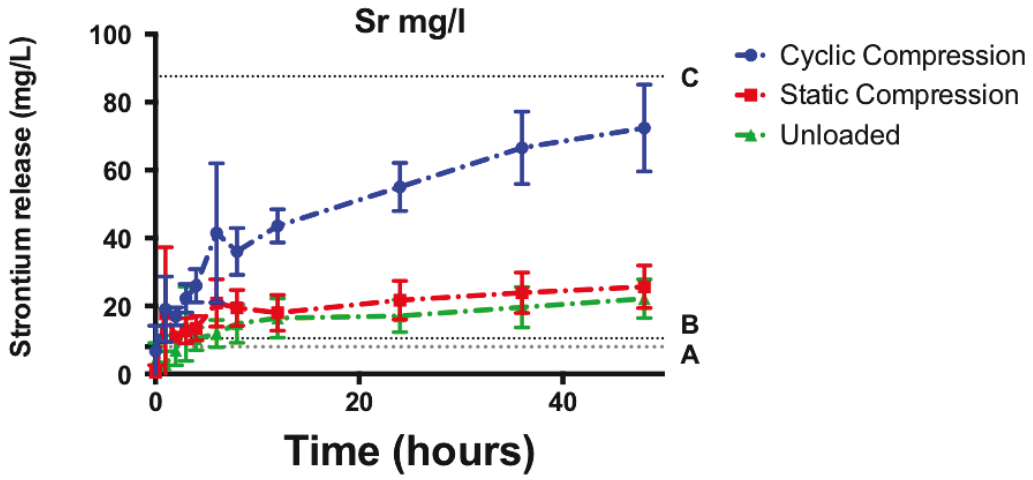

Figure 4.22: Sr release from cements into SBF in mg/l, relative to (A) *in vitro* OBL activation threshold[9] (B) serum Sr concentration reported in the Treatment of Peripheral Osteoporosis (TROPOS) study[10], and (C) *in vitro* OCL inhibition threshold [8].

incubation conditions widely used for the investigation of Sr releasing bone cements will underestimate the true release levels and therefore impact effective local dosing. While cyclic loading increased therapeutic Sr release, it also increased the release of B raising a potential concern for cytotoxicity. However, while bioactive glass extracts containing B at concentrations of 5.2 mM (56 mg/l) demonstrated decreased bone marrow proliferation in *in vitro* assays[312], animal implantation models have demonstrated favorable bone response to high borate glass bone graft materials[313]. Cumulative B release of 58 mg in 48 h under cyclic loading is well below the NOAEL of 6.1 mg/kg/d for chronic B exposure indicating that borate glass reinforced cements are likely a safe vector for TII delivery[314]. As such the increase of boron release due to cyclic loading is unlikely to impart detrimental effects to cement biocompatability. The ability of cyclic loading to prevent the significant decrease in the ratio of Sr to B release could also serve to mitigate potentially toxic effects of boron.

While previous studies have reported a $t^{1/2}$ dependence for ion release from bioactive glass reinforced composite resin dental materials[315], such kinetics were only seen in the cyclic loading conditions of this study. In the static compression and

unloaded conditions the power model coefficients were below 0.5, characteristic of less Fickian release[316]. This finding suggests that the polymer chain relaxation rate under the unloaded, and static compressive conditions is much faster than the rate of water penetration. This increased rate of relaxation is likely an effect of the high mono-functional HEMA content, decreasing the fraction of bi-functional monomers reducing cross-linking. Previous studies into the release of gentamicin from PMMA bone cements reported crack surface mediated increases in drug release rates. A study of antibiotic loaded cements under uniaxial sinusoidal tension-compression ($\pm$10 MPa at a frequency of 2 Hz) resulted in a three-fold increase in the rate of gentamicin released versus statically incubated samples; with both conditions displaying surface controlled release[191]. It was proposed that the increased rate of release was due to crack formation providing an increased surface area for drug elution. When a 400 KPa 5Hz compressive force was applied to the stem of a cemented hip prosthesis in a model elution environment (cement stresses of -2 MPa to 6 MPa) minor increases in antibiotic elution were seen only in a highly porous cement formulation over 28 d of elution testing but no alterations to the mechanism of release were reported[192]. While crack surface mediated release mechanisms are considered in the literature, such a mechanism is unlikely to explain the results seen in this study, as any increase in surface area would result in increased water sorption.

Results from this study, in contrast, indicate significant alterations to the mechanism of release of Sr^{2+} as a result of physiological loading variations. Increases to power law release coefficients suggest that compressive loading decreased both the rate of water sorption and polymer chain relaxation in both cyclic and static conditions. Mechanical loading of hydrogels has been demonstrated to alter release kinetics only for reversibly bound growth factors. Such an effect may explain the alteration in kinetics seen in this study. Polar pendant groups in hydrophilic poly HEMA materials are associated with cation chelation in their hydrated state[317], providing both a mechanism of hydrogel calcification and bone integration. While cyclic loading alters

local concentration gradients, allowing for increased ion release, compressive loading also limits water sorption, and polymer chain relaxation reducing the number of exposed polar sites. Increases in cation release under cyclic loading may thus be twofold; (i) increased filler degradation due to decreased degradation product accumulation within the material, as well as (ii) decreased polymer cation interactions. The decrease is the ratio of Sr to B release seen only in unloaded conditions would similarly be explained by increased chain relaxation resulting in increased Sr chelation.

While continuous cyclic loading is standard in material testing, *in vivo* loading would present fewer, intermittent loading cycles, with ASTM F2118 standards for cyclic testing of acrylic bone cement reporting an average of 2-3 million steps a year[318]. As such the 7,200 loading cycles per hour used in this study would approximate a full day of activity, with the 48 h duration approximating 48 d of activity. Strontium release rate based on equivalent loading days (7,200 loading cycles) is represented in Figure 4, along with the unloaded release rate over the 48 h study. No statistical difference is seen between Sr release in unloaded conditions after 1 and 2 d, and the equivalent rate of release of Sr corrected for loading cycles (1 and 2 h sampling points respectively). Release rates exceed therapeutic efficacy thresholds for OBL proliferation but not *in vitro* OCL inhibition, demonstrating potential for therapeutic efficacy only for the first sampling point when assessed as a daily rate of release. While this is a short duration study, this may indicate a potential mechanism to extend the effective window of testing.

The loading levels selected in this study were based on computational models assessing the cement stress levels during walking following vertebral body augmentation, assuming fill volumes of ca. 8 ml[319]. True loading values may vary significantly due to the variability in fill pattern and irregularly shaped cement volume seen following PVP[193]. Previous models have predicted cement stress as low as 1.5 MPa within the cement bolus (based on an assumption of 70 % fill)[320]. Furthermore the elastic

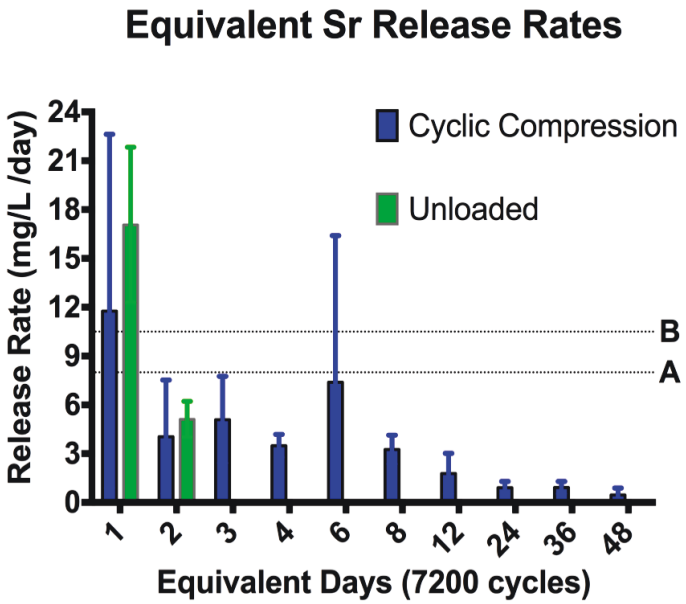

Figure 4.23: Rate of Sr release as equivalent days (7,200 cycles of compression) relative to (A) *in vitro* OBL activation threshold[9] (B) serum Sr concentration reported in the Treatment of Peripheral Osteoporosis (TROPOS) study[10].

modulus of trabecular bone can vary by orders of magnitude in even healthy individuals, adding variability to the extent of stress shielding, while kyphotic angle has been reported in increased quasi-static compressive forces by as much as 2-3 % per degree of kyphosis[144, 321]. As such our limitations in predicting the loading levels in augmented vertebrae limits our ability to predict cement behaviour, including ion release kinetics. While the results of this study demonstrate the ability of cyclic loading conditions to alter ion release kinetics over a short period of investigation, further investigation into the threshold of this effect, as well as long-term release behaviour is merited. Along with variations in loading conditions, alterations to solution media, notably the inclusion of serum proteins would serve to better mimic the true implantation environment deepening our understanding of material host interactions which mediate ion release.

4.3.7 Conclusion

Both cyclic and static compressive stress has been demonstrated to shown to yield a significant increase in ion release from a borate glass filled composite resins (relative to unloaded release conditions). Cyclic loading conditions may provide a mechanism of extending the time frame for diffusion-controlled release of TIIs from such systems, despite the decrease in water sorption caused by compression. The study results indicate that the mechanical loading environment should be considered when assessing the release kinetics of a drug loaded bone augmentation material for both toxic and therapeutic effects.

4.3.8 Methods

A two paste chemically cured resin blend was fabricated from a blend of Bis-GMA and HEMA based on the compositions in Table 4.7, mixed in the appropriate weight ratios with either BPO, or DHEPT, to initiate the free radical polymerisation reaction upon mixing. Resin blends were shielded from light and mixed in a shaking incubator at 37°C, 2 Hz overnight to achieve homogeneous mixtures. The borate-glass reinforcing phase was fabricated as described by MacDonald et al[285], ground and sieved to retrieve <45 μm particles. Each cement paste was formed from a mixture of glass filler (60 wt%) mixed to homogeneity with either resin part one or two (40 wt%), through hand spatulation. Cement cylinders were fabricated using a cylindrical aluminum split mold (4 cm diameter, 3 cm height) filled with an equal mixture of the two pastes (40 g/paste, 80 g total) through hand spatulation, clamped between two stainless steel plates, and allowed to cure for an hour. Samples were removed from the mould, and stored in a desiccator overnight until the elution study.

Table 4.7: Two paste chemically cured resin system (wt%).

Component	Paste 1	Paste 2
Bis-GMA	54 %	53 %
HEMA	45 %	45 %
BPO	1 %	0 %
DHEPT	0 %	2 %

Incubation conditions

Cylindrical cement samples (n=4) were incubated at 37°C in 950 ml (surface to volume ration of 15 ml/cm^2) SBF[322] for 48 h under three loading conditions: a) no mechanical loading, b) cyclic compressive loading and c) static compressive loading. Both cyclic and static compressive loading was performed using a Bose Electroforce 3510 system (TA Instruments, MN). Environmental control tank volume was reduced to approximately 1.5 l by the fixation of an acrylic cylinder (approximately 12.5 cm diameter, 25 cm height) to the chamber base centred around the loading platform using silicone marine adhesive on the outside rim. The outer tank was filled with water during testing to improve heat conduction from elements and stabilize temperature. Cyclic loading was performed as a compression-compression sinusoidal waveform, oscillating between 0.3 to 6 MPa at a frequency of 2 Hz. Static compressive loading was performed at 4.3 MPa (the equivalent RMS value of the cyclic loading conditions). Incubation media was sampled through the removal of 5 ml of SBF at 1, 2, 3, 5, 6, 8, 12, 24, 36 and 48 h, and replaced with 5 ml of fresh SBF.

Water sorption measurements

Cement cylinders were removed from solution and patted dry of excess SBF before the measurement of wet weight. Cylinders were then dried in a 45 °C oven until constant mass was achieved and dry weight was recorded (approximately 7 d). Water sorption was recorded as the difference between wet and dry weights.

Ion release

Ion release profiles were assessed through the use of ICP OES, for the presence of both B and Sr in solution. Extract media was diluted in 2 % HCl to 1:100 and 1:1000 dilutions for the assessment of B and Sr respectively. ICP-OES measurements were performed in triplicate, against a standard calibration curve, and corrected for the removal of SBF during sampling. Ion release profiles were fitted through least squares regression to diffusion controlled release models, with model parameters compared between elution conditions using a corrected Akaikes Information Criterion.

4.4 A pilot implantation study of borate glass filled hydrophilic bone cements

K. MacDonald[1], K. O'Connell,[2] D. Boyd[1,2]

[1]School of Biomedical Engineering, Dalhousie University, Halifax, NS B3H 1X7, Canada;

[2]Department Applied Oral Sciences, Dalhousie University, Halifax, NS B3H 1X7, Canada

4.4.1 Author contribution statement

All authors contributed to the development of the study protocol, the selection of sample processing techniques, and the interpretation of the study results. K.M. prepared all test article samples for implantation. K.M. wrote the manuscript, and contributed to the editing of the manuscript with D.B.

4.4.2 Abstract

Hydrophilic composite resin cements reinforced with degradable borate glasses may provide a mechanism of providing long term strontium release to improve local bone quality. A pilot implantation study in a New Zealand white (NZW) rabbit femoral defect model was conducted to evaluate the local response to these novel materials. A favorable tissue response with evidence of direct new bone formation was observed. Highly hydrophilic glass filled cements may present benefits of rapid surface mineralization, and a press fit coupling to bone.

4.4.3 Introduction

Systemic strontium salt administration has demonstrated increased new bone formation while simultaneously decreasing bone resorption, resulting in increased BMD and strength [305]. These effects, mediated through direct local signalling pathways,

may be possible through the local release of strontium ions from biomaterials[29]. To provide such an effect, a strontium releasing borate-glass reinforced composite-resin bone cement has been investigated for therapeutic potential[306]. The cement comprises two principle differences to conventional resins (e.g. Cortoss®). The first difference, is the incorporation of up to 45 % HEMA providing a highly hydrophilic resin phase. The second is the utilization of highly degradable borate glasses as the filler phase, for sustained strontium release[306, 285]. However, given the substantive differences in composite chemistry, three critical issues arise. Firstly, it is important to understand if the local response after implantation is appropriate to allow sustained ion release in the intended application (i.e. fibrous encapsulation eliminated or minimized). Secondly, if fibrous encapsulation occurs, it is important to establish if it has been mediated by changes to the organic versus inorganic compositional chemistry. Finally, histopathology methods must be verified for appropriateness to assess the ability of local strontium release to alter bone metabolism and integration.

4.4.4 Materials and methods

Glass comprising 70 mol% B_2O_3, 26 mol% SrO and 4 mol% $Na_2$2O was fabricated as per MacDonald et al[285], to retrieve sub 25 μm particles. Two-part resin blends containing 45 wt% HEMA was mixed per the literature[306]. Unfilled resin cylinders were fabricated through the hand spatulation of equal weight measures of the two resin components, filled into split ring cylindrical moulds (3.5 mm diameter, 6 mm depth), clamped between acetate sheets and allowed to cure for 1 h. Glass filled composite cylinders were fabricated by mixing 65 wt% glass filler, with 35 wt% resin blend were prepared as per MacDonald et al[306]. Once cured all cylinders were scraped of excess flashing and sterilized using 25 kGy gamma irradiation (Nordion, Laval QC), and shipped to the animal testing facility. Further ethylene oxide surface sterilization (55°C 1 h) was performed at the animal testing facility with implants allowed to off-gas for 8 d prior to implantation.

Animal Model

The protocol for a non-critical sized femoral defect model in a NZW rabbit was reviewed and approved by an Institutional Animal Care and Use Committee (IACUC: Accell Lab Inc, Laval QC, Canada) in accordance with the Canadian Council on Animal Care guidelines. Four male rabbits (four months old, 3.35-3.83 kg, Charles River Laboratories, Wilmington, Mass) were individually housed, with collecting trays located below perforated floors. Animals acclimated at the testing facility for six d prior to implantation procedures. High fibre food (Teckland, Ind USA) was supplied at 180 g/d, along with supplements of hay, fruits, and vegetables or bunny block treats. Water was provided ad libitum. Animals were subject to a physical examination by the supervising veterinarian (including cardiac and pulmonary auscultations) to ensure fitness. Animals were identified by a unique study number, tattooed on the ear at the time of the surgical procedure.

Surgical Procedure

Rabbits were sedated using subcutaneous Acepromazine (1 mg/kg), following by IV propofol (7.5 mg/kg) to induce anaesthesia. Animals were intubated, and ventilated through passive balloon ventilation, with oxygen and isoflurane used to maintain surgical anaesthesia. Lactate Ringers solution was used to provide warm fluid therapy (10 ml/kg/h) through the procedure, and adjusted to correct for changes in blood pressure. Prophylactic antibiotic therapy and pre-emptive analgesia was administered per the literature[323]. Surgical sites were accessed and prepared as per O'Connell et al[313]. Unfilled resin composites were inserted in the left femoral defects, while filled composites were inserted into the right femoral defects on the three test animals. The fourth control animal had bilateral defects left unfilled. Bupivacane (0.25 % up to 1.5 ml/ surgical site) was infiltrated to provide local anaesthesia, soft tissue layers were reflected back and sutured, and the wound was treated with an antibiotic ointment.

Post-surgery, animals were closely monitored until the completion of the study. After eight weeks, animals were anaesthetized, and euthanized through rapid IV administration of Euthanyl (240 mg/ml). Gross necropsy was performed and implant sites were removed, dissected from connecting soft tissue, and micro CT scans were collected using a Nikon skyscan model 1172. All samples were processed per O'Connell et al. and stained with a Goldners trichrome[313] . Histologic evaluation (n=3/test article) was performed under 400x magnification and rated as per ISO 10993 by the study pathologist. Histomorphometry was performed on whole section images (n=3/ test article) using Image Pro-Premier version 9.2 image analysis software using a polygon tool to identify the boundary area of the defect area (fracture edge), test article residual area, area of bone apposition, percentage new bone area, soft tissue area and void area.

4.4.5 Results

All animals survived the procedure. At day 24 of the study the sham animal was euthanized due to dehydration and prolonged refusal of food. For clarity, sham defect sites showed 91.8 $\pm$0.8 % new bone area (Figure 4.24 a, d), with moderate fibro-connective tissue formation and fatty infiltrate/marrow formation at the time of sacrifice; confirming a normal wound healing response to the surgical procedure, without evidence of infection (Table 4.8).

A summary of histopathological findings is presented in Table 4.8. Both unfilled resin (Figure 4.24 b, e) and composite resin (Figure 4.24 c,f) sites showed no polymorphic nuclear cells, lymphocytes, plasma cells, evidence of necrosis, infection, fibrous exudate, tissue degeneration, void spaces or fluid/material buildup surrounding the defects. Slight decreases in the observed number of giant cells was noted between materials with a narrow band of fibrous encapsulation being present for all of the glass filled resin cylinders. Conversely, the unfilled resin cylinders showed no fibrous encapsulation. Implant irregularity was not significantly increased in the unfilled resins

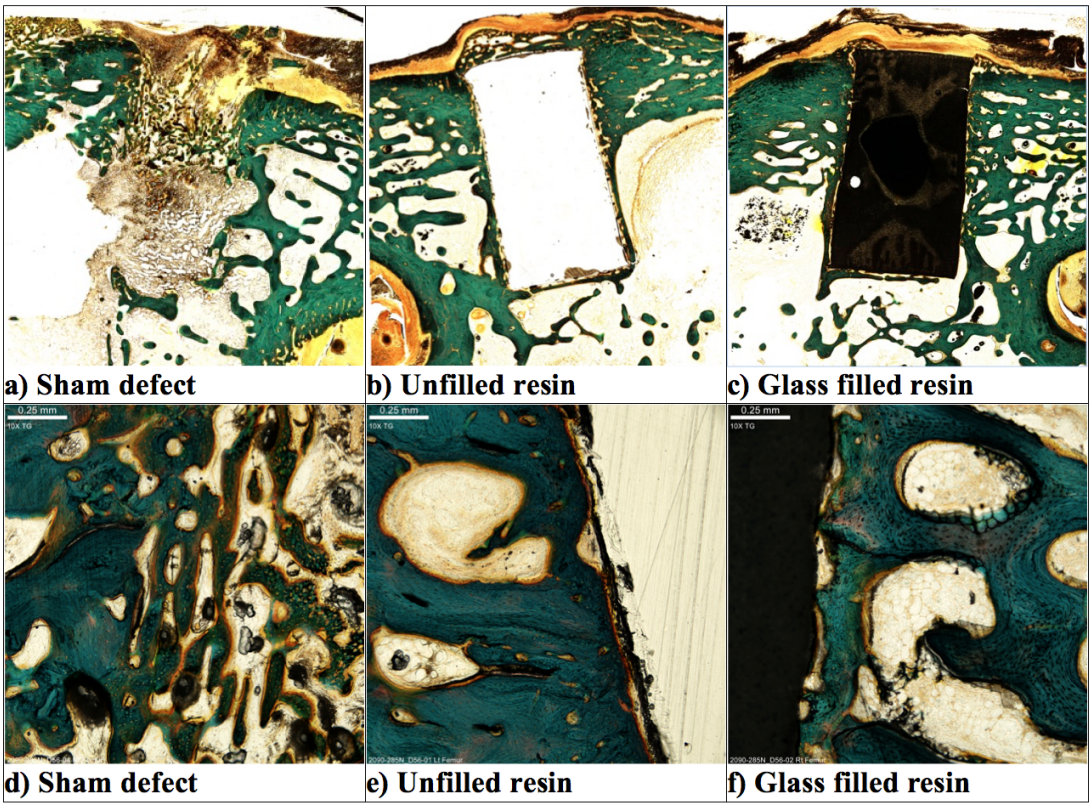

Figure 4.24: Histologic response, 8 w post implantation, Goldners Trichrome stain low magnification (10 x, subfigures a, b,c) and high magnification (subfigures d, e, f). Sham defects (a, d) showing fibrous infiltrate, unfilled resins (b, e) showing mineralized bone formation at implant surface (stained green) and glass filled resins (c, f) evidence of unmineralised osteoid formation (stained red/orange) and implant surface irregularity.

Table 4.8: Histological and histomorphometry results for sham, glass filled, and unfilled defect sites, 8 weeks post implantation.

Parameters (Mean ± SD)	**Glass Filled Resin (n=3)**	**Unfilled Resin (n=3)**	**Sham Defect (n=2)**
Polymorphonuclear cells	0.00 ± 0.00	0.00 ± 0.00	0.00 ± 0.00
Lymphocytes	0.00 ± 0.00	0.00 ± 0.00	0.00 ± 0.00
Plasma cells	0.00 ± 0.00	0.00 ± 0.00	0.00 ± 0.00
Macrophages	1.00 ± 0.00	1.00 ± 0.00	1.00 ± 0.00
Giant cells	1.00 ± 0.00	0.67 ± 0.58	0.00 ± 0.00
Necrosis	0.00 ± 0.00	0.00 ± 0.00	0.00 ± 0.00
Infection	0.00 ± 0.00	0.00 ± 0.00	0.00 ± 0.00
Fibrous Exudates	0.00 ± 0.00	0.00 ± 0.00	0.00 ± 0.00
Tissue Degeneration	0.00 ± 0.00	0.00 ± 0.00	0.00 ± 0.00
Neovascularization	1.00 ± 0.00	1.00 ± 0.00	1.50 ± 0.71
Fibrocytes/ fibroconnective tissue, fibrosis/encapsulation	1.00 ± 0.00	0.67 ± 0.58	3.00 ± 0.00
Fatty infiltrate/marrow	1.33 ± 0.58	1.33 ± 0.58	3.00 ± 0.00
New bone formation	1.00 ± 0.00	1.00 ± 0.00	3.00 ± 0.00
Bone-implant contact/ apposition (including marrow)	3.67 ± 0.58	3.67 ± 0.58	-
Void Spaces	0.00 ± 0.00	0.00 ± 0.00	0.00 ± 0.00
Fluid/material	0.00 ± 0.00	0.00 ± 0.00	0.00 ± 0.00
Implant irregularity	0.33 ± 0.58	0.67 ± 0.58	-
Bone Apposition (%)	71.4 ± 4.5	91.3 ± 15.0	-
Bone Area (%)	6.4 ± 2.5	13.0 ± 2.9	91.8 ± 0.8
Test Article Residual Area (%)	93.3 ± 2.6	86.9 ± 2.7	-
Soft Tissue Area (%)	0.4 ± 0.2	0.1 ± 0.2	8.2 ± 0.8
Void Area (%)	0.0 ± 0.0	0.0 ± 0.0	0.0 ± 0.0

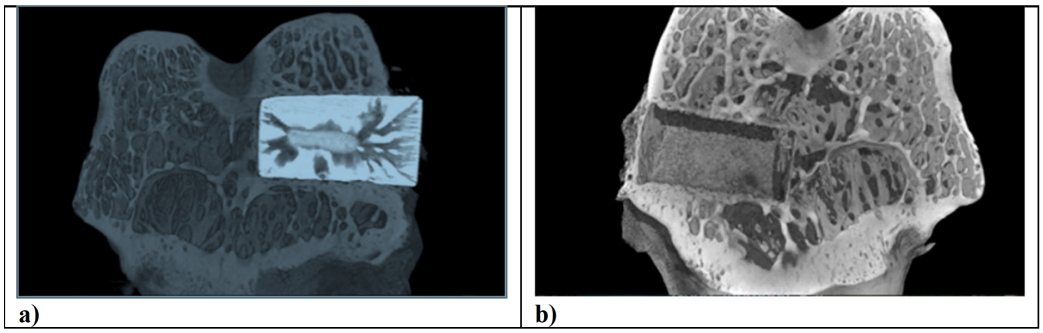

Figure 4.25: Mirco CT of implants sites, 8 weeks post implantation, (a) glass filled resin cylinder showing high contrast between glass filled material and surrounding bone tissue, along with the protrusion of the cement cylinder out of the defect site and (b)unfilled showing the formation of mineralized bone covering the defect opening

relative to the glass filled resins.

Histomorphometry results (Table 4.8) revealed limited soft tissue area and high rates of bone apposition. Bone area, and bone apposition were both greater with the unfilled resin, which also demonstrated increased resorption relative to the glass filled resin. Conversely, residual sample area for glass filled resins (24.14 ± 0.59 mm^2) was significantly higher than both the initial implant area (21 mm^2) and the residual sample area for the unfilled resins (17.57 ± 3.49 mm^2), indicating that implant swelling occurred in the glass filled resin samples. Micro CT images of the glass filled resin showed strong contrast between the glass filled resin and the surrounding bone tissues. Glass filled cement cylinder was noted to be extruding from the defect site at the time of sacrifice, extending beyond the surrounding bone (Figure 4.25 a). While visualization of the unfilled cylinder using micro CT image is not possible due to radiolucency, evidence of new bone formation over the surface of the implant encapsulating the cylinder can be seen, both on the micro CT (Figure 4.25 b) and on histological slides (Figure 4.24 b), indicating osteoconduction, consistent with the high degree of new bone apposition reported.

4.4.6 Discussion

The beneficial effects of Sr^{2+} at levels as low at 8.7 mg/l has been demonstrated *in vitro*[6]. Previous literature has established that the glass filled test article in this study is capable of exceeding this threshold over a 60 d evaluation period[306]. However, in order to achieve these therapeutic levels of release, significant alterations to the composite chemistry were required. This study observed low levels of fibrous encapsulation and high rates of new bone apposition demonstrating a favourable bone integration response for both the glass filled and unfilled resin specimens. Similar models have reported mild to moderate layers of fibrous encapsulation in response to the implantation of PMMA, or Cortoss® at 8 weeks[28] . While direct bone deposition was reported in implantation studies of Cortoss® , the onset of new bone formation was longer than was seen in this study. Specifically, new bone formation was reported after 12 weeks for Cortoss® , as opposed to the 8-week onset of new bone formation observed with the test articles. These observations may be impacted by specimen preparation, specifically, the selection of pre cast cylinders, which precluded, for example, an evaluation of the effects of exothermic setting reaction on host response. This implant form was selected to facilitate the comparison with the unfilled resin, which would lack the required viscosity for safe injection. In comparing the glass filled test article to the unfilled test article it was noted that the filled resin did not appear to provide increased bone formation, or bone apposition relative to the unfilled resin. In fact, decreased new bone formation, and increased fibrous encapsulation was noted for the glass filled resins. Contrastingly, and of particular interest is the layer of mineralized bone formed over the unfilled resin implant surface, attributable to spontaneous mineralization promoted by the highly hydrophilic resin [via a mechanism equivalent to HEMA hydrogels][297]. The unfilled resin samples also showed decreased residual material volume, and increased surface irregularity when compared to the glass filled resin samples. The increase in residual material

volume for the glass filled resin (despite the mass loss known to occur for the filler phase) was unexpected and may be an artefact of increased cement swelling arising from increased surface area imparted by the irregularly shaped, uncoupled glass filler particles, as well as potential capillary action into the voids generated by glass degradation. While cement swelling has been recognized as a detrimental effect of hydrophilic monomer additions in the field of dental materials[324], no adverse response was seen in this study. Cement swelling may also have been promoted by the selection of a predrilled surface defect, allowing room for material expansion. Irrespectively, swell-able hydrophilic cements can counteract shrinkage forces and reduce trabecular damage thereby providing improved interfaces with press fit bone bonding[325, 152]. As such, this attribute may be beneficial in the stabilization and retention of orthopaedic implants.

Conclusion

The composite materials examined presented high levels of new bone deposition, without evidence of fibrous encapsulation. The inclusion of strontium releasing glass imparted implant swelling, which may provide for improved bone integration. High rates of bone formation in the hydrophilic resin suggest surface mediated mineralization is the driving factor for the favourable tissue response and not strontium release.

Acknowledgements

The authors would like to acknowledge the funding support of the ACOA, and the technical support of AccellLAB, Boisbriand QB, Canada.

Chapter 5

Conclusion

Vertebral compression fractures are the most common outcome of osteoporotic bone loss, resulting in significant pain, and disability. While PVP has demonstrated significant pain relief for osteoporotic patients, mechanical changes to spinal loading, and osteoporotic progression result in high rates of subsequent fracture. Due to the progressive nature of the disease, clinical guidelines for the treatment of osteoporotic VCFs recommend that the primary treatment focus is the prevention of subsequent fracture. Prophylactic PVP has demonstrated efficacy in achieving this goal, by reducing the rate of adjacent fractures. This protective effect is provided by the procedures ability to compensate for the alteration in spinal biomechanics which accompany PVP. The benefit of such a procedure could be further expanded through the use of materials capable of releasing strontium, a divalent cation capable of imparting anti-osteoporotic effect. While the incorporation of strontium has been attempted through various approaches in the past, a focus on the modulation of strontium release, aiming to achieve therapeutically relevant levels has been lacking in the literature.

While bioactive glasses are frequently used as a delivery vehicle for TII's due to their easy integration into a variety of materials, they offer limited ion release time frames. As the majority of bioactive glasses studied are silicate based, significant reductions in their corrosion rate can be expected within hours of ageing. This decay in reaction rate occurs as a dense corrosion layer prevents further water infiltration at physiological pH. Borate based glasses in turn provide a significant extension of the degradation time frame, providing more uniform network degradation, and may offer benefits for long term ion release. While promising, these materials are less well

understood, with less predictable glass network structures. Furthermore, challenges to their use in bone cements are presented by their inability to be coupled into the resin network and significant mass loss, potentially negatively affecting the mechanical integrity of the material. In order to utilise borate glasses effectively as TII delivery vehicles, better understanding of their degradation properties and ability to be used as reinforcing agents in bone cements is required.

In working towards a better understanding of the long term release of strontium from a borate glass reinforced composite cement, first the dissolution of the borate glass in isolation was investigated. This experimental work "Modulation of strontium release from a tertiary borate glass through substitution of alkali for alkali earth oxide" was published in the Journal of Non Crystalline Solids, and detailed the investigation of nine glasses composed of 70 mol% B_2O_3, 30-14 mol% SrO, and 0-16 mol% Na_2O. Post fabrication compositional analysis was performed for all glasses through acid digestion, revealing B losses of up to 4 mol% during firing. Glass density increased linearly with increasing strontium content (2.62 to 2.98 g/cm^3) and a similar linear increase was observed for glass transition temperature (520 to 641°C). While B coordination was not significantly correlated to the prefired strontium content, multi-linear regression, (accounting for firing losses), revealed significant decreases in tetrahedral coordination with increasing strontium. These finding highlighted the importance of post compositional analysis in the investigation of borate glasses, where volatile losses during oxide melting could result in a significant variation between intended, and true composition. As such acid digest compositional analysis offers an important tool which is underutilized in this field.

Along with the investigation of glass structural properties, the release of both B and Sr into PBS was measured over 60 d at 37°C. Sr release was diffusion controlled for all compositions, reaching a maximum of 1418 mg/l for the 30 % Sr composition after 60 d. The diffusion coefficient for Sr release showed a strong linear correlation to the Sr content of the glass, demonstrating a high degree of tailorability of ion

release though compositional selection and structural control. While Sr release was continuous throughout the experimental period, B release kinetics varied between glass compositions. Glasses which contained low amounts of Na showed continuous B network degradation and release, however, in compositions containing 6 mol% Na_2O or greater, the measured B level in solution peaked at 14 to 30 d, before decreasing. While such analysis of Na release was precluded by the high initial Na content of the elution media, borate-alkali metal interactions were the likely cause of this finding. While glass modifier release and precipitation effects have been reported in silicate glass studies, the finding is unusual for borate glasses, which have previously been reported to undergo uniform degradation. The time frame selected for this investigation may have been critical in allowing for this observation, as many previous studies ended after 14 to 30 d. While such time-lines are common in silicate glass literature and allow for the capture of degradation up until saturation and steady state is reached, they would be insufficient to capture the full degradation reaction of the glasses investigated in this study. Borate glasses must undergo a greater degree of degradation before saturation is reached due to the high solubility of borates, and thus may require longer investigation periods to fully capture the degradation process. While high Na content resulted in B precipitation, it is of note that Sr release kinetics remained unchanged. As such, the incorporation of Na (or other alkali oxides) may offer beneficial effects in reducing the release of B, offering a potential method of mitigating cytotoxicity, without limiting TII release from the glass.

While this work demonstrated two significant methods to improve our understanding of borate glass behaviour (i.e. the importance of post fabrication compositional analysis and the selection of appropriate dissolution time lines), it was limited in its ability to assess only bulk dissolution of the glass. While this focus is common in the study of bioactive glasses in which TII release is of interest, emerging findings from the field of nuclear glasses are pointing to the importance of surface structural

changes. The use of high resolution atom probe tomography, or scanning transmission electron microscopy with a high angle annular dark field to assess compositional depth profile changes has been used successfully in the study of nuclear glasses to provide information on the progression of the hydration front[227]. Such techniques could potentially be utilised for highly degradable borate glasses to further our understanding of the degradation reaction, thus providing improved guidance for the development of TII releasing glasses. Furthermore, as surface water transport and diffusivity are being highlighted as governing factors in these reactions, the importance of organic extracellular fluid components is also drawn into question. To best utilize surface analysis techniques the incorporation of both organic and inorganic components of the elution solution would be ideal. While such research has been conducted on the original Bioglass^{TM} series, investigating the role of plasma components on the formation of an altered surface layer[326], similar experiments are needed to understand the role of surface protein interactions in borate glass reaction. Of particular importance for the study of glasses for use in mineralized tissues would be the interaction of dentin matrix protein 1 (DMP-1), which serves as nucleation sites for HA, and as, such could substantially reduce both calcium and phosphate levels in solution, altering release kinetics[327]. Ultimately, the application of such analytical techniques to a broader range of glass compositions will help to better explain the role of both the glass components and the glass surface in the reaction process.

From the information gained in the first study, a glass composed of 70 mol% B_2O_3, 26 mol% SrO, and 4 mol% Na_2O was selected for use as the reinforcing phase moving forward. This composition was selected as it demonstrated continuous diffusion controlled release of both Sr, and B over the 60 d investigated. This selection allowed for predictable release kinetics over the investigation period, exceeding therapeutic thresholds for Sr on bone, without concern of decreased degradation due to precipitate formation on the glass surface. Furthermore, this glass composition resulted in the lowest peak B release of the three diffusion controlled compositions, decreasing

concerns of potential B toxicity. This glass composition was studied in the second publication in this work "The Feasibility and Functional Performance of Ternary Borate-Filled Hydrophilic Bone Cements: Targeting Therapeutic Release Thresholds for Strontium" which was published in the Journal of Functional Biomaterials and focused on the effects of resin hydrophilicity and glass filler content on composite resin properties and ion release kinetics. In this work the effect of varying glass content (55 to 65 wt% of the cement) and HEMA content (15 to 45 wt% of the resin phase) on handling properties, resin conversion, biaxial strength, and ion release was observed. These investigations revealed that while no appreciable effect was seen on cement setting time, with all cements setting within 209 to 263 s, working times in turn decreased from 255 to 150 s with increasing HEMA content. These results suggested that the cement formulations have potential clinical applications as snap set cements from a two paste system. ATR FTIR degree of cure analysis revealed that increased HEMA content resulted in increased methacrylate conversion (42 % to 81 %). While high HEMA content composites have previously been reported to increase cytotoxicity due to the increased leachability of the small monomer, cytotoxicity testing of these materials (Appendix B) confirmed that no increased cytotoxicity was present, likely due to the increased degree of cure reducing leaching from the resin.

Biaxial flexural strength following ageing in PBS ranged from 44 to 16 MPa after 24 h, decreasing with increased HEMA content. After 60 d of ageing however, cement strength ranged from 28 to 16 MPa, with cements containing 30 % HEMA or less demonstrating a significant decrease from their initial strength at 24 h. Such a decrease in materials strength is common in composite resins containing degradable fillers, and was expected to have a significant effect on the investigated materials in which the filler was designed to provide prolonged degradation. The finding of maintained, or improved strength over time for cements containing 37.5 or 45 % HEMA were thus an unexpected, and unique finding. While residual curing could explain such a finding, the greatest increases in strength were observed in the materials with

the greatest degree of cure, leaving this explanation unlikely.

The release of both Sr and B from these cements was investigated, following ageing in PBS. While increasing HEMA content resulted in increased B release, as was expected by the increased water sorption, no such effect was seen for Sr release. B release was high (between 67.7 and 183.6 mg/l at 60 d), but no longer diffusion controlled. Similar to the release profiles observed for the high Na content glasses a peak and fall in boron concentration was observed for all but the highest HEMA content cements. Maximum B release of 15 % of the initial B loading was observed for the 45 % HEMA, 65 % glass cement after 60 d. Sr release was much lower than B release (9 to 32 mg/l), reaching a maximum of 1.3 % of the loaded Sr, with the greatest release seen in the 30 % HEMA cements. While investigations into the glass in isolation resulted in preferential Sr release, no preferential release was seen from the cement samples. This change can be explained by the formation of a strontium-phosphate phase on the surface of the materials as observed under SEM EDS. These finding suggest that glass degradation is hydration controlled as expected, however Sr release may be prevented due to the surface charge generated on the highly hydrophilic resins, resulting in the formation of the precipitate. The selection of a calcium free media may have favoured the precipitation of strontium, as calcium phosphates are less soluble and would be expected to form under such conditions *in vivo*, decreasing the phosphate concentration and sparing strontium precipitation.

The evidence of precipitates was observed not only on the surface of the glasses, as altered layers, but also on the resin phase, suggesting that their formation was not generated by decreased transport phenomena and supersaturation. These findings highlight the importance of matrix filler interactions, and is likely the factor which provided the unusual increase in strength seen in these materials, with precipitates serving to reinforce the composite. As such highly hydrophilic materials may offer a unique ability to compensate for the loss of strength associated with small molecular weight monomers, as well as the plasticizing effects of water uptake. This surface

reaction may also provide improved tissue integration in a mechanism similar to bioactive glass integration, in which the formation of an HA like surface layer is an important step. As such the ability of highly polar polymers to spontaneously generate mineral phases could be beneficial in long term implantation environments providing increased mechanical reinforcement over time.

The interaction between solution and surface effects which govern the formation of the precipitates on these materials, while similar to those which govern bioactive glass degradation, is poorly understood in the field of biomaterials. Peak concentrations of strontium released into solution were much greater in the investigation of the glass phase in isolation (up to 1418 mg/l), and remained stable in solution, indicating an important role of surface charge. A similar dependence on surface charge and not supersaturation has been reported with the formation of a HA alteration layer on calcium free silicate glasses[218]. While such forces are recognized as important, research into the reaction of bioactive glasses frequently relies upon degradation models which lack a mechanistic basis, and are thus unable to adequately explain or predict the effect of altering surface conditions. While interfacial dissolution and reprecipitation models allow for better predictive power, based on the relative solubility of the various glass components, they also lack consideration of surface charge. These models however do highlight the importance of secondary precipitates in preventing saturation, and permitting prolonged glass degradation. For example, it has been demonstrated that fluctuations in natural soil bacteria can alter geological glass corrosion due to metaloprotease secretion, altering the metal content of the solution and accelerating the surface reaction[328]. Such findings are of particular relevance to the application of glasses in hard tissue engineering, where spontaneous physiological mineralization reactions would be expected to alter the local composition of the solution, and thus the reaction progress. Similarly to the importance of bacterial metaloproteases in geological glass weathering, the ability of both naturally occurring proteins (i.e. DMP-1) and poly HEMA to precipitate divalent cations from solution could greatly alter the

glass degradation reaction. While *in vitro* ion release experiments are a valuable tool for the comparison between compositions, they can not be directly linked to true *in vivo* release. In order to better understand what factors govern the release *in vivo*, adaptations to the ageing environment to better mimic both the chemical as well as mechanical environment would be needed.

Building upon this work, the third publication of this thesis aimed to deepen our understanding of the impact of mechanical loading on ion release from such cement under simulated physiological conditions. Mechanically responsive hydrogel drug delivery devices have previously demonstrated significant increases in the release of reversibly bound hydrophilic drugs under cyclic loading conditions, due to hydrostatic pulses generated in the materials. While material stiffness would be expected to be much greater in bone cements, so would be the mechanical loads on the cements. Despite the mechanically demanding implantation environment which would be experienced by these materials, the majority of drug loaded bone cements are tested under non mechanically loaded environments. While some limited investigations have taken place, they have focused on the release of sparingly soluble gentamicin from hydrophobic PMMA cements[192, 191]. While these investigations both revealed that drug release was significantly increased over unloaded *in vitro* testing, the investigations focused on hip arthroplasty models where high levels of tension generated crack-surface mediated release. While these studies demonstrated significant possibility for mechanical loading to alter drug release, the topic has gained little research interest, with no focus on hydrophilic cements, ion release, or the mechanical loading experienced by PVP materials. Along with investigating mechanical loading, this third study employed SBF, aiming to give a better representation of the ionic conditions, and thus the precipitation effects expected to occur following implantation. This change in extract conditions was made to test the hypothesis that strontium precipitation was caused, in part, by the calcium free media used, and that strontium

release would be significantly increased if calcium ions were present. The cement composition selected for this third experiment was the 45 % HEMA, 60 % glass loading composition. This cement formulation was selected as it had provided the highest degree of boron release, and thus presented the greatest extent of network degradation while allowing for sustained mechanical strength over the 60 d period. This experiment looked at the release of Sr and B over 48 h under three loading conditions, cyclic compressive loading (0.3 to 6 MPa, 2 Hz sinusoidal waveform), static compressive loading (equivalent RMS value, 4.3 MPa) as well as unloaded. While the compressive cyclic loading conditions served to mimic the loading expected to occur during gait, both the static compressive and unloaded conditions were used as controls to better assess the effects of the loading cycles. ICP analysis of incubation media revealed that, while both compressive loading conditions resulted in significant decreases in water uptake, concurrent increases in ion release were observed. Cyclic compressive loading increased strontium release 4 fold over unloaded conditions, while a modest but statistically significant increase was seen under static compression. While pulsatile fluid flow, similar to what has been used to control hydrogel drug delivery would explain the increase seen under cyclic loading, static compressive loading likely increased release rates due to decreased interaction with the resin components due to decreased swelling. In this study the preferential release of Sr was again seen, for all loading conditions, demonstrating that the precipitation of Sr was prevented by the inclusion of Ca in the incubation media. Such a finding is important, as the use of SBF has fallen out of favour for investigation of HA formation on bioactive glasses, due to inconsistent results which translate poorly to *in vivo* HA formation[329, 330]. The significant impact of mechanical loading also points to the importance of mechanical loading in the release of therapeutic in bone tissue engineering, where considerable load bearing would be expected to occur.

While this work is important in its demonstration of the significant impact of mechanical loading on ion release, a factor frequently overlooked in the design of drug

delivery for hard tissue applications, it offers several avenues through which further investigation could be conducted. First of note would be to extend the duration of testing which was limited in this initial evaluation. While the experiment covered 345,600 cycles, the equivalent of 48 d of mechanical loading, dissolution time was limited at 48 h, which would greatly reduce the potential for glass network hydrolysis. Extension to 60 or even 90 d would be relevant for such a material as it would represent a normal fracture healing window[331, 332]. While regularly shaped cement samples were investigated in this work to maintain consistent surface area, the injection of cements into the interconnected pores of a tissue phantom could serve to further the knowledge gained from this work. Such a testing method would allow for more accurate representation of the final geometry of the implanted cement, which has been linked to significant alterations in loading[319]. As the swelling of the injected cement would be limited not only by the constraints of mechanical loading, but also by the tissue phantom, a more accurate representation of cement swelling, and thus ion release would also be gained. Similar constrained models have been utilized for the fatigue testing of acrylic bone cements to better represent the stress distribution in the implanted cement environment and could be adapted for ion release investigations[333].

While loading amplitude and frequency was selected to represent the mechanical environment of an augmented vertebral body during walking, the constant cyclic loading regime utilized is not representative of typical human activity. Intermittent periods of rest, low activity, and more intense activity would be more representative of true activity levels, and may serve to better predict true response. Variations in both loading frequency, and amplitude could serve to alter water transport surrounding the materials and thus may alter the release of ions or other soluble drugs. While mimicking the natural activity of a target patient demographic could be beneficial in terms of assessing ion release for threshold targeting, testing through a variety of frequencies and amplitudes could help to better understand the underlying mechanisms which

govern ion release The mechanical response demonstrated in this work may offer a method of mimicking natural mechanosensory response in bone tissue, with increased drug release under periods of increased activity. While using more natural loading conditions, including constrained phantoms and variable loading regimes could better mimic the mechanical environment, alterations to the elution media could also be made to better understand the implantation environment, as previously discussed. Flow through environments, which allow for media circulation could also be used to better mimic a true implantation environment in which blood flow would limit the accumulation of release products. The selection of appropriate flow rates however is unclear, and difficult to correlate to *in vivo* conditions. Ultimately the closest match to the implantation environment would likely be the use of *ex vivo* spinal segments, which would provide mechanical constraint to injected tissue, best mimic loading distribution, and provide natural nucleation sites. Furthermore, the field of dental biomaterials has provided improved insight into the movement of water through composite resins using silver nitrate staining which can identify areas of hydrophilicity and water infiltration[334]. While the extended periods of stain infiltration required (over 24 h) precluded the application of such a method in this study, if extended timeframes of loading were used this could provide useful insight into alteration of fluid flow. If combined with the use of tissue phantoms, such a method could be useful in identifying how tissue geometry alters water movement, and its correlation with potential for soluble drug release.

In vivo responses to the 45 % HEMA 60 % glass loading cement was evaluated through a pilot implantation study which compared response to precast cylinders of both the resin in isolation, and the glass filled resin (full results in Appendix C). This selection was made to allow for the isolation of the response to each component, as Bis-GMA resins have previously been demonstrated to improve tissue response[28]. As such, the hydrophilic resin phase was used as a negative control to isolate any potential beneficial effect from strontium release. To accommodate this comparison,

and prevent interference from differences in peak exothermic temperatures, pre cast cylinders were used as the implanted material. This investigation was performed as a pilot animal study, in an aim to gain better insight into the appropriateness of this design to test the efficacy of strontium releasing cements. While favourable healing responses, with direct bone deposition, was observed for both materials the highest degree of direct bone deposition and new bone formation as seen surrounding the glass free resin. The resin phase in isolation provided very high rates of direct bone deposition, with bone formation evident over the defect surface through both histological and micro CT analysis. In contrast, the glass reinforced resin demonstrated significant swelling with minor areas of fibrous encapsulation. While the use of a pre-drilled defect in a New Zealand white rabbit is a common model for the evaluation of bone tissue engineering materials, it is possible that this model provided a favourable environment for the high level of swelling seen (allowing for the implant to protrude past the bone surface), obscuring measurement of new bone formation. More accurate swelling response could be gained through the direct injection of the cement into trabecular voids.

Due to the limited sample size of the study, it can not conclusively be determined if the inclusion of strontium had any detrimental or beneficial effect on the surrounding tissue. The high level of new bone formation surrounding the resin phase in isolation however was unexpected, and likely linked to the material's ability to form spontaneous phosphate containing precipitates as observed *in vitro*. This beneficial effect from increased hydrophilicity may provide a simple method of improving integration of acrylic cements without the need for increasing complexity through bioactive glass inclusion. While such a cement would not offer any anti-osteoporotic efficacy it would offer substantial benefit over PMMA cement by reducing fibrous encapsulation, without the unpredictable remodelling observed with CPCs.

Further investigation is merited both into the unexpectedly positive response to the unfilled resin, as well as to assess if strontium release provided any appreciable

beneficial effect. To accomplish this goal a large animal study which allows for direct injection of the materials into trabecular voids would be ideal, allowing for better approximation of both swelling and loading *in vivo*. Better understanding of the movement of strontium and its distribution through the bone network could be gained through analysis of the HA crystal lattice in the tissues surrounding the implant. This technique has been used in the early investigations oral strontium therapy, to assess the mechanism of strontium incorporation into bone[335]. Such investigations could provide information as to the fate of strontium released from the material, allowing for a greater understanding of its accumulation, potential for therapeutic benefit, and region of distribution. This information could be gained by a number of micro analysis techniques (both X ray and infra-red spectroscopy based), and would provide valuable information not only in relation to the development of strontium releasing cements, but would offer unique insight into the distribution of inorganic ions from bioactive glasses used in tissue engineering. As the greatest limit to our understanding of the degradation of bioactive glasses is our lack of knowledge of ion transport surrounding the implant, information gained from such experiments could prove highly valuable in furthering our understanding of the topic.

While borate glasses offer a method of providing sustained TII delivery, the translation of such findings into therapeutically relevant release levels remains challenging. Controlled substitution of strontium for sodium in a high borate glass provided a method of tailoring the diffusion coefficient for strontium allowing for a high degree of control over strontium release. The extension of degradation timelines allowed for the observation of borate precipitation effects, a possible mechanism of mitigating borate toxicity while prolonging TII release. When incorporated into a highly hydrophilic composite resin cement however, preferential release was lost due to interactions between strontium and the resin phase under *in vivo* conditions, leaving ion release difficult to assess. While these interactions were favoured by the selection of calcium free media, the ability of strontium to readily incorporate into a calcium phosphate

phase leads to difficulty in extrapolating true release behaviour as would be observed *in vivo*. This work highlighted the importance of resin-filler interactions, with the formation of precipitates serving to reinforce the material counteracting strength loss from filler degradation. The investigation of mechanical loading on ion release highlighted that mechanical loading, similarly to the ionic environment, can greatly alter the release of TIIs from a biomaterial and is an important consideration in the design and investigation of drug releasing orthopaedic materials subject to mechanical loading. These findings are significant due to the current predominance of non mechanically loaded elution testing environments for orthopaedic materials. While the ultimate therapeutic efficacy could only be determined through animal implantation models, further investigation into mechanically loaded simulated implantation environments could deepen our understanding of ion release mechanisms and provide for more accurate estimates of true *in vivo* release. While a pilot animal study showed positive tissue response to the strontium releasing cement, no benefit was seen over a strontium free Bis-GMA, TEG DMA, HEMA implant. These findings, similarly to the findings of spontaneous precipitate formation on the resin surface draw attention to the ability of the hydrophilic resin phase to induce mineralization, allowing for osteointegration. The findings of this work highlight the importance of hydrophilicity, mechanical loading and ionic environment in the assessment of TII release, presenting avenues to further our understanding of biomaterial response to the implantation environment and guide development of novel products. While the inclusion of a borate glass into a highly hydrophilic composite resin cement provides a novel mechanism of significantly increasing ion release over conventional materials, while simultaneously mitigating the decrease in strength typically observed during ageing, further work is required to understand the true therapeutic potential of such a material. As such this material may present a novel mechanism of providing long term mechanical stability, coupled with load responsive anti-osteoporotic therapy to address the ever growing burden of age related osteoporotic fractures on the health care system.

Bibliography

[1] Gladius Lewis. Injectable bone cements for use in vertebroplasty and kyphoplasty: Stateoftheart review. *Journal of Biomedical Materials Research Part B: Applied Biomaterials*, 76(2):456–468, 2006.

[2] Stryker. Stryker interventional spine, 2013.

[3] SW Wade, C. Strader, LA Fitzpatrick, MS Anthony, and CD OMalley. Estimating prevalence of osteoporosis: examples from industrialized countries. *Archives of osteoporosis*, 9(1):182, 2014.

[4] R. Bartl and B. Frisch. *Osteoporosis: Diagnosis, Prevention, Therapy*. Springer, 2009.

[5] Cardiovascular and interventional radiology society of europe, vertebral augmentation, 2017.

[6] Edith Bonnelye, Anne Chabadel, Frdric Saltel, and Pierre Jurdic. Dual effect of strontium ranelate: Stimulation of osteoblast differentiation and inhibition of osteoclast formation and resorption in vitro. *Bone*, 42(1):129–138, 2008.

[7] Pierre J. Meunier, Christian Roux, Ego Seeman, Sergio Ortolani, Janusz E. Badurski, Tim D. Spector, Jorge Cannata, Adam Balogh, Ernst-Martin Lemmel, Stig Pors-Nielsen, Ren Rizzoli, Harry K. Genant, and Jean-Yves Reginster. The effects of strontium ranelate on the risk of vertebral fracture in women with postmenopausal osteoporosis. *N Engl J Med*, 350(5):459–468, 01/29; 2013/04 2004.

[8] DP Wornham, MO Hajjawi, IR Orriss, and TR Arnett. Strontium potently inhibits mineralisation in bone-forming primary rat osteoblast cultures and reduces numbers of osteoclasts in mouse marrow cultures. *Osteoporosis International*, 25(10):2477–2484, 2014.

[9] N. Chattopadhyay. The calcium-sensing receptor (car) is involved in strontium ranelate-induced osteoblast proliferation. *Biochemical pharmacology*, 74(3):438, 2007.

[10] Jean-Yves Reginster, E. Seeman, MC De Vernejoul, S. Adami, J. Compston, C. Phenekos, JP Devogelaer, M. Diaz Curiel, A. Sawicki, and S. Goemaere. Strontium ranelate reduces the risk of nonvertebral fractures in postmenopausal women with osteoporosis: Treatment of peripheral osteoporosis (tropos) study. *Journal of Clinical Endocrinology and Metabolism*, 90(5):2816–2822, 2005.

[11] Juliet Compston. Osteoporosis: social and economic impact. *Radiologic clinics of North America*, 48(3):477–482, 2010.

[12] Erik F. Eriksen, Adolfo Dez-Prez, and Steven Boonen. Update on long-term treatment with bisphosphonates for postmenopausal osteoporosis: A systematic review. *Bone*, 58:126–135, 1 2014.

[13] Jean-Yves Reginster, Marie-Paule Lecart, Rita Deroisy, and Christian Lousberg. Strontium ranelate: a new paradigm in the treatment of osteoporosis. *Expert opinion on investigational drugs*, 13(7):857–864, 2004.

[14] Becky A. Briesacher, Susan E. Andrade, Robert A. Yood, and Kristijan H. Kahler. Consequences of poor compliance with bisphosphonates. *Bone*, 41(5):882–887, November 2007 2007.

[15] Manisha Mulgund, Karen A. Beattie, Andy KO Wong, Alexandra Papaioannou, and Jonathan D. Adachi. Assessing adherence to teriparatide therapy, causes of nonadherence and effect of adherence on bone mineral density measurements in osteoporotic patients at high risk for fracture. *Therapeutic advances in musculoskeletal disease*, 1(1):5–11, 2009.

[16] Sundeep Khosla, Jane A. Cauley, Juliet Compston, Douglas P. Kiel, Clifford Rosen, Kenneth G. Saag, and Elizabeth Shane. Addressing the crisis in the treatment of osteoporosis: a path forward. *Journal of Bone and Mineral Research*, 32(3):424–430, 2017.

[17] Osteoporosis Canada. Osteoporosis, facts and statistics, 2013.

[18] Michael C. Hurley, Rami Kaakaji, Guilherme Dabus, Ali Shaibani, Mathew T. Walker, Richard G. Fessler, and Bernard R. Bendok. Percutaneous vertebroplasty. *Neurosurgery clinics of North America*, 20(3):341–359, 07/01 2009.

[19] Eric Heffernan. The current status of percutaneous vertebroplasty in canada. *Canadian Association of Radiologists Journal*, 59(2):77–82, 2008.

[20] N. Tanigawa. Percutaneous vertebroplasty for osteoporotic compression fractures: long-term evaluation of the technical and clinical outcomes. *AJR, American journal of roentgenology*, 196(6):1415, 2011.

[21] G. Baroud, J. Nemes, P. Heini, and T. Steffen. Load shift of the intervertebral disc after a vertebroplasty: a finite-element study. *European Spine Journal*, 12(4):421–426, Aug 2003.

[22] Andreas Boger, Paul Heini, Markus Windolf, and Erich Schneider. Adjacent vertebral failure after vertebroplasty: a biomechanical study of low-modulus pmma cement. *European Spine Journal*, 16(12):2118–2125, 2007.

[23] H. Bae. A prospective randomized fda-ide trial comparing cortoss with pmma for vertebroplasty: a comparative effectiveness research study with 24-month follow-up. *Spine (Philadelphia, Pa.1976)*, 37(7):544, 2012.

[24] Y. Y. Tseng. Repeated and multiple new vertebral compression fractures after percutaneous transpedicular vertebroplasty. *Spine (Philadelphia, Pa.1976)*, 34(18):1917, 2009.

[25] Jaw-Lin Wang, Chun-Kai Chiang, Ya-Wen Kuo, Wen-Kai Chou, and Been-Der Yang. Mechanism of fractures of adjacent and augmented vertebrae following simulated vertebroplasty. *Journal of Biomechanics*, 45(8):1372–1378, 5/11 2012.

[26] W. F. Lems, K. E. Dreinhofer, H. Bischoff-Ferrari, M. Blauth, E. Czerwinski, J. da Silva, A. Herrera, P. Hoffmeyer, T. Kvien, G. Maalouf, D. Marsh, J. Puget, W. Puhl, G. Poor, L. Rasch, C. Roux, S. Schuler, B. Seriolo, U. Tarantino, T. van Geel, A. Woolf, C. Wyers, and P. Geusens. Eular/efort recommendations for management of patients older than 50 years with a fragility fracture and prevention of subsequent fractures. *Annals of the Rheumatic Diseases*, 76(5):802–810, May 2017.

[27] Alexander Hoppe, Viviana Mourio, and Aldo R. Boccaccini. Therapeutic inorganic ions in bioactive glasses to enhance bone formation and beyond. *Biomaterials Science*, 1(3):254–256, 2013.

[28] E. M. Erbe, T. D. Clineff, and G. Gualtieri. Comparison of a new bisphenol-a-glycidyl dimethacrylate-based cortical bone void filler with polymethyl methacrylate. *European spine journal*, 10 Suppl 2:S147–S152, 2001.

[29] P. J. Marie. Mechanisms of action and therapeutic potential of strontium in bone. *Calcified tissue international*, 69(3):121, 2001.

[30] A. S. Hurtel-Lemaire, R. Mentaverri, A. Caudrillier, F. Cournarie, A. Wattel, S. Kamel, E. F. Terwilliger, E. M. Brown, and M. Brazier. The calcium-sensing receptor is involved in strontium ranelate-induced osteoclast apoptosis. new insights into the associated signaling pathways. *The Journal of biological chemistry*, 284(1):575–584, Jan 2 2009.

[31] Larry L. Hench. Bioceramics: from concept to clinic. *Journal of the American Ceramic Society*, 74(7):1487–1510, 1991.

[32] Larry L. Hench, Arjan Andersson, June Wilson, Antti Yli-Urpo, and Risto-Pekka Happonen. *BIOACTIVE GLASSES; BIOACTIVE GLASSES: CLINICAL APPLICATIONS*, chapter 3; 4, pages 41; 63–62; 73. An Introduction to Bioceramics: An Introduction to Bioceramics.

[33] L. L. Hench and D. E. Clark. Physical chemistry of glass surfaces. *Journal of Non-Crystalline Solids*, 28(1):83, 1978.

[34] Jaime L. George and Richard K. Brow. In-situ characterization of borate glass dissolution kinetics by -raman spectroscopy. *Journal of Non-Crystalline Solids*, 426:116–124, 2015.

[35] Muhammad S. Hasan, Ulrike WernerZwanziger, and Daniel Boyd. Compositionstructureproperties relationship of strontium borate glasses for medical applications. *Journal of Biomedical Materials Research Part A*, 2014.

[36] Adrian C. Wright. My borate life: An enigmatic journey. *International Journal of Applied Glass Science*, 6(1):45–63, 2015.

[37] F. M. Collares, F. A. Ogliari, C. H. Zanchi, C. L. Petzhold, E. Piva, and S. M. Samuel. Influence of 2-hydroxyethyl methacrylate concentration on polymer network of adhesive resin. *The journal of adhesive dentistry*, 13(2):125–129, Apr 2011.

[38] J. M. Powers and R. L. Sakaguchi. *Craig's Restorative Dental Materials*. Mosby, 2006.

[39] Alexandra Papaioannou, Suzanne Morin, Angela M. Cheung, Stephanie Atkinson, Jacques P. Brown, Sidney Feldman, David A. Hanley, Anthony Hodsman, Sophie A. Jamal, Stephanie M. Kaiser, Brent Kvern, Kerry Siminoski, and William D. Leslie. 2010 clinical practice guidelines for the diagnosis and management of osteoporosis in canada: summary. *Canadian Medical Association journal*, October 12 2010.

[40] P. McDonnell, P. E. McHugh, and D. O'Mahoney. Vertebral osteoporosis and trabecular bone quality. *Annals of Biomedical Engineering*, 35(2):170–189, 2007.

[41] A. Tenenhouse, L. Joseph, N. Kreiger, S. Poliquin, TM Murray, L. Blondeau, C. Berger, DA Hanley, JC Prior, and CaMos Research Group. Estimation of the prevalence of low bone density in canadian women and men using a population-specific dxa reference standard: the canadian multicentre osteoporosis study (camos). *Osteoporosis International*, 11(10):897–904, 2000.

[42] Elizabeth BarrettConnor, Ethel S. Siris, Lois E. Wehren, Paul D. Miller, Thomas A. Abbott, Marc L. Berger, Arthur C. Santora, and Louis M. Sherwood. Osteoporosis and fracture risk in women of different ethnic groups. *Journal of bone and mineral research*, 20(2):185–194, 2005.

[43] Gerrads Tortora J. and Mark Nielsen T. *Principles of Human Anatomy*. Wiley, Hoboken, N. J., 11 edition, 2009.

[44] Steve Weiner, Wolfie Traub, and H. Daniel Wagner. Lamellar bone: Structure-function relations. *Journal of structural biology*, 126(3):241–255, 6/30 1999.

[45] E. R. Myers and S. E. Wilson. Biomechanics of osteoporosis and vertebral fracture. *Spine (Philadelphia, Pa.1976)*, 22(24 Suppl):25S–31S, 1997.

[46] Bart Clarke. Normal bone anatomy and physiology. *Clinical Journal of the American Society of Nephrology*, 3(Supplement 3):S131–S139, November 2008 November 2008.

[47] Erik Fink Eriksen. Cellular mechanisms of bone remodeling. *Reviews in Endocrine and Metabolic Disorders*, 11(4):219–227, 2010.

[48] K. Henriksen, J. Bollerslev, V. Everts, and M. A. Karsdal. Osteoclast activity and subtypes as a function of physiology and pathologyimplications for future treatments of osteoporosis. *Endocrine reviews*, 32(1):31–63, February 01 2011.

[49] Sandrine Theoleyre, Yohann Wittrant, Steeve Kwan Tat, Yannick Fortun, Francoise Redini, and Dominique Heymann. The molecular triad opg/rank/rankl: involvement in the orchestration of pathophysiological bone remodeling. *Cytokine & growth factor reviews*, 15(6):457–475, 12 2004.

[50] Astrid Liedert, Daniela Kaspar, Robert Blakytny, Lutz Claes, and Anita Ignatius. Signal transduction pathways involved in mechanotransduction in bone cells. *Biochemical and biophysical research communications*, 349(1):1–5, 10/13 2006.

[51] Fanxin Long. Building strong bones: molecular regulation of the osteoblast lineage. *Nature reviews Molecular cell biology*, 13(1):27–38, 2012.

[52] Donald A. Glass II and Gerard Karsenty. Molecular bases of the regulation of bone remodeling by the canonical wnt signaling pathway. *Current topics in developmental biology*, 73:43–84, 2006.

[53] Jacob Tfelt-Hansen and Edward M. Brown. The calcium-sensing receptor in normal physiology and pathophysiology: a review. *Critical reviews in clinical laboratory sciences*, 42(1):35–70, 2005.

[54] Pierre J. Marie. Signaling pathways affecting skeletal health. *Current osteoporosis reports*, 10(3):190–198, 2012.

[55] B. Lawrence Riggs, Sundeep Khosla, and L. Joseph Melton. A unitary model for involutional osteoporosis: estrogen deficiency causes both type i and type ii osteoporosis in postmenopausal women and contributes to bone loss in aging men. *Journal of bone and mineral research*, 13(5):763–773, 1998.

[56] L. G. Raisz. Pathogenesis of osteoporosis: concepts, conflicts, and prospects. *The Journal of clinical investigation*, 115(12):3318–3325, Dec 2005.

[57] N. K. Arden, J. Baker, C. Hogg, K. Baan, and T. D. Spector. The heritability of bone mineral density, ultrasound of the calcaneus and hip axis length: A study of postmenopausal twins. *Journal of Bone and Mineral Research*, 11(4):530–534, 1996.

[58] - *Calcified Tissue International*, (- 3):– 181.

[59] J. A. Riancho, J. M. Olmos, B. Pineda, C. Garcia-Ibarbia, M. I. Perez-Nunez, D. N. Nan, J. Velasco, A. Cano, M. A. Garcia-Perez, M. T. Zarrabeitia, and J. Gonzalez-Macias. Wnt receptors, bone mass, and fractures: gene-wide association analysis of lrp5 and lrp6 polymorphisms with replication. *European journal of endocrinology*, 164(1):123–131, Jan 2011.

[60] G. Eghbali-Fatourechi, S. Khosla, A. Sanyal, W. J. Boyle, D. L. Lacey, and B. L. Riggs. Role of rank ligand in mediating increased bone resorption in early postmenopausal women. *The Journal of clinical investigation*, 111(8):1221–1230, Apr 2003.

[61] Michael F. Holick. Vitamin d deficiency. *N Engl j Med*, 2007(357):266–281, 2007.

[62] F. Grassi, G. Tell, M. Robbie-Ryan, Y. Gao, M. Terauchi, X. Yang, M. Romanello, D. P. Jones, M. N. Weitzmann, and R. Pacifici. Oxidative stress causes bone loss in estrogen-deficient mice through enhanced bone marrow dendritic cell activation. *Proceedings of the National Academy of Sciences of the United States of America*, 104(38):15087–15092, Sep 18 2007.

[63] J. Vina, J. Sastre, FV Pallardo, J. Gambini, and C. Borras. Role of mitochondrial oxidative stress to explain the different longevity between genders. protective effect of estrogens. *Free radical research*, 40(12):1359–1365, 2006.

[64] K. Y. Lin, A. Ito, T. Asagami, P. S. Tsao, S. Adimoolam, M. Kimoto, H. Tsuji, G. M. Reaven, and J. P. Cooke. Impaired nitric oxide synthase pathway in diabetes mellitus: role of asymmetric dimethylarginine and dimethylarginine dimethylaminohydrolase. *Circulation*, 106(8):987–992, Aug 20 2002.

[65] Elena A. Ostrakhovitch and Igor B. Afanasev. Oxidative stress in rheumatoid arthritis leukocytes: suppression by rutin and other antioxidants and chelators. *Biochemical pharmacology*, 62(6):743–746, 2001.

[66] J. J. Cao and M. J. Picklo. N-acetylcysteine supplementation decreases osteoclast differentiation and increases bone mass in mice fed a high-fat diet. *The Journal of nutrition*, 144(3):289–296, Mar 2014.

[67] Grahame Elder. Pathophysiology and recent advances in the management of renal osteodystrophy. *Journal of Bone and Mineral Research*, 17(12):2094–2105, 2002.

[68] A. Bouquegneau, S. Salam, P. Delanaye, R. Eastell, and A. Khwaja. Bone disease after kidney transplantation. *Clinical journal of the American Society of Nephrology : CJASN*, 11(7):1282–1296, Jul 7 2016.

[69] Nobuhiro Sasaki, Eiji Kusano, Yasuhiro Ando, Kazuki Yano, Eisuke Tsuda, and Yasushi Asano. Glucocorticoid decreases circulating osteoprotegerin (opg): possible mechanism for glucocorticoid induced osteoporosis. *Nephrology Dialysis Transplantation*, 16(3):479–482, March 01 2001.

[70] Keizo Ohnaka, Hiroshi Taniguchi, Hisaya Kawate, Hajime Nawata, and Ryoichi Takayanagi. Glucocorticoid enhances the expression of dickkopf-1 in human osteoblasts: novel mechanism of glucocorticoid-induced osteoporosis. *Biochemical and biophysical research communications*, 318(1):259–264, 5/21 2004.

[71] Jill Waalen. Current and emerging therapies for the treatment of osteoporosis. *J Exp Pharmacol*, 2:121–134, 2010.

[72] Sian Yik Lim, Joon Hee Lim, Dan Nguyen, Rie Okamura, Hoda Mojazi Amiri, Michael Calmes, and Kenneth Nugent. Screening for osteoporosis in men aged 70 years and older in a primary care setting in the united states. *American journal of men's health*, 7(4):350–354, 2013.

[73] A. Spiegel. How a bone disease grew to fir the perscription (internet), December 21, 2009 2009.

[74] Smita Jha, Zhong Wang, Nicholas Laucis, and Timothy Bhattacharyya. Trends in media reports, oral bisphosphonate prescriptions, and hip fractures 19962012: An ecological analysis. *Journal of Bone and Mineral Research*, 30(12):2179–2187, 2015.

[75] Richard Eastell, Sandra L. Cedel, Heinz W. Wahner, B. Lawrence Riggs, and L. Joseph Melton. Classification of vertebral fractures. *Journal of Bone and Mineral Research*, 6(3):207–215, 1991.

[76] Fraser P. Coxon, Keith Thompson, and Michael J. Rogers. Recent advances in understanding the mechanism of action of bisphosphonates. *Current Opinion in Pharmacology*, 6(3):307–312, 6 2006.

[77] H. Molvik and W. Khan. Bisphosphonates and their influence on fracture healing: a systematic review. *Osteoporosis International*, 26(4):1251–1260, 2015.

[78] Pirow J. Bekker, Donna L. Holloway, Amy S. Rasmussen, Robyn Murphy, Steven W. Martin, Philip T. Leese, Gregory B. Holmes, Colin R. Dunstan, and Alex M. DePaoli. A singledose placebocontrolled study of amg 162, a fully human monoclonal antibody to rankl, in postmenopausal women. *Journal of Bone and Mineral Research*, 19(7):1059–1066, 2004.

[79] E. M. Lewiecki, Paul Miller, Michael McClung, Stanley Cohen, Michael Bolognese, Yu Liu, Andrea Wang, Suresh Siddhanti, and Lorraine Fitzpatrick. Two-year treatment with denosumab (amg 162) in a randomized phase 2 study of postmenopausal women with low bmd. *Journal of bone and mineral research*, 22(12):1832–1841, 2007.

[80] Steven R. Cummings, Javier San Martin, Michael R. McClung, Ethel S. Siris, Richard Eastell, Ian R. Reid, Pierre Delmas, Holly B. Zoog, Matt Austin, and Andrea Wang. Denosumab for prevention of fractures in postmenopausal women with osteoporosis. *New England Journal of Medicine*, 361(8):756–765, 2009.

[81] Armen H. Tashjian and Bruce A. Chabner. Commentary on clinical safety of recombinant human parathyroid hormone 134 in the treatment of osteoporosis in men and postmenopausal women. *Journal of Bone and Mineral Research*, 17(7):1151–1161, 2002.

[82] Jean-Yves Reginster, Rita Deroisy, and Isabelle Jupsin. Strontium ranelate: a new paradigm in the treatment of osteoporosis. *Drugs Today*, 39(2):89–101, 2003.

[83] Glen M. Blake, E. Michael Lewiecki, David L. Kendler, and Ignac Fogelman. A review of strontium ranelate and its effect on dxa scans. *Journal of Clinical Densitometry*, 10(2):113–119, 2007.

[84] S. C. Skoryna. Effects of oral supplementation with stable strontium. *Canadian Medical Association journal*, 125(7):703–712, 1981.

[85] P. J. Marie. The calcium-sensing receptor in bone cells: a potential therapeutic target in osteoporosis. *Bone*, 46(3):571, 2010.

[86] Joseph Caverzasio and Cyril Thouverey. Activation of fgf receptors is a new mechanism by which strontium ranelate induces osteoblastic cell growth. *Cellular physiology and biochemistry*, 27(3-4):243–250, 2011.

[87] Alex Rojas Bie Thomsen, Jesper Worm, Stine Engesgaard Jacobsen, Martin Stahlhut, Markus Latta, and Hans Brauner-Osborne. Strontium is a biased agonist of the calcium-sensing receptor in rat medullary thyroid carcinoma 6-23 cells. *Journal of Pharmacology and Experimental Therapeutics*, August 31 2012.

[88] Zuzana Saidak and Pierre J. Marie. Strontium signaling: Molecular mechanisms and therapeutic implications in osteoporosis. *Pharmacology & therapeutics*, 136(2):216–226, 11 2012.

[89] Iris Schrooten, Monique M. Elseviers, Ludwig V. Lamberts, Marc E. De Broe, and Patrick C. D'Haese. Increased serum strontium levels in dialysis patients: An epidemiological survey. *Kidney International*, 56(5):1886–1892, November 1999 1999.

[90] Servier Laboratories. *SUMMARY OF PRODUCT CHARACTERISTICS: Protelos*. 2012.

[91] Christian Roux, Jacques Fechtenbaum, Sami Kolta, Giancarlo Isaia, JB Cannata Andia, and Jean-Pierre Devogelaer. Strontium ranelate reduces the risk of vertebral fracture in young postmenopausal women with severe osteoporosis. *Annals of the Rheumatic Diseases*, 67(12):1736–1738, 2008.

[92] P. J. Marie. Effective doses for strontium ranelate. *Osteoporosis International*, 19(12):1813, 2008.

[93] PJ Meunier, DO Slosman, PD Delmas, JL Sebert, ML Brandi, C. Albanese, R. Lorenc, S. Pors-Nielsen, MC De Vernejoul, and A. Roces. Strontium ranelate: dose-dependent effects in established postmenopausal vertebral osteoporosisa 2-year randomized placebo controlled trial. *The Journal of Clinical Endocrinology and Metabolism*, 87(5):2060–2066, 2002.

[94] Seamus Looby and Adam Flanders. Spine trauma. *Radiologic clinics of North America*, 49(1):129–163, 2011.

[95] Jerilynn C. Prior, Lisa Langsetmo, Brian C. Lentle, Claudie Berger, David Goltzman, Christopher S. Kovacs, Stephanie M. Kaiser, Jonathan D. Adachi, Alexandra Papaioannou, Tassos Anastassiades, Tanveer Towheed, Robert G. Josse, Jacques P. Brown, William D. Leslie, and Nancy Kreiger. Ten-year incident osteoporosis-related fractures in the population-based canadian multicentre osteoporosis study comparing site and age-specific risks in women and men. *Bone*, 71:237–243, February 2015 2015.

[96] G. Ioannidis, A. Papaioannou, W. M. Hopman, N. Akhtar-Danesh, T. Anastassiades, L. Pickard, C. C. Kennedy, J. C. Prior, W. P. Olszynski, K. S. Davison, D. Goltzman, L. Thabane, A. Gafni, E. A. Papadimitropoulos, J. P. Brown, R. G. Josse, D. A. Hanley, and J. D. Adachi. Relation between fractures and mortality: results from the canadian multicentre osteoporosis study. *CMAJ : Canadian Medical Association journal = journal de l'Association medicale canadienne*, 181(5):265–271, Sep 1 2009.

[97] S. A. Jackson, A. Tenenhouse, and L. Robertson. Vertebral fracture definition from population-based data: preliminary results from the canadian multicenter osteoporosis study (camos). *Osteoporosis international : a journal established as result of cooperation between the European Foundation for Osteoporosis and the National Osteoporosis Foundation of the USA*, 11(8):680–687, 2000.

[98] Michael Adams and Patricia Dolan. Biomechanics of vertebral compression fractures and clinical application. *Archives of Orthopaedic and Trauma Surgery*, 131(12):1703–1710, 2011.

[99] Hwan Mo Lee, Si Young Park, Soon Hyuck Lee, Seung Woo Suh, and Jae Young Hong. Comparative analysis of clinical outcomes in patients with osteoporotic vertebral compression fractures (ovcfs): conservative treatment versus balloon kyphoplasty. *The Spine Journal*, 12(11):998–1005, 2012.

[100] A. M. Briggs, A. M. Greig, and J. D. Wark. The vertebral fracture cascade in osteoporosis: a review of aetiopathogenesis. *Osteoporosis International*, 18(5):575–584, 2007.

[101] Sri Harsha Tella and J. Christopher Gallagher. Prevention and treatment of postmenopausal osteoporosis. *The Journal of steroid biochemistry and molecular biology*, 142:155–170, 2014.

[102] A. O. Ortiz and R. Bordia. Injury to the vertebral endplate-disk complex associated with osteoporotic vertebral compression fractures. *American Journal of Neuroradiology*, 32(1):115–120, January 01 2011.

[103] P. R. Landham, S. J. Gilbert, H. L. Baker-Rand, P. Pollintine, K. A. Robson Brown, M. A. Adams, and P. Dolan. Pathogenesis of vertebral anterior wedge deformity: A 2-stage process? *Spine*, 40(12):902–908, Jun 15 2015.

[104] Mehrsheed Sinaki. Critical appraisal of physical rehabilitation measures after osteoporotic vertebral fracture. *Osteoporosis International*, 14(9):773–779, 2003.

[105] Umile Giuseppe Longo, Mattia Loppini, Luca Denaro, Nicola Maffulli, and Vincenzo Denaro. Osteoporotic vertebral fractures: current concepts of conservative care. *British medical bulletin*, 102(1):171–189, June 01 2012.

[106] JASON McCARTHY and Amy Davis. Diagnosis and management of vertebral compression fractures. *American Family Physician*, 94(1), 2016.

[107] S. I. Esses, R. McGuire, J. Jenkins, J. Finkelstein, E. Woodard, W. C. Watters 3rd, M. J. Goldberg, M. Keith, C. M. Turkelson, J. L. Wies, P. Sluka, K. M. Boyer, and K. Hitchcock. The treatment of symptomatic osteoporotic spinal compression fractures. *The Journal of the American Academy of Orthopaedic Surgeons*, 19(3):176–182, Mar 2011.

[108] I. G. Hide and A. Gangi. Percutaneous vertebroplasty: history, technique and current perspectives. *Clinical radiology*, 59(6):461–467, /6 2004.

[109] Giovanni Anselmetti, Stefano Marcia, Luca Saba, Mario Muto, Giuseppe Bonaldi, Paolo Carpeggiani, Stefano Marini, Antonio Manca, and Salvatore Masala. Percutaneous vertebroplasty: multi-centric results from everest experience in large cohort of patients. *European Journal of Radiology*, 81(12):4083–4086, 2012.

[110] Vadim Goz, Thomas J. Errico, Jeffrey H. Weinreb, Steven M. Koehler, Andrew C. Hecht, Virginie Lafage, and Sheeraz A. Qureshi. Vertebroplasty and kyphoplasty: national outcomes and trends in utilization from 2005 through 2010. *The Spine Journal*, 13(0), 2013.

[111] A. Venmans, P. N. M. Lohle, W. J. van Rooij, H. J. J. Verhaar, and W. P. Th M. Mali. Frequency and outcome of pulmonary polymethylmethacrylate embolism during percutaneous vertebroplasty. *American Journal of Neuroradiology*, 29(10):1983–1985, November 2008 November 2008.

[112] Chris Gu, Waleed Brinjikji, Avery Evans, Mohammad Murad, and David Kallmes. Outcomes of vertebroplasty compared with kyphoplasty: a systematic review and meta-analysis. *Journal of NeuroInterventional Surgery*, 8(6):636–642, 2016.

[113] Medical Advisory Secretariat. Balloon kyphoplasty: an evidence-based analysis. Technical Report 4(12), Ontario Health Technology Assessment Series, 2004.

[114] Caroline AH Klazen, Paul NM Lohle, Jolanda de Vries, Frits H. Jansen, Alexander V. Tielbeek, Marion C. Blonk, Alexander Venmans, Willem Jan J van Rooij, Marinus C. Schoemaker, and Job R. Juttmann. Vertebroplasty versus conservative treatment in acute osteoporotic vertebral compression fractures (vertos ii): an open-label randomised trial. *The Lancet*, 376(9746):1085–1092, 2010.

[115] Jordi Blasco, Angeles Martinez-Ferrer, Juan Macho, Luis San Roman, Jaume Poms, Josep Carrasco, Ana Monegal, Nuria Guaabens, and Pilar Peris. Effect of vertebroplasty on pain relief, quality of life, and the incidence of new vertebral fractures: A 12-month randomized follow-up, controlled trial. *Journal of Bone and Mineral Research*, 27(5):1159–1166, 2012.

[116] Majid Reza Farrokhi, Ehsanali Alibai, and Zohre Maghami. Randomized controlled trial of percutaneous vertebroplasty versus optimal medical management for the relief of pain and disability in acute osteoporotic vertebral compression fractures. *Journal of Neurosurgery: Spine*, 14(5):561–569, 2011.

[117] David F. Kallmes, Bryan A. Comstock, Patrick J. Heagerty, Judith A. Turner, David J. Wilson, Terry H. Diamond, Richard Edwards, Leigh A. Gray, Lydia Stout, Sara Owen, William Hollingworth, Basavaraj Ghdoke, Deborah Annesley-Williams, Stuart H. Ralston, and Jeffrey G. Jarvik. A randomized trial of vertebroplasty for osteoporotic spinal fractures. *N Engl J Med*, 361(6):569–579, 08/06; 2012/09 2009.

[118] William Clark, Paul Bird, Peter Gonski, Terrence H. Diamond, Peter Smerdely, H. Patrick McNeil, Glen Schlaphoff, Carl Bryant, Elizabeth Barnes, and Val Gebski. Safety and efficacy of vertebroplasty for acute painful osteoporotic fractures (vapour): a multicentre, randomised, double-blind, placebo-controlled trial. *The Lancet*, 388(10052):1408–1416, 2016.

[119] Rachelle Buchbinder, Richard H. Osborne, Peter R. Ebeling, John D. Wark, Peter Mitchell, Chris Wriedt, Stephen Graves, Margaret P. Staples, and Bridie Murphy. A randomized trial of vertebroplasty for painful osteoporotic vertebral fractures. *N Engl J Med*, 361(6):557–568, 08/06; 2013/03 2009.

[120] Douglas Wardlaw, Steven R. Cummings, Jan Van Meirhaeghe, Leonard Bastian, John B. Tillman, Jonas Ranstam, Richard Eastell, Peter Shabe, Karen Talmadge, and Steven Boonen. Efficacy and safety of balloon kyphoplasty compared with non-surgical care for vertebral compression fracture (free): a randomised controlled trial. *The Lancet*, 373(9668):1016–1024, 2009.

[121] M. Dohm, C. M. Black, A. Dacre, J. B. Tillman, G. Fueredi, and KAVIAR investigators. A randomized trial comparing balloon kyphoplasty and vertebroplasty for vertebral compression fractures due to osteoporosis. *AJNR.American journal of neuroradiology*, 35(12):2227–2236, Dec 2014.

[122] Jane Johnson, Wendy Rogers, and Rosalind Jeffree. The controversy over vertebroplasty: an analysis of the debate and proposals for a way forward. *Journal of medical imaging and radiation oncology*, 56(4):449–451, 2012.

[123] Juan-Francisco Asenjo and Felipe Rossel. Vertebroplasty and kyphoplasty: new evidence adds heat to the debate. *Current Opinion in Anesthesiology*, 25(5):577–583, 2012.

[124] Arif Hussain and Michael Erdek. Vertebroplasty augmentation procedures: examining the controversy. *Pain physician*, 16:E483–E490, 2013.

[125] Afshin Gangi, Tarun Sabharwal, Farah G. Irani, Xavier Buy, Jose P. Morales, and Andreas Adam. Quality assurance guidelines for percutaneous vertebroplasty. *Cardiovascular and interventional radiology*, 29(2):173–178, 2006.

[126] David J. Wilson, Sara Owen, and Rufus A. Corkill. Facet joint injections as a means of reducing the need for vertebroplasty in insufficiency fractures of the spine. *European radiology*, 21(8):1772–1778, 2011.

[127] Steven Boonen, Jan Van Meirhaeghe, Leonard Bastian, Steven R. Cummings, Jonas Ranstam, John B. Tillman, Richard Eastell, Karen Talmadge, and Douglas Wardlaw. Balloon kyphoplasty for the treatment of acute vertebral compression fractures: 2year results from a randomized trial. *Journal of Bone and Mineral Research*, 26(7):1627–1637, 2011.

[128] Robert Oakland, Navin Furtado, Ruth Wilcox, Jake Timothy, and Richard Hall. Preliminary biomechanical evaluation of prophylactic vertebral reinforcement adjacent to vertebroplasty under cyclic loading. *The spine journal*, 9(2):174–181, 2009.

[129] U. Berlemann. Adjacent vertebral failure after vertebroplasty a biomechanical investigation. *The journal of bone and joint surgery.British volume*, 84(5):748, 2002.

[130] S. P. J. Muijs, A. R. van Erkel, and P. D. S. Dijkstra. Treatment of painful osteoporotic vertebral compression fractures. *Journal of Bone and Joint Surgery*, 93-B(9):1149, 2011.

[131] Sandro D. Badilatti, Patrik Christen, Stephen J. Ferguson, and Ralph Mller. Computational modeling of long-term effects of prophylactic vertebroplasty on bone adaptation. *Proceedings of the Institution of Mechanical Engineers, Part H: Journal of Engineering in Medicine*, 231(5):423–431, 2017.

[132] C. H. Yen, M. M. Teng, W. H. Yuan, Y. C. Sun, and C. Y. Chang. Preventive vertebroplasty for adjacent vertebral bodies: a good solution to reduce adjacent vertebral fracture after percutaneous vertebroplasty. *AJNR.American journal of neuroradiology*, 33(5):826–832, May 2012.

[133] Peter Diel, Lorenz Freiburghaus, Christoph Rder, Lorin Michael Benneker, Albrecht Popp, Gosia Perler, and Paul Ferdinand Heini. Safety, effectiveness and predictors for early reoperation in therapeutic and prophylactic vertebroplasty: short-term results of a prospective case series of patients with osteoporotic vertebral fractures. *European spine journal*, 21(6):792–799, 2012.

[134] Nobuo Kobayashi, Yuji Numaguchi, Sokun Fuwa, Akihiro Uemura, Masaki Matsusako, Yuka Okajima, Mitsutomi Ishiyama, and Osamu Takahashi. Prophylactic vertebroplasty: cement injection into non-fractured vertebral bodies during percutaneous vertebroplasty. *Academic Radiology*, 16(2):136–143, 2009.

[135] Dong-Hyun Kim, Kyeong-Lok Kim, Ho-Hwan Chun, Tae-Wan Kim, Hong-Chae Park, and Seog-Young Yoon. In vitro biodegradable and mechanical performance of biphasic calcium phosphate porous scaffolds with unidirectional macro-pore structure. *Ceramics International*, 40(6):8293–8300, 2014.

[136] WCG Peh and LA Gilula. Percutaneous vertebroplasty: indications, contraindications, and technique. *The British journal of radiology*, 76(901):69–75, 2003.

[137] Ren Aquarius, Jasper Homminga, Allard Jan Frederik Hosman, Nico Verdonschot, and Esther Tanck. Prophylactic vertebroplasty can decrease the fracture risk of adjacent vertebrae: An in vitro cadaveric study. *Medical Engineering and Physics*, 36(7):944–948, July 2014 2014.

[138] Ying-Chou Sun, Michael Mu Huo Teng, Wei-Shin Yuan, Chao-Bao Luo, Feng-Chi Chang, Jiing-Feng Lirng, Wan-Yuo Guo, and Cheng-Yen Chang. Risk of post-vertebroplasty fracture in adjacent vertebral bodies appears correlated with the morphologic extent of bone cement. *Journal of the Chinese Medical Association*, 74(8):357–362, August 2011 2011.

[139] Martin C. Eichler, Christian Spross, Alexander Ewers, Ryan Mayer, and Fabrice A. Klling. Prophylactic adjacent-segment vertebroplasty following kyphoplasty for a single osteoporotic vertebral fracture and the risk of adjacent fractures: a retrospective study and clinical experience. *Journal of Neurosurgery: Spine*, 25(4):528–534, 2016.

[140] Masashi Makita, Koichiro Yamakado, Atsuhiro Nakatsuka, Haruyuki Takaki, Tadashi Inaba, Fumiyoshi Oshima, Hidetaka Katayama, and Kan Takeda. Effects of barium concentration on the radiopacity and biomechanics of bone cement: experimental study. *Radiation Medicine*, 26(9):533–538, 2008.

[141] Naomi Kobayashi, Daisuke Togawa, Takaaki Fujishiro, Kimberly A. Powell, A. Simon Turner, Howard B. Seim, and Thomas W. Bauer. Histological and radiographic evaluation of polymethylmethacrylate with two different concentrations of barium sulfate in a sheep vertebroplasty model. *Journal of Biomedical Materials Research Part A*, 75A(1):123–127, 2005.

[142] A. Boger, K. D. Wheeler, B. Schenk, and P. F. Heini. Clinical investigations of polymethylmethacrylate cement viscosity during vertebroplasty and related in vitro measurements. *European spine journal*, 18(9):1272–1278, 2009.

[143] Jean-Denis Laredo and Bassam Hamze. Complications of percutaneous vertebroplasty and their prevention. *Skeletal radiology*, 33(9):493–505, 2004.

[144] Liliana Rincn-Kohli and Philippe K. Zysset. Multi-axial mechanical properties of human trabecular bone. *Biomechanics and modeling in mechanobiology*, 8(3):195–208, 2009.

[145] Ian Henry Parkinson, Arash Badiei, M. Stauber, J. Codrington, R. Mller, and Nicola L. Fazzalari. Vertebral body bone strength: the contribution of individual trabecular element morphology. *Osteoporosis International*, 23(7):1957–1965, 2012.

[146] MA Tyndyk, V. Barron, and PE McHugh. Effect of osteoporosis on the biomechanics of the thoracolumbar spine: finite element study. *European Cells and Materials*, 10(Suppl 3):73, 2005.

[147] MA Tyndyk, V. Barron, PE McHugh, and D. O Mahoney. Generation of a finite element model of the thoracolumbar spine. *Acta of Bioengineering and Biomechanics*, 9(1):35, 2007.

[148] Giovanni Carlo Anselmetti, Antonio Manca, Khanna Kanika, Kieran Murphy, Haris Eminefendic, Salvatore Masala, and Daniele Regge. Temperature measurement during polymerization of bone cement in percutaneous vertebroplasty: an in vivo study in humans. *Cardiovascular and interventional radiology*, 32(3):491–498, 2009.

[149] Gladius Lewis. Properties of acrylic bone cement: state of the art review. *Journal of Biomedical Materials Research*, 38(2):155–182, 1997.

[150] Gladius Lewis. Effect of mixing method and storage temperature of cement constituents on the fatigue and porosity of acrylic bone cement. *Journal of Biomedical Materials Research Part A*, 48(2):143–149, 1999.

[151] Jingtao Zhang, Weizhen Liu, Verena Schnitzler, Franck Tancret, and Jean-Michel Bouler. Calcium phosphate cements for bone substitution: chemistry, handling and mechanical properties. *Acta biomaterialia*, 10(3):1035–1049, 2014.

[152] Michael Kinzl, Andreas Boger, PK Zysset, and Dieter H. Pahr. The mechanical behavior of pmma/bone specimens extracted from augmented vertebrae: a numerical study of interface properties, pmma shrinkage and trabecular bone damage. *Journal of Biomechanics*, 45(8):1478–1484, 2012.

[153] David Nussbaum, Philippe Gailloud, and Kieran Murphy. The chemistry of acrylic bone cements and implications for clinical use in image-guided therapy. *Journal of vascular and interventional radiology*, 15(2):121–126, 2004.

[154] Klaus-Dieter Kuhn. *Bone Cements*. Springer, 2000.

[155] S. M. Kenny. Bone cements and fillers: a review. *Journal of materials science.Materials in medicine*, 14(11):923, 2003.

[156] Huilin Yang and Jun Zou. Filling materials used in kyphoplasty and vertebroplasty for vertebral compression fracture: a literature review. *Artificial Cells, Blood Substitutes, and Immobilization Biotechnology*, 39(2):87–91, 2011.

[157] David A. Nussbaum, Philippe Gailloud, and Kieran Murphy. A review of complications associated with vertebroplasty and kyphoplasty as reported to the food and drug administration medical device related web site. *Journal of Vascular and Interventional Radiology*, 15(11):1185–1192, 2004.

[158] G. J. Pomrink, M. P. DiCicco, T. D. Clineff, and E. M. Erbe. Evaluation of the reaction kinetics of cortoss, a thermoset cortical bone void filler. *Biomaterials*, 24(6):1023–1031, 2003.

[159] D. Boyd, M. Towler, A. Wren, and O. Clarkin. Comparison of an experimental bone cement with surgical simplex p, spineplex and cortoss. *Journal of Materials Science: Materials in Medicine*, 19(4):1745–1752, 2008.

[160] Laurence C. Chow and Shozo Takagi. A natural bone cement-a laboratory novelty led to the development of revolutionary new biomaterials. *JOURNAL OF RESEARCH-NATIONAL INSTITUTE OF STANDARDS AND TECHNOLOGY*, 106(6):1029–1034, 2001.

[161] Marc Bohner. Reactivity of calcium phosphate cements. *Journal of Materials Chemistry*, 17(38):3980–3986, 2007.

[162] M. Bohner. Physical and chemical aspects of calcium phosphates used in spinal surgery. *European Spine Journal*, 10(2):S114–S121, 2001.

[163] S. S. Bajammal, M. Zlowodzki, A. Lelwica, P. Tornetta 3rd, T. A. Einhorn, R. Buckley, R. Leighton, T. A. Russell, S. Larsson, and M. Bhandari. The use of calcium phosphate bone cement in fracture treatment. a meta-analysis of randomized trials. *The Journal of bone and joint surgery.American volume*, 90(6):1186–1196, Jun 2008.

[164] S. Panzavolta, P. Torricelli, B. Bracci, M. Fini, and A. Bigi. Alendronate and pamidronate calcium phosphate bone cements: setting properties and in vitro response of osteoblast and osteoclast cells. *Journal of inorganic biochemistry*, 103(1):101–106, 2009.

[165] OM Clarkin, D. Boyd, S. Madigan, and MR Towler. Comparison of an experimental bone cement with a commercial control, hydroset. *Journal of Materials Science: Materials in Medicine*, 20(7):1563–1570, 2009.

[166] Jorrit-Jan Verlaan, F. Cumhur Oner, and Wouter J. A. Dhert. Anterior spinal column augmentation with injectable bone cements. *Biomaterials*, 27(3):290–301, January 2006 2006.

[167] Elise Verron, Marie-Line Pissonnier, Julie Lesoeur, Verena Schnitzler, Borhane Hakim Fellah, Hugues Pascal-Moussellard, Paul Pilet, Olivier Gauthier, and Jean-Michel Bouler. Vertebroplasty using bisphosphonate-loaded calcium phosphate cement in a standardized vertebral body bone defect in an osteoporotic sheep model. *Acta biomaterialia*, 10(11):4887–4895, 2014.

[168] Gianluca Maestretti, Claus Cremer, Philippe Otten, and Roland Peter Jakob. Prospective study of standalone balloon kyphoplasty with calcium phosphate cement augmentation in traumatic fractures. *European Spine Journal*, 16(5):601–610, 2007.

[169] Mohamed Habib, Gamal Baroud, Francois Gitzhofer, and Marc Bohner. Mechanisms underlying the limited injectability of hydraulic calcium phosphate paste. *Acta Biomaterialia*, 4(5):1465–1471, September 2008 2008.

[170] Iwan Palmer, John Nelson, Wolfgang Schatton, Nicholas J. Dunne, Fraser J. Buchanan, and Susan A. Clarke. Biocompatibility of calcium phosphate bone cement with optimized mechanical properties. *Journal of Biomedical Materials Research Part B: Applied Biomaterials*, 104(2):308–315, 2016.

[171] Jie An, Hongbing Liao, Nathan W. Kucko, RalfPeter Herber, Joop GC Wolke, Jeroen JJP van den Beucken, John A. Jansen, and Sander CG Leeuwenburgh. Longterm evaluation of the degradation behavior of three apatiteforming calcium phosphate cements. *Journal of Biomedical Materials Research Part A*, 104(5):1072–1081, 2016.

[172] Brent R. Constantz, Bryan M. Barr, Ira C. Ison, Mark T. Fulmer, Joy Baker, LuAnn McKinney, Stuart B. Goodman, Subramanian Gunasekaren, David C. Delaney, and John Ross. Histological, chemical, and crystallographic analysis of four calcium phosphate cements in different rabbit osseous sites. *Journal of Biomedical Materials Research Part A*, 43(4):451–461, 1998.

[173] Long Xin, Matthias Bungartz, Stefan Maenz, Victoria Horbert, Max Hennig, Bernhard Illerhaus, Jens Gnster, Jrg Bossert, Sabine Bischoff, Juliane Borowski, Harald Schubert, Klaus D. Jandt, Elke Kunisch, Raimund W. Kinne, and Olaf Brinkmann. Decreased extrusion of calcium phosphate cement versus high viscosity pmma cement into spongious bone marrowan ex vivo and in vivo study in sheep vertebrae. *The Spine Journal*, 16(12):1468–1477, December 2016 2016.

[174] L. Nystrom, R. Raw, J. Buckwalter, and J. A. Morcuende. Acute intraoperative reactions during the injection of calcium sulfate bone cement for the treatment of unicameral bone cysts: a review of four cases. *The Iowa orthopaedic journal*, 28:81–84, 2008.

[175] Norihisa Goto, Hiroshi Kato, Jun ichi Maeyama, Michiko Shibano, Takuya Saito, Junji Yamaguchi, and Shinobu Yoshihara. Local tissue irritating effects and adjuvant activities of calcium phosphate and aluminium hydroxide with different physical properties. *Vaccine*, 15(12-13):1364–1371, 1997.

[176] Fabien Wauquier, Laurent Leotoing, Vronique Coxam, Jrme Guicheux, and Yohann Wittrant. Oxidative stress in bone remodelling and disease. *Trends in molecular medicine*, 15(10):468–477, 10 2009.

[177] J. Palussire. Clinical results of an open prospective study of a bis-gma composite in percutaneous vertebral augmentation. *European spine journal*, 14(10):982, 2005.

[178] Sune Larsson and Gerjon Hannink. Injectable bone-graft substitutes: current products, their characteristics and indications, and new developments. *Injury*, 42:S30–S34, 2011.

[179] E. T. Middleton, C. J. Rajaraman, D. P. O'Brien, S. M. Doherty, and A. D. Taylor. The safety and efficacy of vertebroplasty using cortoss cement in a newly established vertebroplasty service. *British journal of neurosurgery*, 22(2):252–256, 04 2008.

[180] M. M. Panjabi, V. Goel, T. Oxland, K. Takata, J. Duranceau, M. Krag, and M. Price. Humand lumbar vertebrae quantitative three dimensional anatomy. *Spine*, 17(3):299–299–306, 1992.

[181] Jiaxing Wang, Chen Zhu, Tao Cheng, Xiaochun Peng, Wen Zhang, Hui Qin, and Xianlong Zhang. A systematic review and meta-analysis of antibiotic-impregnated bone cement use in primary total hip or knee arthroplasty. *PloS one*, 8(12):e82745, 2013.

[182] J. S. Cummins, I. M. Tomek, S. R. Kantor, O. Furnes, L. B. Engesaeter, and S. R. Finlayson. Cost-effectiveness of antibiotic-impregnated bone cement used in primary total hip arthroplasty. *The Journal of bone and joint surgery.American volume*, 91(3):634–641, Mar 1 2009.

[183] P. Zwolak, J. C. Manivel, P. Jasinski, M. N. Kirstein, A. Z. Dudek, J. Fisher, and E. Y. Cheng. Cytotoxic effect of zoledronic acid-loaded bone cement on giant cell tumor, multiple myeloma, and renal cell carcinoma cell lines. *The Journal of bone and joint surgery.American volume*, 92(1):162–168, Jan 2010.

[184] D. Corry and J. Moran. Assessment of acrylic bone cement as a local delivery vehicle for the application of non-steroidal anti-inflammatory drugs. *Biomaterials*, 19(14):1295–1301, 1998.

[185] Marshall R. Urist. *Polymethylmethacrylate delivery system for bone morphogenetic protein*, 1985.

[186] Maria-Pau Ginebra, Tania Traykova, and JA Planell. Calcium phosphate cements as bone drug delivery systems: a review. *Journal of Controlled Release*, 113(2):102–110, 2006.

[187] Susmita Bose and Solaiman Tarafder. Calcium phosphate ceramic systems in growth factor and drug delivery for bone tissue engineering: a review. *Acta biomaterialia*, 8(4):1401–1421, 2012.

[188] Daniel G. Arkfeld and Elyse Rubenstein. Quest for the holy grail to cure arthritis and osteoporosis: Emphasis on bone drug delivery systems. *Advanced Drug Delivery Reviews*, 57(7):939–944, 25 May 2005 2005.

[189] Gladius Lewis. Properties of antibioticloaded acrylic bone cements for use in cemented arthroplasties: A stateoftheart review. *Journal of Biomedical Materials Research Part B: Applied Biomaterials*, 89(2):558–574, 2009.

[190] Javad Parvizi, Khaled J. Saleh, Phillip S. Ragland, Aidin Eslam Pour, and Michael A. Mont. Efficacy of antibioticimpregnated cement in total hip replacement. *Acta orthopaedica*, 79(3):335–341, 2008.

[191] Gladius Lewis and Si Janna. The in vitro elution of gentamicin sulfate from a commercially available gentamicinloaded acrylic bone cement, versabond ab. *Journal of Biomedical Materials Research Part B: Applied Biomaterials*, 71(1):77–83, 2004.

[192] Johannes GE Hendriks, Danille Neut, Jan G. Hazenberg, Gijsbertus J. Verkerke, Jim R. van Horn, Henny C van der Mei, and Henk J. Busscher. The influence of cyclic loading on gentamicin release from acrylic bone cements. *Journal of Biomechanics*, 38(4):953–957, 2005.

[193] MAKOTO OTSUKA, KAZUKI YONEOKA, YOSHIHISA MATSUDA, JEFFREY L. FOX, WILLIAM I. HIGUCHI, and YUICHI SUGIYAMA. Oestradiol release from selfsetting apatitic bone cement responsive to plasmacalcium level in ovariectomized rats, and its physicochemical mechanism. *Journal of pharmacy and pharmacology*, 49(12):1182–1188, 1997.

[194] WM Lam, HB Pan, MK Fong, WS Cheung, KL Wong, ZY Li, KDK Luk, WK Chan, CT Wong, and C. Yang. In vitro characterization of low modulus linoleic acid coated strontiumsubstituted hydroxyapatite containing pmma bone cement. *Journal of Biomedical Materials Research Part B: Applied Biomaterials*, 96(1):76–83, 2011.

[195] Solene Tadier, Reine Bareille, Robin Siadous, Olivier Marsan, Cedric Charvillat, Sophie Cazalbou, Joelle Amde, Christian Rey, and Christle Combes. Strontium-loaded mineral bone cements as sustained release systems: Compositions, release properties, and effects on human osteoprogenitor cells. *Journal of Biomedical Materials Research Part B: Applied Biomaterials*, 100(2):378–390, 2012.

[196] Christian Behl, Thomas Skutella, Frank LezoualcH, Anke Post, Martina Widmann, Christopher J. Newton, and Florian Holsboer. Neuroprotection against oxidative stress by estrogens: Structure-activity relationship. *Molecular pharmacology*, 51(4):535–541, American Society for Pharmacology and Experimental Therapeutics 1997.

[197] Matthias Schumacher and Michael Gelinsky. Strontium modified calcium phosphate cementsapproaches towards targeted stimulation of bone turnover. *Journal of Materials Chemistry B*, 3(23):4626–4640, 2015.

[198] J. Christoffersen, M. R. Christoffersen, N. Kolthoff, and O. Brenholdt. Effects of strontium ions on growth and dissolution of hydroxyapatite and on bone mineral detection. *Bone*, 20(1):47–54, 1 1997.

[199] Mohammad Hamdan Alkhraisat, Claus Moseke, Luis Blanco, Jake E. Barralet, Enrique Lopez-Carbacos, and Uwe Gbureck. Strontium modified biocements with zero order release kinetics. *Biomaterials*, 29(35):4691–4697, 2008.

[200] S. Panzavolta, P. Torricelli, L. Sturba, B. Bracci, R. Giardino, and A. Bigi. Setting properties and in vitro bioactivity of strontiumenriched gelatincalcium phosphate bone cements. *Journal of Biomedical Materials Research Part A*, 84(4):965–972, 2008.

[201] D. Guo. Development of a strontium-containing hydroxyapatite bone cement. *Biomaterials*, 26(19):4073, 2005.

[202] Xiupeng Wang, Jiandong Ye, and Yingjun Wang. Influence of a novel radiopacifier on the properties of an injectable calcium phosphate cement. *Acta Biomaterialia*, 3(5):757–763, 9 2007.

[203] Kenneth MC Cheung, FHKAM Orth FHKCOS, William W. Lu, CT Wong, Danny Chan, JX Shen, GX Qiu, ZM Zheng, CH Li, and SL Liu. Vertebroplasty by use of a strontium-containing bioactive bone cement. *Spine*, 30(17S):S84–S91, 2005.

[204] KK Johal, G. Mendoza-Suarez, JI Escalante-Garcia, RG Hill, and IM Brook. In vivo response of strontium and zinc-based ionomeric cement implants in bone. *Journal of Materials Science: Materials in Medicine*, 13(4):375–379, 2002.

[205] Dong Xie, Dingsong Feng, Il-Doo Chung, and Alan W. Eberhardt. A hybrid zinccalciumsilicate polyalkenoate bone cement. *Biomaterials*, 24(16):2749–2757, 2003.

[206] D. Boyd, M. R. Towler, S. Watts, R. G. Hill, A. W. Wren, and O. M. Clarkin. The role of sr2+ on the structure and reactivity of sro-cao-zno-sio2 ionomer glasses. *Journal of materials science.Materials in medicine*, 19(2):953–957, Feb 2008.

[207] Larry L. Hench, R. J Splinter, WC Allen, and TK Greenlee. Bonding mechanisms at the interface of ceramic prosthetic materials. *Journal of Biomedical Materials Research*, 5(6):117–141, 1971.

[208] Julian R. Jones. Review of bioactive glass: from hench to hybrids. *Acta biomaterialia*, 9(1):4457–4486, 2013.

[209] Alexander Hoppe, Nusret S. Gldal, and Aldo R. Boccaccini. A review of the biological response to ionic dissolution products from bioactive glasses and glass-ceramics. *Biomaterials*, 32(11):2757–2774, 2011.

[210] Valentina Miguez-Pacheco, Larry L. Hench, and Aldo R. Boccaccini. Bioactive glasses beyond bone and teeth: Emerging applications in contact with soft tissues. *Acta Biomaterialia*, 13:1–15, 2 2015.

[211] AE Clark, CG Pantano, and LL Hench. Auger spectroscopic analysis of bioglass corrosion films. *Journal of the American Ceramic Society*, 59(12):37–39, 1976.

[212] H Andersson, Guizhi Liu, KH Karlsson, L. Niemi, J. Miettinen, and J. Juhanoja. In vivo behaviour of glasses in the sio2-na2o-cao-p2o5-al2o3-b2o3 system. *Journal of Materials Science: Materials in Medicine*, 1(4):219–227, 1990.

[213] Kouichiro Ohura, Takashi Nakamura, Takao Yamamuro, Tadashi Kokubo, Yukihiro Ebisawa, Yoshihiko Kotoura, and Masanori Oka. Bonebonding ability of p2o5free cao sio2 glasses. *Journal of Biomedical Materials Research*, 25(3):357–365, 1991.

[214] K. Ohura, T. Nakamura, T. Yamamuro, Y. Ebisawa, T. Kokubo, Y. Kotoura, and M. Oka. Bioactivity of cao sio2 glasses added with various ions. *Journal of Materials Science: Materials in Medicine*, 3(2):95–100, 1992.

[215] RW Douglas and TMM ELSHAMY. Reactions of glasses with aqueous solutions. *Journal of the American Ceramic Society*, 50(1):1–8, 1967.

[216] A. Paul. Chemical durability of glasses; a thermodynamic approach. *Journal of Materials Science*, 12(11):2246–2268, 1977.

[217] CY. Kim, AE. Clark, and LL. Hench. Early stages of calcium-phosphate layer formation in bioglasses. *Journal of Non-Crystalline Solids*, 113(2-3):195–202, 1989.

[218] Satoshi Hayakawa, Kanji Tsuru, Chikara Ohtsuki, and Akiyoshi Osaka. Mechanism of apatite formation on a sodium silicate glass in a simulated body fluid. *Journal of the American Ceramic Society*, 82(8):2155–2160, 1999.

[219] R. Hill. An alternative view of the degradation of bioglass. *Journal of Materials Science Letters*, 15(13):1122–1125, 1996.

[220] Jia Ning, Aihua Yao, Deping Wang, Wenhai Huang, Hailuo Fu, Xin Liu, Xinquan Jiang, and Xiuli Zhang. Synthesis and in vitro bioactivity of a borate-based bioglass. *Materials Letters*, 61(30):5223–5226, 12 2007.

[221] Qiang Fu, Mohamed N. Rahaman, Hailuo Fu, and Xin Liu. Silicate, borosilicate, and borate bioactive glass scaffolds with controllable degradation rate for bone tissue engineering applications. i. preparation and in vitro degradation. *Journal of Biomedical Materials Research Part A*, 95A(1):164–171, 2010.

[222] Xin Liu, M. Rahaman, and D. Day. Conversion of melt derrrived microfibrous borate (13-93b3) and silicate (45s5) bioactive glass in a simulated body fluid, 2013.

[223] Wenhai Huang, Delbert E. Day, Kanisa Kittiratanapiboon, and Mohamed N. Rahaman. Kinetics and mechanisms of the conversion of silicate (45s5), borate, and borosilicate glasses to hydroxyapatite in dilute phosphate solutions. *Journal of Materials Science: Materials in Medicine*, 17(7):583–596, 2006.

[224] Jaime Lynn George. Dissolution of borate glasses and precipitation of phosphate compounds. 2015.

[225] Xuanyong Liu, Chuanxian Ding, and Paul K. Chu. Mechanism of apatite formation on wollastonite coatings in simulated body fluids. *Biomaterials*, 25(10):1755–1761, 2004.

[226] Hiroaki Takadama, HyunMin Kim, Tadashi Kokubo, and Takashi Nakamura. Xray photoelectron spectroscopy study on the process of apatite formation on a sodium silicate glass in simulated body fluid. *Journal of the American Ceramic Society*, 85(8):1933–1936, 2002.

[227] Roland Hellmann, Richard Wirth, Damien Daval, Jean-Paul Barnes, Jean-Michel Penisson, Delphine Tisserand, Thierry Epicier, Brigitte Florin, and Richard L. Hervig. Unifying natural and laboratory chemical weathering with interfacial dissolutionreprecipitation: a study based on the nanometer-scale chemistry of fluidsilicate interfaces. *Chemical Geology*, 294:203–216, 2012.

[228] Roland Hellmann, Stphane Cotte, Emmanuel Cadel, Sairam Malladi, Lisa S. Karlsson, Sergio Lozano-Perez, Martiane Cabi, and Antoine Seyeux. Nanometre-scale evidence for interfacial dissolutionreprecipitation control of silicate glass corrosion. *Nature materials*, 14(3):307–311, 2015.

[229] Pierre Frugier, Stphane Gin, Yves Minet, Tony Chave, Bernard Bonin, Nicole Godon, J-E Lartigue, Patrick Jollivet, Andr Ayral, and Laurent De Windt. Son68 nuclear glass dissolution kinetics: Current state of knowledge and basis of the new graal model. *Journal of Nuclear Materials*, 380(1):8–21, 2008.

[230] Maxime Fournier, Stphane Gin, and Pierre Frugier. Resumption of nuclear glass alteration: State of the art. *Journal of Nuclear Materials*, 448(13):348–363, 5 2014.

[231] Lars Dohmen, Christoph Lenting, Ral OC Fonseca, Thorsten Nagel, Alexander Heuser, Thorsten Geisler, and Rene Denkler. Pattern formation in silicate glass corrosion zones. *International Journal of Applied Glass Science*, 4(4):357–370, 2013.

[232] Rachid Bouakkaz, Abdesselam Abdelouas, Yassine El Mendili, Bernd Grambow, and Stphane Gin. Son68 glass alteration under si-rich solutions at low temperature (3590 c): kinetics, secondary phases and isotopic exchange studies. *RSC Advances*, 6(76):72616–72633, 2016.

[233] Stphane Gin, Patrick Jollivet, Maxime Fournier, Claude Berthon, Zhaoying Wang, Alexandre Mitroshkov, Zihua Zhu, and Joseph V. Ryan. The fate of silicon during glass corrosion under alkaline conditions: a mechanistic and kinetic study with the international simple glass. *Geochimica et Cosmochimica Acta*, 151:68–85, 2015.

[234] Andrew Putnis. Glass corrosion: Sharpened interface. *Nature materials*, 14(3):261–262, 2015.

[235] Michael Anthony Velbel. Formation of protective surface layers during silicate-mineral weathering under well-leached, oxidizing conditions. *American Mineralogist*, 78:405–405, 1993.

[236] Viviana Mourio, Juan Pablo Cattalini, and Aldo R. Boccaccini. Metallic ions as therapeutic agents in tissue engineering scaffolds: an overview of their biological applications and strategies for new developments. *Journal of The Royal Society Interface*, 9(68):401–419, 2012.

[237] W. Jonathan Ryves and Adrian J. Harwood. Lithium inhibits glycogen synthase kinase-3 by competition for magnesium. *Biochemical and Biophysical Research Communications*, 280(3):720–725, 26 January 2001 2001.

[238] Aldo R. Boccaccini, Delia S. Brauer, and Leena Hupa. *Bioactive Glasses: Fundamentals, Technology and Applications*, volume 23. Royal Society of Chemistry, 2016.

[239] Marta Cerruti, David Greenspan, and Kevin Powers. Effect of ph and ionic strength on the reactivity of bioglass 45s5. *Biomaterials*, 26(14):1665–1674, 2005.

[240] Liane Bingel, Daniel Groh, Natalia Karpukhina, and Delia S. Brauer. Influence of dissolution medium ph on ion release and apatite formation of bioglass 45s5. *Materials Letters*, 143:279–282, 3/15 2015.

[241] Eileen Gentleman, Yann C. Fredholm, Gavin Jell, Nasrin Lotfibakhshaiesh, Matthew D. O'Donnell, Robert G. Hill, and Molly M. Stevens. The effects of strontium-substituted bioactive glasses on osteoblasts and osteoclasts in vitro. *Biomaterials*, 31(14):3949–3956, 5 2010.

[242] K. Crapse and E. Kyser. *Literature Review of Boric Acid Solubility Data*, 2011.

[243] Arun K. Varshneya. *Fundamentals of inorganic glasses*. Gulf Professional Publishing, 1994.

[244] Xue Han and Delbert E. Day. Reaction of sodium calcium borate glasses to form hydroxyapatite. *Journal of Materials Science: Materials in Medicine*, 18(9):1837–1847, 2007.

[245] Kathleen O'Connell, Margaret Hanson, Helen O'Shea, and Daniel Boyd. Linear release of strontium ions from high borate glasses via lanthanide/alkali substitutions. *Journal of Non-Crystalline Solids*, 430:1–8, 2015.

[246] John C. Mauro, Charles S. Philip, Daniel J. Vaughn, and Michael S. Pambianchi. Glass science in the united states: current status and future directions. *International Journal of Applied Glass Science*, 5(1):2–15, 2014.

[247] Shichang Zhao, Le Li, Hui Wang, Yadong Zhang, Xiangguo Cheng, Nai Zhou, Mohamed N. Rahaman, Zhongtang Liu, Wenhai Huang, and Changqing Zhang. Wound dressings composed of copper-doped borate bioactive glass microfibers stimulate angiogenesis and heal full-thickness skin defects in a rodent model. *Biomaterials*, 53:379–391, 2015.

[248] Murat Bengisu. Borate glasses for scientific and industrial applications: a review. *Journal of Materials Science*, 51(5):2199–2242, 2016.

[249] Jason C. Eck, Dean Nachtigall, S. Craig Humphreys, and Scott D. Hodges. Comparison of vertebroplasty and balloon kyphoplasty for treatment of vertebral compression fractures: a meta-analysis of the literature. *The Spine Journal*, 8(3):488–497, MayJune 2008 2008.

[250] Elsie S. Place, Nicholas D. Evans, and Molly M. Stevens. Complexity in biomaterials for tissue engineering. *Nature materials*, 8(6):457–470, 2009.

[251] S. Pors Nielsen. The biological role of strontium. *Bone*, 35(3):583–588, 2004.

[252] N. Minakova. The structure of borate glass. *Glass and ceramics*, 65(3-4):70–73, 2008.

[253] EI Kamitsos. Modifying role of alkali-metal cations in borate glass networks. *The Journal of physical chemistry*, 93(4):1604–1611, 1989.

[254] YD Yiannopoulos, Georgios D. Chryssikos, and EI Kamitsos. Structure and properties of alkaline earth borate glasses. *Physics and Chemistry of Glasses-European Journal of Glass Science and Technology Part B*, 42(3):164–172, 2001.

[255] M. Hashimoto. Effect of monomer composition on crystal growth by resin containing bioglass. *Journal of biomedical materials research.Part B, Applied biomaterials*, 94(1):127, 2010.

[256] Kuen Yong Lee, Martin C. Peters, Kenneth W. Anderson, and David J. Mooney. Controlled growth factor release from synthetic extracellular matrices. *Nature*, 408(6815):998–1000, 2000.

[257] Y. Issa, D. C. Watts, P. A. Brunton, C. M. Waters, and A. J. Duxbury. Resin composite monomers alter mtt and ldh activity of human gingival fibroblasts in vitro. *Dental Materials*, 20(1):12–20, 1 2004.

[258] Mohamed N. Rahaman, Delbert E. Day, B. Sonny Bal, Qiang Fu, Steven B. Jung, Lynda F. Bonewald, and Antoni P. Tomsia. Bioactive glass in tissue engineering. *Acta biomaterialia*, 7(6):2355–2373, 2011.

[259] HW Kim, HE Kim, and Jonathan C. Knowles. Production and potential of bioactive glass nanofibers as a nextgeneration biomaterial. *Advanced Functional Materials*, 16(12):1529–1535, 2006.

[260] Yinan Lin, Roger F. Brown, Steven B. Jung, and Delbert E. Day. Angiogenic effects of borate glass microfibers in a rodent model. *Journal of Biomedical Materials Research Part A*, 102(12):4491–4499, 2014.

[261] Richard M. Day. Bioactive glass stimulates the secretion of angiogenic growth factors and angiogenesis in vitro. *Tissue engineering*, 11(5-6):768–777, 2005.

[262] Qiang Fu, Mohamed N. Rahaman, B. Sonny Bal, Lynda F. Bonewald, Keiichi Kuroki, and Roger F. Brown. Silicate, borosilicate, and borate bioactive glass scaffolds with controllable degradation rate for bone tissue engineering applications. ii. in vitro and in vivo biological evaluation. *Journal of Biomedical Materials Research Part A*, 95A(1):172–179, 2010.

[263] Roger F. Brown, Mohamed N. Rahaman, Agatha B. Dwilewicz, Wenhai Huang, Delbert E. Day, Yadong Li, and B. Sonny Bal. Effect of borate glass composition on its conversion to hydroxyapatite and on the proliferation of mc3t3-e1 cells. *Journal of Biomedical Materials Research Part A*, 88A(2):392–400, 2009.

[264] AM Abdelghany, MA Ouis, MA Azooz, HA ElBatal, and GT El-Bassyouni. Role of sro on the bioactivity behavior of some ternary borate glasses and their glass ceramic derivatives. *Spectrochimica Acta Part A: Molecular and Biomolecular Spectroscopy*, 152:126–133, 2016.

[265] Nathan P. Lower, Justin L. McRae, Heidi A. Feller, Ashlea R. Betzen, Shalini Kapoor, Mario Affatigato, and Steven A. Feller. Physical properties of alkaline-earth and alkali borate glasses prepared over an extended range of compositions. *Journal of Non-Crystalline Solids*, 293:669–675, 2001.

[266] Jianhui Zhong and Philip J. Bray. Change in boron coordination in alkali borate glasses, and mixed alkali effects, as elucidated by nmr. *Journal of Non-Crystalline Solids*, 111(1):67–76, 1989.

[267] CT Moynihan and AV Lesikar. Weakelectrolyte models for the mixedalkali effect in glass. *Journal of the American Ceramic Society*, 64(1):40–46, 1981.

[268] Paulo Costa and Jose Manuel Sousa Lobo. Modeling and comparison of dissolution profiles. *European journal of pharmaceutical sciences*, 13(2):123–133, 2001.

[269] KE Wallace, RG Hill, JT Pembroke, CJ Brown, and PV Hatton. Influence of sodium oxide content on bioactive glass properties. *Journal of Materials Science: Materials in Medicine*, 10(12):697–701, 1999.

[270] CJ Brinker, KJ Ward, KD Keefer, E. Holupka, PJ Bray, and RK Pearson. *Synthesis and Structure of Borate Based Aerogels*, pages 57–67. Aerogels. Springer, 1986.

[271] K. Er. Cytotoxicity analysis of strontium ranelate on cultured human periodontal ligament fibroblasts: a preliminary report. *Journal of the Formosan Medical Association*, 107(8):609, 2008.

[272] MD Grynpas and PJ Marie. Effects of low doses of strontium on bone quality and quantity in rats. *Bone*, 11(5):313–319, 1990.

[273] Patrick Ammann, Victor Shen, Bruno Robin, Yves Mauras, JeanPhilippe Bonjour, and Rene Rizzoli. Strontium ranelate improves bone resistance by increasing bone mass and improving architecture in intact female rats. *Journal of bone and mineral research*, 19(12):2012–2020, 2004.

[274] Jan J. Stepan. Strontium ranelate: in search for the mechanism of action. *Journal of bone and mineral metabolism*, 31(6):606–612, 2013.

[275] PJ Marie, D. Felsenberg, and ML Brandi. How strontium ranelate, via opposite effects on bone resorption and formation, prevents osteoporosis. *Osteoporosis International*, 22(6):1659–1667, 2011.

[276] M. Hamdan Alkhraisat, C. Rueda, J. Cabrejos-Azama, J. Lucas-Aparicio, F. Tamimi Mario, J. Torres Garca-Denche, L. Blanco Jerez, U. Gbureck, and E. Lopez Cabarcos. Loading and release of doxycycline hyclate from strontium-substituted calcium phosphate cement. *Acta Biomaterialia*, 6(4):1522–1528, 2010.

[277] Meng Tian, Feng Chen, Wei Song, Yancheng Song, Yuanwei Chen, Changxiu Wan, Xixun Yu, and Xiaohua Zhang. In vivo study of porous strontium-doped calcium polyphosphate scaffolds for bone substitute applications. *Journal of Materials Science: Materials in Medicine*, 20(7):1505–1512, 2009.

[278] US Department of Health and Human Services. Toxicological profile for strontium. *Public Health Service, Agency for Toxic Substances and Disease Registry*, 2004.

[279] F. Zhao, WW Lu, KDK Luk, KMC Cheung, CT Wong, JCY Leong, and KD Yao. Surface treatment of injectable strontiumcontaining bioactive bone cement for vertebroplasty. *Journal of Biomedical Materials Research Part B: Applied Biomaterials*, 69(1):79–86, 2004.

[280] YW Li, JCY Leong, WW Lu, KDK Luk, KMC Cheung, KY Chiu, and SP Chow. A novel injectable bioactive bone cement for spinal surgery: a developmental and preclinical study. *Journal of Biomedical Materials Research*, 52(1):164–170, 2000.

[281] Elke Vorndran, Nikola Spohn, Berthold Nies, Sophie Rler, Sandra Storch, and Uwe Gbureck. Mechanical properties and drug release behavior of bioactivated pmma cements. *Journal of Biomaterials Applications*, 26(5):581–594, 2012.

[282] P. Frutos, E. Diez-Pena, G. Frutos, and JM Barrales-Rienda. Release of gentamicin sulphate from a modified commercial bone cement. effect of (2-hydroxyethyl methacrylate) comonomer and poly (n-vinyl-2-pyrrolidone) additive on release mechanism and kinetics. *Biomaterials*, 23(18):3787–3797, 2002.

[283] Wailan D. Chan, Lifang Yang, Wankei Wan, and Amin S. Rizkalla. Fluoride release from dental cements and composites: a mechanistic study. *Dental Materials*, 22(4):366–373, 2006.

[284] D. Skrtic. Effect of the monomer and filler systems on the remineralizing potential of bioactive dental composites based on amorphous calcium phosphate. *Polymers for Advanced Technologies*, 12(6):369, 2001.

[285] Kathleen MacDonald, Margaret A. Hanson, and Daniel Boyd. Modulation of strontium release from a tertiary borate glass through substitution of alkali for alkali earth oxide. *Journal of Non-Crystalline Solids*, 443:184–191, 2016.

[286] Jukka P. Matinlinna, Lippo VJ Lassila, Mutlu zcan, Antti Yli-Urpo, and Pekka K. Vallittu. An introduction to silanes and their clinical applications in dentistry. *International Journal of Prosthodontics*, 17(2), 2004.

[287] Joseph M. Antonucci, Bruce O. Fowler, Michael D. Weir, Drago Skrtic, and Jeffrey W. Stansbury. Effect of ethyl--hydroxymethylacrylate on selected properties of copolymers and acp resin composites. *Journal of Materials Science: Materials in Medicine*, 19(10):3263–3271, 2008.

[288] L. Balachandera, G. Ramadevudub, Md Shareefuddina, R. Sayannac, and YC Venudharc. Ir analysis of borate glasses containing three alkali oxides. *ScienceAsia*, 39:278, 2013.

[289] S. E. Stein. *"Infrared Spectra" by NIST Mass Spec Data Center,.* NIST Chenistry WebBook NIST Standard Reference Database Number 69. National Institute of Standards and Technology, Gaithersburg MD, 2016.

[290] Garry JP Fleming, Adam H. Dowling, and Owen Addison. The crushing truth about glass ionomer restoratives: exposing the standard of the standard. *Journal of dentistry*, 40(3):181–188, 2012.

[291] Po-Liang Lai, Ching-Lung Tai, I-Ming Chu, Tsai-Sheng Fu, Lih-Huei Chen, and Wen-Jer Chen. Hypothermic manipulation of bone cement can extend the handling time during vertebroplasty. *BMC musculoskeletal disorders*, 13:198–198, 2012.

[292] J. L. Ferracane and E. H. Greener. Fourier transform infrared analysis of degree of polymerization in unfilled resins–methods comparison. *Journal of dental research*, 63(8):1093–1095, Aug 1984.

[293] Athina Bakopoulou, Triantafillos Papadopoulos, and Pavlos Garefis. Molecular toxicology of substances released from resinbased dental restorative materials. *International journal of molecular sciences*, 10(9):3861–3899, 2009.

[294] S. Imazato, J. F. McCabe, H. Tarumi, A. Ehara, and S. Ebisu. Degree of conversion of composites measured by dta and ftir. *Dental Materials*, 17(2):178–183, 3 2001.

[295] Flavia Goncalves, Yoshio Kawano, Carmem Pfeifer, Jeffrey W. Stansbury, and Roberto R. Braga. Influence of bisgma, tegdma, and bisema contents on viscosity, conversion, and flexural strength of experimental resins and composites. *European journal of oral sciences*, 117(4):442–446, 2009.

[296] SM Chung, AUJ Yap, SP Chandra, and CT Lim. Flexural strength of dental composite restoratives: Comparison of biaxial and threepoint bending test. *Journal of Biomedical Materials Research Part B: Applied Biomaterials*, 71(2):278–283, 2004.

[297] Zainuddin, David JT Hill, Traian V. Chirila, Andrew K. Whittaker, and Anne Kemp. Experimental calcification of hema-based hydrogels in the presence of albumin and a comparison to the in vivo calcification. *Biomacromolecules*, 7(6):1758–1765, 2006.

[298] M. Schumacher, A. Lode, A. Helth, and M. Gelinsky. A novel strontium (ii)-modified calcium phosphate bone cement stimulates human-bone-marrow-derived mesenchymal stem cell proliferation and osteogenic differentiation in vitro. *Acta biomaterialia*, 9(12):9547–9557, 2013.

[299] ISO ISO. 9917-1: dentistry-water-based cementspart 1: powder/liquid acidbase cements. *International Organization for Standardization, Geneva, Switzerland*, 2007.

[300] ISO Standard. 5833-2002. implants for surgeryacrylic resin cements. *Geneva, Switzerland: International Standards Organization*, 2002.

[301] B. T. Dickey, S. Kehoe, and D. Boyd. Novel adaptations to zincsilicate glass polyalkenoate cements: The unexpected influences of germanium based glasses on handling characteristics and mechanical properties. *Journal of the Mechanical Behavior of Biomedical Materials*, 23(0):8–21, 7 2013.

[302] Theodore Eliades, George Eliades, William A. Brantley, and William M. Johnston. Polymerization efficiency of chemically cured and visible light-cured orthodontic adhesives: Degree of cure. *American Journal of Orthodontics and Dentofacial Orthopedics*, 108(3):294–301, 9 1995.

[303] M. J. Bolland and A. Grey. A comparison of adverse event and fracture efficacy data for strontium ranelate in regulatory documents and the publication record. *BMJ open*, 4(10):e005787–2014–005787, Oct 7 2014.

[304] Anthony Grosso, Ian Douglas, Aroon Hingorani, Raymond MacAllister, and Liam Smeeth. Postmarketing assessment of the safety of strontium ranelate; a

novel caseonly approach to the early detection of adverse drug reactions. *British journal of clinical pharmacology*, 66(5):689–694, 2008.

[305] Jean-Yves Reginster, DO Slosman, PD Delmas, JL Sebert, ML Brandi, R. Lorenc, S. Pors-Nielsen, MC de Vernejoul, A. Roces, and PJ Meunier. Strontium ranelate: Dose-dependent effects in postmenopausal osteoporosis: The stratos 2-year randomised trial. *Clinical rheumatology*, 20:427–428, 2001.

[306] Kathleen MacDonald, Richard B. Price, and Daniel Boyd. The feasibility and functional performance of ternary borate-filled hydrophilic bone cements: Targeting therapeutic release thresholds for strontium. *Journal of Functional Biomaterials*, 8(3):28, 2017.

[307] M. Regina Filgueiras, Guy La Torre, and Larry L. Hench. Solution effects on the surface reactions of a bioactive glass. *Journal of Biomedical Materials Research Part A*, 27(4):445–453, 1993.

[308] V. Mourino and A. R. Boccaccini. Bone tissue engineering therapeutics: controlled drug delivery in three-dimensional scaffolds. *Journal of the Royal Society, Interface*, 7(43):209–227, Feb 6 2010.

[309] Uwe Gbureck, Elke Vorndran, and Jake E. Barralet. Modeling vancomycin release kinetics from microporous calcium phosphate ceramics comparing static and dynamic immersion conditions. *Acta biomaterialia*, 4(5):1480–1486, 2008.

[310] Shuichi Ito, Masanori Hashimoto, Bakul Wadgaonkar, Nadia Svizero, Ricardo M. Carvalho, Cynthia Yiu, Frederick A. Rueggeberg, Stephen Foulger, Takashi Saito, and Yoshihiro Nishitani. Effects of resin hydrophilicity on water sorption and changes in modulus of elasticity. *Biomaterials*, 26(33):6449–6459, 2005.

[311] P. Frutos Cabanillas, E. Dez Pea, JM Barrales-Rienda, and G. Frutos. Validation and in vitro characterization of antibiotic-loaded bone cement release. *International journal of pharmaceutics*, 209(1):15–26, 2000.

[312] Hailuo Fu, Qiang Fu, Nai Zhou, Wenhai Huang, Mohamed N. Rahaman, Deping Wang, and Xin Liu. In vitro evaluation of borate-based bioactive glass scaffolds prepared by a polymer foam replication method. *Materials Science and Engineering: C*, 29(7):2275–2281, 8/31 2009.

[313] Kathleen O'Connell, Caitlin Pierlot, Helen O'Shea, Diane Beaudry, Madeleine Chagnon, Michel Assad, and Daniel Boyd. Host responses to a strontium releasing high boron glass using a rabbit bilateral femoral defect model. *Journal of Biomedical Materials Research Part B: Applied Biomaterials*, 105(7):1818–1827, 2017.

[314] Mike Lumpkin and Malcolm Williams. Toxicological profile for boron. 2010.

[315] Annette Wiegand, Wolfgang Buchalla, and Thomas Attin. Review on fluoride-releasing restorative materialsfluoride release and uptake characteristics, antibacterial activity and influence on caries formation. *Dental materials*, 23(3):343–362, 2007.

[316] Fariba Ganji, Samira Vasheghani-Farahani, and Ebrahim Vasheghani-Farahani. Theoretical description of hydrogel swelling: a review. *Iran Polym J*, 19(5):375–398, 2010.

[317] Teodora Zecheru, Robert Filmon, Edina Rusen, Bogdan Mrculescu, Amar Zerroukhi, Corneliu Cincu, and Daniel Chappard. Biomimetic potential of some methacrylatebased copolymers: A comparative study. *Biopolymers*, 91(11):966–973, 2009.

[318] Standard test method for constant amplitude of force controlled fatigue testing of acrylic bone cement materials, 27 Sep 2017 2014.

[319] Antonius Rohlmann, Hadi Nabil Boustani, Georg Bergmann, and Thomas Zander. A probabilistic finite element analysis of the stresses in the augmented vertebral body after vertebroplasty. *European Spine Journal*, 19(9):1585–1595, 2010.

[320] Celene Hadley, Omer Abdulrehman Awan, and Gregg H. Zoarski. Biomechanics of vertebral bone augmentation. *Neuroimaging Clinics of North America*, 20(2):159–167, May 2010 2010.

[321] Alexander G. Bruno, Dennis E. Anderson, John D'Agostino, and Mary L. Bouxsein. The effect of thoracic kyphosis and sagittal plane alignment on vertebral compressive loading. *Journal of Bone and Mineral Research*, 27(10):2144–2151, 2012.

[322] T. Kokubo, H. Kushitani, C. Ohtsuki, S. Sakka, and T. Yamamuro. Chemical reaction of bioactive glass and glass-ceramics with a simulated body fluid. *Journal of Materials Science: Materials in Medicine*, 3(2):79–83, 1992.

[323] CM Pierlot, L. Kiri, K. MacDonald, B. Dickey, E. Valliant, M. Chagnon, M. Assad, MJ Filiaggi, and D. Boyd. A pilot evaluation of an aluminum free glass ionomer cement using a sub-chronic osseous defect model in new zealand white rabbits. *Materials Letters*, 184:301–304, 2016.

[324] Jack L. Ferracane. Hygroscopic and hydrolytic effects in dental polymer networks. *Dental Materials*, 22(3):211–222, March 2006 2006.

[325] Luciano F. Boesel and Rui L. Reis. The effect of water uptake on the behaviour of hydrophilic cements in confined environments. *Biomaterials*, 27(33):5627–5633, 2006.

[326] Markian S. Bahniuk, Hamidreza Pirayesh, Harsh D. Singh, John A. Nychka, and Larry D. Unsworth. Bioactive glass 45s5 powders: effect of synthesis route and resultant surface chemistry and crystallinity on protein adsorption from human plasma. *Biointerphases*, 7(1-4):1–15, 2012.

[327] Gen He, Tom Dahl, Arthur Veis, and Anne George. Nucleation of apatite crystals in vitro by self-assembled dentin matrix protein 1. *Nature materials*, 2(8):552–558, 2003.

[328] Anne Perez, Stphanie Rossano, Nicolas Trcera, Aurlie Verney-Carron, David Huguenot, Eric D. van Hullebusch, Gilles Catillon, Angelina Razafitianamaharavo, and Franois Guyot. Impact of iron chelators on short-term dissolution of basaltic glass. *Geochimica et Cosmochimica Acta*, 162:83–98, 8/1 2015.

[329] Marc Bohner and Jacques Lemaitre. Can bioactivity be tested in vitro with sbf solution? *Biomaterials*, 30(12):2175–2179, 2009.

[330] Dana Rohanov, Aldo Roberto Boccaccini, Darmawati Mohamad Yunos, Diana Horkavcov, Iva Bezovsk, and Ale Helebrant. Tris buffer in simulated body fluid distorts the assessment of glassceramic scaffold bioactivity. *Acta biomaterialia*, 7(6):2623–2630, 2011.

[331] Vassilios S. Nikolaou, Nicolas Efstathopoulos, George Kontakis, Nikolaos K. Kanakaris, and Peter V. Giannoudis. The influence of osteoporosis in femoral fracture healing time. *Injury*, 40(6):663–668, 2009.

[332] Peter Giannoudis, Christopher Tzioupis, Talal Almalki, and Richard Buckley. Fracture healing in osteoporotic fractures: is it really different?: A basic science perspective. *Injury*, 38(1):S90–S99, 2007.

[333] Dana Rohanov, Diana Horkavcov, Ale Helebrant, and Aldo Roberto Boccaccini. Assessment of in vitro testing approaches for bioactive inorganic materials. *Journal of Non-Crystalline Solids*, 432:53–59, 15 January 2016 2016.

[334] F. R. Tay, D. H. Pashley, and M. Yoshiyama. Two modes of nanoleakage expression in single-step adhesives. *Journal of dental research*, 81(7):472–476, Jul 2002.

[335] SG Dahl, P. Allain, PJ Marie, Y. Mauras, G. Boivin, P. Ammann, Y. Tsouderos, PD Delmas, and C. Christiansen. Incorporation and distribution of strontium in bone. *Bone*, 28(4):446–453, 2001.

[336] H. Deramond, N. T. Wright, and S. M. Belkoff. Temperature elevation caused by bone cement polymerization during vertebroplasty. *Bone*, 25(2, Supplement 1):17S–21S, August 1999 1999.

Appendix A

Peak Exothermic Setting Temperatures

Exothermic setting temperatures were assessed during setting time evaluations using methods described in section 4.2.6. Peak temperatures (Figure A.1) varied between 70°C for 15% HEMA 65% glass cement, and 114°C for the 45% HEMA 55% glass cement. Significant increases in exothermic temperatures when compared to PMMA cements are likely due to the high HEMA content. Temperatures were largely greater than the temperatures previously reported for PMMA (41-95°C)[148, 158]. While exothermic temperatures are well above the thermal damage thresholds often used as guidelines for vertebroplasty cement design [1], the direct comparison between setting time evaluation temperatures and implantation temperatures can not be made due to variability in the thermal environment, including blood flow presenting potential cooling. While presented by Lewis as potentially deleterious, there is controversy about exothermic curing heat proving potential clinical benefit through thermal albalation of local nociceptors providing further pain relief to the patient [336]. While such a mechanism is possible, no significant decrease in pain relief has been reported at early time points with the use of Cortoss®, despite it's reduced setting temperatures[23].

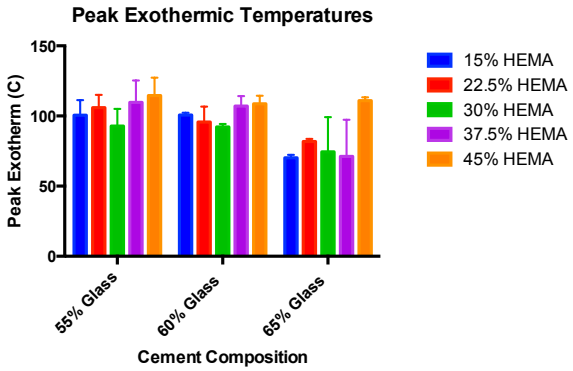

Figure A.1: Peak exothermic temperatures of cement curing.

Appendix B

Cytotoxicity testing of cement extracts

Cytotoxicity testing of cement extracts generated in PBS under unloaded simulated physiological conditions as per section 4.2.6 was performed out of house by WuXi AppTec (St. Paul, MN, USA). Cement extracts containing 15 % and 45 % HEMA (65 wt% glass) generated over both 1 and 60 d of incubation were tested to represent the extremes of the design space. Cement extracts (n=3/composition time point) were sterilized through use of 0.2 μm syringe tip filters, sealed in sterile polypropylene tubes, and sent to the testing facility. Cytotoxicity testing was performed as per ISO 10993 utilizing an L-929 mouse fibroblast cell line. Test articles were mixed in equal parts with 2X Eagle's Minimum Essential Medium (E-MEM) + 10 % Foetal Bovine Serum (FBS) to generate a 50 % exposure medium. A positive control of E-MEM +5 % FBS was used, along with a negative control of E-MEM +5 % FBS with 100 μM $CdCl_2$ to validate the analysis. Cell cultures were incubated with all test media in triplicate, under humidified conditions, and evaluated for cytopathic effects (as per Table B.1) at 24, 48 and 72 h. Cytotoxicity results (Table B.2) indicated no cytotoxic effects were observed after 24 or 48 h. For the 72 h exposure samples, slight cytopathic changes were seen for all test samples, indicating that all materials tested were non cytotoxic.

Table B.1: Criteria for the evaluation of cytotoxicity. Materials with cytopathology scores below 2 considered non cytotoxic. Positive cytotoxic response considered mild for scores of 3, and severe for scores of 4.

Grade	Reactivity	Conditions of All Cultures
0	**None**	Discrete intracytoplasmic granules; no cell lysis, no reduction of cell growth
1	**Slight**	Not more than 20 % of the cells are round, loosely attached, and without intra-cytoplasmic granules, or show changes in morphology; occasional lysed cells are present; only slight growth inhibition observable
2	**Mild**	Not more than 50 % of the cells are round, devoid of intra-cytoplasmic granules, no extensive cell lysis; not more than 50 % growth inhibition observable.
3	**Moderate**	Not more than 70 % of the cell layers contain rounded cells or are lysed; cells layers not completely destroyed, but more than 50 % grown inhibition observable
4	**Severe**	Nearly complete or complete destruction of the cell layers

Table B.2: Cytotoxicity scoring results

HEMA	Incubation Time	Cytotoxicity Scores		
		24 h	**48 h**	**72 h**
15 %	**1 d**	0 ± 0	0 ± 0	1 ± 0
15 %	**60 d**	0 ± 0	0 ± 0	1 ± 0
45 %	**1 d**	0 ± 0	0 ± 0	1 ± 0
45 %	**60 d**	0 ± 0	0 ± 0	1 ± 0
Positive Control		0 ± 0	0 ± 0	0 ± 0
Negative Control		4 ± 0	4 ± 0	4 ± 0

Appendix C

Additional animal study data

Table C.1: Histologic evaluation scoring rubric used for the evaluation of implant response, adapted from ISO 10993

Response	Score (*phf = per high powered (x400) field)			
	0	**1**	**2**	**3**	**4**
Polymorphonuclear cells	0	Rare, 1-5/phf*	6-10/phf	Heavy infiltrate	Packed
Lymphocytes	0	Rare, 1-5/phf*	6-10/phf	Heavy infiltrate	Packed
Plasma cells	0	Rare, 1-5/phf*	6-10/phf	Heavy infiltrate	Packed
Macrophages	0	Rare, 1-5/phf*	6-10/phf	Heavy infiltrate	Packed
Giant cells	0	Rare, 1-5/phf*	6-10/phf	Heavy infiltrate	Packed
Necrosis	0	Minimal	Mild	Moderate	Marked
Infection	0	Minimal	Mild	Moderate	Marked
Fibrinous exudates	0	Minimal	Mild	Moderate	Marked
Tissue degeneration	0	Minimal	Mild	Moderate	Marked
Neovascularisation	0	Minimal capillary proliferation focal, 1-3 buds	Groups of 4-7 capillaries with supporting fibroblastic structures	Broad band of capillaries with supporting fibroblastic structures	Extensive band of capillaries with supporting fibroblastic structures
Fibrocytes/ fibroconnective tissue, fibrosis/encapsulation	0	Narrow band	Moderately thick band	Thick band	Extensive band
Fatty infiltrate	0	Minimal amount of fat associated with fibrosis	Several layers of fat and fibrosis	Elongated and broad accumulation of fat cells about the implant site	Extensive fat completely surrounding the implant
New bone formation	0	Minimal	Mild	Moderate	Marked
Bone-implant contact/apposition	0	Minimal	Mild	Moderate	Marked
Cartilage formation	0	Minimal	Mild	Moderate	Marked

Table C.2: Detailed histomorphometry findings of implant response to glass filled (strontium releasing) implant sites, evaluated 8 weeks post implantation.

Animal Number	Location/Site	Bone Apposition	Area									
			Total (mm^2)	Bone (mm^2)	Test Article Residual (mm^2)	Soft Tissue (mm^2)	Void (mm^2)	Bone (%)	Test Article Residual (%)	Soft Tissue (%)	Void (%)
D56-01	Right Femur	66.7%	26.72	2.45	24.12	0.15	0.00	9.2	90.3	0.6	0.0
D56-02	Right Femur	75.7	24.94	1.30	23.57	0.07	0.00	5.2	94.5	0.3	0.0
D56-03	Right Femur	71.9	26.02	1.22	24.74	0.06	0.00	4.7	95.1	0.2	0.0
Mean		71.4	25.89	1.66	24.14	0.09	0.00	6.4	93.3	0.4	0.0
Standard Deviation		4.5	0.90	0.69	0.59	0.05	0.00	2.5	2.6	0.2	0.0
Number		3	3	3	3	3	3	3	3	3	3

Table C.3: Detailed histomorphometry findings of implant response to unfilled resin (non strontium releasing) implant sites, evaluated 8 weeks post implantation.

Animal Number	Location/Site	Bone Apposition	Unfilled Resin									
			Area									
			Total (mm^2)	Bone (mm^2)	Test Article Residual (mm^2)	Soft Tissue (mm^2)	Void (mm^2)	Bone (%)	Test Article Residual (%)	Soft Tissue (%)	Void (%)
D56-01	Left Femur	74.0	21.44	2.18	19.18	0.08	0.00	10.2	89.5	0.4	0.0
D56-02	Left Femur	100	23.73	3.77	19.96	0.00	0.00	15.9	84.1	0.0	0.0
D56-03	Left Femur	100	15.58	2.02	13.56	0.00	0.00	13.00	87.0	0.0	0.0
Mean		91.3	20.25	2.66	24.1417.57	0.03	0.00	13.0	86.9	0.1	0.0
Standard Deviation		15.0	4.2	0.97	3.49	0.05	0.00	2.9	2.7	0.2	0.0
Number		3	3	3	3	3	3	3	3	3	3

Table C.4: Detailed histomorphometry findings of sham defect sites, evaluated 24 days post operation due to early sacrifice related to decreased appetite.

Animal Number	Location Site	Bone Apposition	Area									
			Total (mm^2)	Bone (mm^2)	Test Article Residual (mm^2)	Soft Tissue (mm^2)	Void (mm^2)	Bone (%)	Test Article Residual (%)	Soft Tissue (%)	Void (%)
D56-04	Right Femur	-	19.71	17.98	-	1.73	0.00	91.2	-	8.8	0.0
D56-04	Left Femur	-	24.46	22.60	-	1.86	0.00	92.4	-	7.6	0.0
Mean		-	22.09	20.29	-	1.8	0.00	91.8	-	8.2	0.0
Standard Deviation		-	3.36	3.27	-	0.09	0.00	0.8	-	0.8	0.0
Number		-	2	2	-	2	2	2	-	2	2

Table C.5: Detailed histological findings of glass filled (strontium releasing) implant sites 8 weeks post implantation.

Animal Number	Location Site	Polymorphic nuclear cells	Lymphocytes	Plasma Cells	Macrophages	Giant Cells	Necrosis	Infection	Fibrous exudate	Tissue degeneration	Neovascularization	Fibroconnective tissue, fibrosis, encapsulation	Fatty infiltrate/marrow	New bone formation	Bone Implant contact/apposition	Void spaces	Fluid/material	Implant irregularity
D56-01	Right Femur	0	0	0	1	1	0	0	0	0	1	1	2	1	3	0	0	0
D56-02	Right Femur	0	0	0	1	1	0	0	0	0	1	1	1	1	4	0	0	1
D56-03	Right Femur	0	0	0	1	1	0	0	0	0	1	1	1	1	4	0	0	0
Mean		0.00	0.00	1.00	1.00	1.00	0.00	0.00	0.00	0.00	1.00	1.00	1.33	1.00	3.67	0.00	0.00	0.33
Standard Deviation		0.00	0.00	0.00	0.00	0.00	0.00	0.00	0.00	0.00	0.00	0.00	0.58	0.00	0.58	0.00	0.00	0.58
Number		3	3	3	3	3	3	3	3	3	3	3	3	3	3	3	3	3

Table C.6: Detailed histological findings of unfilled resin (non strontium releasing) implant sites 8 weeks post implantation

Animal Number	Location Site	Polymorphic nuclear cells	Lymphocytes	Plasma Cells	Macrophages	Giant Cells	Necrosis	Infection	Fibrous exudate	Tissue degeneration	Neovascularization	Fibroconnective tissue, fibrosis, encapsulation	Fatty infiltrate/marrow	New bone formation	Bone Implant contact/apposition	Void spaces	Fluid/material	Implant irregularity
D56-01	Left Femur	0	0	0	1	0	0	0	0	0	1	1	1	1	3	0	0	1
D56-02	Left Femur	0	0	0	1	1	0	0	0	0	1	1	1	1	4	0	0	0
D56-03	Left Femur	0	0	0	1	1	0	0	0	0	1	0	2	1	4	0	0	1
Mean		0.00	0.00	1.00	1.00	0.67	0	0	0.00	0.00	1.00	0.67	1.33	1.00	3.67	0.00	0.00	0.67
Standard Deviation		0.00	0.00	0.00	0.00	0.58	0	0	0.00	0.00	0.00	0.58	0.58	0.00	0.58	0.00	0.00	0.58
Number		3	3	3	3	3	3	3	3	3	3	3	3	3	3	3	3	3

Table C.7: Detailed histological findings of sham defect sites, evaluated 24 days post operation due to early sacrifice related to decreased appetite.

Animal Number	Location Site	Polymorphic nuclear cells	Lymphocytes	Plasma Cells	Macrophages	Giant Cells	Necrosis	Infection	Fibrous exudate	Tissue degeneration	Neovascularization	Fibroconnective tissue, fibrosis, encapsulation	Fatty infiltrate/marrow	New bone formation	Bone Implant contact/apposition	Void spaces	Fluid/material	Implant irregularity
D56-04	Right Femur	0	0	0	1	0	0	0	0	0	1	3	3	3	-	0	0	-
D56-04	Left Femur	0	0	0	1	0	0	0	0	0	2	3	3	3	-	0	0	-
Mean		0.00	0.00	0.00	1.00	0.00	0	0	0.00	0.00	1.50	3.00	3.00	3.00	-	0.00	0.00	-
Standard Deviation		0.00	0.00	0.00	0.00	0.00	0	0	0.00	0.00	0.71	0.00	0.00	0.00	-	0.00	0.00	-
Number		2	2	2	2	2	2	2	2	2	2	2	2	2	-	2	2	-